Miscellaneous Paper CERC-94-8
May 1994

US Army Corps of Engineers
Waterways Experiment Station

Fisherman's Wharf Breakwater Monitoring Study, San Francisco, California

by Jonathan W. Lott

Prepared for Headquarters, U.S. Army Corps of Engineers

Miscellaneous Paper CERC-94-8
May 1994

Fisherman's Wharf Breakwater Monitoring Study, San Francisco, California

by Jonathan W. Lott

U.S. Army Corps of Engineers
Waterways Experiment Station
3909 Halls Ferry Road
Vicksburg, MS 39180-6199

Final report

Approved for public release; distribution is unlimited

Prepared for U.S. Army Corps of Engineers
Washington, DC 20314-1000

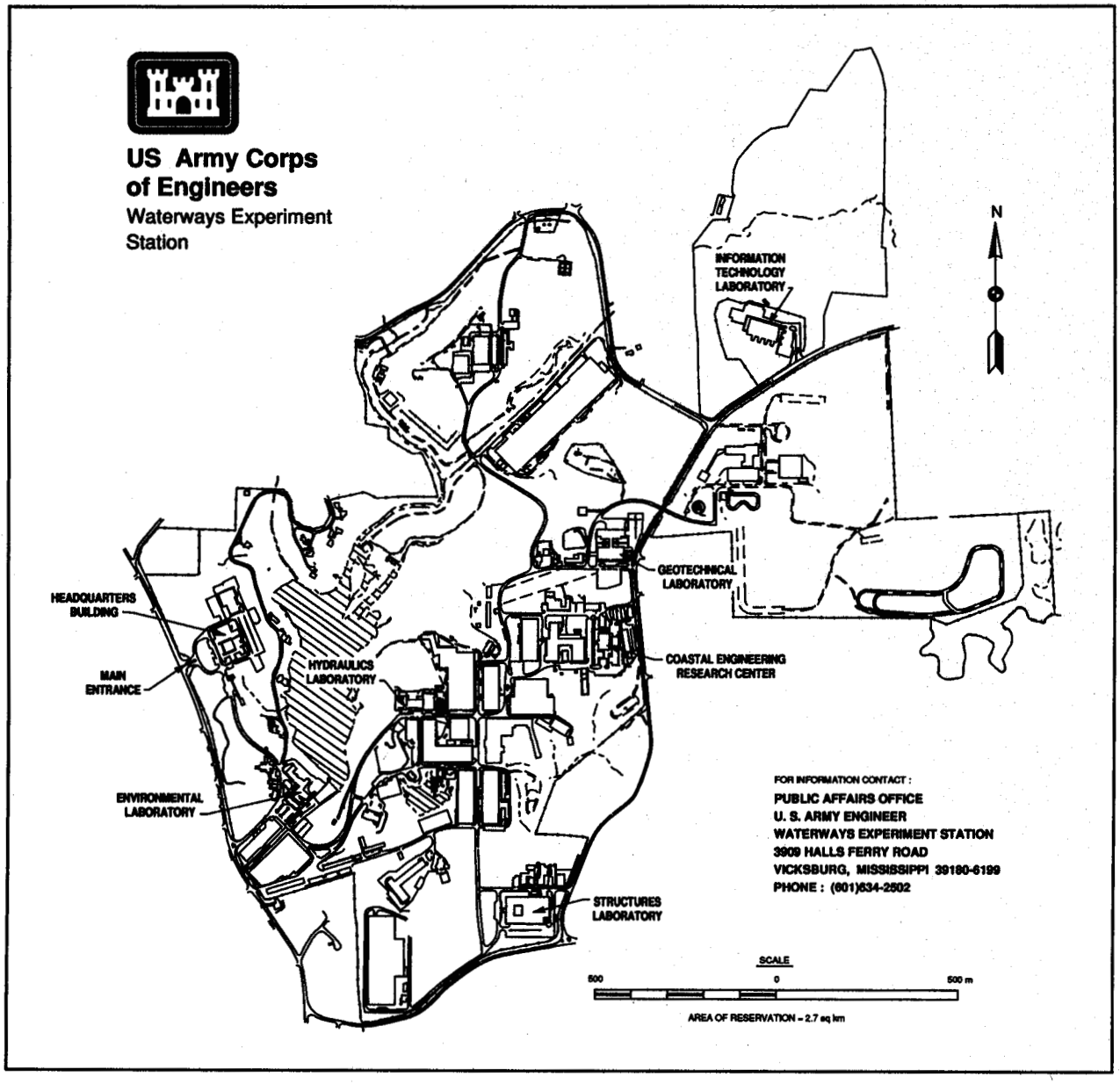

Waterways Experiment Station Cataloging-in-Publication Data

Lott, Jonathan W.
Fisherman's Wharf breakwater monitoring study, San Francisco, California / by Jonathan W. Lott. ; prepared for U.S. Army Corps of Engineers.
188 p. : ill. ; 28 cm. — (Miscellaneous paper ; CERC-94-8)
Includes bibliographic references.
1. Breakwaters — California — San Francisco — Evaluation. 2. Fisherman's Wharf (San Francisco, Calif.) 3. Harbors — California — San Francisco — Design and construction. I. United States. Army. Corps of Engineers. II. U.S. Army Engineer Waterways Experiment Station. III. Coastal Engineering Research Center (U.S.) IV. Title. V. Series: Miscellaneous paper (U.S. Army Engineer Waterways Experiment Station) ; CERC-94-8.
TA7 W34m no.CERC-94-8

Contents

List of Figures

List of Tables

Preface

This report was prepared as part of the Monitoring Completed Coastal Projects (MCCP) Program, regulated by Engineer Regulation 1110-2-8151. The program calls for intensive monitoring of selected Civil Works coastal projects, to assure adequate information as a basis for improving project purpose attainment, design procedures, construction methods, and operations and maintenance techniques. Overall program management is by the Hydraulic Design Section of Headquarters, U.S. Army Corps of Engineers (HQUSACE). The U.S. Army Engineer District, San Francisco (SPN) is the Field Operating Agency within whose jurisdiction the Fisherman's Wharf breakwater project falls. The work was carried out under the Fisherman's Wharf breakwater monitoring effort, MCCP Work Unit 22115. For the MCCP Program, the HQUSACE Technical Monitors are Messrs. John H. Lockhart, Jr., John G. Housley, and Barry W. Holliday. MCCP Program Manager is Ms. Carolyn M. Holmes, succeeding Mr. J. Michael Hemsley, of the U.S. Army Engineer Waterways Experiment Station (WES) Coastal Engineering Research Center (CERC).

The report presents the results of the MCCP effort focusing on the concrete sheet-pile breakwater structures located in the Fisherman's Wharf area of the San Francisco, California, waterfront. The breakwater was built to provide wave protection for the existing small craft harbor at Fisherman's Wharf, for the fleet of historic ships berthed at Hyde Street pier, and for the planned expansion of small craft berthing facilities between Hyde Street pier and Pier 45.

This MCCP effort was performed under the general direction of Dr. James R. Houston, Director, CERC, and Mr. Charles C. Calhoun, Jr., Assistant Director, CERC, and under the direct supervision of Mr. Thomas W. Richardson, Chief, Engineering Development Division, CERC, and Mr. William L. Preslan, Chief, Prototype Measurement and Analysis Branch (PMAB), CERC. The Principal Investigator was originally Mr. Hemsley, succeeded by Mr. David D. McGehee, (PMAB), and then Mr. Jonathan W. Lott, (PMAB). SPN partners in this effort were (in time order) Mr. Dennis Thuet, Mr. Kerry Guy, Ms. Emy Tatami, and Mr. Jay Hawkins. Field measurements conducted during the MCCP study involved personnel from CERC's PMAB, SPN, the National Park Service, and the Ocean Engineering Research Group, Scripps Institution of Oceanography (SIO). The prototype wave data

analysis and model comparisons were based on a report prepared for CERC by Mr. David Castel of SIO with assistance from other personnel of the Ocean Engineering Research Group of the Marine Research Division. A physical model investigation during this MCCP study was conducted by Messrs. Hugh F. Acuff and William G. Henderson, Wave Processes Branch (WPB), CERC, under the supervision of Mr. Robert R. Bottin, Jr., WPB, who also prepared the written documentation of the model effort. This report was prepared by Mr. Lott.

Dr. Robert W. Whalin is Director of WES. COL Bruce K. Howard, EN, is Commander of WES.

Conversion Factors, Non-SI to SI Units of Measurement

Non-SI units of measurement used in this report can be converted to SI units as follows:

Multiply	By	To Obtain
cubic yards	0.7645549	cubic meters
degrees (angle)	0.01745329	radians
feet	0.3048	meters
inches	2.540	centimeters
knots	0.5148	meters per second
miles	1.609347	kilometers
pounds (mass)	0.4535924	kilograms
pounds (force) per square foot	47.88026	pascals

1 Introduction

Project Location and Description

The area of San Francisco traditionally known as Fisherman's Wharf is located along the north-facing waterfront of the city opposite Alcatraz Island (see Figures 1 and 2). The Fisherman's Wharf study area is bordered to the west by the Golden Gate National Recreation Area (GGNRA). To the east is a succession of piers and waterfront structures. Located only about 3 statute miles[1] east of the narrowest part of the Golden Gate (the connecting entrance between the Pacific Ocean and San Francisco Bay), the site is subject to both ocean and bay influences.

Three discrete structures together constitute the Corps' project called "the Fisherman's Wharf breakwater" in this report (see Figure 3). Appendix A presents construction plans showing details of the structures. All of the structures are constructed of reinforced concrete. A brief description of the as built Fisherman's Wharf breakwater is given below; the later sections on breakwater design include additional details. The breakwater lies within the jurisdiction of the San Francisco District (SPN) of the U.S. Army Corps of Engineers (USACE).

An impermeable, vertical-wall, detached breakwater structure forms the main element of the breakwater system (Figure 4). This 1,509-ft-long detached breakwater was built using driven prestressed-precast interlocking sheet piles. A curvilinear alignment was used, made up of individually straight wall sections. It is buttressed by inclined batter piles on both sides for the easternmost 1,083 ft, and on the harbor side only for the curving westerly section. A cast-in-place reinforced cap beam ties the piles together into eight continuous wall sections, separated by expansion joints. The 10-ft-wide overhanging cap has a symmetrical "beveled" shape. The west end of the wall abuts a decorative feature--a ring of individual vertical and batter piles topped by a circular cap platform which is level with the main wall's cap. This platform was also included for its potential future use, along with the cap beam, as a pedestrian walkway and recreational fishing area. For most of its length the

[1] A table of factors for converting non-SI units of measurement to SI units is presented on page x.

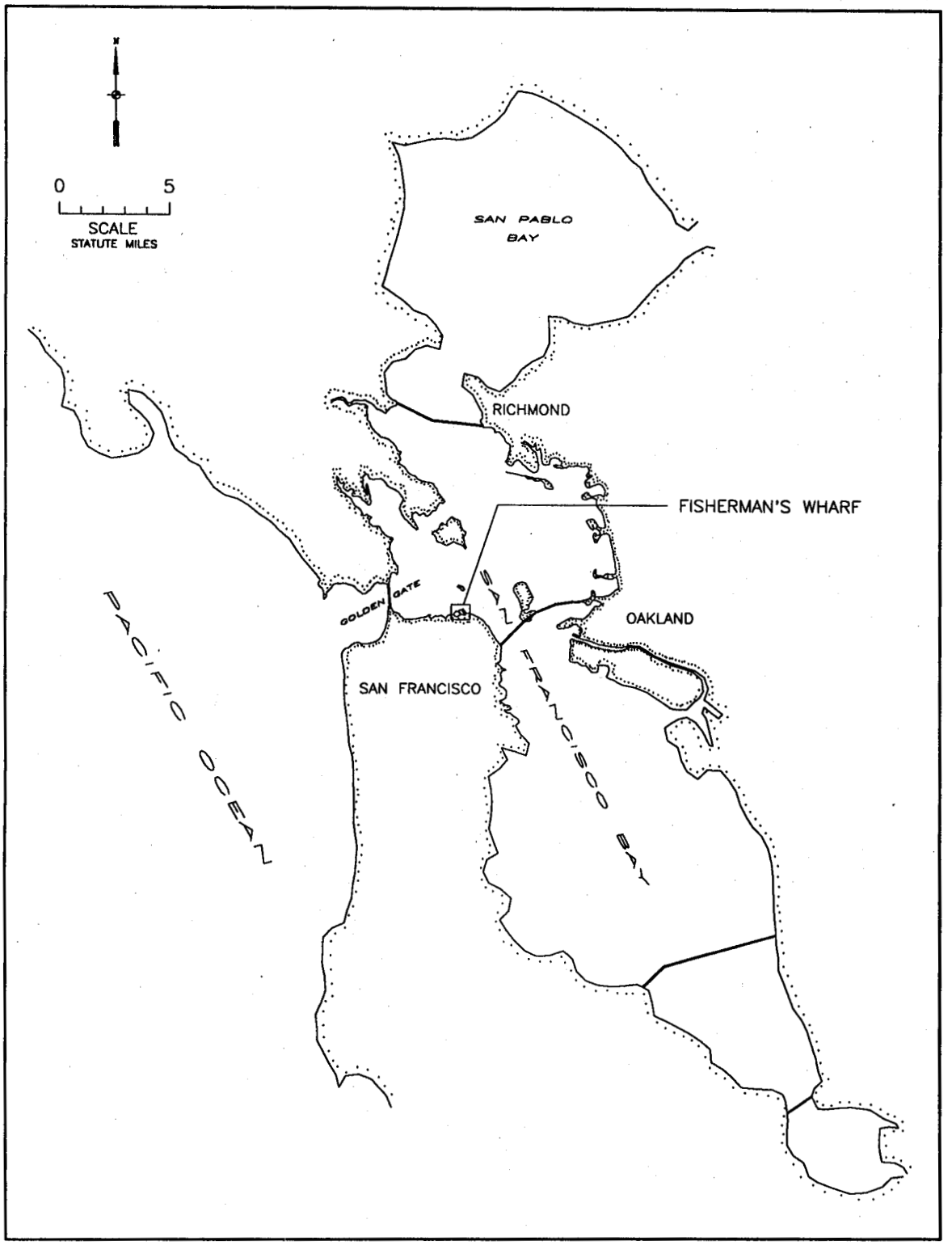

Figure 1. Project location map

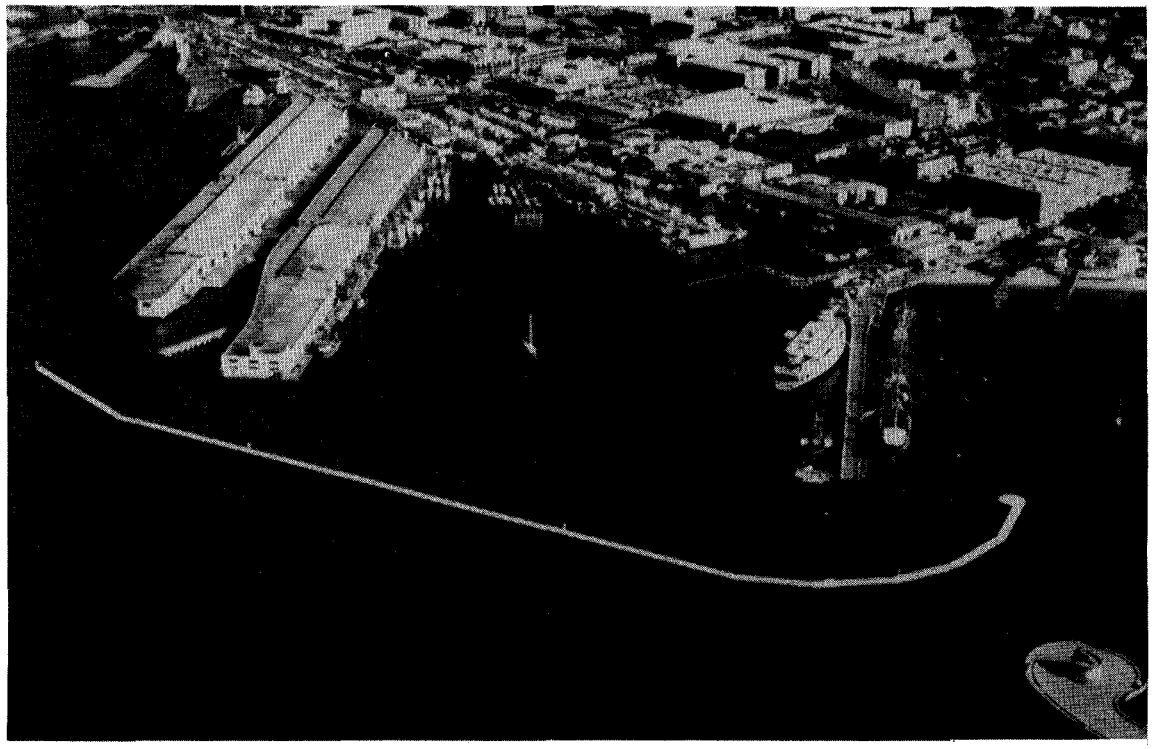

Figure 2. Oblique view of Fisherman's Wharf area (looking southeast)

detached structure is oriented approximately in the shore-parallel west-southwest to east-northeast direction. This alignment intercepts waves from the northwest, yet is essentially parallel to the prevailing tidal currents.

The two other components of the breakwater system are also interlocking sheet pile vertical-wall structures, but they are segmented by openings at evenly spaced intervals, to allow a controlled amount of tidal circulation and wave transmission. Construction is similar to the detached breakwater, except for the gaps which extend all the way from the cap beam to the seabed. Although both segmented breakwaters are attached at deck level to Pier 45 (which is pile-supported at the seaward end), they are designed to be self-supporting. No expansion joints are used. The two segmented structures are oriented to work in conjunction with Pier 45 to reduce incident waves from easterly and northeasterly fetches. Since their orientation puts them nearly perpendicular to the prevailing tidal currents, openings were needed in the attached breakwaters to reduce their interference with circulation through Fisherman's Wharf harbor. The portion of Pier 45 landward from the segmented breakwaters is bulkheaded underneath, forming a total barrier to circulation.

The west segmented breakwater (Figure 5) is adjacent to and aligned with the western edge of Pier 45. It has seven openings (width about 6 ft each) in the otherwise solid, 258-ft-long sheet-pile wall. Batter piles are used only on the interior (east) side, toward Pier 45. The exterior (west) side is faced with

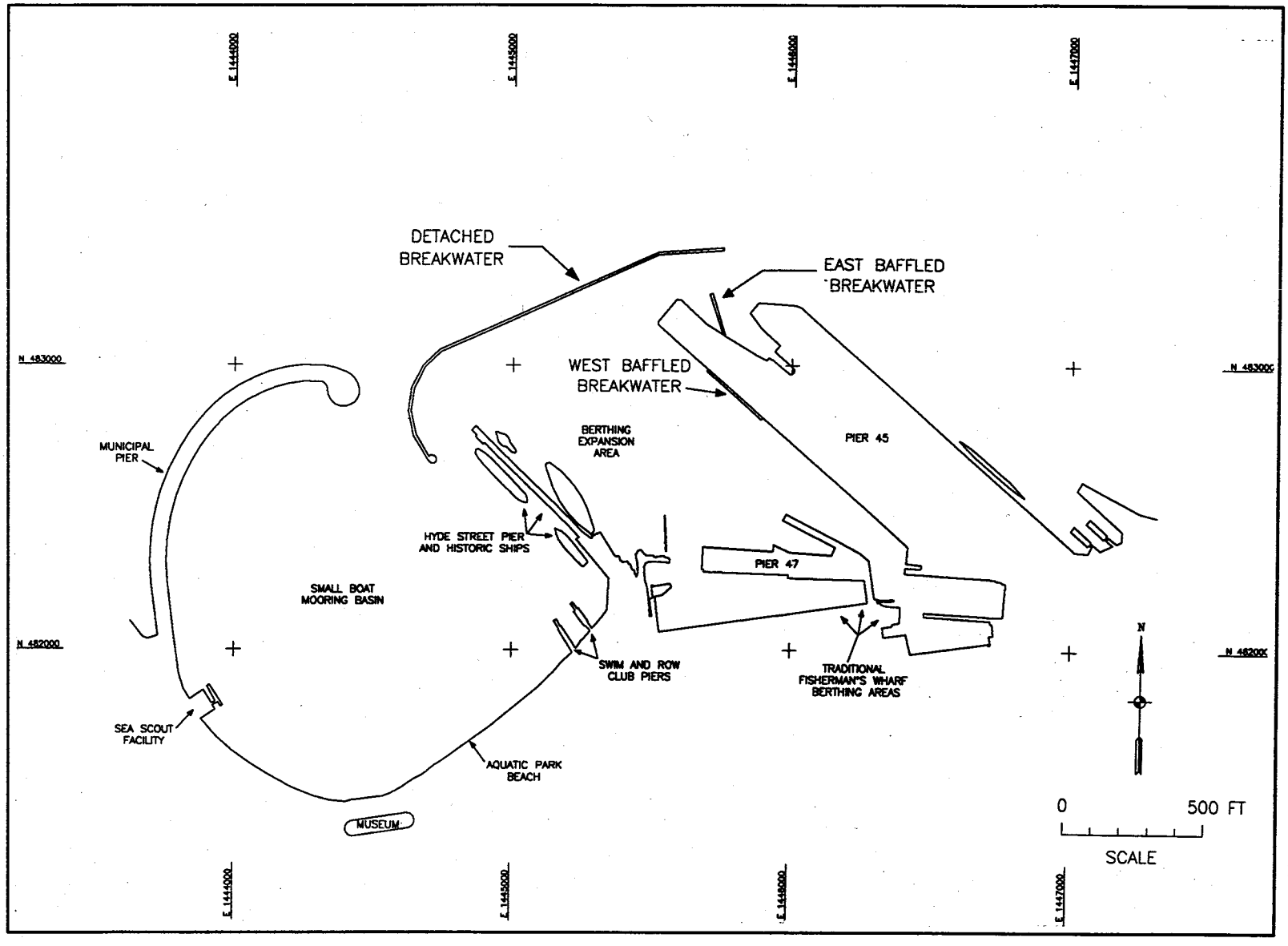

Figure 3. Site plan of Fisherman's Wharf breakwater and vicinity

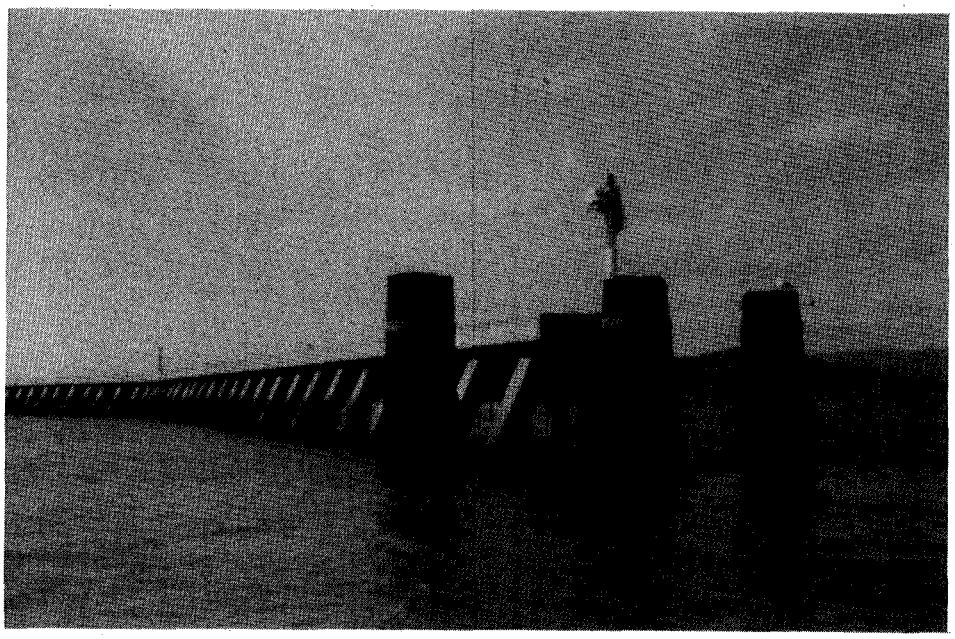

a. East end looking west--timber fender pile clusters in foreground

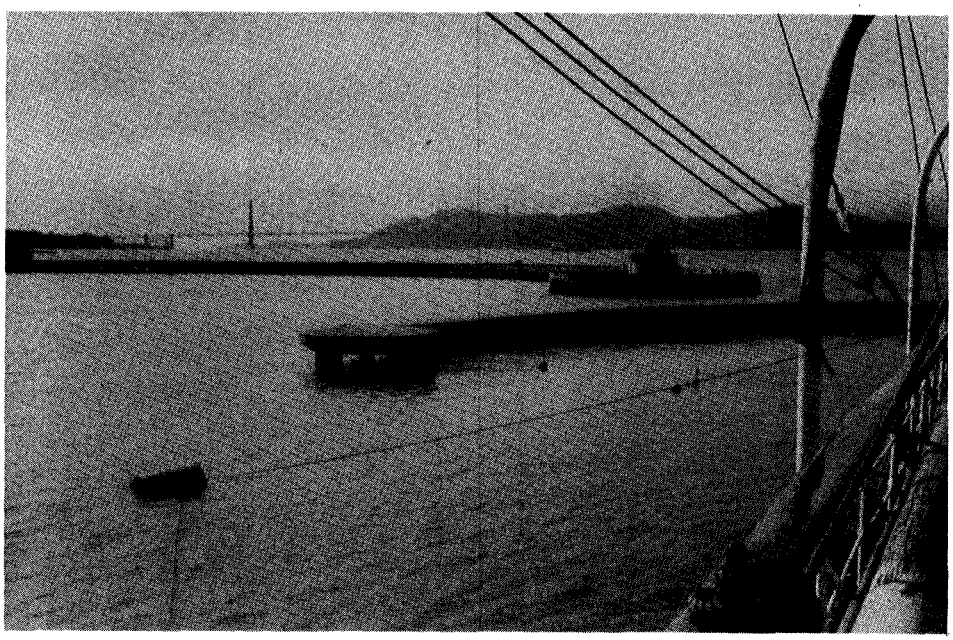

b. West end looking northwest--Municipal pier and Golden Gate Bridge in background

Figure 4. Detached breakwater

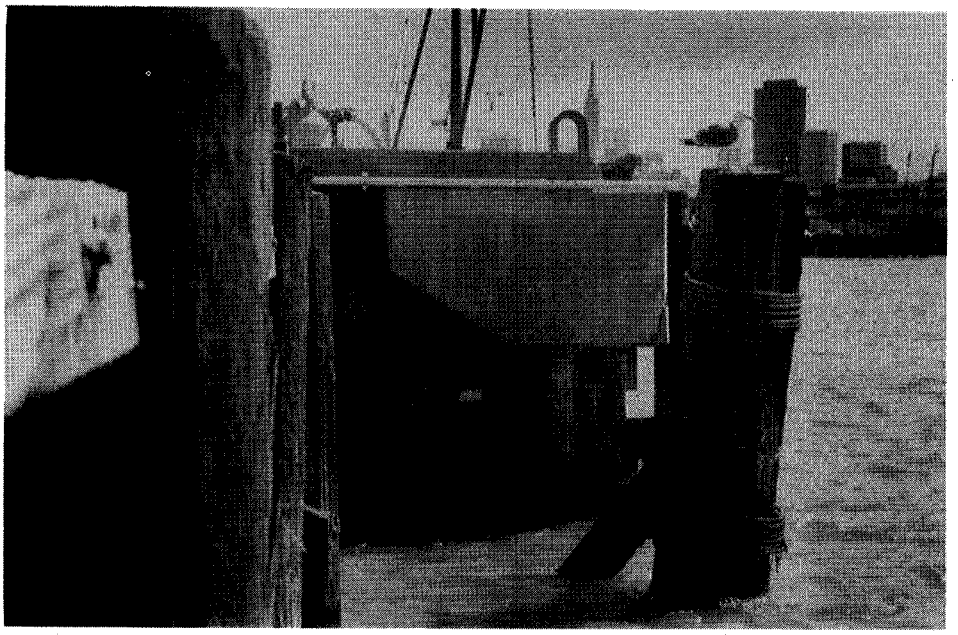

a. Bayward end looking southeast

b. Looking east, across berthing expansion area (from Hyde Street pier)

Figure 5. West segmented breakwater

a timber fender system; cleats along the cap are often used to tie up fishing vessels unloading their catch. The continuous cap beam is asymmetrical in section (beveled on the outside only) with a top width of 7 ft.

The east segmented breakwater (Figure 6) projects out into the notch on the opposite side of Pier 45 at about a 33-deg angle from the pier's long axis. It has four openings spaced along its 150-ft length, and is supported by batter piles on both sides (except for a short section adjacent to its junction with Pier 45, where batter piles are on the exterior side only). It has a continuous 10-ft-wide cap beam similar to that on the detached breakwater. The cap is designed for pedestrian use, including a handrail around the perimeter and handicapped access bridge, both of which are made of aluminum. The exposed north end of the structure is protected with three clusters of timber fender piles, as is the east end of the detached breakwater. The designated navigational entrance to the Fisherman's Wharf berthing areas is located between these two sets of fender pile clusters. The entrance provides a total channel width of 165 ft.

The study area for the Monitoring Completed Coastal Projects (MCCP) project also encompasses several zones influenced by the Fisherman's Wharf breakwater.

Municipal pier extends out from the shoreline westward of the Fisherman's Wharf breakwater in a semicircular arc, curving to the east. The pier was built around 1930. Constructed entirely of concrete, it has a wave baffle system of inclined panels integrated with the supporting piles and underside of the deck (Figure 7). The wave baffle system is relatively permeable and only spans the top part of the water column near mean tide level. The gap between Municipal pier and the detached breakwater is not used by commercial vessels as a second navigational entrance to the Fisherman's Wharf berthing areas, although there is no structural barrier to prevent vessel passage.

The small boat mooring basin and sandy beach, (Figure 8) enclosed by Municipal pier to the west and Hyde Street pier to the east, are part of Aquatic Park. The promenade, beach, and basin are open to the public for recreational uses. A Sea Scout facility is located on the western edge of the basin. Clubhouse and pier facilities for South End Rowing Club and the Dolphin Swimming and Boating Club are located at the eastern end of the beach, adjacent to the foot of Hyde Street pier. Members of the clubs have a very long tradition of using the basin for rowing and long-distance swimming. A few small boats cross through the gap between the detached breakwater and the end of Municipal pier to moor in the basin. Hyde Street pier is home to several historic ships and maritime museum facilities (Figure 9). Aquatic Park, Hyde Street pier, and the historic ships are managed by the GGNRA of the U.S. Department of the Interior's National Park Service.

The zone surrounded on four sides by the detached breakwater, Pier 45, the traditional Fisherman's Wharf berthing area, and Hyde Street pier is referred to as the basin and berthing expansion area in this report. The Port of

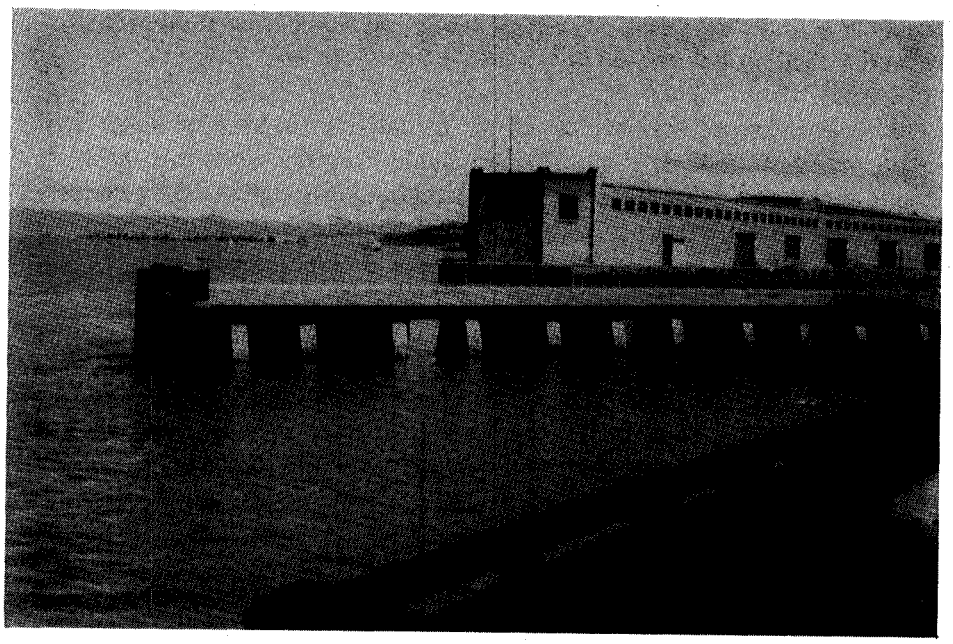

a. Looking east

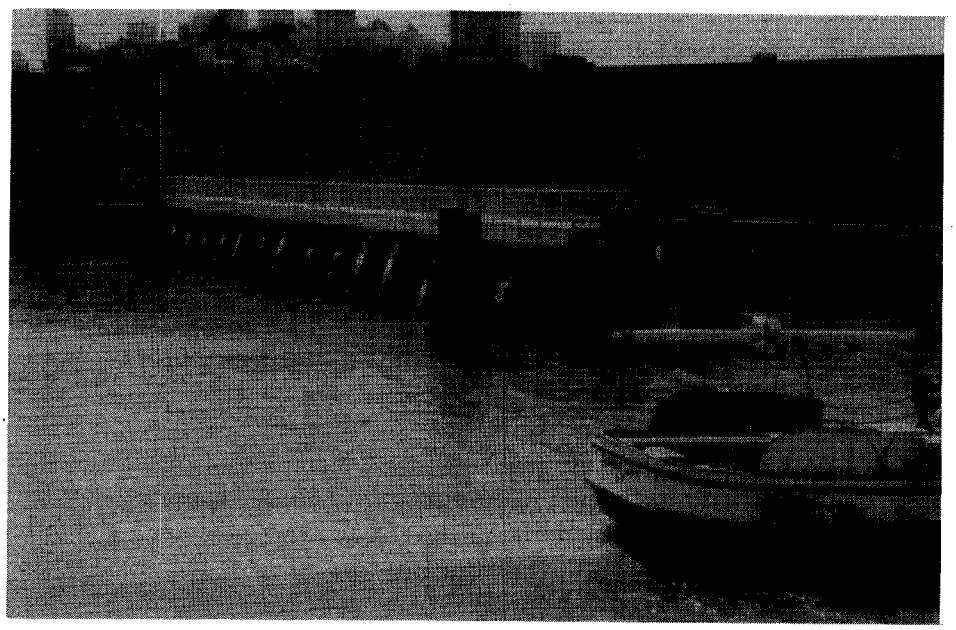

b. Looking south--Pier 45 in background

Figure 6. East segmented breakwater

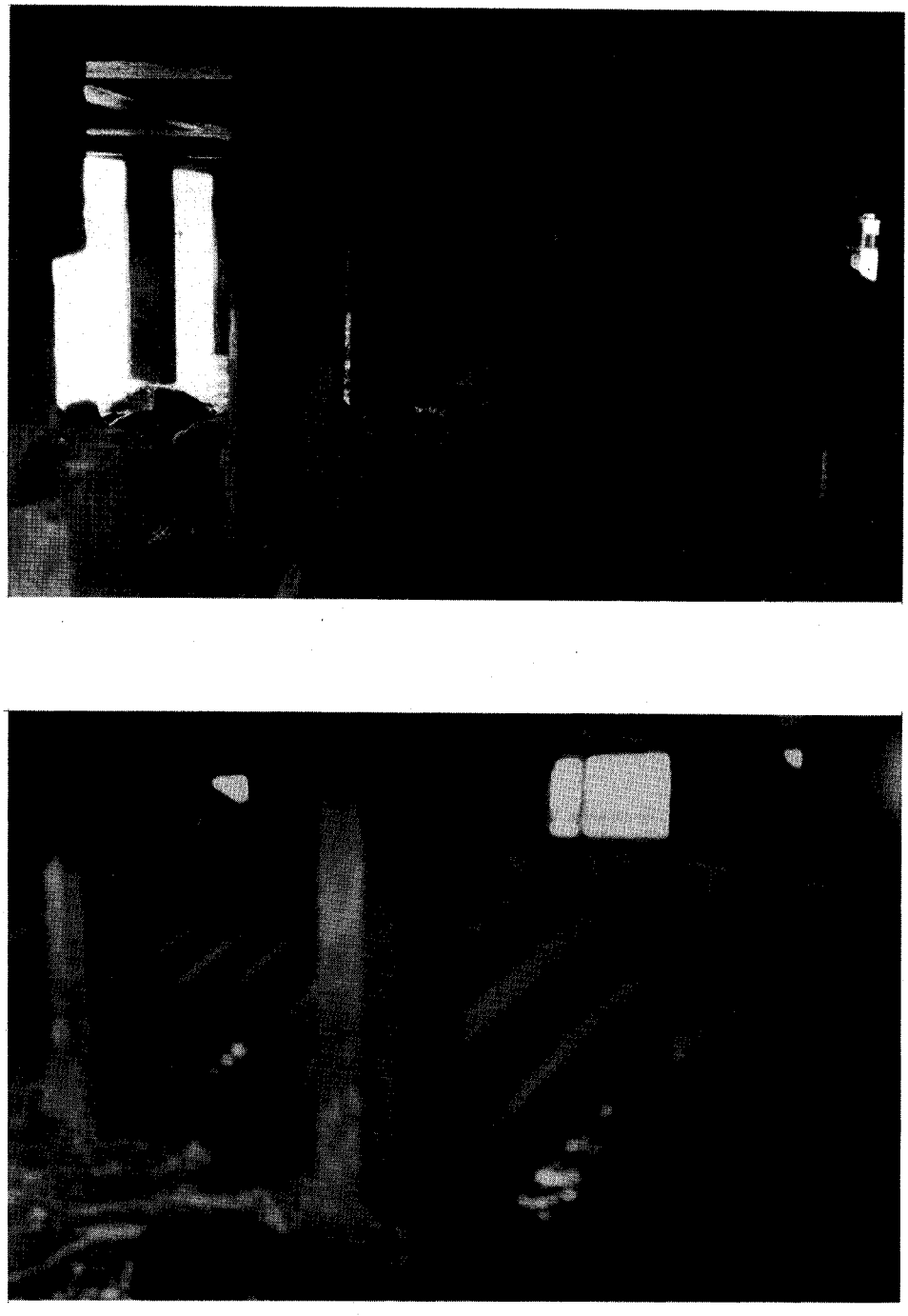

Figure 7. Wave baffle under Municipal pier

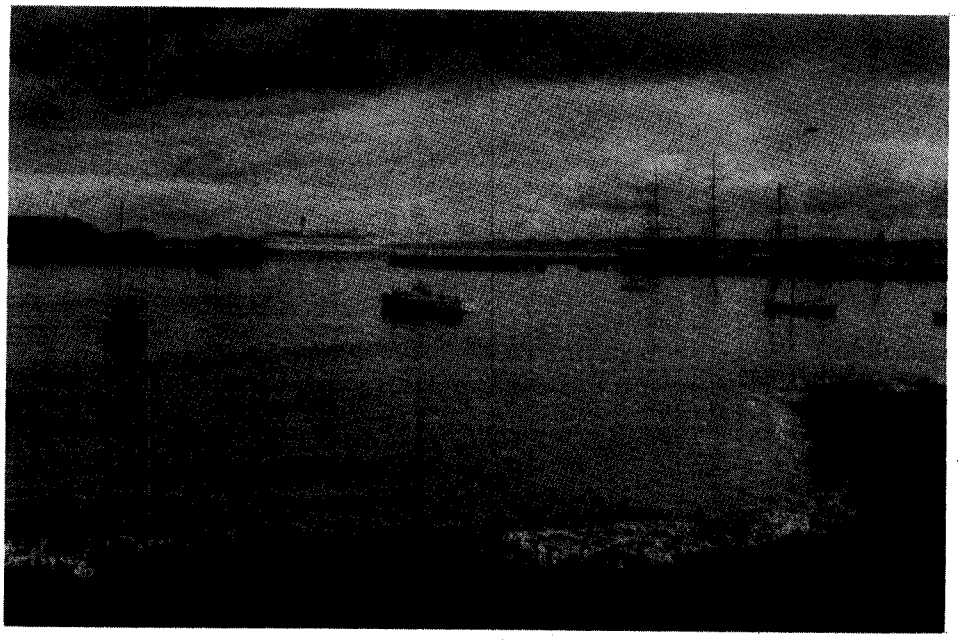

a. Small boat mooring area looking northeast

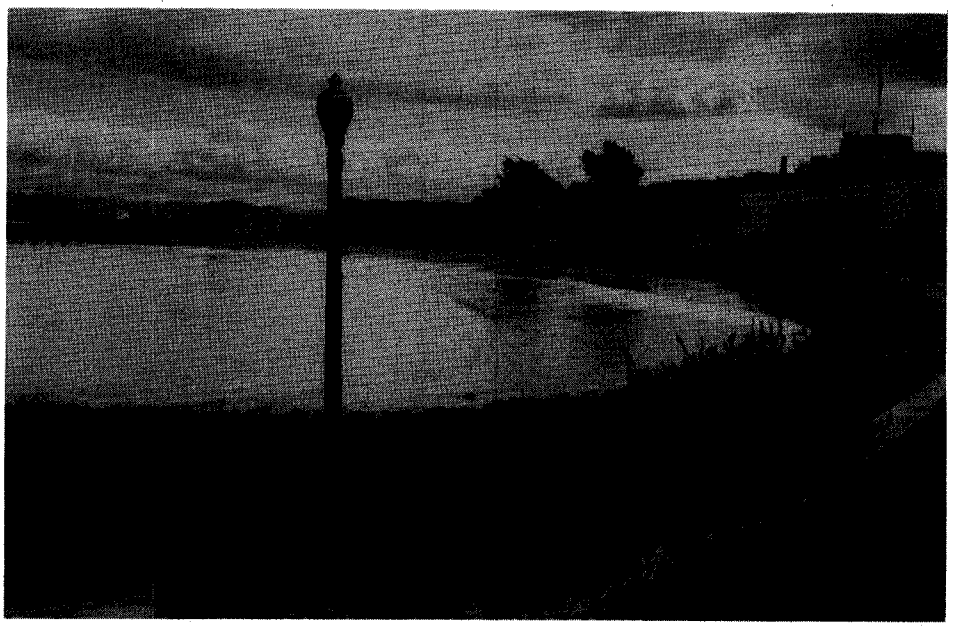

b. Swimming area and beach looking east

Figure 8. Aquatic Park mooring area and beach

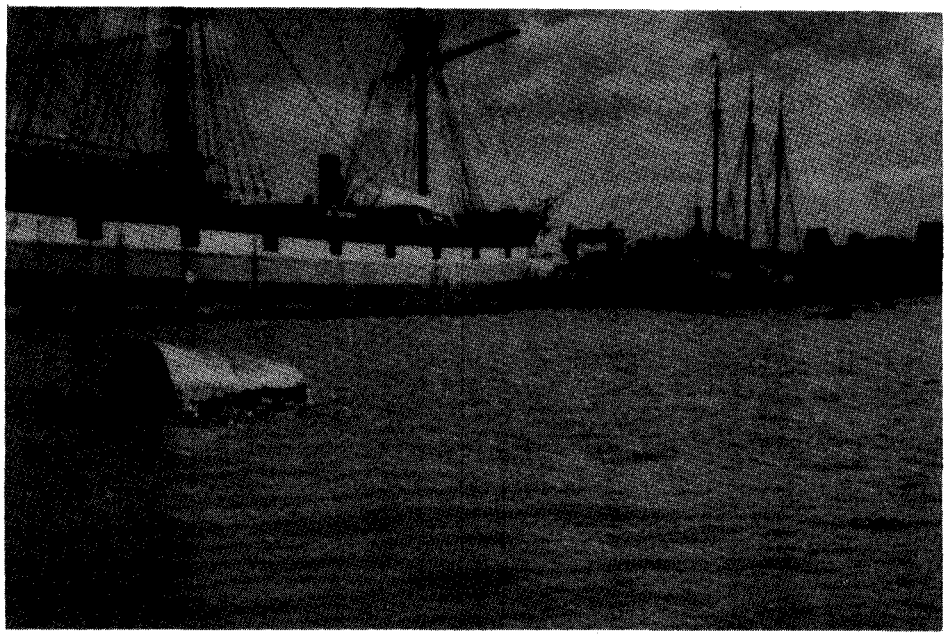

Figure 9. Hyde Street pier and Historic Fleet (looking southeast--*Balclutha* at left)

San Francisco is undertaking a series of improvements in the Fisherman's Wharf area. The proposed Fisherman's Wharf Seafood Center envisions modernization and expansion of shoreside facilities and a new berthing area. The latter involves reconstruction at the foot of Hyde Street pier and new docks along the west side of the basin, taking advantage of the protection offered by the Corps breakwater. Renovations to Pier 45 are also included in the plan. The current basin and the berthing expansion area are shown in Figure 10.

The traditional Fisherman's Wharf berthing area occupies the entirely man-made shoreline of piers, wharves, and bulkheads between Hyde Street pier and Pier 45. Figure 11 shows a typical view from Alioto's restaurant, the easternmost point in the traditional berthing area. The shoreline is made of highly reflective vertical walls, except for a sloped, revetted fill underneath Pier 47, and a rubble groin structure at the foot of Hyde Street pier.

Project History

Fisherman's Wharf has historically been Northern California's center for commercial fishing by light-draft vessels. However, prior to the completion of the breakwater, it was the most exposed small craft harbor in the San Francisco Bay area. Although attenuated ocean-generated waves penetrate to the site under certain conditions, the most troublesome wave agitation in the harbor resulted from short-period waves generated along northerly fetches within the bay. Damage to berthed boats and difficulties in unloading catches during these "norther" events caused many boats to relocate to more protected sites. Loss of fishing activity at Fisherman's Wharf had negative implications for the related landside activities, notably seafood processing and the tourism industry. Other important considerations were the need to provide safe

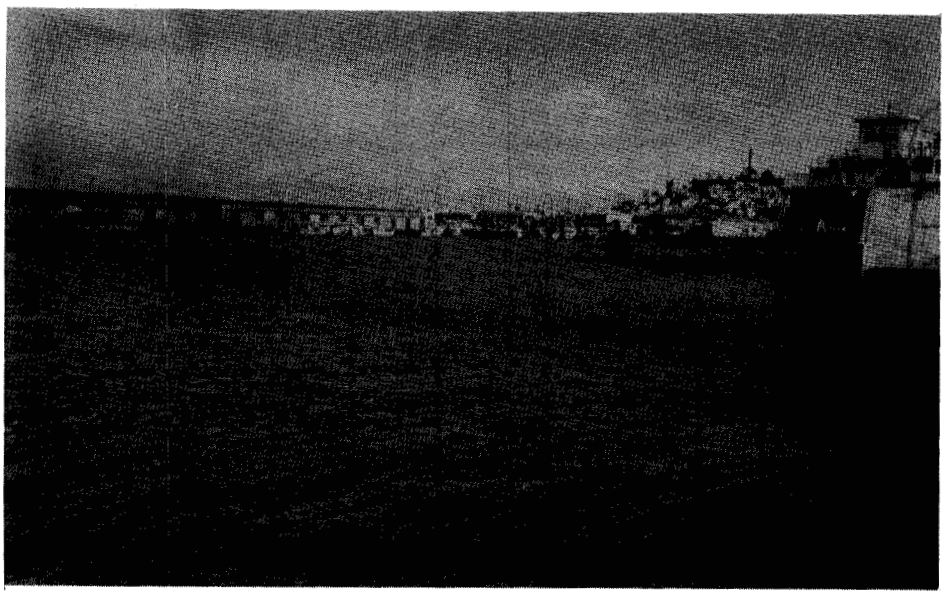

Figure 10. Basin and berthing expansion area (looking southeast from Hyde Street pier)

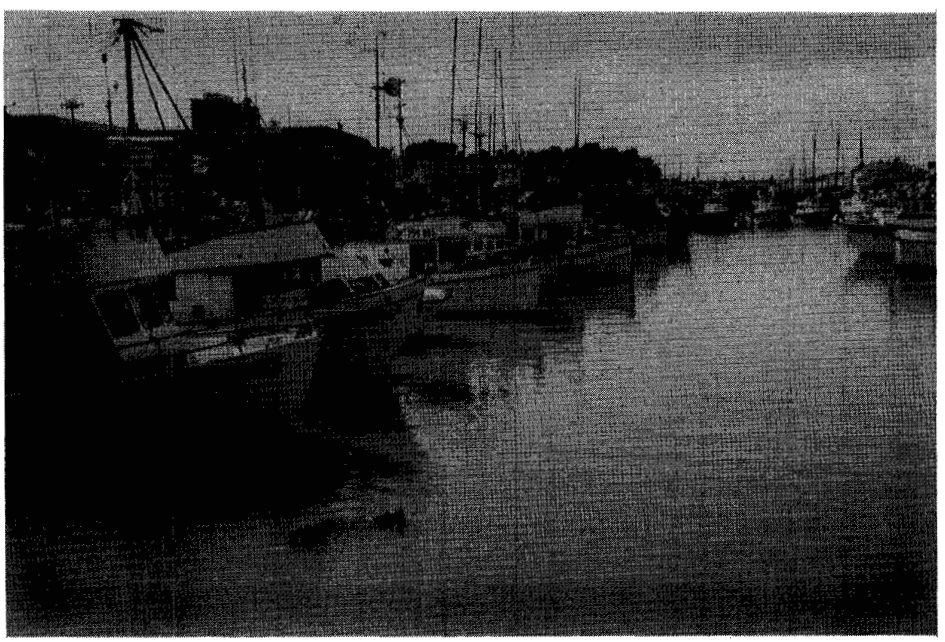

Figure 11. Traditional berthing area (looking west)

berthing conditions for the fleet of Federally owned historic ships located along Hyde Street pier, and the planned expansion of small craft berthing and redevelopment of landside facilities to be undertaken by local interests.

The need for improvements to light-draft harbor facilities in the Fisherman's Wharf area was recognized by the early 1960's. A Congressional Resolution in 1966 called for a review to determine whether modifications and improvements to existing facilities were advisable. By 1969 the City of San Francisco had adopted a Northern Waterfront Plan, which emphasized land uses centered around commercial fishing. Several economic and engineering feasibility studies and a Draft Environmental Impact Statement were completed by 1976; a Final Environmental Impact Statement was completed in 1981.

In FY 1982, the U.S. Army Engineer District, San Francisco (SPN), began the process of compiling the General Design Memorandum (GDM) (U.S. Army Engineer District (USAED), San Francisco 1985). This document presents the Corps of Engineers' recommended plan for the Fisherman's Wharf breakwater. On November 14, 1983, the project was authorized for construction under Section 135 of Public Law No. 98-151. The authorized plan reads as follows (USAED San Francisco 1985):

> ...a 700-foot baffled wall with a 10-foot walkway connected to and extending alongside the Hyde Street pier. A 1,200-foot sheet pile wall, with a 10-foot walkway, would extend from the baffled wall towards Pier 45. A 370-foot baffled wall, without walkway, would be attached to the west side of the central opening of Pier 45. Local interests would provide berthing spaces inside the protected area for about 350 additional fishing craft. The walkway would be used for pier fishing and sightseeing. The five historic ships located at the Hyde Street pier would be relocated inside the protected harbor...

(USAED San Francisco 1985). The authorizing document also called for investigation into using a more aesthetically acceptable curvilinear breakwater alignment, in keeping with the curved shape of Municipal pier.

Several studies, as discussed below, were conducted during development of the recommended plan presented in the GDM. SPN incorporated their main findings into the GDM.

The Los Angeles District (SPL) of the USACE acted as SPN's prime engineering design consultant. SPL conducted and coordinated studies of shoreline processes, and coastal engineering and structural design (including estimated costs) of the proposed breakwater, and a geotechnical investigation. The results are documented in Appendixes A and B, respectively, of the GDM. SPL also managed a prototype data collection effort by Scripps Institution of Oceanography (SIO) which obtained information on the wave climate for use in verifying numerical and physical models and in checking design wave predictions. Wave gages and a meteorological station were installed at the site starting in December 1982.

The Coastal Engineering Research Center (CERC) of the U.S. Army Engineer Waterways Experiment Station (WES) performed a physical model study of short-period waves and numerical model studies of long-period waves and historic ship motions for SPL. Technical Report CERC-85-7, "Fisherman's Wharf Area, San Francisco Bay, California, Design for Wave Protection: Physical and Numerical Model Investigations" documents the CERC effort (Bottin, Sargent, and Mize 1985).

The Hydrologic Engineering Center (HEC) of USACE performed prototype data collection and numerical model studies relating to hydrodynamics and water quality for SPN. A comprehensive review of existing reports resulted in Special Projects Memo No. 83-9, "Second Interim Report for the Fisherman's Wharf Harbor Study: Data Summary" (USACE HEC 1983). HEC's hydrodynamic and water quality simulations are documented in Special Projects Report No. 84-10, "Numerical Simulation of the Circulation and Water Quality Within Fisherman's Wharf Harbor" (USACE HEC 1984b). HEC also contracted a study of seabed scour potential, Special Projects Report No. 84-8, "Evaluation of Scour Potential Around the Proposed Fisherman's Wharf Harbor Breakwater" (USACE HEC 1984a) in support of SPL's Appendix A to the GDM.

The GDM presents a recommended plan for the Fisherman's Wharf breakwater that differs somewhat from the authorized plan. Two phases of construction were envisioned. The curvilinear as-built breakwater described above and shown in the figures and photos of this report is very similar to the recommended plan's Phase I construction. The recommended plan avoided the need to relocate the historic ships, since the 700-ft-long baffled wall along Hyde Street pier had been eliminated. Phase II construction included items to facilitate pedestrian access to the detached breakwater (handrails, access bridge from the end of Hyde Street pier, and sanitary facilities). Estimated total project first cost (including construction, contingencies, engineering and design, and supervision and administration) was $12,100,000 for Phase I, and $500,000 for Phase II (October 1984 prices). Annual costs were estimated assuming a 50-year period of economic evaluation corresponding to the assumed 50-year project lifetime. Although the structures were designed to withstand a certain amount of scouring at the mudline, maintenance cost estimates included a one-time cost of $100,000 for the placement of rock to prevent additional scour. This cost was assumed to occur within the first 10 years of the project life. The uniform annual Operation and Maintenance costs were estimated at $10,000 per year for 50 years. Annual benefit-to-cost ratio was computed at the time of the GDM to be 1.9 to 1.0 for the total project (both Phases I and II). Phase I construction (driving of detached breakwater piles) started November 6, 1985, and was essentially completed by the end of August 1986. The construction contractor had completed all construction and demobilized by November 1, 1986, one month ahead of schedule. The final construction contract cost was $7,820,000, below the Government estimate. Phase II construction was deferred pending improvements to Hyde Street pier. At the time of this report, the Phase II construction continues to be deferred. The project received an Award of Merit in the USACE 20th Design Awards Program in 1989.

During the development of the GDM, the South Pacific Division (SPD) of USACE suggested that SPN nominate the Fisherman's Wharf breakwater for the MCCP program. At SPN's request, a monitoring proposal was prepared by HEC in June 1984. In addition to items that fall within the realm of coastal engineering, the proposal included monitoring of water quality and evaluation of water quality modeling efforts. Participation by CERC was envisioned for the coastal engineering aspects. SPN submitted the proposal to Headquarters, USACE (HQUSACE) for evaluation in July 1984. The HQUSACE ruled that, in accordance with established policy, the MCCP program would not address the water quality issues at Fisherman's Wharf. Since the proposal called for participation by CERC, and because of mission considerations, it was eventually determined that responsibility for a Fisherman's Wharf MCCP study--without water quality monitoring--should be borne by CERC and SPN. Fisherman's Wharf breakwater was accepted into the MCCP program in FY 1986, and CERC and SPN began developing the MCCP monitoring plan. Initial prototype monitoring under MCCP funding began in 1987.

2 Project Design

Site Characterization: Baseline Conditions

Tides, water levels, and waves

Tides and water levels. Tides at Fisherman's Wharf harbor are of the mixed type, normally having two high and two low waters per day. The magnitudes of the two highs or two lows (or both) are unequal most of the time. However, at Fisherman's Wharf the diurnal inequality (difference in height of the two high waters or of the two low waters of each day) is not large, so the extreme tide range is expressed as the diurnal range, that between mean lower low water (mllw) and mean higher high water (mhhw). The mean tidal range is that between mean low water (mlw) and mean high water (mhw), where all of the high waters and all of the low waters are included in the averaging. The mean tide level is the elevation halfway between mlw and mhw. The datum used as a vertical reference for reported depths (chart depths) and tide stages is mllw (= 0.0-ft elevation). Depths are given as positive when the seabed is below mllw. Tide stages and water levels are given as positive elevations when they are above mllw. The GDM presents values for the vicinity of Fisherman's Wharf based on the National Oceanic and Atmospheric Administration (NOAA) primary reference station at the Golden Gate (Presidio):

Diurnal tide range	5.8 ft
Mean tide range	4.1 ft
Mean tide level	+3.1 ft

The GDM also presents the following extreme tidal elevations, observed at the Golden Gate NOAA station:

Highest observed tide	+8.4 ft
Lowest observed tide	-2.7 ft

The NOAA Tide Tables (U.S. Department of Commerce 1988) indicate that times of high and low waters at the Fisherman's Wharf site occur approximately 15 min later than at the Golden Gate station. There is essentially no difference in tide stage between the two locations. The GDM reports several different values for still-water level (swl) used in the design process. For a

preliminary check on cap elevation, SPN used +5.9 ft mllw, which is described as the mhhw elevation at the Presidio. For the physical model study, SPL selected swl's of +5.7 ft and 0.0 ft mllw to represent mhhw and MC mllw conditions, respectively. In a second check on overtopping potential, SPL used an swl of +6.0 ft mllw, described as a maximum tide level. For calculations of structural loading due to waves, SPL used swl's of +5.9 ft and 0.0 ft mllw to represent mhhw and mllw conditions, respectively. SPL's seismic loading calculations considered an swl of +3.2 ft mllw.

Prototype wave measurements and wave height projection. As stated in the GDM, the breakwater site is primarily affected by short-period wind-generated waves from the north. High-frequency wind waves arriving from easterly and westerly directions are less important because Treasure Island and Yerba Buena Island interfere with winds from the east and the Presidio Hills interfere with westerly winds. SPN and SPL determined that while long-period ocean swell waves do enter the bay through the Golden Gate, they are attenuated by diffraction around Point Bonita on the Marin headlands to the north and by refraction crossing the San Francisco Bar at the bay entrance. It was clear that waves generated locally (within the bay) were the primary cause of vessel damages at Fisherman's Wharf. The GDM also notes that while large seagoing vessels pass by the Fisherman's Wharf area as close as 900 ft away at net speeds of 5 knots, the resulting wakes were assumed to be of negligible importance compared to the locally generated waves.

The Ocean Engineering Research Group of SIO conducted prototype non-directional wave measurements in the Fisherman's Wharf area of San Francisco starting in December 1982. These pre-breakwater (pre-BW) prototype measurements were contracted to SIO by the Coastal Engineering Section of SPL, in cooperation with the California Department of Boating and Waterways through the Coastal Data Information Program. Five sensors were installed at four locations as shown in Figure 12. SIO used pressure sensors affixed to pilings or in bottom-sitting tripods to indirectly measure the fluctuations in water depth above the sensors. Sensor type in Figure 12 is denoted as either "surge" or "energy," the difference being due to the sampling rate and duration, and processing scheme used. Surge sensors detected long-period wave energy such as harbor oscillations (energy at periods greater than 22 sec); energy sensors detected short-period, wind-wave energy (at periods less than 22 sec).

Prototype wave data were collected to allow an evaluation of wave conditions for the both the structural design of the breakwater and for the physical model tests. An additional motive for surge data collection was experience with excess long-period wave energy and related damages at the recently built Pier 39 berthing facilities, located about 0.6 mile to the east. Data collection ended prior to the construction of the breakwater for all of the sensors shown, except the surge sensor at Alioto's.

In support of the GDM development, SIO performed spectral analyses of the prototype wave data from the period December 1982 through June 1984.

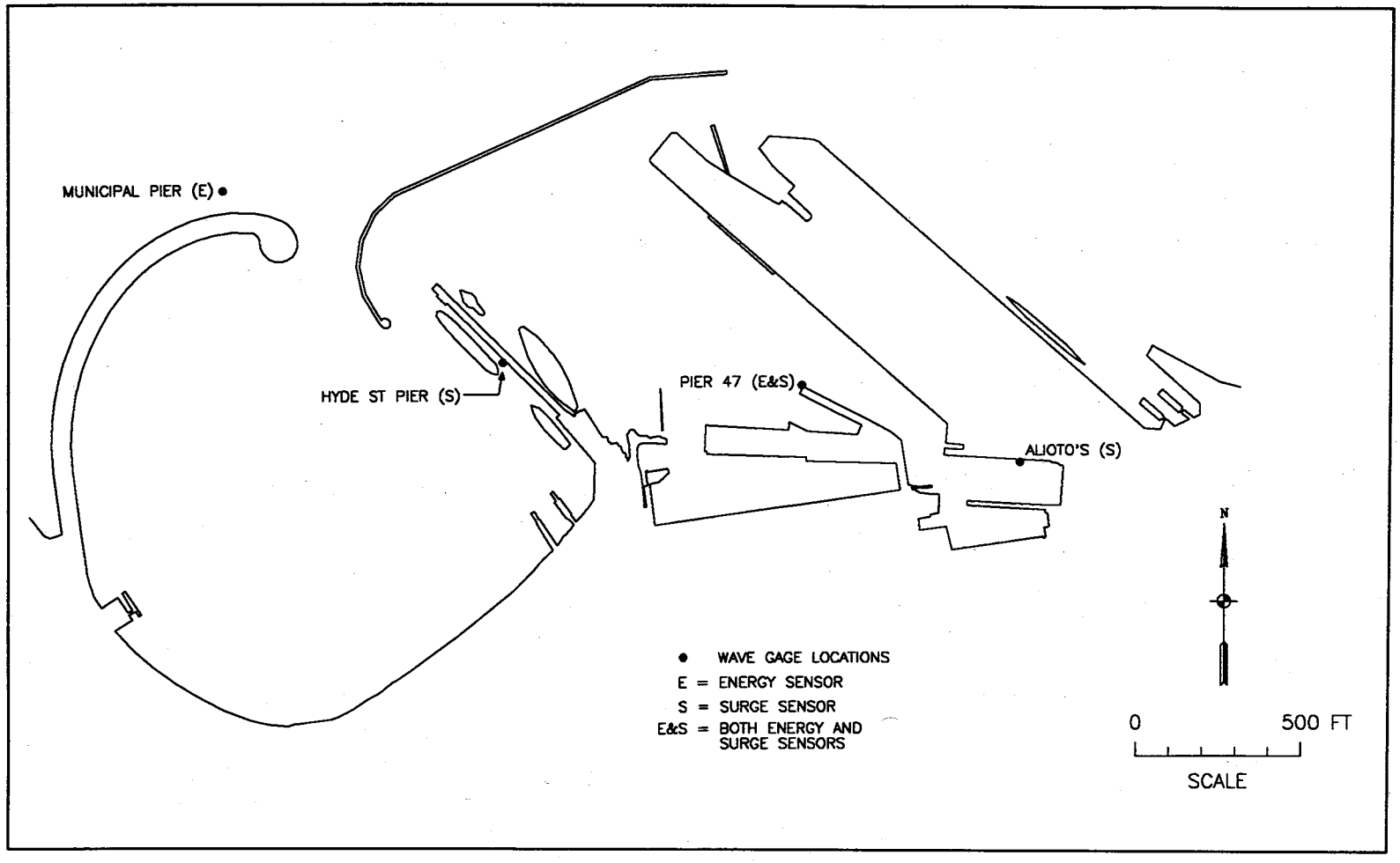

Figure 12. Baseline (pre-breakwater) prototype wave gage locations

Appendix O of the HEC Data Summary report (USACE HEC 1983) contains the complete set of monthly summaries resulting from spectral analyses for all sensors operating in the period December 1982 through September 1983. The GDM contains examples of monthly summary information, and annual summary information for the 12 months of observations from January through December, 1983.

SIO also performed an analysis of extreme wave statistics for the approximately 15-month-long data set obtained by the Municipal pier energy sensor. A joint distribution table was developed for occurrence of significant heights and periods, from which a plot of significant wave height versus return period was created. Figure 13 shows this plot from the GDM, which could be used to estimate an extreme wave projection. As stated in the GDM, SIO noted that the 15-month Municipal pier record would normally allow a projection to about a 4-year return period, although a straight-line fit to the plotted points shows an extrapolation to a 50-year significant wave height of about 1 m (3.3 ft). SIO further noted that this 50-year projection has no statistical or theoretical validity and that the actual significant height could easily be as much as 50 percent greater, considering the small number of observations. The GDM also presents 5-year and 10-year significant wave height projections of 2.6 ft and 2.9 ft, respectively, derived from the information of Figure 13.

Currents

HEC conducted an initial baseline survey of prototype currents throughout the Fisherman's Wharf area on October 25, 1982. The survey gave a reconnaissance overview of circulation characteristics of the site, providing a starting point for the numerical hydrodynamic and water quality modeling and providing insight for planning of further prototype current observations. The survey vessel visited 13 separate stations distributed throughout the Fisherman's Wharf area, taking observations of the horizontal current speed and direction at between 3 and 7 different depths during each station stop. A standard oceanographic side-cast current direction-speed-depth meter with on-deck readout was deployed from an anchored boat at each station. The survey extended over about a 9-hr period, between the two high waters on an average-strength tide. The number of visits at each station ranged from 1 to 4. The GDM presents a tabular summary of the results as simple (i.e., non-vector) depth-averaged speeds and directions by station number and time.

HEC conducted additional prototype hydrodynamic surveys on May 5 and 9, 1983, and July 14, 1983. These surveys used the same measurement technology and approach as the initial baseline survey, but used different sets of stations, selected to characterize the flows across the rectilinear boundaries of the numerical model grid as well as across the outer edge of the existing basin and berthing expansion area. The May 5th survey extended over about a 6-hr period, covering lower low water and most of the flooding tide towards higher high water on an average-strength tide. Four stations were visited, along a north-south line west of Municipal pier. The May 9th survey extended over about a 7-hr period, covering the ebbing tide between lower high and

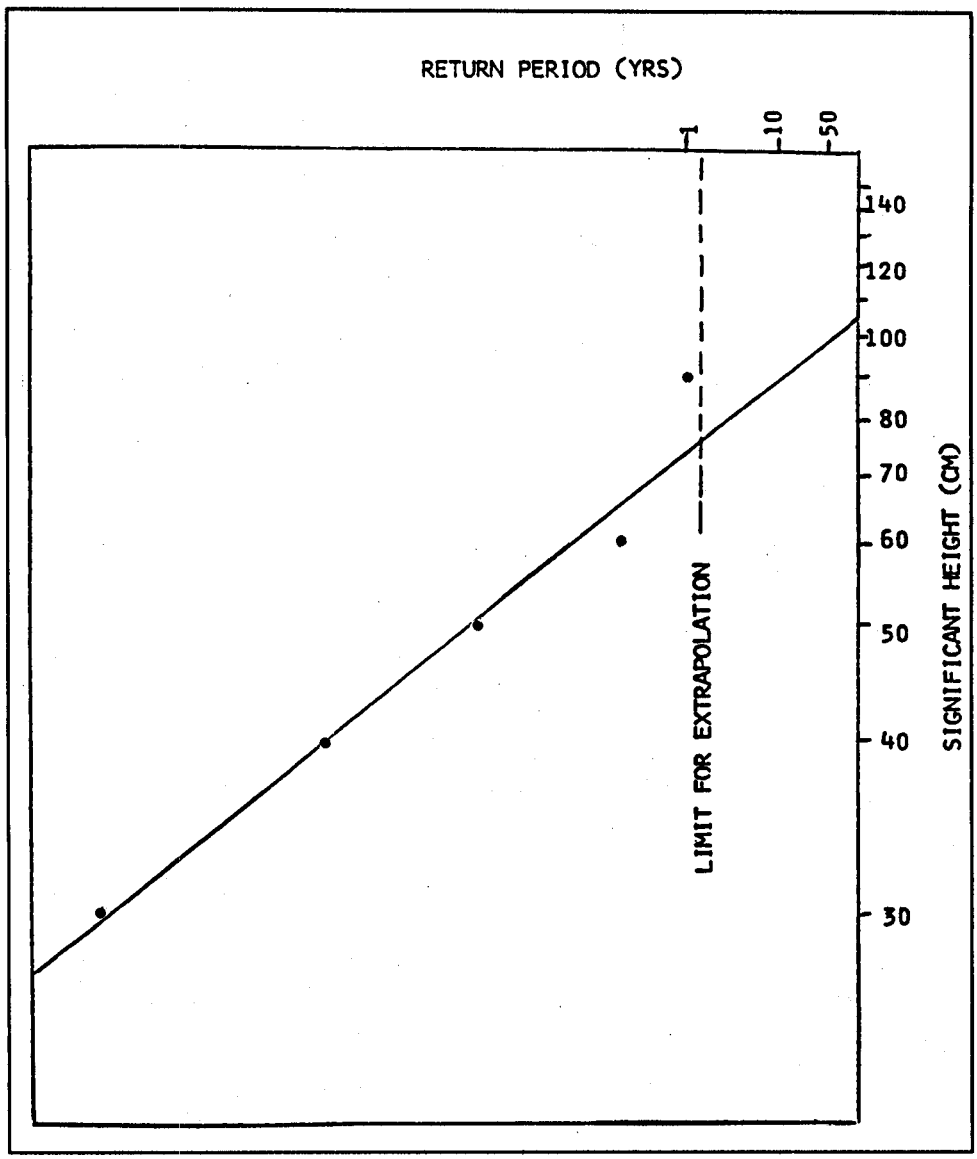

Figure 13. Extreme wave projection from Municipal pier prototype data (from GDM)

lower low water, again on an average-strength tide. The four western stations were visited once at the beginning, then four stations in a north-south line east of Pier 45 were visited for the remainder of the survey. On July 14th the survey extended over about a 7-hr period, covering the flooding tide between lower low and lower high water on a strong tide. Six stations were visited, two of them along an east-west line bayward of the site, and the other four between Pier 45 and Hyde Street pier.

The GDM presents a tabular summary of results from this second set of three surveys as vectorially depth-averaged speeds and directions by station number and time.

A fifth hydrodynamic survey mission was conducted on September 19, 1983. The survey extended over about a 6-hr period, covering the ebbing tide between lower high water and higher low water on an average-strength tide. Five stations were visited in the existing basin and berthing expansion area. Results from this survey were not available at the time HEC's Data Summary report (USACE HEC 1983) was written, but were included in comparisons with model predictions in the final report on the numerical simulations (USACE HEC 1984b).

Concurrent measurements of water quality parameters were obtained during the May 9, July 14, and September 19, 1983 survey missions.

HEC also needed prototype data to evaluate and adjust the hydrodynamic model to account for the hydrodynamic influence of the various piers included within the numerical model boundaries, so a series of in situ continuous current measurements were conducted by SIO (through coordination with SPL) by placing a pair of current meters for a full tidal cycle (approximately 24 hr) on either side of Pier 45 (May 16, 1983), Municipal pier (May 18th), and Hyde Street pier (May 19th). The sensors measured speed and direction of the horizontal component of currents at a single-depth sensor location. Due to problems with the equipment and the data processing, and inconsistency of the direction data, the data set was difficult to interpret for the intended purposes.

In coordination with SPL and HEC, SIO installed in situ recording current meters to measure long-term horizontal currents and depth fluctuations at two sites in the study area. At both sites, SEADATA cassette tape recording meters (with electromagnetic horizontal current sensor and a pressure sensor) were installed on bottom-sitting tripods to measure currents about 4 ft above the seabed. One of the instruments was located just east of Municipal pier, about halfway between the pier end and the shore, from mid-December 1982 to mid-April 1983. The other instrument was located east of Hyde Street pier in the existing basin and berthing expansion area, from mid-December 1982 to mid-May 1983. As a part of the same prototype measurement effort, a weather station was established towards the end of Hyde Street pier from mid-December 1982 to mid-May 1983. The station recorded meteorologic data including wind speed and direction and air temperature. For both the long-term current meters and the weather station, there were gaps in the data sets due to equipment malfunctions and servicing shutdowns. These long-term prototype current and meteorologic data apparently were collected for potential use in checking and evaluating the numerical model results and the prototype wave measurements.

HEC's Data Summary report (USACE HEC 1983) presents more details of the hydrodynamic surveys, including figures showing station locations, complete reduced tabular data, plots of current speed versus depth, and current vector roses (plan view plots of current vectors at each station stop). HEC's Numerical Simulation report (USACE HEC 1984b) also discusses the various prototype measurements of currents and winds. A review of the current roses reveals that it was common to have large differences between simultaneous current vectors (both in direction and magnitude) at different observation

depths at a station. This behavior is common in estuarine environments where density differences due to temperature, salinity, and turbidity gradients or layers can result in flow reversals, vertical current components, and discontinuities. Effects of surface wind stresses and flow around pier structures, moored vessels, and varying seabed topography likely have significant influence at this site as well. It is therefore difficult to develop meaningful depth-averaged current velocities, whether simply or vectorially averaged, for this kind of data. Also, it is very resource-intensive and difficult to obtain prototype data at numerous spatial locations and depths in a simultaneous fashion for direct comparison with the synoptic type of results obtainable from a numerical model.

It should be noted that the prototype current measurement surveys were primarily intended to provide information to guide the establishment of the tidal boundary conditions for the numerical models and for use in their calibration and verification. As such, the model results, not the prototype data, were the primary tool for developing the breakwater design and evaluating its circulation impact.

Bathymetry and bottom sediments

Baseline bathymetry. The GDM states that water depths vary from about 20 to 55 ft below mllw along the proposed alignments of the three breakwater elements. Bathymetry used in the design process was based on an original hydrographic survey conducted by SPN in November 1974, portions of which were updated in June 1980 by the Port of San Francisco. In July and August 1984, Woodward-Clyde Consultants performed a geophysical and geotechnical exploration for SPL (Woodward-Clyde Consultants 1984), including a detailed fathometer survey in the immediate vicinity of the proposed breakwater alignments, a side-scan sonar survey, subbottom profiling, and two subsurface rotary wash borings. The primary purpose of the side-scan sonar survey was to check the site for underwater features and objects that might interfere with the proposed construction, or might be of archaeological value (such as shipwrecks). A sunken steel barge was found at a location corresponding to the bayward end of the proposed east segmented breakwater. It was removed prior to construction. The results of the fathometer survey were used to update the baseline bathymetry. The GDM does not include a figure depicting baseline bathymetry, other than a plate (see Figure B1) showing limited contours based on soundings interpreted from subbottom profiler records obtained in October 1982 by the Port of San Francisco. However, the summer 1984 fathometer survey data were the basis for the bathymetry sheet included in the as-built plan set (dated November 1984) reproduced for this report as Figure B3. Figure A1 (reproduced from the GDM) includes seabed profiles along the proposed breakwater alignments, also based on the summer 1984 bathymetry.

Borings and subsurface conditions. The Port of San Francisco, SPN, and SPL contracted Geotechnical Consultants, Inc. to obtain eight more subsurface borings along the proposed breakwater alignments and to conduct laboratory tests and geotechnical interpretations (Geotechnical Consultants, Inc. 1984).

Some of the laboratory tests on the total set of 10 borings were performed by the USACE South Pacific Division Soils Laboratory. SPL synthesized all the geotechnical information into Geotechnical Appendix B to the GDM. Figure B1 is a plan view showing the location of all 10 borings, the proposed breakwater alignments, and the location of interpreted geotechnical profiles. Figure B2 shows the geotechnical profiles. Both figures are reproduced from the Geotechnical Appendix of the GDM. Figure B2 shows that three stratigraphic sediment units were identified in the project area. Younger Bay Muds, Bay Side Sands, and Older Bay Muds are layered from top to bottom in that order, with artificial fill overlaying the other units for about three-fourths of Pier 45's length. Younger Bay Muds are made up of layers and lenses of silty clay and fine-grained, poorly graded sands, and clayey sands with shell fragments and sandy, clayey silt interbeds. Bay Side Sands consist of fine-grained, poorly graded, dense to very dense sands, and silty and clayey sands with lenses of medium to very stiff, high plasticity clays. Older Bay Muds consist of highly plastic, medium to very stiff clay, which overlay bedrock.

Littoral environment

In the design process leading to the GDM, questions arose about the impact of the breakwaters on the littoral environment of the Aquatic Park area. A stretch of sandy beach extends from in front of the Maritime Museum building to the low-crested, rubble, groin-like structure just to the east of the foot of Hyde Street pier (refer to Figures 2, 3, and 8b). The primary concerns were that waves reflecting from the breakwater, and increased tidal current speeds in Aquatic Park basin (due to redirection of currents by the breakwater) might cause changes in the sand-transport regime of Aquatic Park, resulting in increased erosion of the beach. In order to characterize the baseline conditions and identify the potential for negative littoral impact, SPN contracted Norgaard Consultants (NC) to do a limited study, resulting in a brief report titled "Sand Transport, Erosion, and Accretion at Aquatic Park, San Francisco Bay" (Norgaard Consultants International 1985). NC's study consisted of a review of existing documents, discussions and interviews with individuals familiar with or involved in the management of Aquatic Park, and qualitative onsite observations of the beach on November 2 and 3, 1984. NC reported that, historically, the area was a natural cove, but since the mid-1800's, it has been modified by human activities such as filling and dredging.

According to the NC report, imported sand was added to form a more attractive recreational beach prior to the opening of Aquatic Park as a recreation area in 1939. GGNRA personnel told CERC personnel in a June 1986 conversation that the beach was started with 1 million cu yd of imported sand in 1943. From interviews with GGNRA maintenance department personnel, NC found that current beach management practice consists of moving an estimated 1,000 cu yd per year by bulldozer or front-end loader from the east end of the beach adjacent to the rowing and swim club piers to the west end, where a low-crested, deteriorated rubble mound forms the westerly limit of the beach. Typically this operation takes place each year in February, and the sand moves under natural forces back towards the east throughout the year.

From this information, NC concluded that the net sand movement along the beach is from west to east.

During onsite visits, NC observed traces of cohesive soil mixed with the beach sand at various locations along the beach east from the Maritime Museum building. On November 3, 1984, NC personnel also noted that with 0.5- to 1-ft, 5- to 6-sec waves breaking with crests parallel to the straight eastern reach of the beach, a zone of increased turbidity extended out to about 50 ft beyond the breaker line. NC referred to the rubble mound as a rock "reef," and noted that it is only exposed on lower tide stages. An accumulation of sand was observed at the east end of the park under the swim and rowing club piers and the foot of Hyde Street pier. NC suggested that the structures at the east end of the beach may cause the sand to deposit there rather than moving on to the east and out of the cove.

The movement of Aquatic Park beach sands due to waves was also addressed using qualitative tracer sediment methods during the physical model study which will be discussed later in this report.

Breakwater Design

Design wave conditions

SPL developed design wave predictions for various critical fetch directions using the most up-to-date USACE wave prediction techniques available at the time (Coastal Engineering Tech Notes (CETN) I-5, I-6, I-7 (U.S. Army Engineer Waterways Experiment Station 1981a,b,c) and Engineering Technical Letter (ETL) 1110-2-305 (USACE 1983)). These procedures superseded the techniques presented in CERC's existing *Shore Protection Manual* (SPM) (USAE WES 1977); they have since been incorporated into the more recent edition of the SPM. A chart of the bay was used to determine critical fetch directions for winds crossing the bay to reach the site.

SPL began the design wave prediction by reviewing two prior studies which analyzed a 25-year record (1946 to 1970) of hourly wind data from an anemometer located at the Alameda Naval Air Station (Figure 14). SPL concluded that sustained average wind speeds of over 1-hr duration do not exceed 35 mph, for winds coming from directions between ENE through WNW. Unadjusted design wind speeds were selected based on the prior studies for the six critical fetch directions centered on the project site (NE through WNW) as shown in Table 1 (from the GDM). These wind speeds were adjusted according to CETN I-5 (WES 1981a) procedures assuming a minimum wind duration of 1 hr. The adjustment procedures are intended to remove effects of extraneous factors influencing anemometer data and to produce an equivalent wind speed meeting the assumptions of the USACE wave generation models. The six fetch lengths and depths were determined from chart measurements, using

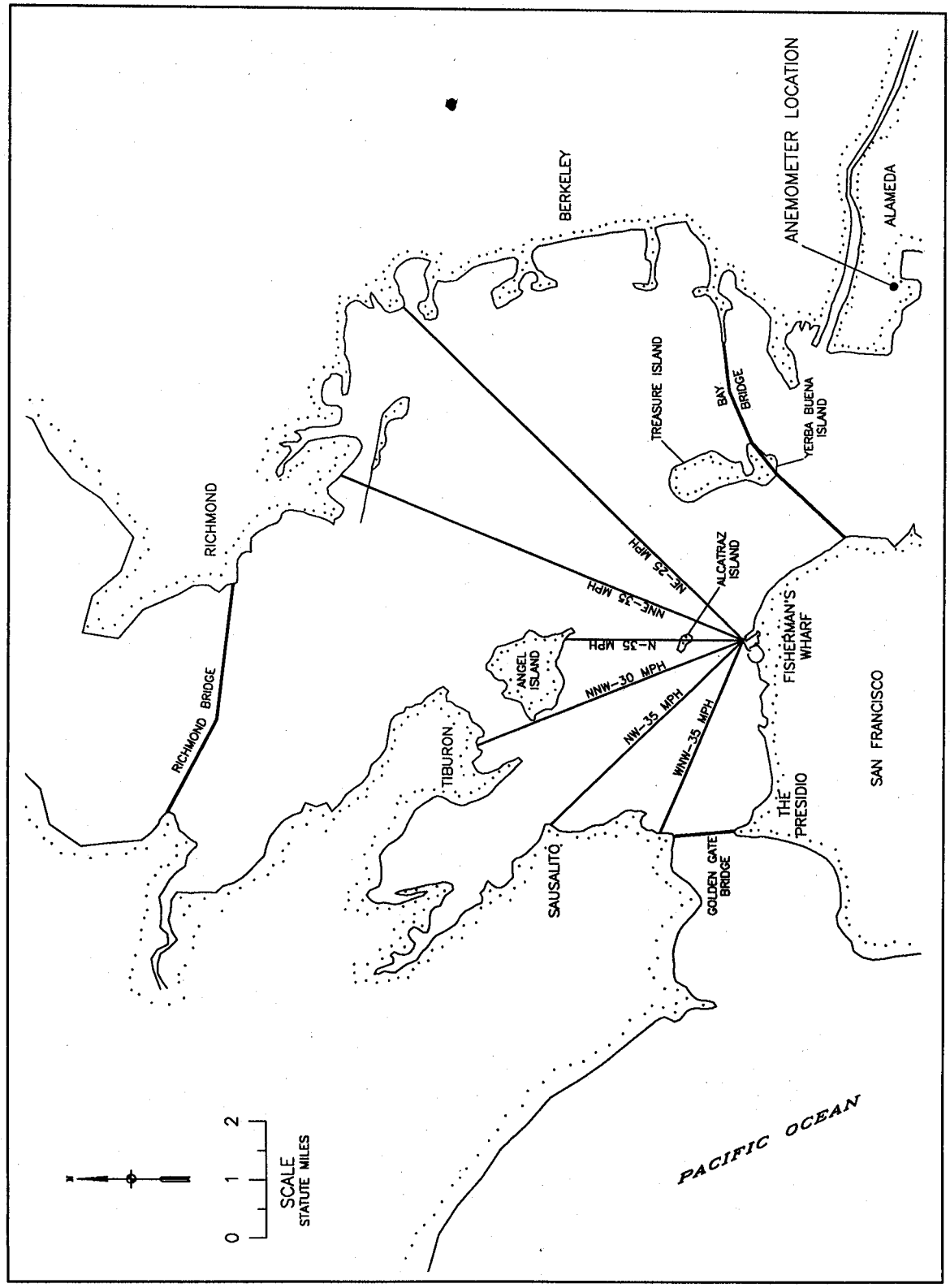

Figure 14. Anemometer location and wave generation fetches

Table 1
Fisherman's Wharf Wave Forecast Summary

Wind Direction	Design Wind Speed (mph)	Adjusted Wind Speed (mph)	Average Fetch Length (ft)	Average Depth (ft)	H_s (ft)	T_s (sec)	H_{10} (ft)	H_1 (ft)	L_0 (ft)	L (ft)
WNW	35	60	18,000	94	3.4	3.3	4.3	5.7	56	56
NW	35	60	27,000	69	4.1	3.8	5.2	6.8	74	74
NNW	30	50	24,000	61	3.3	3.4	4.2	5.5	59	59
N	35	60	16,000	89	3.1	3.2	3.9	5.2	52	52
NNE	35	60	38,000	49	4.8	4.2	6.1	8.0	90	90
NE	25	40	40,000	30	3.3	3.9	4.2	5.5	78	76

the radial averaging methods for sheltered waters contained in ETL 1110-2-305. Significant wave heights and periods (H_s, T_s) reported in Table 1 were calculated by the USACE procedures for fetch-limited conditions (i.e., the forecasting curves for shallow-water waves). Table 1 also lists H_{10}, the average of the highest 10 percent of all waves, and H_1, the average of the highest 1 percent of all waves. H_{10} and H_1 were obtained from the relationships $H_{10} = 1.27\ H_s$ and $H_1 = 1.67\ H_s$ found in ETL 1110-2-305, which result from the assumption that wave heights can be approximated by a Rayleigh distribution. The predicting procedures give the peak spectral period which is, for design purposes, considered equivalent to the significant period T_s. In accordance with ETL 1110-2-305 guidance, T_s was assumed sufficiently accurate for use as the design wave period appropriate to all three design wave height parameters H_s, H_{10}, and H_1. The wavelengths L_o and L in Table 1 represent the deepwater and local (site) wavelengths, computed using the linear wave theory methods found in the SPM. All the fetch directions, except NE, result in deepwater waves at the site.

The GDM states that in accordance with SPM guidance for rigid structures, "For purposes of this Design Memorandum, the design wave refers to H_1." Thus the 8.0-ft H_1 value for the NNE fetch direction was considered the nominal structural design wave.

The GDM points out that the extrapolated 50-year return period significant wave height of approximately 3.3 ft (based on the 15-month Municipal pier prototype wave data set) compares closely with the predicted significant wave heights of 3.4 ft, 3.3 ft, 3.1 ft, and 3.3 ft for directions WNW, NNW, N, and NE, respectively. Note, however, that the predicted heights of 4.8 ft and 4.1 ft for the NNE and NW directions are substantially higher than the prototype-based 50-year H_s value. No frequency of occurrence, such as return period, was specified in the GDM for the selected wind speeds presented in Table 1. In a later section of the GDM it is stated that "the design wave for the life of the structure is eight feet. This wave is expected only once in 50 years..." However, it is not clear that the selected wind speeds (hence predicted waves) were determined to be 50-year values from a quantitative evaluation of the

anemometer record. Consequently, comparison of predicted design waves with the extrapolated 50-year wave height, especially considering the uncertainty inherent in the 50-year extrapolation, may have little meaning.

Due to the location of the project site with respect to the configuration of San Francisco Bay and the limited available wave-generating fetches, it was assumed that magnitude and direction of winds approaching the site would be the governing factors in wave generation. Consequently, no wave refraction analysis was performed and all predicted waves were assumed to be locally generated.

Breakwater type, alignment, and configuration

The process of selecting the planform breakwater alignment and configuration began with desktop studies of various concepts by SPN, the Port of San Francisco, and their consultants. From consideration of construction and material costs, and available space for future berthing expansion, it was evident that the best breakwater alternative would consist of precast, prestressed concrete sheet-pile structures.

Design constraints

Constraints on the breakwater design which affected the selection of alignment included allowable wave heights, existing water depths, berthing locations for the historic fleet, recreational uses of Aquatic Park (beachcombing, swimming, boating), entrance channel dimensions and vessel sizes, water quality and circulation, constructability, and compatibility with future rehabilitation and redevelopment of other Fisherman's Wharf structures. Concepts resulting from the desktop studies sought to keep construction costs down by aligning the detached breakwater in shallower water where possible. The western limit of the detached breakwater was constrained by a requirement to keep the structure out of the recreational swimming and small boat mooring basin area of Aquatic Park. The alignment of the breakwater structures at the eastern end of the site was constrained by navigational considerations. The two-way traffic channel width of 150 ft was determined on the basis of six times the beam of the typical commercial fishing vessel (25-ft beam, 75-ft length). Since additional clearance is needed for vessels to avoid striking the inclined batter piles underwater, a total channel width of 165 ft was specified, which in turn governed the minimum separation between the ends of Pier 45 and the east segmented breakwater, and the detached breakwater. The 165-ft channel width was also sufficient to allow tugboat-assisted passage by the historic ship Eureka under favorable weather conditions. Also, the eastern limit of the detached breakwater was governed by the need to allow a straight-line docking approach to the east side of Pier 45 for the large vessels occasionally berthed there.

HEC's numerical modeling

In the next step HEC performed numerical hydrodynamic and water quality modeling of two proposed alternative alignments (USACE HEC 1984b). Both alignments involved a detached, impermeable-wall breakwater fronting the harbor in conjunction with a baffled section of breakwater along the exterior parts of Pier 45. Alternative A was similar to SPN's configuration resulting from the earlier Corps feasibility study (USAED San Francisco 1976) and consisted of piece-wise linear segments for the detached breakwater. Alternative B was similar to the Port of San Francisco's proposed curvilinear detached breakwater alternative, which was one of several alternatives considered (Bechtel Civil & Minerals 1983). HEC's approach consisted of a combined program of field sampling and application of numerical models. The prototype data were used to establish baseline information for the development of model boundary conditions and for model calibration and verification. Quantification of differences between proposed breakwater design alternatives, emphasizing circulation and water quality performance, was obtained through the use of the RMA-2 (hydrodynamics) and the RMA-4 (water quality) finite element models, originally developed by Resource Management Associates (RMA) of Lafayette, California. These models have since been improved and incorporated into USACE's TABS system of models. Figure 15 shows the initial finite element network for the hydrodynamic study, which was modified as necessary to incorporate the hydraulically important features of the proposed breakwater alternatives and the existing piers and wharves. The hydraulic effects due to the historic ships were not included in the model. HEC conducted a series of hydrodynamic simulations for flood and ebb tides under both steady-state and dynamic tidal conditions. The steady-state runs applied spatially varying, but not time-varying water surface and velocity boundary conditions (like river flow) in order to demonstrate and check model operation. The dynamic runs applied time- and spatially varying boundary conditions representative of actual tides expected in the study area, based on empirically derived relationships between predicted tides at the Golden Gate and tides at Fisherman's Wharf. The empirical relationships were developed using data observed during the prototype hydrodynamic surveys. To calibrate the hydrodynamic model, the appropriate coefficients of the model were manually adjusted to obtain good agreement between depth-averaged model results and prototype observations for conditions on July 14, 1983. Then, for verification, the model was run without further adjustments to predict hydrodynamics for September 19, 1983; the results were judged to be in good agreement with observed prototype data. At this point the hydrodynamic model results could be used as input to the RMA-4 model, a constituent transport water quality model that computed constituent concentrations as mixing occurred during advection and diffusion. The September 19 conditions were selected for production model runs used in making comparisons between breakwater alternatives and existing conditions. The tidal and water quality conditions of that date were considered the most representative of average general conditions at Fisherman's Wharf. It was found that Alternative B had slightly less overall impact on circulation and flushing than Alternative A for the cases considered, compared to existing (no breakwater) conditions. However, neither alternative had a large adverse impact on water quality conditions.

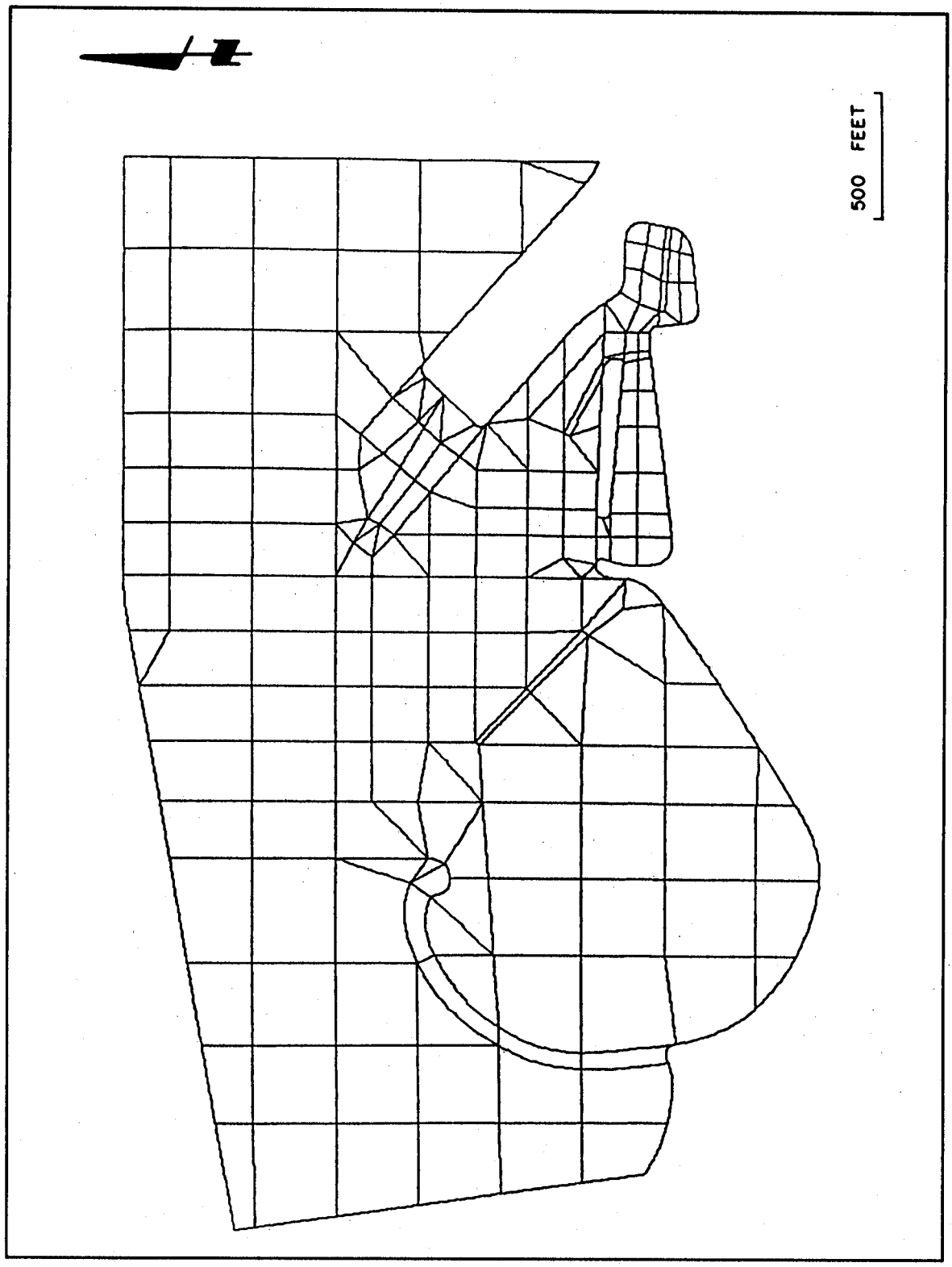

Figure 15. Initial numerical model network for hydrodynamic simulation

CERC's physical modeling

At this point in the design process, CERC began a physical model study to determine short-period wave attenuation performance of various structure configurations (Bottin, Sargent, and Mize 1985). In selection of alternative approaches to project design, CERC considered using a numerical model available at the time (Danish Hydraulic Institute's System 21 model) to simulate the short-period waves for existing conditions and evaluation of breakwater design alternatives. CERC determined that a numerical model approach for short-period waves was not suitable, and recommended a physical model approach. The numerical model lacked certain necessary capabilities, required some types of input data that were difficult to estimate, and would be more expensive to use than a physical model.

A 1:75-scale geometrically undistorted, fixed-bed physical model was built to encompass the entire Fisherman's Wharf area including Municipal pier and Pier 45, extending bayward to approximately the 60-ft depth contour. Figure 16 shows the layout of the physical model basin. The model reproduced the complex system of piers, wharves, pilings, bulkheads, and rubble structures in great detail, as well as the existing bathymetry. The historic ships were not included in the physical model. Figure 17 presents an oblique photograph of the basin during testing of a breakwater configuration alternative; the wave generator is seen at the top of the photo. Test conditions included two values of swl selected by SPL, 0.0 ft and +5.7 ft mllw, corresponding to mllw and mhhw, respectively. Monochromatic, unidirectional (regular) waves were generated using a trapezoidal-shaped, vertical-motion plunger type wave generator. The generator could be positioned within the model basin according to the desired direction of wave propagation. CERC and SPL jointly selected wave conditions to be tested based on preliminary results from the wave prediction analysis described previously, including the same six critical directions. Initial test waves included significant wave height-period combinations as well as a set of less severe, but more frequently occurring height-period combinations. The wave generator could not produce waves with periods less than 3.6 sec, so some of the combinations that called for shorter periods were run at 3.6 sec. During the course of the physical model study, SPL finalized the wave predictions (Table 1), and furnished revised and additional wave height-period combinations for inclusion in the study. The revised combinations were the same (except for the limitations on the shorter periods imposed by the wave generator) as the predicted conditions of Table 1. In some cases the new wave conditions were less severe than the original combinations that had already been tested. Also, several breakwater configurations were tested with wave heights of 2.0 ft, 2.5 ft, and 3.0 ft, all with periods of 10.0 sec from the WNW direction. These additional test wave conditions were included to examine the effects of ocean-generated swell coming through the Golden Gate.

Because small rubble-mound model structures reflect relatively more and absorb or dissipate relatively less wave energy than the prototype structures they represent (Le Mehaute 1965), adjustments to the model rubble-mound structures were needed to ensure correct reproduction of wave reflection and transmission characteristics. Based on past WES physical model experience,

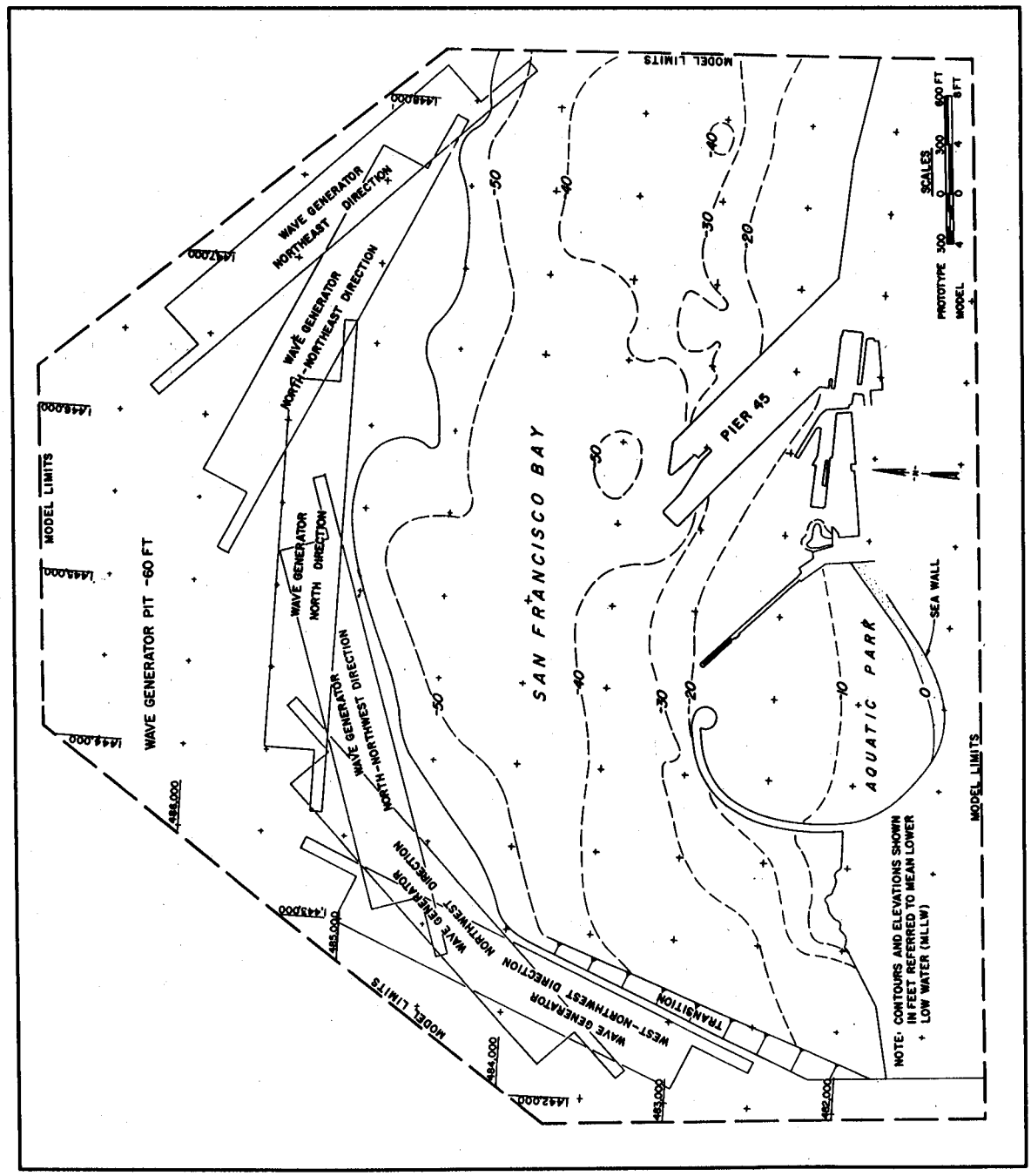

Figure 16. Physical model layout for investigation of breakwater configuration

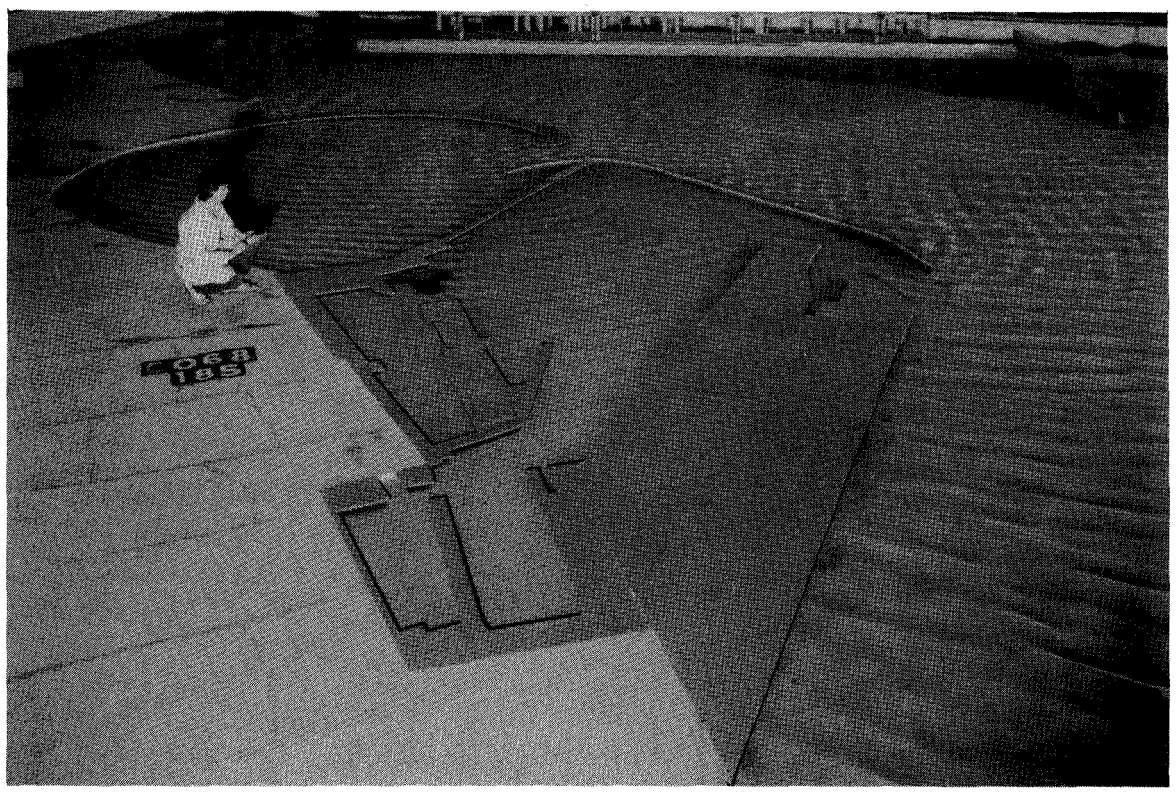

Figure 17. Physical model in operation--wave generator at top of photo

it was determined that rock sizes in the model should be increased to about 1.5 times the sizes required for geometrical similarity.

A second objective of the physical model study was to qualitatively determine the degree of erosion and accretion on the shoreline of Aquatic Park, to address concerns raised about the possible impact of waves reflecting off the breakwater. The approach used was to place small amounts of a crushed coal tracer sediment at five locations along the Aquatic Park beach immediately prior to the start of tests, then to track the movements of the tracer. The selection of the tracer material and its median grain size was based on experimentally derived scaling relations (Noda 1972) and prior experience with model tracers.

A large number of tests were conducted in the physical model using various alternative alignments, lengths, and combinations of baffled and segmented breakwater elements to develop the most economical configuration that would provide adequate protection from short-period waves. A total of 90 different breakwater plans were tested. Not all plans needed to be tested for every wave condition, because changes between plans often affected only waves from one or two directions, and some results from earlier tests could be assumed to apply to plans that were tested later. Sediment tracer movement was examined for existing conditions and, at an intermediate point in the study, for one of the most promising alternatives (Plan 38), which was sufficiently similar to the breakwater configuration finally chosen that there was no need to perform sediment tracer tests again.

An automated data acquisition and control system was used to record the output from wave gages placed at varying locations in the model basin, depending on the breakwater configuration and wave conditions being tested. Parallel-wire, electrical resistance-type wave gages provided the fluctuation of water-surface elevation versus time. The resulting time series of water surface elevation data was analyzed by computer-assisted methods to derive the significant wave heights for each model gage. Since generated waves were monochromatic, the analysis took the average height of the highest one-third of the waves recorded at each gage ($H_{1/3}$) as the significant wave height. These significant wave heights were then adjusted to compensate for the excess viscous bottom friction present in the physical model (compared to that in the prototype) using results obtained by Keulegan (1950)[1]. The resulting wave heights were tabulated and organized by breakwater configuration being tested. The wave attenuation performance of the various breakwater plans was evaluated by comparing the tabulated wave heights with the maximum allowable wave height criteria for the various locations in the study area. At times during the course of the investigation, the "art" of physical modeling came into play when CERC's investigators tried different configurations in informal tests using visual observations as the primary tool to evaluate what approaches were working. Typical wave patterns for each of the breakwater configurations were documented by oblique photographs of the model basin. General patterns of sediment tracer movement were documented using oblique photographs taken after test completion, with arrows indicating the movement paths. The physical model report (Bottin, Sargent, and Mize 1985) presents the tables of wave heights, wave pattern photographs, and sediment movement photographs.

After testing several variations of an initial curvilinear breakwater configuration which combined elements of the two alternatives tested by HEC, a design conference was held involving participants from SPN, SPL, South Pacific Division (SPD), CERC, HEC, and the Port of San Francisco. Port personnel recommended increased allowable wave height criteria, a narrower navigational entrance channel, and elimination of the reverse curvature in the detached breakwater alignment. (The curvilinear alignment had included a reverse curve to bring the central portion of the detached breakwater closer to shore to take advantage of shallower depths, thereby saving on lengths of piles required. However, it was found that the length savings would be outweighed by the reverse curve's increased cost and difficulty of construction). At the outset of physical model testing, SPL and SPN specified that maximum wave heights should not exceed 1.0 ft for all areas of the harbor. Design conference participants agreed to set maximum allowable wave height criteria at 1.0 ft in the existing and future small-craft berthing areas, 1.5 ft in the historic vessel mooring area adjacent to Hyde Street pier, and 2.5 ft in the navigational entrance channel. The GDM's wave height criteria and the zones to which they apply are shown in Figure 18. Names designating the zones are those used in the MCCP monitoring plan, discussed in a later report section. Zone

[1] Unpublished data, entitled "The gradual damping of a progressive oscillatory wave with distance in a prismatic rectangular channel," prepared by G. H. Keulegan, National Bureau of Standards, Washington, DC, at the request of the Director, U.S. Army Engineer Waterways Experiment Station, Vicksburg, MS, by letter of 2 May 1950.

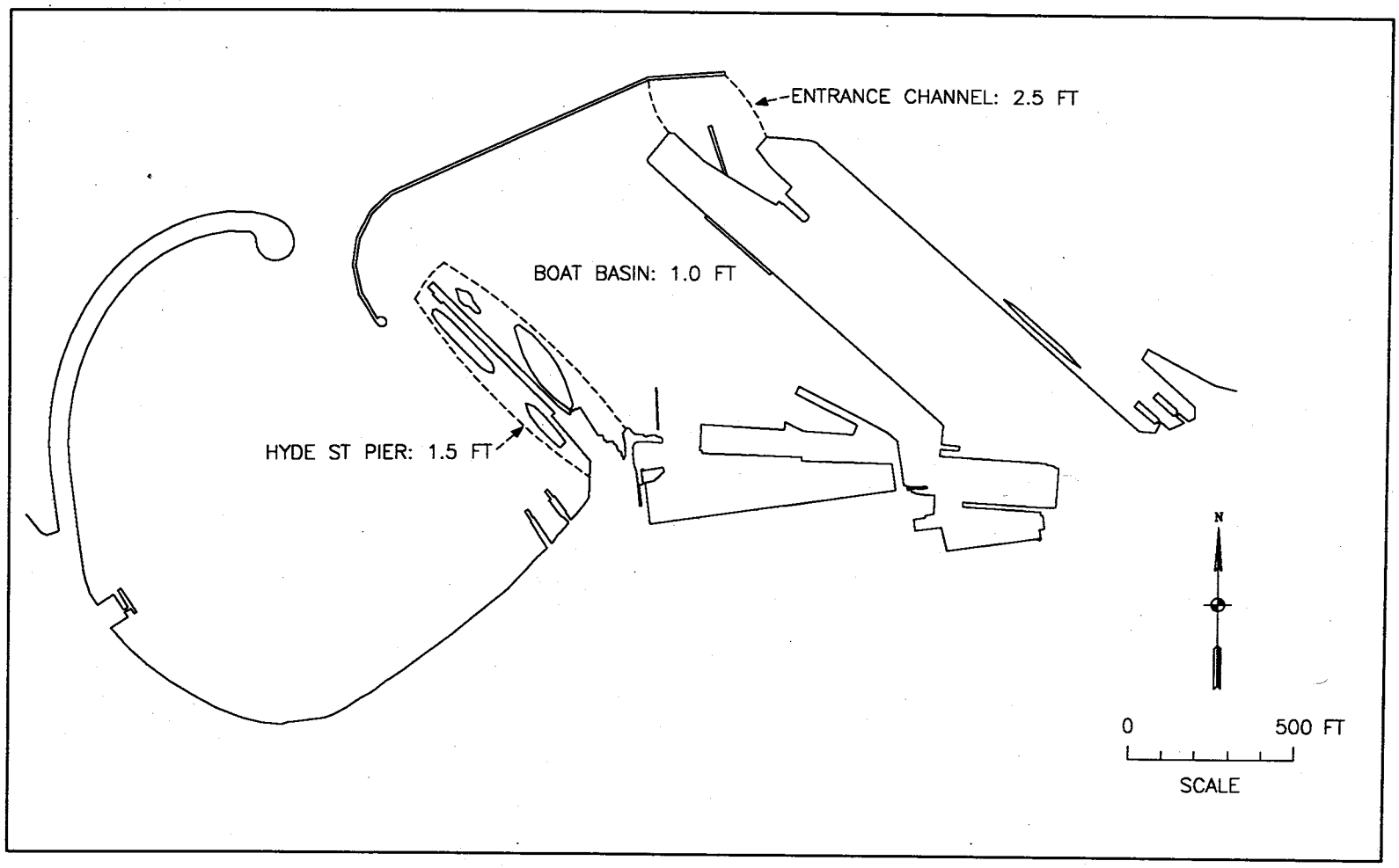

Figure 18. Design wave height criteria

boundaries were not precisely specified during breakwater design. Figure 18 shows zone boundaries, which should be considered approximate, since they were chosen by the author for convenient reference in subsequent sections of this report.

Tests resumed for breakwater configurations incorporating the design conference's recommendations. It was found that no feasible breakwater configuration could attenuate the 2.5-ft and 3.0-ft, 10-sec swell coming from WNW to within the wave height criteria for the harbor during mhhw conditions. Since the frequency of occurrence of these test waves was estimated to be about 50 years or greater, it was felt that they should not be considered further in design evaluation. Consideration was also given to the possible combination of ocean-generated waves (swell) coming through the Golden Gate with locally generated storm waves (sea). Only locally generated waves from WNW and NW directions, in combination with swell from WNW, were considered important. It was felt that local winds occurring with the other locally generated wave directions would be in opposition to the incident swell, thereby reducing or eliminating the net additive effect. Since it was not possible to generate two simultaneous wave trains in the physical model, combined sea/swell significant wave heights for locations of interest were computed from wave heights obtained in separate tests of sea or swell alone. For certain critical combinations, resulting wave heights in the historic fleet mooring area and the future small-craft berthing area slightly exceeded allowable criteria. However, the violations were considered acceptable, given the small frequency of occurrence expected for the combined sea/swell conditions.

A persistent problem that required innovative approaches to breakwater configuration was excessive wave action in the area of the navigational entrance, due to reflected energy being trapped between the end of Pier 45 and the eastern end of the detached main breakwater. In order to limit the penetration of waves from northeasterly directions, several baffled breakwater arrangements around the end of Pier 45 were tested. These configurations improved inner harbor conditions but worsened entrance conditions. After consideration of the constructability of the baffled sections, it was decided that segmented breakwater sections, using impermeable sections of several adjoining sheet piles separated by gaps, would accomplish the same goals with a less expensive construction approach. Various alternative length and orientation treatments for the east end of the detached breakwater were also tried. The Plan 78 breakwater configuration was considered optimum since it provided the best combination of overall wave attenuation performance, entrance navigability, and economy of construction. This plan was very similar to the constructed breakwater described in the introduction of this report.

The reflection problem in the entrance area was mitigated through the use of the angled, segmented east breakwater component, which deflected much of the incoming wave energy back towards the east, away from the entrance. Maximum wave height criteria were met for the existing and future small-craft berthing areas and the historic vessel area (except for under certain sea/swell combination conditions, as previously noted).

Tracer movement results obtained in earlier tests (similar to Plan 78) indicated that only the most severe swell and locally generated storm waves would result in substantial movement of Aquatic Park beach sediment. The predominant movement direction would be toward the east, as found for the existing (no breakwater) condition. Beach erosion due to reflected energy from the breakwater appeared to be inconsequential.

CERC's numerical modeling

Plan 78 was then tested for its impact on harbor-oscillation response due to long-period wave excitation (Bottin, Sargent, and Mize 1985). CERC employed a numerical harbor oscillation model which computed a two-dimensional hybrid finite element solution to the generalized Helmholtz equation in shallow water. Originally developed by Chen and Mei (1974), the harbor response model was improved and expanded prior to the Fisherman's Wharf study (Houston 1976, Chen 1984). The model was run for wave periods ranging from 30 to 600 sec, for an incident direction (azimuth) of 272 deg corresponding to the approach direction of long-period Pacific Ocean energy passing through the Golden Gate. Results from the model included frequency response curves of wave height amplification versus wave period for selected locations. Peak resonant response frequencies were identified from these curves. Contour maps of wave height amplification factors throughout the study area were produced for the peak response frequencies. Maps of normalized maximum horizontal current velocity vectors due to the standing wave field were also produced. Each of these products showed both existing conditions and those with the Plan 78 breakwater in place, to facilitate comparisons.

A simplified numerical ship-motion model was also developed by CERC to evaluate the potential impact of the proposed breakwater on historic fleet mooring conditions (Bottin, Sargent, and Mize 1985). CERC's simplified model was principally based on an earlier model developed by Raichlen (1968).

Since the two numerical models predicted that Plan 78 would not result in significantly changed long-period harbor oscillation or ship mooring conditions, no further changes in the breakwater plan were proposed by CERC.

HEC's numerical tests of Plan 78

The final CERC configuration was then numerically modeled by HEC to determine its circulation, flushing, and water-quality performance, again using the conditions of September 19, 1983 (USACE HEC 1984b). Figure 19 shows model results as vector plots of current velocity fields for the September 19, 1983 tide condition for both existing conditions (without breakwater) and with the final CERC breakwater (Plan 78) in place. Figures 19a and 19b show conditions at peak flood tide. Figures 19c and 19d show peak ebb tide conditions. The model predicted that current speeds would be increased by the presence of the breakwater in the Aquatic Park area, in both ebb and flood

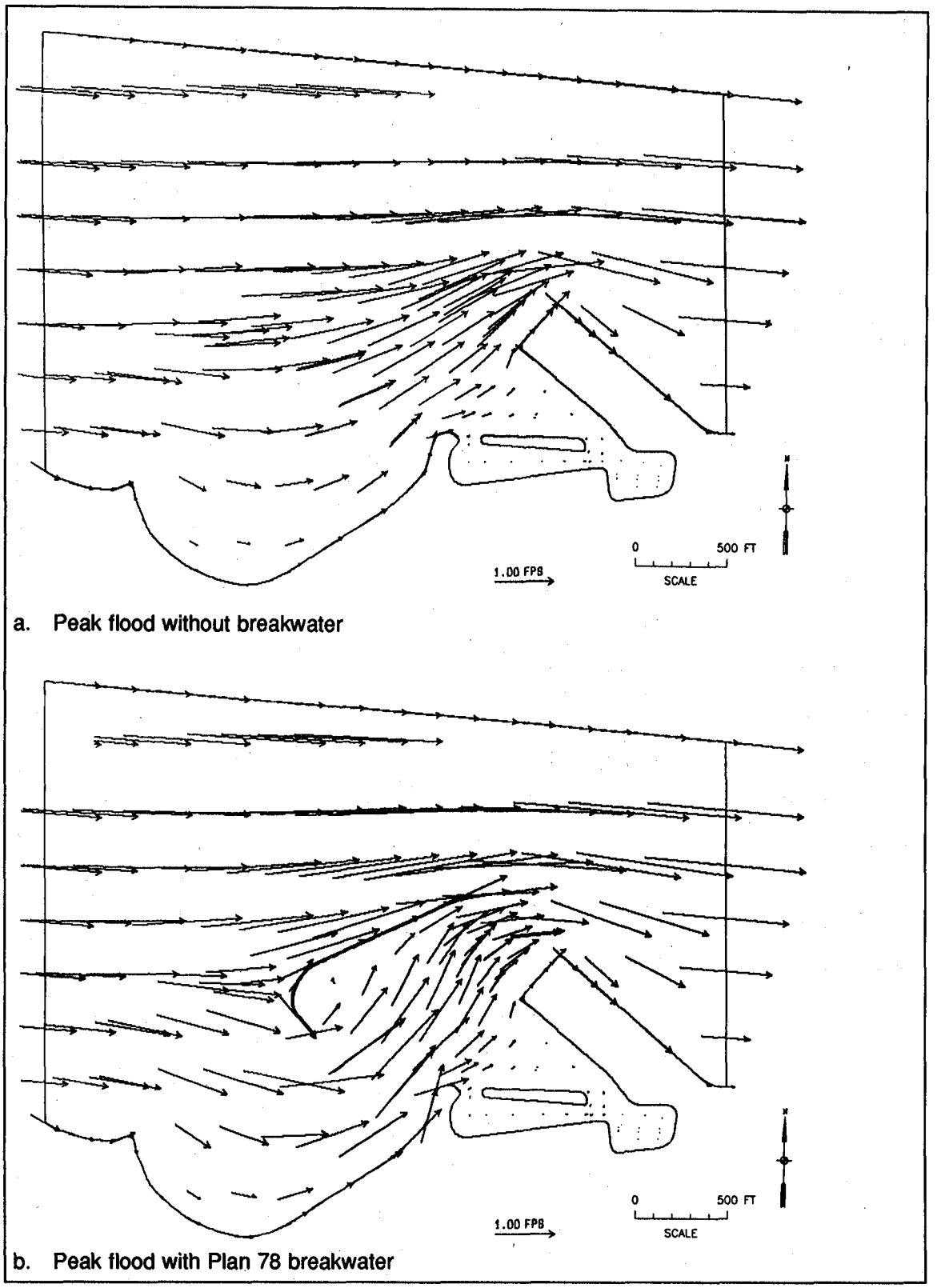

a. Peak flood without breakwater

b. Peak flood with Plan 78 breakwater

Figure 19. Hydrodynamic model currents (Continued)

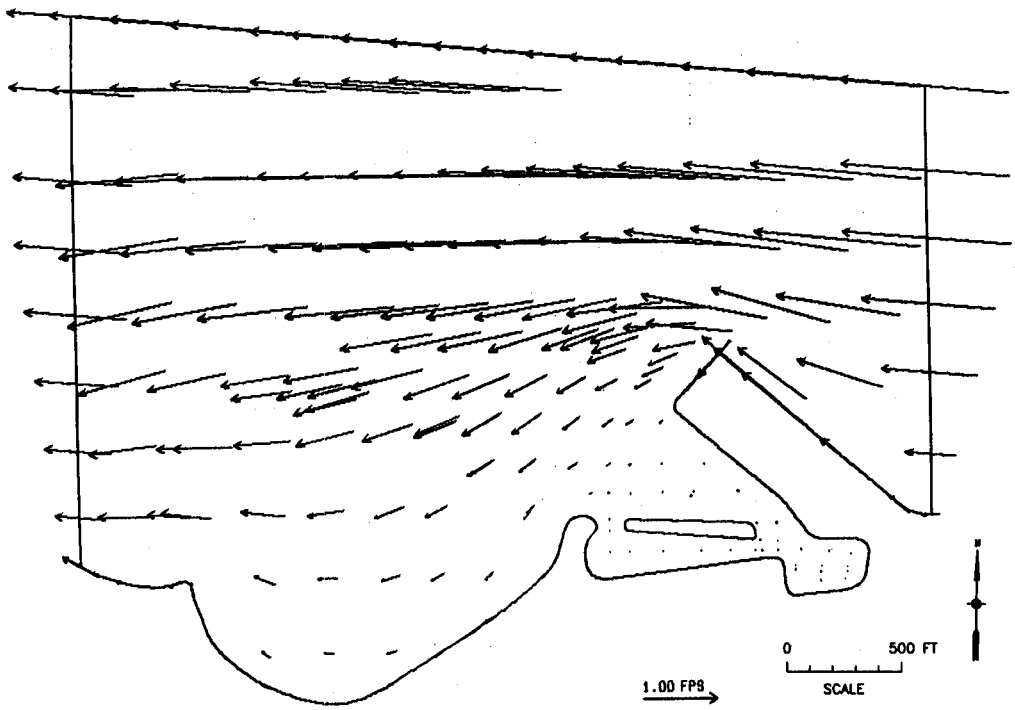

c. Peak ebb without breakwater

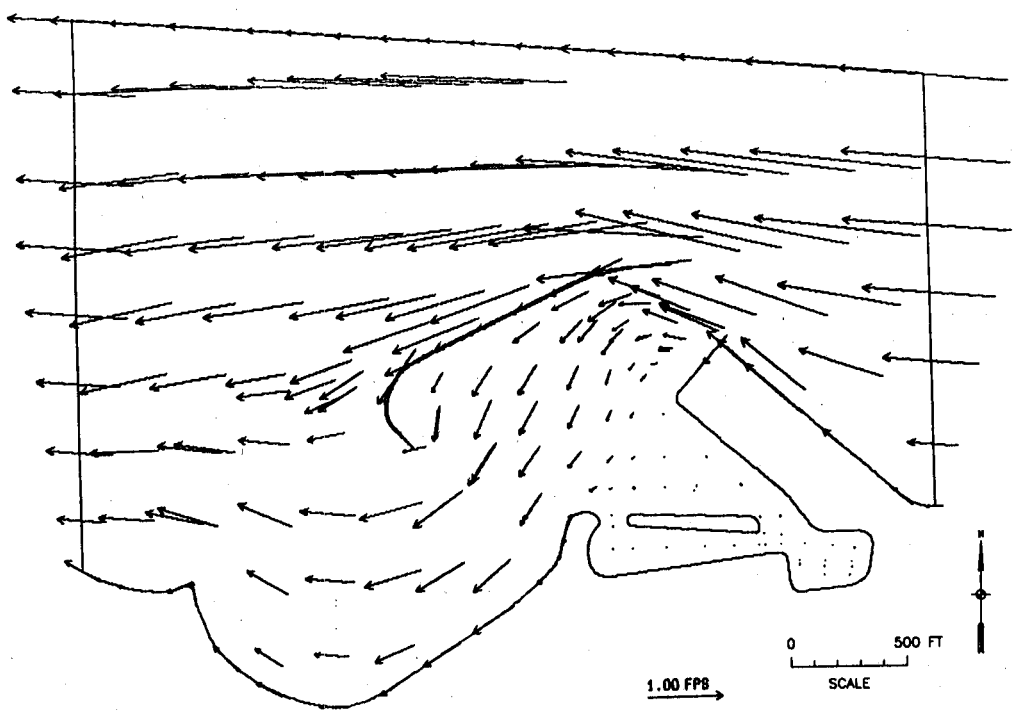

d. Peak ebb with Plan 78 breakwater

Figure 19. (Concluded)

conditions, and in the outer harbor area during flood. HEC concluded that for both flood and ebb conditions, harbor flushing (net exchange) would, on average, be maintained at its present rate or improved slightly. HEC further concluded that the proposed final configuration would provide sufficient circulation and flushing action to maintain the existing level of water quality, with no significant changes likely. The GDM further points out that predicted tidal current velocities in the entrance will not exceed 2 knots (3.4 ft/sec), which apparently was considered an upper limit for navigational safety.

As-built breakwater

The as-built breakwater shown in Figures 2, A1, and A2 has some very slight differences from the Plan 78 configuration (Figure 20). The shape of the western end of the detached breakwater was altered to shorten the length of its curvature, bringing it closer to the end of Hyde Street pier. The smooth curve in the Plan 78 alignment was replaced with a series of straight segments. At the eastern end, a slightly shorter straight end segment replaced the gently curving end segment of Plan 78. The total length of the as-built detached breakwater is 1,509 ft, versus the Plan 78 length of 1,560 ft.

Cap elevation and configuration

The top-of-cap (crest) elevation of the breakwater elements was initially specified at +12 ft mllw, primarily on the basis of aesthetics. This cap elevation was selected to match the deck elevations of the existing Hyde Street pier and Pier 45, allowing the breakwater structures to blend in architecturally with the piers. The matching elevation also would make pedestrian access to the cap safer and easier. Furthermore, the 12-ft crest was low enough that the historic vessels could still be viewed from the bay. Due to possible use of caps on the detached and east segmented breakwaters as pedestrian walkways, a cap top width of 10 ft was specified. The provision of an accessible cap allowed inclusion of additional recreation benefits for fishing and sightseeing.

The cap elevation was checked with regard to wave overtopping. The main body of the GDM mentions briefly that the crest of the clapotis (standing wave) was calculated by the Sainflou method to occur at +13 ft and +12 ft mllw for design wave heights of 5.5 ft and 5.0 ft, respectively, using the mhhw elevation at the Presidio (near the Golden Gate) of +5.9 ft mllw as a design swl.

Since the overtopping potential of the +12-ft elevation seemed minor, it was decided to proceed to the physical modeling study with that elevation for the scale-model breakwaters. The model breakwater included a rectangular-sectioned, 10-ft-wide cap. Although overtopping is not mentioned in Bottin, Sargent, and Mize (1985), the report's wave pattern photograph for Plan 78 subjected to 3.9-sec, 3.3-ft waves from NE at the +5.7-ft swl shows some slight overtopping at the eastern end of the detached breakwater.

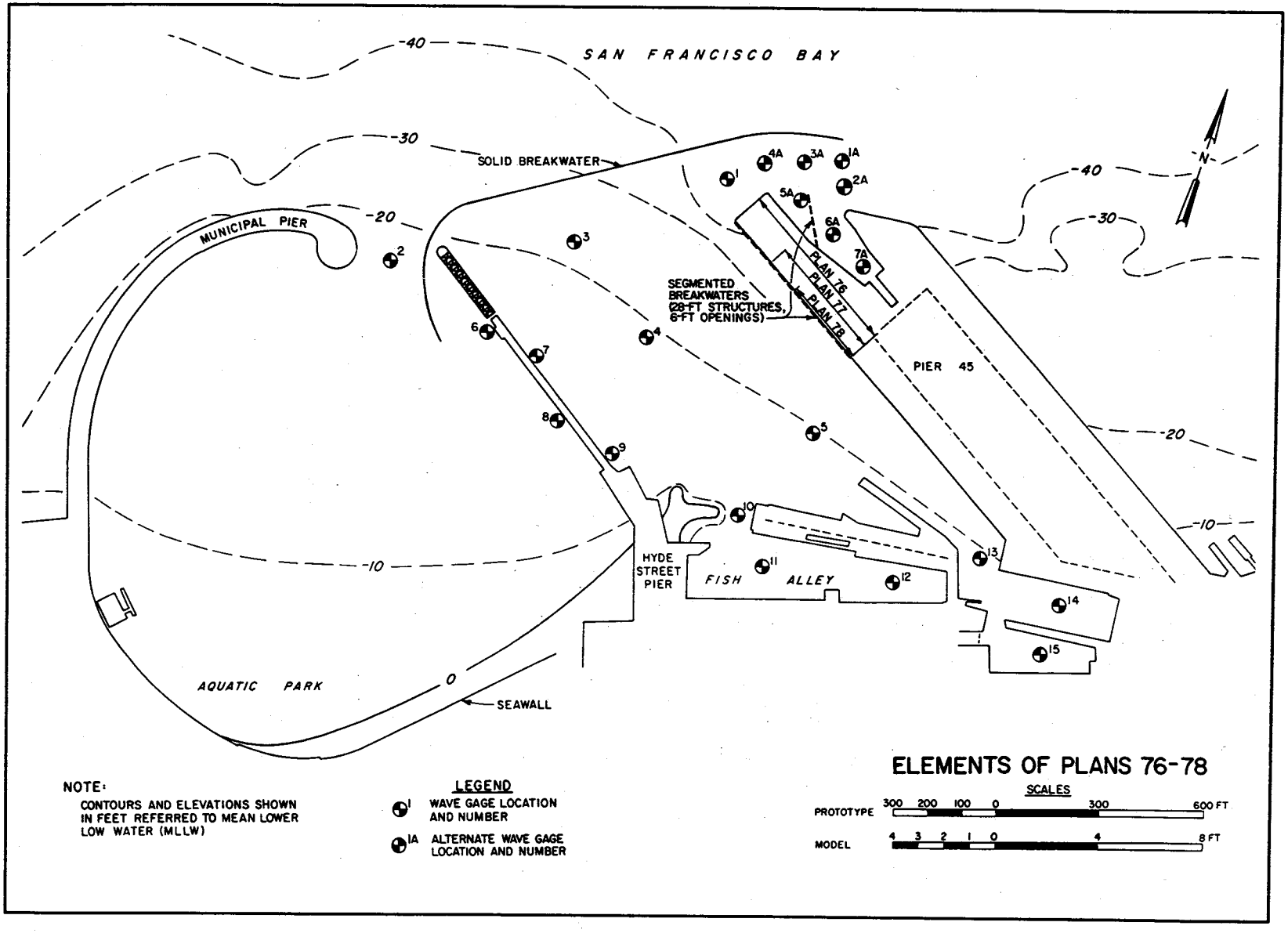

Figure 20. Optimum physical model breakwater configuration and gage locations

SPL performed further calculations of overtopping potential (and wave forces) using an unpublished computer program supplied by CERC. The program combined the Sainflou and Miche-Rundgren methods from the SPM. No overtopping was predicted except under the very conservative condition of perpendicular incidence of the 8-ft design wave, for which the predicted standing wave crest was at +16.2 ft mllw. The GDM states that 8-ft waves were tested in the physical model, resulting in wave heights less than 3 ft in the enclosed area. It was felt that the extreme conditions required to produce overtopping were likely to be very infrequent. The low perceived risk of overtopping was therefore deemed an acceptable one. However, as a precaution, plans called for signs to be posted warning pedestrians to stay off the breakwater during storms.

The overtopping calculations discussed above were made without consideration of the effect of the concrete cap which would be needed to tie together the interlocking sheet piles. To address concerns about the possible uplift forces exerted by the standing waves if their crests contacted the underside of the overhanging cap, initial cap designs included a protuberance, integrated with and extending an additional 1 ft outward from the edge of the cap on the bayward side. This splash deflector was curved on the underside to deflect the uprushing wave outward. During design review a suggestion was made to eliminate the protuberance, and instead to bevel the underside of the cap to accomplish the same effect as the splash deflector. Informal physical model tests of the beveled cap design were conducted by Professor Robert Wiegel at the University of California, Berkeley. The tests confirmed that the beveled design would function as intended, and the breakwater was built with beveled caps on both sides of the detached and east segmented structures, and on the east side of the west segmented structure (see Figures A2 and A3). The construction cost of the beveled caps was comparable to the initial design, since the increased difficulty in forming the sloped underside was offset by the reduction in concrete volume.

Scour and deposition

SPL asked HEC to study the scour potential around the proposed breakwater, which HEC then contracted to RMA. Dr. Ranjan Ariathurai of the University of California, Davis, performed the investigation for RMA. HEC made several additional recommendations following their review of Dr. Ariathurai's results. Details of the analysis procedure and complete results of the study are presented in a separate HEC report, USACE HEC (1984a), with key results presented in Appendix A of the GDM.

The scour analysis considered the combined effects of waves and tidal currents. Orbital velocities due to waves were computed using linear wave theory. Design waves (H_s, H_{10}, and H_1) were selected from Table 1 for the NNE direction, but for the purposes of the study were assumed to be perpendicularly incident to the breakwater, forming standing waves. As a check on which wave conditions could suspend sand at various locations, sand-transport

potentials were calculated for each wave condition and for the range of water depths present along the breakwater. A review of HEC's prototype current measurements and hydrodynamic model results revealed maximum depth-averaged current speeds in the range of 3 to 4 ft/sec along the proposed breakwater alignments. Assuming a value of 4 ft/sec as the maximum velocity of tidal currents, Dr. Ariathurai then superimposed the maximum orbital velocities near the seabed due to 8.0-ft waves (H_1) to calculate a single equivalent scour velocity which varied by depth and therefore by location. Since the near-bed tidal current speed is normally less than the depth-averaged speed, and since the design waves would not be perpendicular to all parts of the breakwater, Dr. Ariathurai used engineering judgment to reduce the computed equivalent scour velocities to a set of more realistic design values. He then computed equilibrium scour depth ranges corresponding to those design scour velocities for the range of water depths occurring along the structures. These maximum scour depths (see Table 2) were obtained using several empirical formulae; iterative calculations were used to account for the reduction in the wave-induced velocities with increasing depth of scour. Although the bed materials at some locations consist of cohesive materials, the empirical formulae were applied assuming a sand bed. Dr. Ariathurai reasoned that despite their higher scour resistance, there would be essentially no resupply of cohesive materials to fill in scoured regions, so scour depths might be similar to those computed for a sand bed. The report had previously defined equilibrium depth of scour for a sand bed as "the result of equilibrium reached between the rate of supply of sediment by the flow and the rate of removal by the scouring process." However, it is not clear that sand resupply rate was considered in the analysis leading to the results of Table 2. Recognizing that the use of a uniform, tidal current velocity of 4 ft/sec throughout could be overly conservative in some locations, Dr. Ariathurai recomputed the scour depths using tidal-current velocities selected from a review of the velocity vectors predicted by HEC's hydrodynamic model. The resulting values, designated "maximum likely scour depths," are shown in Figure 21. The figure shows that a zone of potential deposition lies along the inside of the detached breakwater. Scour potential along the segmented breakwaters was not addressed in USACE HEC (1984a) or the GDM. The maximum likely scour depths are generally smaller than the maximum equilibrium scour ranges, especially near the western end of the detached breakwater.

Table 2
Maximum Equilibrium Scour Depths

Depth of Water (ft)	Maximum Scour Velocity (ft/sec)	Maximum Scour Depth (ft)	
		Wall	Batter Piles
20	6.5	10-12	9-11
30	5.0	8-10	8-10
40	4.5	7-8	6-8
50	4.3	6-7	5-7

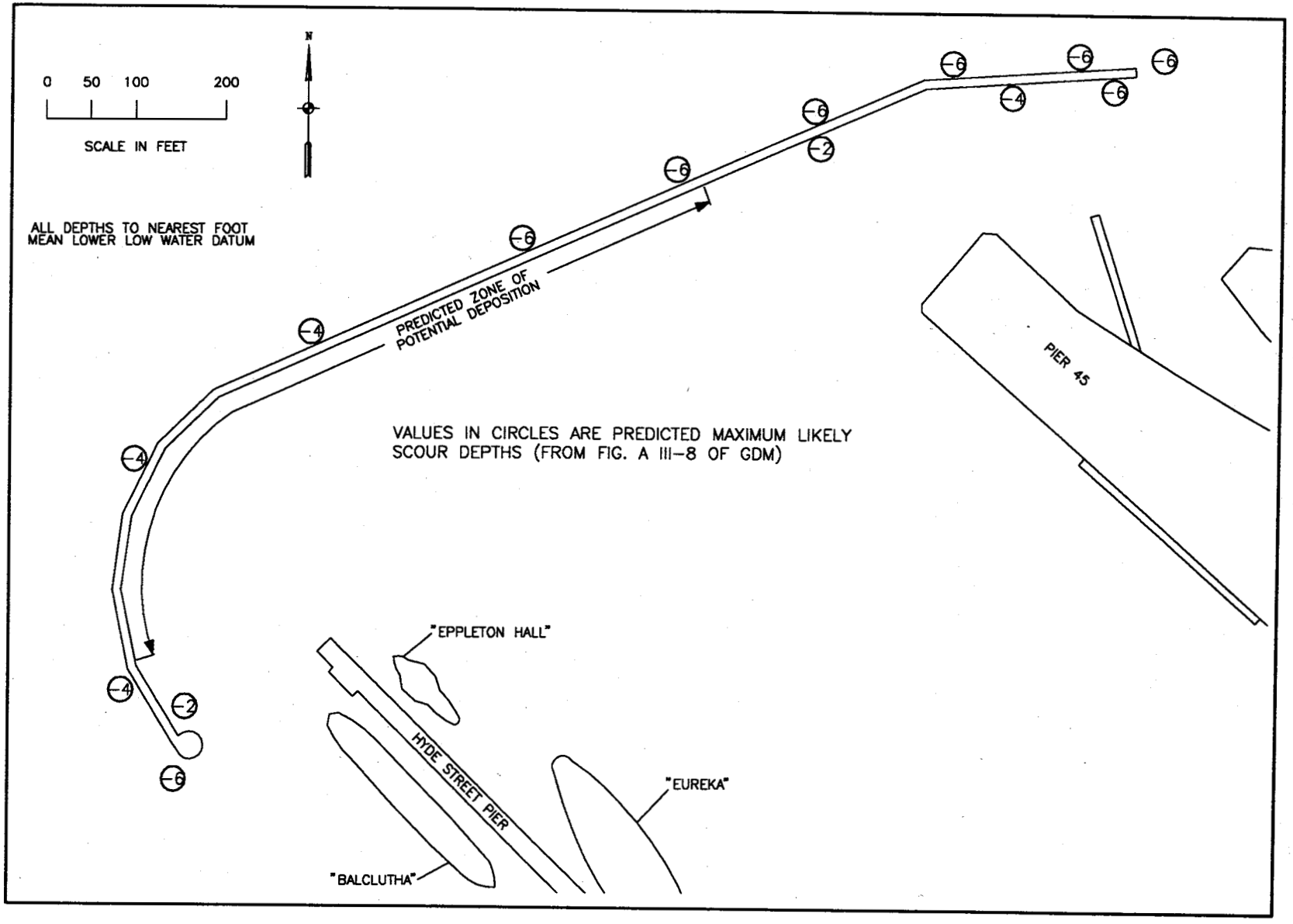

Figure 21. Predicted maximum likely scour depths

The report states that the width of scour holes will probably be about twice their maximum depth. At the end of the report Dr. Ariathurai recommended selecting design scour depths from those in Figure 21 and applying a factor of safety of 1.3, which he chose to reflect the uncertainties of his methods. He also warned that a differential earth pressure could develop due to the deposit on the landward side of the detached breakwater. His further recommendation was to protect all areas of potential scour adjacent to the detached breakwater with an 18-in.-thick layer of 6-in. stone riprap laid on a filter. The width of this scour blanket was specified to be the greater of 9 ft or twice the corresponding maximum likely scour depth.

The first of HEC's additional recommendations (prefacing their report) was that the maximum likely scour depths of Figure 21 be used for design purposes. HEC then recommended that a larger factor of safety, such as 2.0, be used for the scour depth and riprap design at the east and west ends of the detached breakwater. They stated "experience with most structures that end abruptly and that are oriented into the flow, such as the proposed Fisherman's Wharf breakwater, indicates that high energy vortices can cause additional scour at the tips of such a structure." HEC recommended placing a 24-in. thickness of 12-in. riprap on both sides of the wall around the tips, extending a minimum of 50 ft back along the breakwater from the two ends. HEC's final recommendation was to monitor seabed elevations adjacent to the breakwater after construction to ensure that scour depth allowances used in design are not exceeded. They noted that riprap scour protection designed according to Dr. Ariathurai's recommendations could be placed later if scouring problems appeared.

Design review comments presented as Appendix E of the GDM indicate that considerable discussion on the subject of scour and its effect on breakwater design took place following the appearance of HEC's report. Although the figure showing maximum likely scour depths was presented in the GDM, the end result, as stated in Appendix A of the GDM, was that a design scour depth of 10 ft was assumed for the bayward (outer) side of all breakwater elements. The GDM's estimated Operation & Maintenance costs included a one-time cost of $100,000 for placement of riprap scour protection, to be used if scour developed beyond the 10-ft design scour depth.

The site is described in USACE HEC (1984a) as "a net depositional area probably with a low rate of deposition." In discussing the need for maintenance dredging, the GDM refers to HEC's scour evaluation, stating "comparison of existing conditions to those conditions with the project indicate that sufficient current velocity during flood tide will be maintained so as to not exacerbate sedimentation. Based on these studies no maintenance dredging above historic maintenance requirements is anticipated." Later in Appendix A of the GDM, the authors state "investigations indicate that deposition amounts due to the breakwater will be of the same volume as are currently found in the area. However, the amounts due to the breakwater will probably have less impact on the area because the volume will be spread out over a large area and will be thinner on the harbor floor."

Structural loading and design

The focus of this section will be on structural loading, with particular emphasis toward the coastal engineer's point of view. Structural design of the breakwaters was in accordance with standard Corps of Engineers practice at the time of the GDM's publication. Structural engineering aspects of the design are discussed in greater detail in the GDM, which also includes consultants' design review comments and the Corps' responses in an appendix.

Loading conditions

Figure 22 (taken from Appendix A of the GDM) summarizes the critical wave and seismic loading conditions examined during the structural design of the breakwater. The "trough" and "crest" loading conditions assumed waves perpendicularly incident on the breakwater from both sides, forming standing waves and exerting a combination of hydrostatic and dynamic pressures. The trough cases assumed a standing wave crest occurred on the "lee" side of the wall while a standing wave trough simultaneously occurred on the "sea" side. The crest cases assumed the crest occurred on the sea side while the trough occurred on the lee side. The side facing the harbor was considered the lee side for all of the breakwater structures.

SPL divided the Fisherman's Wharf breakwater system into six sections for structural design. The detached breakwater was divided into four sections according to water depth and batter pile configuration. Section IV, the curving western part of the detached breakwater, has batter piles on the lee side only. The fifth and sixth design sections were the east and west segmented breakwaters, respectively (refer to Figure A1, which identifies the sections and the boundaries dividing them).

The GDM states that both mhhw (=5.9 ft mllw) and mllw (0.0 ft) swl conditions were examined in determining the wave loads. The table at the bottom of Figure 22 lists the individual standing wave heights and periods used in the calculations. Note that separate wave conditions were chosen for each side of the wall. The wave condition normally used in Corps of Engineers practice for design wave loading on rigid structures is H_1, the average of the highest 1 percent of all waves, with period T_s. Since in the case of perpendicular wave incidence the (non-breaking) standing wave height from linear theory is twice the incident wave height, one can deduce that incident sea-side wave height for Sections I, II, and III was 8.0 ft (the H_1 height for the NNE direction, from Table 1). Similarly, the Section IV conditions used H_1 of 6.8 ft for the NW direction. The GDM does not discuss the rationale underlying the choice of the lee-side wave conditions, or the lower sea side standing wave heights for the segmented breakwaters. Given the orientation of the segmented breakwaters relative to the possible wave incidence directions, the influence of nearby structures, the effects of the gaps in the breakwaters, etc., it was less clear how their design wave conditions should be determined. Presumably engineering judgment came into play in selecting these other wave conditions.

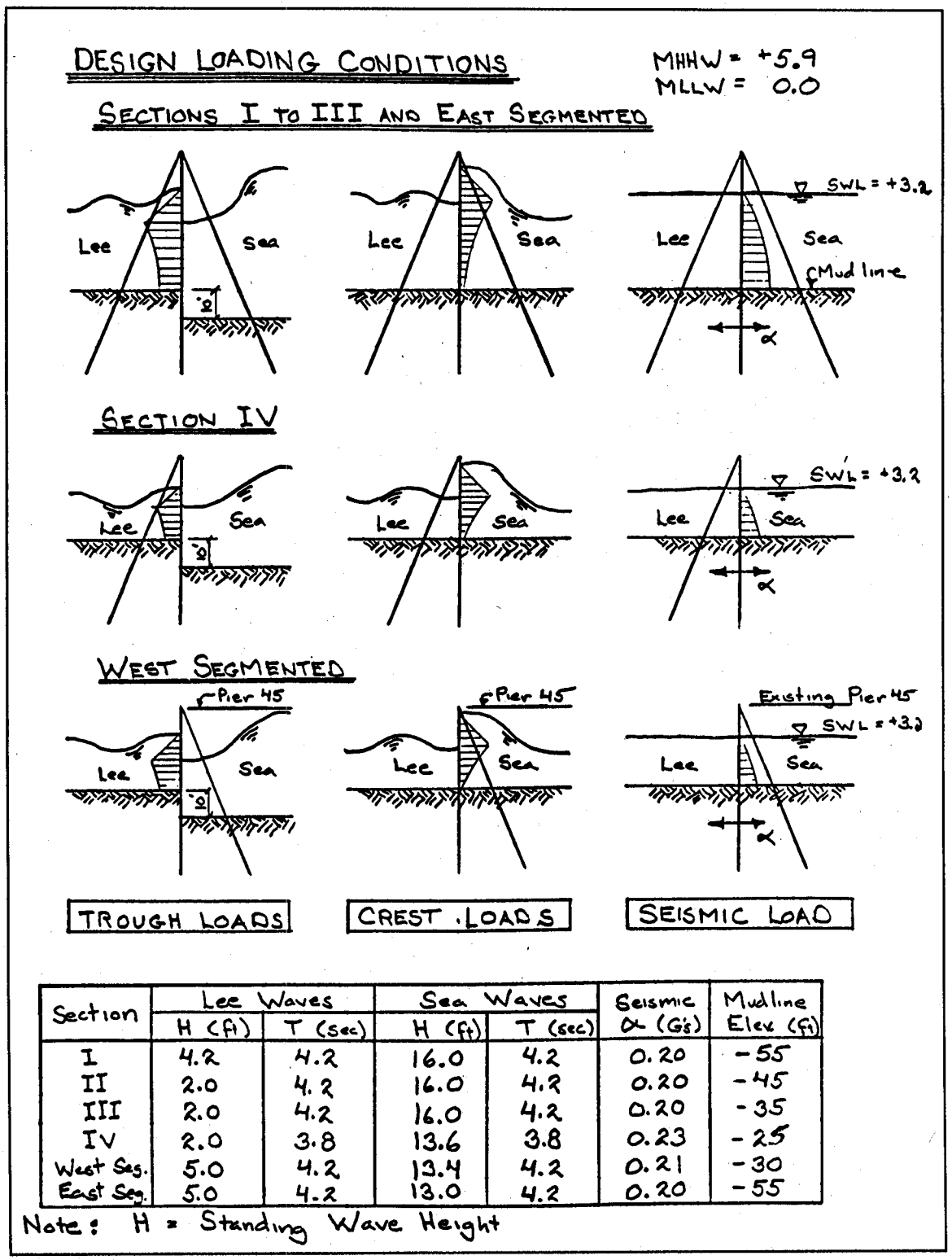

Section	Lee Waves		Sea Waves		Seismic	Mudline
	H (ft)	T (sec)	H (ft)	T (sec)	α (Gs)	Elev (ft)
I	4.2	4.2	16.0	4.2	0.20	-55
II	2.0	4.2	16.0	4.2	0.20	-45
III	2.0	4.2	16.0	4.2	0.20	-35
IV	2.0	3.8	13.6	3.8	0.23	-25
West Seg.	5.0	4.2	13.4	4.2	0.21	-30
East Seg.	5.0	4.2	13.0	4.2	0.20	-55

Note: H = Standing Wave Height

Figure 22. Design loading conditions (from GDM). The mudline elevation of -25 ft for Section IV differs from a value of -27 ft used in Figure A4

Mudline elevations

The six design mudline elevations (referenced to mllw) listed at the bottom of Figure 22 were selected from existing seabed profiles (shown in Figure A1) from the baseline bathymetry. Design mudline elevations approximately equaled the deepest point on the seabed profile within each of the six design sections. The assumed scour depth of 10 ft on the bayward side of all breakwater elements was applied in determining sea-side mudline elevations in the trough loading cases only. A locally flat seafloor was assumed on both sides, i.e., the mudline elevation was the same at the base of the wall sheet piles and the adjacent batter piles.

Wave forces

SPL computed wave pressures for each of the wave loading conditions using the computer program described in the foregoing discussion of overtopping. The program provided pressures from both the Sainflou and Miche-Rundgren methods for non-breaking waves. Since results of the two methods differed, SPL decided, after consultation with CERC, to use the Sainflou results for wave crest pressures and the Miche-Rundgren results for the trough pressures. Although breaking wave forces can be much higher than those from non-breaking waves, water depths at all parts of the breakwater were theoretically sufficient to preclude breaking of the design waves.

Earthquake design

Seismic loading on the breakwater was calculated in accordance with standard Corps of Engineers earthquake design practice at the time, which required seismic coefficients (maximum ground accelerations) be no less than 0.20 g. The table in Figure 22 lists the actual seismic coefficients used, which varied by design section. The coefficients resulted from a seismic analysis contracted to Geotechnical Consultants, Inc. (1984). They correspond to a 6.5 Richter-magnitude design earthquake along the San Andreas Fault, which passes within 9 miles of the breakwater site. This design earthquake has an estimated 50 percent probability of occurrence during the 50-year design life of the structure. The seismic analysis also looked at liquefaction potential of the sediments at the site and the likelihood of ground rupture due to underlying faults. Liquefaction potential was deemed very low for the bulk of the sediments present, with the exception of some lenses of relatively loose, clean sands within the Younger Bay Muds. However, damage to the breakwater was felt to be unlikely, since the piles penetrate into the Bay Side Sands and Older Bay Muds, which have low liquefaction potential. Since no active or potentially active faults underlie the site, ground rupture was deemed unlikely.

The seismic loading condition of Figure 22 considered horizontal earthquake acceleration in both directions with an swl of +3.2 ft mllw. Resulting dynamic water pressures were determined using Westergaard's theory.

The GDM does not discuss which of the loading conditions governed the structural design, or whether wave or seismic forces dominated. Considering the likelihood of the simultaneous circumstances required to produce some of the wave loading cases shown in Figure 22, it appears that wave-induced stressing of the breakwater to design limits may be a very infrequent occurrence.

Pile design

Six size classes of piles were designed, corresponding to each design section (see the Pile Schedule table at the upper right of Figure A4). All piles in each class have the same length and cross-sectional dimensions. The effects of the assumption of an additional bayward side depth of 10 ft due to scour were increases in pile length ranging from 8 to 20 ft, and increases in the amount of reinforcing steel needed to resist the greater moments. In order to minimize settlements, the sheet-pile tips were required to penetrate a minimum of 10 ft into the Bay Side Sands layer.

Uplift loads

Due to the use of a beveled cap configuration, wave uplift loads were subordinate to other loadings which governed the design of the cap tie beam. Wave uplift forces of 450 lb/sq ft were, however, included in the design of the circular platform at the western end of the detached breakwater. Other loading conditions included in the platform design included live load of 100 lb/sq ft (not acting simultaneously with the uplift load) and seismic load from a horizontal acceleration of 0.20 g.

Structural details and plans of the as-built breakwater are included in Appendix A of this report.

3 Monitoring Program

Monitoring Objectives

SPN and CERC jointly developed a monitoring plan during the first year of the Fisherman's Wharf MCCP study. The stated overall objective of the MCCP study was to monitor and evaluate the performance of the completed breakwater and its impact on the surrounding area. Furthermore, the study was to provide data with which to evaluate the various models used to predict post-construction conditions, and to determine the effectiveness of the pre-construction modeling activities. Several elements of the monitoring plan were included to address concerns raised by SPN, the Port of San Francisco and its consultants, and local interests during the breakwater design and review process. The monitoring plan listed the specific objectives to be investigated as follows:

a. Document wave attenuation of the structure compared to the model studies and design criteria.

b. Evaluate the effect of the structure on surge within the harbor complex.

c. Determine the effect of the structure on water circulation within the harbor and surrounding areas and currents, especially at the entrance.

d. Determine the actual scour. Measure the scour, evaluate the cause, and compare with the predicted scour.

e. Evaluate the effect of the structure on the littoral process, including shoreline response and deposition within the harbor.

f. Monitor the structural integrity of the structure, investigating spalling, cracking, and settlement of the wall.

Criteria for Evaluation of Success

The monitoring plan also specified a set of performance criteria for use in evaluating the success of the structure and its design, as follows:

Feature	Limiting Criteria
Waves	
• Boat Basin	Not to exceed 1.0 ft.
• Hyde Street pier	Not to exceed 1.5 ft.
• Entrance Channel	Not to exceed 2.5 ft.
Surge	No increase in surge.
Currents	Not to exceed 2 knots in the entrance channel.
Scour	Must be within the design scour depth of 10 ft along the wall.
Beach Erosion	Does not increase net sediment loss to the Aquatic Park littoral system.
Circulation	Does not impact shoaling rates to the point of requiring maintenance dredging.
Alignment	Vertical and horizontal alignment changes, visual cracking and spalling not sufficient to impact the function of the structure.

Prototype Data Collection, Analysis, Comparisons, Interpretation

Like any engineering project extending over several years, the objectives, evaluation criteria, and approach to monitoring laid out in the joint monitoring plan underwent changes as the MCCP study progressed. Certain plan elements were found to be too ambitious with respect to cost, logistical complexity, or technical feasibility. Some of the monitoring objectives set out in the monitoring plan had to be modified. The performance and evaluation criteria, however, were generally acceptable as originally stated. In keeping with the evolution of the overall MCCP research program (Fisherman's Wharf was just one of several simultaneous studies), an increased emphasis was placed on the critical review of design procedures and tools, and on providing information useful for planning of Operation and Maintenance and prevention of problems needing later repair.

This section of the report is organized by subsections, each of which discusses an element (physical process or feature) of the MCCP prototype monitoring effort at Fisherman's Wharf. Within each subsection, monitoring objectives and the approach to data collection and analysis are described first.

Results, including comparisons with baseline data and design predictions, follow. Interpretations and specific conclusions are included, forming the basis for Chapter 4, "Summary, Evaluation, and Recommendations."

Waves

Although the preceding monitoring objectives refer to "waves" and "surge" separately, the separation between the two is somewhat arbitrary from a monitoring standpoint, since surge is simply a lower-frequency wave phenomenon. The SPM defines surge as "the name applied to wave motion with a period intermediate between that of the ordinary wind wave and that of the tide, say from 1/2 to 60 minutes. It is low height; usually less than 0.09 meter (0.3 foot)....See also SEICHE." The SPM defines seiche as "(a) standing wave oscillation of an enclosed waterbody that continues, pendulum fashion, after the cessation of the originating force, which may have been either seismic or atmospheric; and (b) an oscillation of a fluid body in response to a disturbing force having the same frequency as the natural frequency of the fluid system...." "Harbor oscillation" is another term used for the phenomenon. The Fisherman's Wharf study area is only partially enclosed; thus, the water surface variations measured within included a mix of wind-wave frequencies and lower surge frequencies. The prototype gaging technology was similar for both, with the difference being in the sampling scheme and the data processing approach.

Monitoring objectives for waves and surge. Primary objectives stated in the monitoring plan can be reformulated as the following simple questions:

a. Have post-breakwater (post-BW) wave heights been within criteria?

b. Has surge increased as a result of the breakwater?

Going beyond just answering these questions, secondary objectives of the monitoring were as follows:

a. Quantify the wave attenuation of the breakwater.

b. Compare the prototype results to the predictions of the numerical surge model and physical model.

c. Compare the design wave conditions with prototype conditions experienced by the breakwater.

d. Suggest improvements in Corps coastal engineering tools and the way they are used, including improvements to prototype gaging for monitoring and evaluating project performance.

Data collection. The Corps of Engineers contracted with SIO to conduct prototype measurements of waves and surge at Fisherman's Wharf from December 1982 through December 1989. SIO's measurements from five sensors at four locations during the pre-breakwater period and corresponding

analyses supporting the breakwater design process have been described previously in Chapter 2.

Table 3 provides names and characteristics for all of SIO's prototype wave gages in the Fisherman's Wharf study area from December 1982 to December 1989. Gage depths shown in Table 3 have been approximately corrected to reference the mllw datum. SIO provided measured gage depths, computed as the long-term average height of the water column above the sensors. The mean tide level (+3.1 ft mllw) was assumed to be at approximately the same elevation as the long-term average water level (the two levels may not have been at exactly the same elevation, however). Depths listed in Table 3 were computed by subtracting 3.1 ft from the depths provided by SIO. Figure 23 shows the gage locations and wave height criteria. Figure 24 graphically depicts the gaging coverage over time. Figure 24 is accurately scaled with respect to time. Horizontal bands indicate periods in which usable data were obtained, rather than simply periods when gages were in place. All gaps in useable data longer than 7 days are indicated. All wave data are archived at SIO.

Table 3
Prototype Wave Gage Names and Characteristics

Name	Sensor Type	Depth ft	Interrogation Interval hr	Sample Rate Hz	Samples Per Record	Samples Analyzed
Alioto's	Surge	11.3	6	0.125	2,048	2,048
Alioto's Wharf	Energy	8.5	6	1.0	1,024	1,024
Alioto's Wharf	Surge	8.5	6	0.125	2,048	2,048
Municipal pier	Energy	29.0	6	1.0	1,024	1,024
Hyde St. pier	Surge	18.6	6	0.125	2,048	2,048
Pier 47	Energy	13.1	6	1.0	1,024	1,024
Pier 47	Surge	13.1	6	0.125	2,048	2,048
Pier 45	Energy	11.4	6	1.0	1,024	1,024
Pier 45	Surge	11.4	6	0.125	2,048	2,048
Incident	Energy	41.6	3	1.0	8,192	1,024
Basin	Energy	21.5	3	1.0	8,192	1,024
Basin	Surge	21.5	3	0.125	2,048	2,048

The Pier 47 surge and energy sensors ended data collection during July 1984. The Hyde Street pier surge sensor and the Municipal pier energy sensor ended data collection during October 1984. The surge sensor at the Alioto's location continued collecting data throughout breakwater construction and the post-breakwater (MCCP) period. In March 1986, part way through the

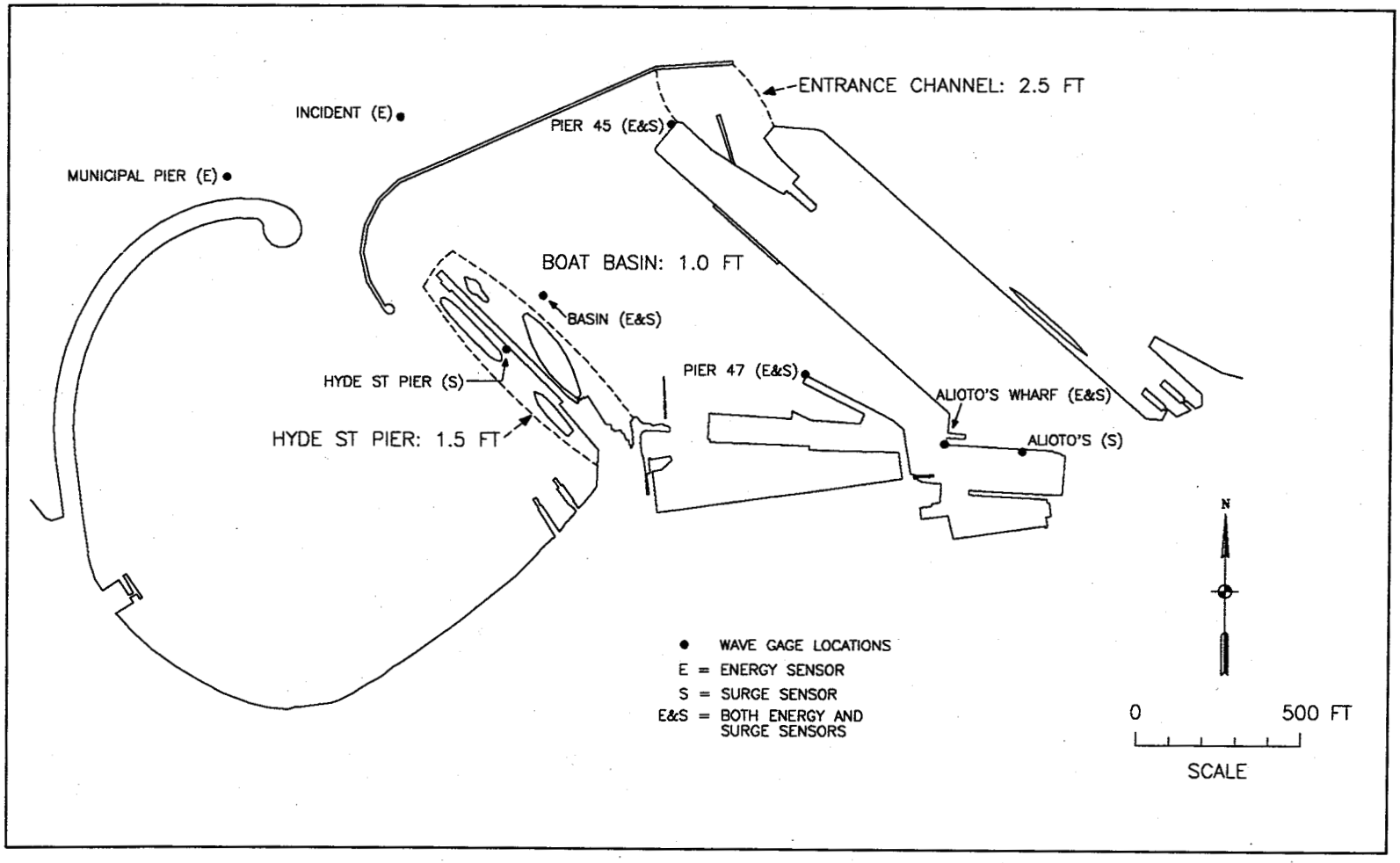

Figure 23. Prototype wave gage locations

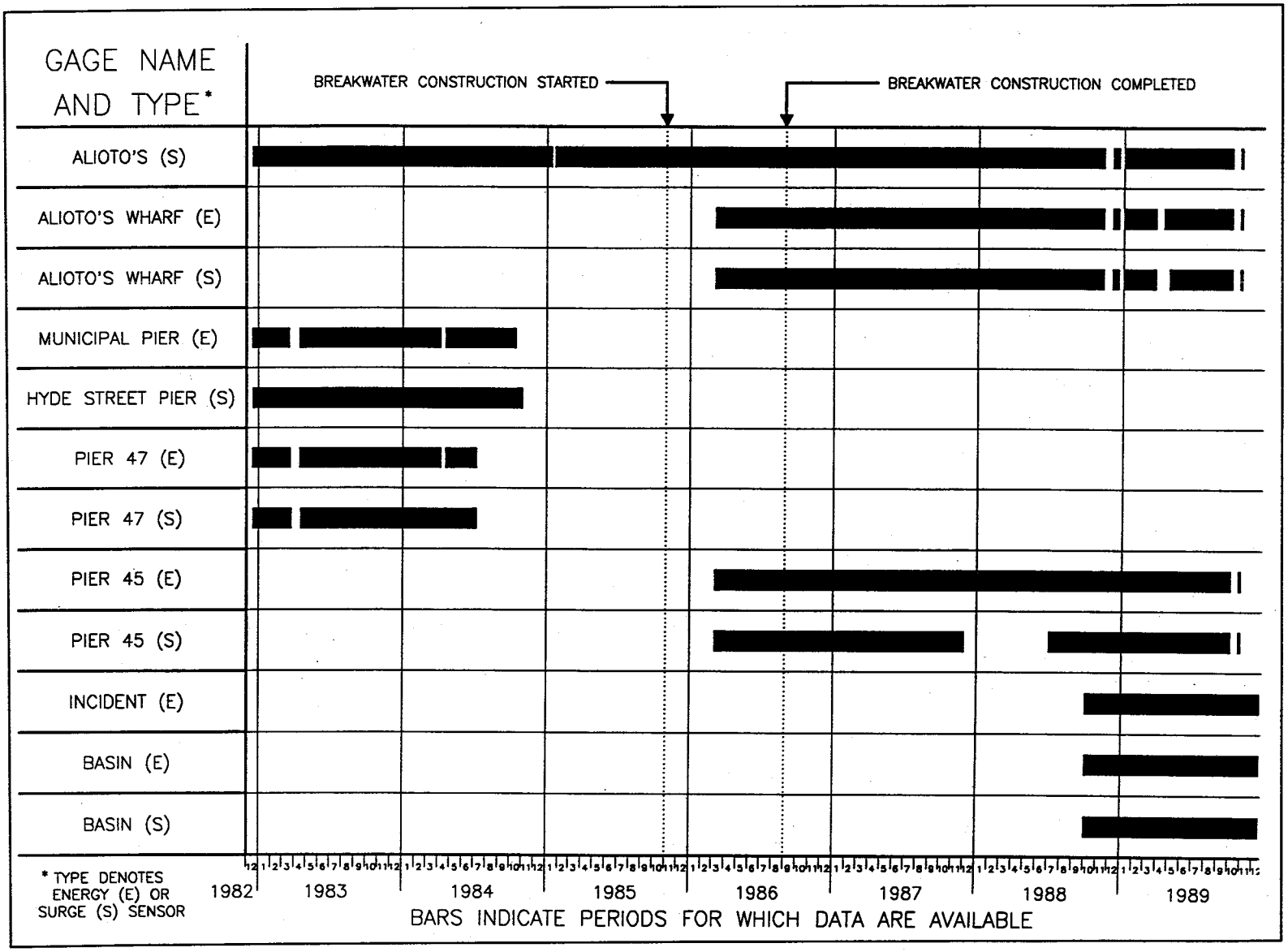

Figure 24. Prototype wave gaging coverage

construction of the breakwater, two new gage locations were added, one several hundred feet west of the Alioto's surge sensor, and the other at the end of Pier 45 (denoted Alioto's Wharf and Pier 45, respectively). Both locations measured surge *and* energy. SPN funded SIO's installation of the gages in order to have a record of wave conditions during the remaining construction for evaluation of claims by the pile-driving contractor about the effects of wave conditions on construction operations. CERC was involved in arranging for SIO's services, and was interested in wave measurements in the Fisherman's Wharf area because the Corps breakwater was in the process of being approved for study under the MCCP research program.

After breakwater completion, SIO established two more gage locations in the fall of 1988, to the east of Hyde Street pier in the basin, and bayward of the western part of the detached breakwater (denoted Basin and Incident, respectively). Energy measurements were taken at both locations; the Basin location also measured surge. SIO installed these CERC-funded gages specifically to collect data for the MCCP study. The Incident gage was intended to monitor the incoming wave climate, while the Basin gages would provide the climate in the basin and future berthing expansion area. CERC also funded the continuation of data collection at the Alioto's Wharf and Pier 45 surge and energy sensors as well as the Alioto's surge sensor. By the end of 1989, all prototype wave data collection had ended.

Later, CERC contracted SIO to perform data processing and analysis of the cumulative data set, and to provide a report for the MCCP study. Selected figures from SIO's report are included as Appendix C herein.

Decisions concerning sensor type and siting of the earlier gages were largely guided by the needs of the breakwater designers, and then later by the needs of construction monitoring. With the onset of the MCCP study, the emphasis shifted toward documenting completed breakwater performance and providing information for comparison with models.

All wave gages at Fisherman's Wharf were pressure-sensor based. Wave gaging by the indirect method of measuring subsurface pressure fluctuation is a well-established technique; a thorough discussion of the technology and data analysis is beyond the scope of this report. In brief, the pressure sensor detects fluctuations in water pressure at a known depth. Sensor output is recorded through time, resulting in a pressure time series. Measured pressure includes both hydrostatic and dynamic components, resulting from the instantaneous height of the water column above the sensor, and the acceleration of the water mass, respectively. The wave pressure spectrum (distribution of energy density by frequency of pressure fluctuation) is computed using standard time-series analysis techniques (Fourier analysis) which transform measured time-domain information into frequency-domain (spectral) information. The Fourier transformation procedure used has become relatively standardized, and was similar to that used at CERC. The wave pressure spectrum is converted to a wave height (or amplitude) spectrum via a frequency-dependent pressure response factor (also known as depth attenuation factor) derived from linear wave theory. (Refer to Chapter 2, Section II.3.f. of the SPM for a derivation

of the pressure response factor and an example problem.) Typically, wave data analysis results are presented as a plot of the energy spectrum, where the vertical (energy) axis has units of length squared, rather than as a wave height or amplitude spectrum, where the vertical axis has length units.

Because the degree of wave pressure attenuation increases with both depth and frequency, there are limits on how deep a pressure sensor can be mounted for accurate measurement of waves, particularly short-period waves such as the locally generated wind waves encountered at Fisherman's Wharf. Attachment of sensors to existing pilings has the advantages of lower installation cost, easier relocation and serviceability, flexibility in choosing sensor depth, and good protection of sensors and cables from boat anchoring and construction operations. Deployment of sensors on bottom-sitting mounts with shore cables strung along the seabed has the advantage of siting flexibility, provided that depth attenuation of wave pressure fluctuation can be kept within acceptable limits. At Fisherman's Wharf, pile mounting was used for sensors at the Alioto's, Alioto's Wharf, Pier 45, Pier 47, and Hyde Street pier locations. The sensors were installed by divers. Sensors at the Municipal pier, Incident, and Basin locations were mounted on bottom-sitting tripods deployed by a crane from the SPN debris-removal vessel *Grizzly* (Figure 25). Divers assisted in deploying, servicing, and retrieving the tripod-mounted gages. All sensors were hard-wired to above-water shore stations via telemetry cables.

An alternative approach would have been use of self-contained recording gages. The hard-wired gage approach has the advantage that one can determine remote site wave conditions in near real-time, and gage malfunctions can be detected and corrected promptly. Self-contained gages available at the time of the Fisherman's Wharf study would have required relatively frequent site visits by divers to service gages and retrieve data stored on cassette tapes. In the event of self-contained gage malfunction, large gaps in coverage can occur. SIO's experience using hard-wired remote gaging technology made it the most reliable, flexible, and cost-effective approach at Fisherman's Wharf.

Each shore station consisted of a data-logging system and telephone connection to SIO's central computer processing and archival facility in La Jolla, California. The data logger included a memory buffer that stored the most recent telemetered data coming in from the sensors. The central computer telephoned the shore stations at regular intervals, initiating the transfer of the buffer's contents to the computer for subsequent processing and storage. SIO has used this automated approach for many years to operate a large remote network of Pacific coast wave gages, of which Fisherman's Wharf was just one part. (Refer to Seymour, Sessions, and Castel (1985) for a description of the automated SIO system.)

Site selection for most of the sensors was straightforward because of the abundance of pilings in the area. The selection of the incident gage type and location was more difficult, and required compromise. Considerations included budget, vessel traffic, vandalism, available inventory of components, influence of reflections off the vertical wall breakwater, and existing bathymetry. In a situation where the intention is to measure the incident wave climate

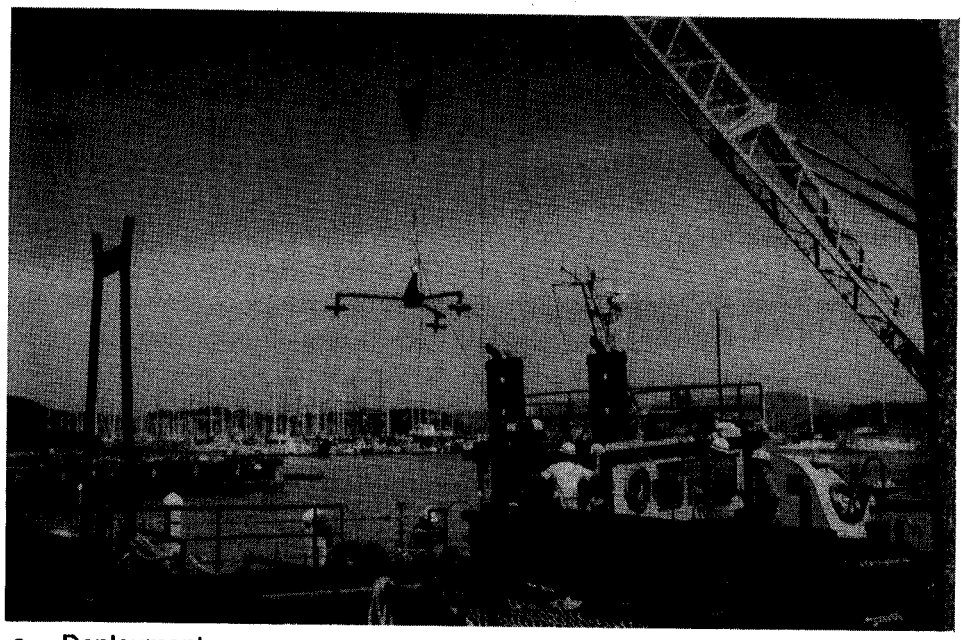

a. Deployment

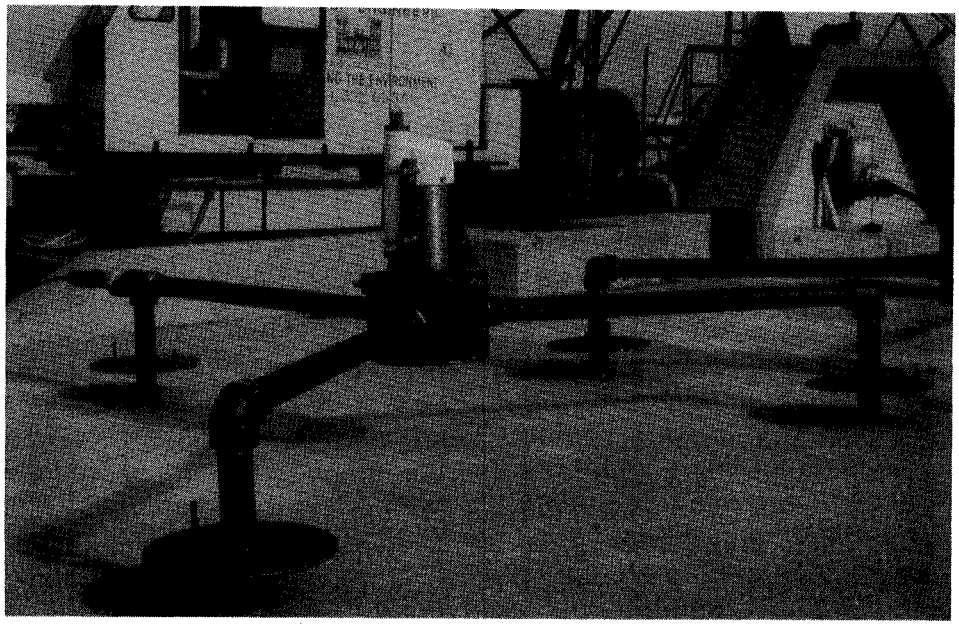

b. Close-up of tripod--pressure sensor is at center

Figure 25. Pressure sensor tripod installation

approaching a vertical wall structure, ideally one would measure the directional characteristics of the wave field in addition to the wave heights. The gage would be sited far enough away from the wall to avoid significant reflected wave energy, and the area between the gage and the wall would have a flat seabed to minimize distortions of the wave field induced by irregular bathymetry. Due to budgetary constraints, a directional gage was ruled out. Also, a visual observations program (discussed in a later section) was planned, to include estimated wave incidence directions, particularly during storm events. Remaining options included either a surface-following buoy (e.g., Waverider type) or a tripod-mounted pressure sensor. The buoy option was also ruled out. No reasonably safe buoy location was available, given the high vessel traffic zone just bayward of the breakwater. Also, existing buoys are not well-proven for use with short moorings in a shallow-water, short-period wave environment. Given the expected wave climate, a bottom-sitting pressure sensor would have to be sited in depths less than about 50 ft in order to resolve wave energy at frequencies as high as 0.25 Hz (4-sec period). Inspection of existing bathymetry revealed that it would not be possible to locate the tripod in sufficiently shallow depths without also being within the zone of reflected wave influence. Displacing the gage site westward or eastward (away from directly bayward of the breakwater) would also be unsatisfactory, given the complexity of the bathymetry and the logistical problems posed by a long telemetry cable along the seabed. Therefore the incident gage was sited approximately 170 ft bayward of the detached breakwater at a depth of about 42 ft, with the telemetry cable brought in to the Hyde Street pier.

Sensor sampling schemes were designed with an intention to measure waves in the two frequency regimes of interest: wind waves and swell, from 0.50 Hz to 0.0625 Hz (periods from 2 sec to 16 sec), and surge, from 0.0625 Hz up to tidal frequencies (periods from 16 sec to several hours). Continuous, around-the-clock wave data collection is seldom conducted in coastal engineering practice due to the enormous amounts of data that result and because wave conditions on the open coast usually change gradually. Typical data collection schemes sample intensively for relatively short durations, separated by intervals when no data are collected. At Fisherman's Wharf, sampling schemes for sensors installed prior to the MCCP study (all except those at Incident and Basin locations) were as follows. Energy (i.e., wind, wave, and swell) sensors were sampled at 1 Hz obtaining a total of 1,024 data points per "burst" (time interval of sequential data collection), thus collecting one instantaneous measurement of pressure every second for about 17 min. Since the central computer interrogated the energy shore stations four times daily, data representing a 17-min time series "snapshot" of the wave activity were transferred for processing every 6 hr. Note that at a 1-Hz sampling rate, the shortest wave period reliably resolved is typically taken to be 4.0 sec. Surge sensor outputs were first low-pass filtered to remove frequencies higher than 0.0625 Hz (16-sec period), then were sampled at 0.125 Hz (every 8 sec), obtaining 2,048 data points per burst. Under the same data transfer schedule, 4.55 hr of sequential surge data were obtained every 6 hr.

Somewhat different sampling schemes were implemented for the sensors at the Incident and Basin locations. Their shore stations were interrogated every

3 hr. The surge sensor output was not low-pass filtered. Otherwise, the Basin surge sensor was sampled in the same fashion as the other existing surge sensors. A sample rate of 1 Hz was used for the energy sensors at the Incident and Basin locations. Bursts of 2.27-hr duration (8,192 data points) were collected at these latter sensors. Analysis procedures for the Incident and Basin energy sensors used only 17 min of the burst, however, conforming to the burst length analyzed for all other energy sensors. Table 3 summarizes sampling and interrogation parameters for all of the Fisherman's Wharf wave sensors.

Data processing and analysis. SIO subjected incoming wave data to quality assurance procedures upon transfer to the central computer center. Many data screening procedures were performed automatically by computer processing algorithms which recognized certain classes of anomalies, correcting some, and rejecting others as instances of bad data. A list of some of the more common types of errors that could be detected is given in Seymour, Sessions, and Castel (1985).

After completing the data quality assurance step, SIO performed the analysis processing, including removal of tidal fluctuations, Fourier transformation, and pressure depth attenuation correction, leading to distributions of energy versus wave frequency (energy spectra). The long-term averaged water level from each sensor defined its depth used for attenuation correction. The analysis provided a separate energy spectrum for each burst of wave data. The energy spectrum was specified by reporting energy contained within discrete frequency bands of limited width. Significant spectral wave height (H_s) was then calculated as four times the square root of the total energy content in the burst record. (Recall that the total energy content of an energy spectrum is given by the area under the curve). The peak period T_p of a burst record is defined as the period corresponding to the central frequency of the frequency band containing the highest wave energy in the record. Individual burst energy spectra are not presented in this report or SIO's contract report (they analyzed a total of approximately 41,000 burst records in preparing their report). However, to properly interpret the meaning of significant wave height and peak period results discussed in subsequent sections, the reader should be aware of the manner in which energy spectra were calculated. For energy sensors, the total energy content used in computing significant wave height came from the period range 4 to 2,048 sec, divided into the following period bands (sec): 4-6, 6-8, 8-10, 10-12, 12-14, 14-16, 16-18, 18-22, and 22-2,048. For surge sensors, the total energy content range was from 16 to 9,999 sec divided into the following period bands (sec): 16-21, 21-26, 26-31, 31-36, 36-46, 46-51, 51-56, 56-61, 61-73, 73-85, 85-102, 102-128, 128-171, 171-256, 256-512, and 512-9,999. Thus, the spectra for the energy and surge sensors have a certain amount of overlap in frequency coverage. Because of this fact, the reported significant wave height for an energy sensor was, in some instances, primarily associated with long-period energy in the 22- to 2,048-sec band. In interpreting reported wind wave and swell significant wave heights, it is therefore sometimes necessary to dig deeper and look at the spectral information to determine which frequencies contained the bulk of the energy.

In order to evaluate the effects of the breakwater, SIO had to select a date separating the gaging period into data sets representing the pre- and post-breakwater construction periods. The construction of the detached breakwater started from the west end in November 1985. About half of its length was in place by the end of June 1986. The remainder of the detached breakwater and the segmented breakwaters had been essentially completed by the end of August 1986. In early stages of completion, the breakwater probably had only minor effect on the interior wave climate; therefore, July 1, 1986, was taken as the data set dividing date. Note that as a consequence of this choice, about four months of the data sets from the Alioto's Wharf and Pier 45 sensors (installed in March 1986) were classified as pre-breakwater data.

Results of monitoring and comparisons with design and models. In Appendix C, Figures C1 through C42 plot the variations of significant wave height (H_s) throughout the prototype gaging period for each of the sensors. Surge time-series plots are arranged in order from most-interior gage to most-exterior gage. Energy time-series plots are arranged in the converse manner. The continuous lines in these time-series plots connect H_s values computed individually for each burst record. Apparent gaps in the time-series records (other than those shown in Figure 24) indicate instances of no data or invalid data, due to malfunctions of the sensor or telemetry system, or rejection by the data quality screening procedures. Recall that the analysis process results in only a single significant wave height (and peak period) being associated with each measured burst. For bursts with multiple peaks of energy at different frequencies, the peak period was assigned to the highest energy peak, and the significant wave height value was computed from the total energy including all the peaks. Thus, for events when both ocean-generated and locally generated waves simultaneously affected the site, the significant wave height and peak period are somewhat unsatisfactory descriptors of the actual wave activity. This is an inherent shortcoming of the "standard" measured wave data analysis procedure, and should be kept in mind by anyone planning a prototype wave measurement program at sites where simultaneous wave trains from fundamentally different generating areas can occur.

Review of the time series plots revealed that at some locations, surge significant wave heights were of comparable magnitude to energy sensor significant wave heights. For example, the H_s time series for the surge and energy sensors at Alioto's Wharf are very similar with the exception of the most severe events, when the energy sensor's peaks were generally higher. The Alioto's surge sensor also measured surprisingly large significant wave heights--values greater than 1 ft were not uncommon. Part of the reason for these similarities between surge and energy time series is the overlap in frequency coverage; i.e., often the two sensor types were measuring waves in the same part of the frequency spectrum. One should remember that because the surge sensors were measuring waves of long period, the water surface elevation change was slow. Surge "wave height" is a somewhat confusing terminology, since one normally associates wave height with a much shorter- period (and readily visible) change in water surface elevation. Nonetheless, large surge significant wave heights can be critical for design of vessel moorings and floating berthing facilities, particularly since relatively strong and long-

duration horizontal water motions can occur even when surge wave height is low.

Scrutiny of the surge time-series plots (Figures C1 through C24) gives a qualitative indication of the spatial variability of surge activity around the study area. Looking at 1983 data from the pre-breakwater (pre-BW) period, surge significant waves at Alioto's were highest, followed by Pier 47, with Hyde Street pier the lowest. Surge significant waves for 1989 (post-BW) were highest at Alioto's and Alioto's Wharf (which match closely), followed by Basin, with Pier 45 the lowest. Thus it appears that the interior corner near Alioto's was a zone of relatively high surge both before and after breakwater construction.

The Alioto's surge sensor is the only one that operated over a long portion of both the pre- and post-BW periods. No general trend of increased or decreased surge significant wave heights can be seen. Similarly, no evidence of breakwater-induced change can be detected from the plots for the two surge sensors installed in March 1986 (Alioto's Wharf and Pier 45).

Looking at the time series of wind-wave and swell significant wave heights for the energy sensors in the early pre-BW period (Figures C25 through C42), plots for Municipal pier and Pier 47 are nearly identical. This suggests there was little spatial variability of wind-wave and swell significant wave heights throughout most of the study area prior to the presence of the breakwater.

Comparing plots for all four of the post-BW energy sensors (e.g., during 1989), the Incident location had the highest significant waves, followed by Basin, then Alioto's Wharf, with Pier 45 the lowest. Note that significant wave heights for the Incident sensor include reflections from the detached breakwater. The differences between plots for Alioto's Wharf and Pier 45 are slight. This pattern of spatial variability is consistent with the locations of the gages with respect to the breakwater and other sheltering structures.

No energy sensor operated for a long portion of both the pre- and post-BW periods. Perhaps a valid comparison can be made between the early pre-BW Municipal pier and post-BW incident records, however, because the two locations were close in proximity and similarly exposed to the incoming waves. Generally their significant wave height time series look similar, with the incident gage's record showing slightly greater heights. If differences in the characteristics of the two gages (depth of sensor, influence of reflected waves, nearby bathymetry, etc.) and differences in the length and timing of gaging coverage can be considered negligible, one might conclude that the pre- and post-BW periods experienced similar incident wave heights. Note that while the Incident gage record very likely included influence of reflections from the breakwater, Municipal pier has a partial wave baffle system underneath that also likely reflected some short-period energy to influence the adjacent sensor.

Comparison of wind-wave and swell time series at Alioto's Wharf versus Pier 45 (both gages installed March 1986) gives some indication of the effects

of the breakwater on wave heights, because the two gages' records cover the same time period. Significant waves were initially higher at Pier 45. After the breakwater was completed, the situation reversed as wave heights at Pier 45 generally dropped, while those at Alioto's Wharf remained about the same.

The primary usefulness of the time series plots is for examining qualitative aspects of the wave climate record. They show spatial variations within the study area, passage of "events" (storms), and seasonal variations. Typically the most energetic wave activity at Fisherman's Wharf occurs during late fall, winter, and early spring. At some locations (for example, the Municipal pier and Incident gages) the influence of variations in tide range can be seen as oscillations in the time series, corresponding to daily, fortnightly (spring-neap), and annual cycles. This water level influence occurs because higher water levels allow greater penetration of ocean-generated energy through the Golden Gate.

SIO also developed two types of cumulative statistics for the energy sensors: joint distributions of height and period, and cumulative distribution functions for significant wave height. These products provide another dimension of information about the measured waves, that is, the spread of energy across the frequency range. Figures C43 through C58 are the joint distribution tables and corresponding three-dimensional figures (conveying the same information as the tables) for each energy sensor. The figures are grouped by sensor location in the same order as in Table 3. When a sensor only operated in the pre-BW period or only operated in the post-BW period, a single joint distribution table and figure set were produced. For the energy sensors at Alioto's Wharf and Pier 45, two sets were made, one for March-June 1986 (pre-BW), and the other for the post-BW record.

Joint distributions were formed from the many individual energy spectra by counting the number of occurrences of particular combinations of significant wave height and peak period. The three-dimensional figures indicate number of occurrences as height of the plotted surface. Each figure gives a visual indication of which period and height combinations were most common over the long term at that location. For example, Figures C47 and C48 indicate that in the pre-BW period, the most commonly experienced waves at Municipal pier were at the high frequency end of the spectrum (around 5-sec periods) with significant heights on the order of 0.5 ft. In contrast, Figures C43 and C44 show a prevalence of small significant wave heights at long periods (greater than 22 sec) at Alioto's Wharf. Figures C55 and C56 show that the Incident gage had frequent occurrences of both short- and long-period waves. Note that the vertical scale is not the same on all of the figures. Also, since the joint distributions only show occurrence, and since no energy sensor operated for a long part of both the pre- and post-BW gaging periods, the three-dimensional figures are not very useful for determining effects of the breakwater.

It can also be seen that the relatively large significant wave heights at the Alioto's Wharf energy sensor were in fact associated with long-period energy. The comparison between the Alioto's Wharf and Pier 45 time series revealed

the somewhat puzzling trend of significant heights remaining high at Alioto's Wharf, while dropping at Pier 45 as the breakwater was completed. The additional information provided by the joint distributions shows that this behavior was primarily due to the fact that at Alioto's Wharf, energy at the ordinary wind-wave frequencies was relatively low even before the breakwater was built. The bulk of the energy at that location was nearly always in the highest band, 22-2,048 sec; consequently, most of the plotted significant wave heights were actually for waves in the surge frequency regime. In contrast, at Pier 45, much more of the energy was distributed into the higher frequencies normally associated with wind waves (which the breakwater attenuates more effectively).

Figures C59 through C66 present sets of cumulative distribution function plots for significant wave height at each energy sensor. Separate plots were produced for pre- and post-BW data sets, as was done for the joint distributions. The figures are ordered by gage location as in Table 3. The wave height distribution functions indicate how often a particular significant wave height was exceeded during the gaging period. For example, in Figure C59, it is seen that significant wave heights greater than about 1 ft (0.3 m) were exceeded for less than 6 hr out of the pre-BW gaging period at the Alioto's Wharf location, whereas wave heights were greater than about 1 in. (0.03 m) throughout the gaging period. A stretched-out distribution indicates that large significant wave heights (or long peak periods) were infrequent, whereas a more vertical distribution resulted when large wave heights (or long peak periods) were relatively common.

Review of the distribution function plots confirms previously discussed trends noted from the qualitative review of the significant wave height time series plots. As before, comparing pre- and post-BW data sets to determine effects of the breakwater is hampered since long-term pre- and post-BW data sets are not available at any energy sensor location. Much of the difference between pre- and post-BW cumulative distribution functions (for example, at the Alioto's Wharf sensor) can be attributed to the differences in duration of the gaging period. The pre-BW gaging period for the two energy sensors installed in March 1986 is simply too short (much less than a year) to form a good basis for quantitative comparison with the corresponding post-BW record. Ideally, a *minimum* of one full year of observations should be obtained to characterize the wave climate at a location. To reduce bias that could result should the chosen gaging period be unusually calm or stormy, several years of record are preferable. Also, data sets being compared to determine pre- and post-structure effects should include the same length of gaged record, so that seasonal variations do not bias one of the two data sets. Perhaps the best available comparison to point out changes in the interior short-period wave heights due to the breakwater is between the pre-BW Pier 47 record and the post-BW Basin record. The joint distributions and cumulative distribution functions clearly show that short-period waves were substantially attenuated by the breakwater, while longer-period waves were not. Thus, in effect, the surge action became dominant at the Basin location once the breakwater reduced the incoming short-period wave action. Whereas the Boat Basin design wave height criterion of 1.0 ft was exceeded for about 1,050 hr out of the 19-month

pre-BW gaging record at Pier 47, the criterion was never exceeded during the 15-month post-BW record at the Basin location.

The wave height distribution functions from the post-BW period are useful for answering the question of whether wave heights inside the breakwater have met design criteria. Recall that Figure 18 shows the wave height criteria for various zones within the area protected by the breakwater.

The Alioto's Wharf energy sensor was well-situated to characterize short-period waves in the traditional Fisherman's Wharf small-craft berthing area. Figure C60 shows that the 1.0-ft (30-cm) design wave height criterion was exceeded for about 300 hr out of the approximately 11,900-hr (16-month) post-BW gaging record; i.e., about 2.5 percent of the time. Similarly, the 1.5-ft level was exceeded about 11 hr (less than 0.1 percent) of the time. However, it is misleading to call these exceedances wave height criteria violations. The joint distribution table (Figure C45) indicates that all the exceeding significant wave heights had corresponding peak periods in the 22- to 2,048-sec band, i.e., they were actually surges.

The Pier 45 energy sensor was located within the Boat Basin wave height criterion zone, yet it was near the (somewhat ill-defined) boundary with the adjacent Entrance Channel zone. The cumulative distribution function (Figure C64) shows that the 1.0-ft Boat Basin criterion was exceeded for about 12.5 hr out of the approx. 11,900-hr post-BW gaging record; i.e., about 0.1 percent of the time. The 2.5-ft Entrance Channel criterion was never exceeded in the post-BW period. However, from examination of the joint distribution table (Figure C53), all but one of the few 1.0-ft criterion exceedances were in the 22- to 2,048-sec band. The single wind-wave frequency exceedance was just barely over the 1.0-ft level.

The Basin energy sensor was located within the Boat Basin wave height criterion zone, and was well-situated to define the wave climate in the future berthing expansion area. It was also very close to the Hyde Street pier zone. The cumulative distribution function (Figure C66) shows that the 1.0-ft Boat Basin criterion was approached infrequently, and never exceeded.

Therefore, the measured data show that post-BW wave height criteria have been met at all of the prototype gaging locations within Fisherman's Wharf harbor.

It was desired to make comparisons between prototype-measured short-period wave data and physical-model measured data in order to critique the performance of the physical model as a design tool. Ideally, cases where prototype incident conditions matched those generated by the model wavemaker would be compared. A satisfactory physical model would correctly predict the spatial variation trends of wave heights around the harbor, and predict the degree of wave height attenuation due to the breakwater. If the model predicted that wave height criteria would be met, then the criteria should also be met in the prototype. Separate comparisons should be made for pre-BW model versus prototype and post-BW model versus prototype.

A pre-BW comparison is hindered by lack of directional information for prototype incident waves, limited length of gaging record, poor correspondence between prototype and model wave gage locations, sparse spatial coverage, and inability to force nature to create the desired wave conditions. Because the directional characteristics of the prototype incident waves are unknown, it is impossible to select specific prototype events as being good approximations of model-tested cases. Furthermore, since the model-tested conditions represent severe, if not extreme prototype conditions, even a very long-duration prototype gaging record could easily fail to capture truly comparable natural events. Moreover, recall that the numbers, types, and locations of early gages were not based on MCCP objectives. While the pre-BW prototype wave data sets are not entirely adequate for MCCP purposes, considering the timing of the selection of the breakwater as an MCCP site, this study is fortunate (compared to those projects selected for MCCP monitoring *after* their completion) to have at least *some* pre-construction wave data.

Nonetheless, some limited model:prototype comparisons can be made for the pre-BW period. Table 4 compares maximum significant wave heights observed at prototype and model gages for pre-BW conditions. Model gage locations are shown in Figure 26. The choice of "closest" model gage was judgmental, and considered proximity to the prototype location, exposure to arriving waves, and bathymetry. Model wave heights and test conditions were obtained from CERC's physical model study results, reported in Bottin, Sargent, and Mize (1985). At some locations, more than one test condition produced the same maximum wave height value. Prototype maximum wave heights are limited to those for which the analysis assigned a peak period within the ordinary wind wave regime. Recall that prototype peak period (T_p) represents the midpoint of the period band (e.g., T_p = 5 sec when the 4- to 6-sec band was the highest energy band of the burst).

Table 4
Maximum Pre-Breakwater Significant Wave Heights Observed in Prototype (p) and Model (m)

Prototype Gage	Closest Model Gage	Max H_s (p/m) (ft)	T_p (p) (sec)	Test Conditions (m), T (sec), H (ft), Direction, SWL (ft)
Municipal pier	No. 3	2.6/4.8	5	4.9, 5.8, NNE, 0.0
Pier 47	No. 5	2.7/4.6	5	4.9, 5.8, NNE, 0.0
Pier 45	No. 1	1.5/5.2	5	4.9, 5.8, NNE, +5.7
Alioto's Wharf	No. 13	0.5/2.3	9	3.8, 4.1, NW, 0.0 and 3.6, 3.4, WNW, 0.0

The prototype H_s of 2.7 ft (81 cm) at Pier 47 was the highest H_s observed in the pre-BW data set; it occurred on December 3, 1983.

Pre-BW maximum model significant wave heights were consistently higher than maximum prototype values at comparable locations, ranging from 1.7 to 4.6 times higher. The closest match was between the Pier 47 gage and model

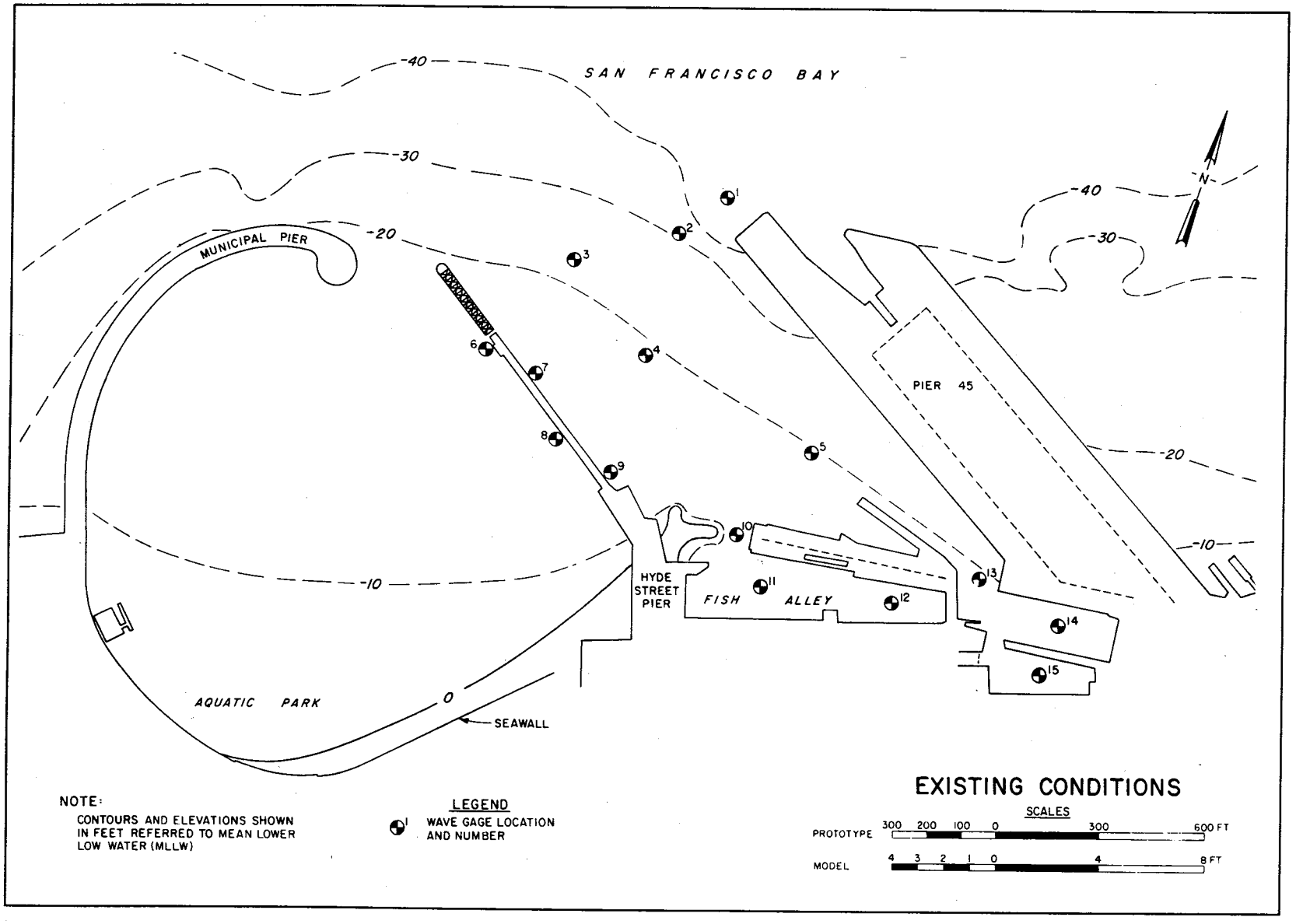

Figure 26. Pre-breakwater physical model wave gage locations

gage No. 5. The relatively low prototype maximum wave heights at Pier 45 and Alioto's Wharf may be partly due to the short pre-BW record available for those sensors (less than 4 months). Maximum prototype heights occurred in the 4- to 6-sec period band (except at Alioto's Wharf), which agrees well with model results.

Table 4 also shows that the physical model predicted exceedances of design wave height criteria throughout the harbor for pre-BW conditions. Prototype data confirm that wave height criteria were exceeded prior to completion of the breakwater (except at Alioto's Wharf).

Of the aforementioned restrictions on comparing model and prototype, perhaps the most important is the relative severity of the design (test) conditions versus the relatively short gaging record of the prototype. In other words, the more severe design wave conditions were not experienced during the pre-BW prototype gaging period. If the Municipal pier gage represents incident conditions, its highest H_s value of 2.6 ft is substantially lower than the highest pre-BW incident conditions generated in the model (5.8 ft), so it is not surprising that prototype maximum wave heights were lower than model wave heights.

Recall that some of the most severe model wave combinations used for testing pre-BW (existing) conditions were revised downward during the course of the physical model investigation. For example, the 5.8 ft/4.9 sec NNE case used in early testing was revised to 4.8 ft/4.2 sec for later tests, including the Plan 78 final breakwater configuration. Although the no-breakwater model was not run again with the lower design wave conditions, it is very likely that had pre-BW tests been re-run, the resulting maximum wave heights would have been closer to the prototype values.

Post-BW model:prototype comparisons are hampered by all of the same limitations listed above for the pre-BW comparison, except for the poor correspondence between prototype and model wave gage locations.

The gage location incompatibility problem was eliminated by re-activating the physical model specifically for the MCCP study, with model gages relocated to the same sites gaged by SIO in the prototype (Incident, Pier 45, Basin, and Alioto's Wharf). CERC's Wave Dynamics Division, Wave Processes Branch, conducted the second model study. The still-extant model at CERC was "taken out of mothballs" for a limited series of tests, including 40 variations.

The primary intent of this second model investigation was to provide model results for a direct comparison with prototype data, using the same model technology available at the time of the original investigation. The Plan 78 breakwater configuration was still in place from the first investigation. Of the wave directions tested in the original model study, the NNE and WNW directions were selected for the new series of tests, since they were the most critical directions in producing interior harbor waves. Wave height and period combinations and swls were the same as in the original tests. In order to exactly

replicate the original investigation, monochromatic (regular) waves were generated.

However, taking advantage of the new CERC wavemaker (similar to the original wavemaker) that can generate irregular or regular waves, an additional series of irregular wave tests were conducted. Wave conditions were developed by adapting Joint North Sea Wave Project (JONSWAP) spectral distributions so that peak period and significant spectral wave height matched the corresponding monochromatic (regular) wave height and period.

For the WNW cases only, an additional series of tests were conducted with scale replicas of the historic ships' hulls placed at the correct locations along Hyde Street pier to simulate wave barrier effects of the actual vessels. The replicas were fixed in place, but adjusted in vertical position according to swl to maintain constant draft.

While use of irregular waves and the historic ship replicas was not part of the original model procedure, a secondary intent of the second model investigation was to try to replicate one or more prototype events included in the post-BW gaging record. Unfortunately, lacking prototype wave incidence direction information, or even local wind records upon which to base estimated direction, there was no rational way to select events from the prototype data set to be re-created in the model. In spite of that, the test cases with irregular waves and historic ships were conducted anyway, to provide some model results more closely resembling the actual post-BW prototype environment, and also to take advantage of an opportunity to compare monochromatic versus irregular waves in the same model. The results of the second model investigation are documented in an in-house memorandum prepared by Mr. Robert R. Bottin of CERC.[1] Photographic and videotape documentation were also obtained.

Figure 27 shows locations of the four sites gaged in the second physical model study of post-BW conditions. Model gages were located according to information supplied by SIO, but since the prototype locations were not precisely surveyed in, some siting discrepancy may have existed between model and prototype, especially for the tripod-mounted Incident and Basin gages. Table 5 compares maximum significant wave heights observed at prototype and model gages for post-BW conditions. As for the pre-BW comparison, prototype wave heights are limited to those that occurred at ordinary wind wave frequencies. Model wave heights and test conditions were obtained from the memorandum documenting CERC's second physical model investigation. Only monochromatic test results (with no historic ships present) are included in Table 5, in keeping with the intention to compare only the model technology and procedure actually used for breakwater design.

---

[1] In-house memorandum, 26 Mar 90, Robert R. Bottin, Research Physical Scientist, Coastal Engineering Research Center, U.S. Army Engineer Waterways Experiment Station, Vicksburg, MS.

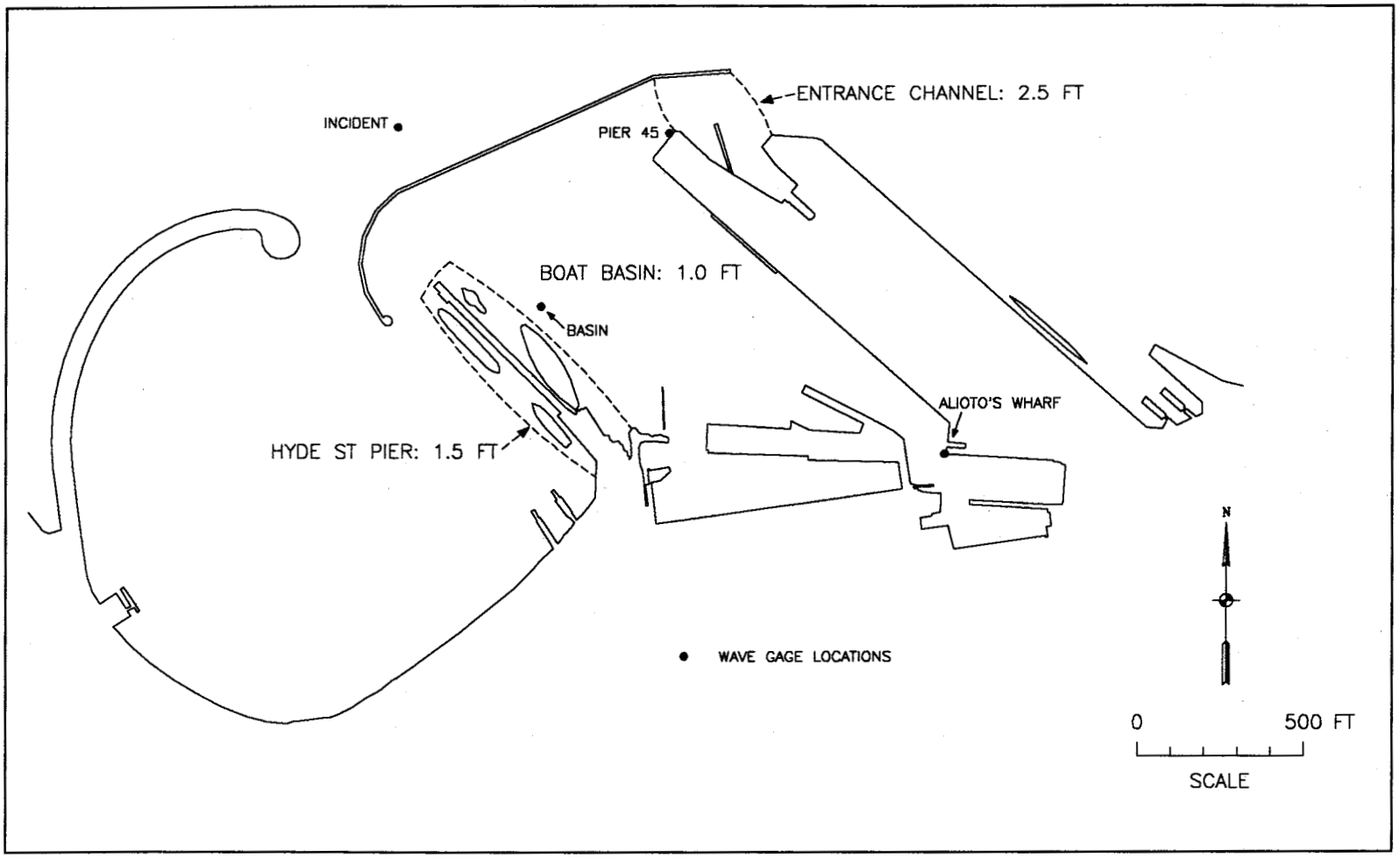

Figure 27. Post-breakwater physical model wave gage locations (second model study)

Table 5
Maximum Post-Breakwater Significant Wave Heights Observed in Prototype (p) and Model (m)

Gage	Max H_s (p/m) (ft)	T_p (p) (sec)	Test Conditions (m), T (sec), H (ft), Direction, SWL (ft)
Incident	2.0/8.1	5	4.2, 4.8, NNE, 0.0
Basin	0.9/1.0	5	4.2, 4.8, NNE, 0.0 and 10.0, 3.0, WNW, 0.0
Pier 45	1.0/1.6	5	4.2, 4.8, NNE, 0.0 and 4.2, 4.8, NNE, +5.7
Alioto's Wharf	0.3/0.6	9	10.0, 3.0, WNW, +5.7

The prototype H_s of 1.0 ft (32 cm) at Pier 45, which occurred on December 15, 1988, was the highest post-BW H_s observed within the protected harbor area. Local observers noted this event to be a good example of a strong "norther," a type of weather condition seen in the San Francisco area associated with passage of a cold front. During a norther, strong winds blow from northwesterly, then northerly, then northeasterly directions. The same norther produced an H_s value of 1.6 ft (50 cm) in the same period band at the Incident gage--one of the highest values observed there--showing that this norther was one of the most energetic events of the post-BW record. Since the Pier 45 gage was relatively unprotected from waves from northeasterly directions, it is not surprising that the difference between its H_s and that at the Incident gage was only 0.6 ft (18 cm) for this event.

Of the interior gages, the maximum model H_s of 1.6 ft (exceeding the Boat Basin criterion of 1.0 ft) was also at Pier 45. However, the Pier 45 gage is near the boundary between zones, and the Entrance Channel criterion (2.5 ft) should apply there. (Also, in the first physical model study a gage slightly farther out from the end of Pier 45 recorded a maximum height of 1.0 ft under the same test conditions.)

The model maximum wave height at the Incident gage was 8.1 ft. Obviously, the Incident gage in the model was influenced by reflection off the breakwater, and was probably very near an antinode of the standing-wave pattern. Visual observations and photographs confirm that well-defined standing-wave patterns quickly became established in the model basin after the wavemaker started. Irregular wave tests produced less well-defined standing wave patterns than the monochromatic tests (see Figure 28). These two examples show that wave heights obtained in the model were very sensitive to gage position.

For the pre-BW comparison, maximum model significant wave heights were consistently higher than maximum prototype values at comparable locations, although there is better model:prototype agreement for the post-BW

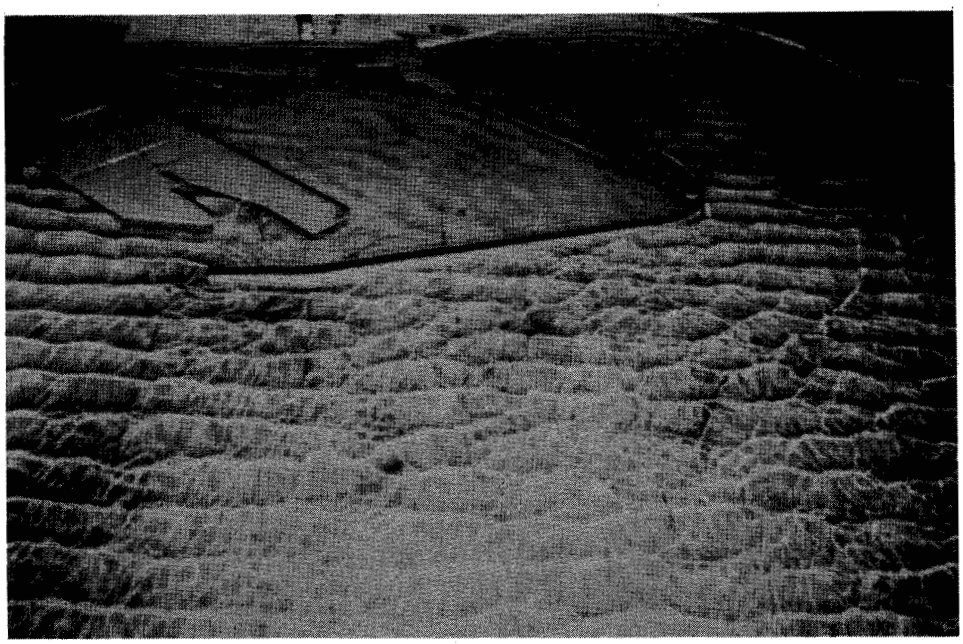

a. Typical monochromatic wave patterns for 4.2-sec, 4.8-ft waves from NNE

b. Typical irregular wave patterns for 4.2-sec, 4.8-ft waves from NNE

Figure 28. Monochromatic and irregular test wave patterns (Continued)

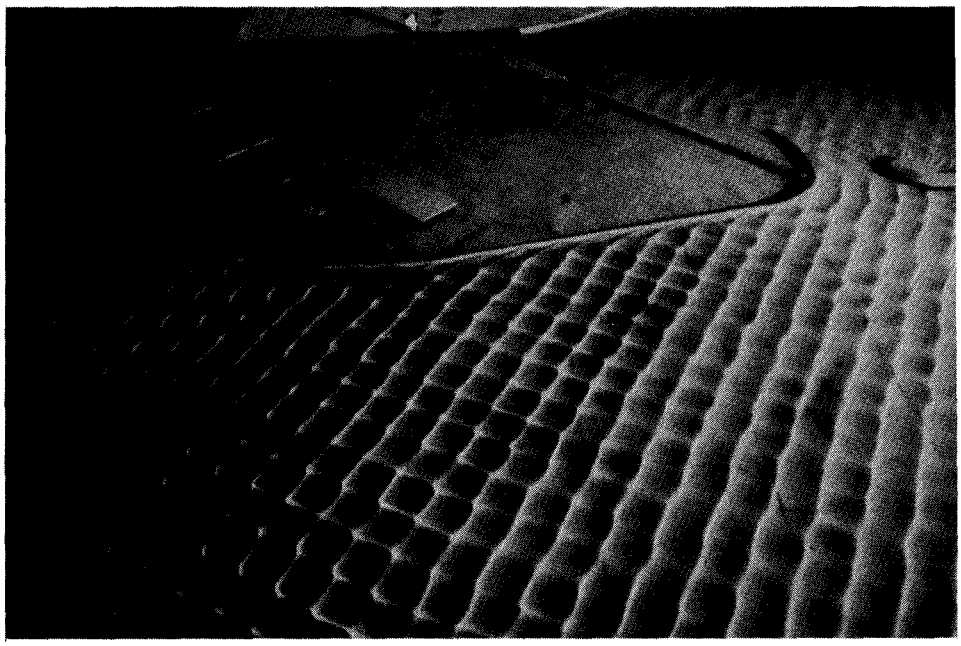

c. Typical monochromatic wave patterns for 3.6-sec, 3.4-ft waves from WNW

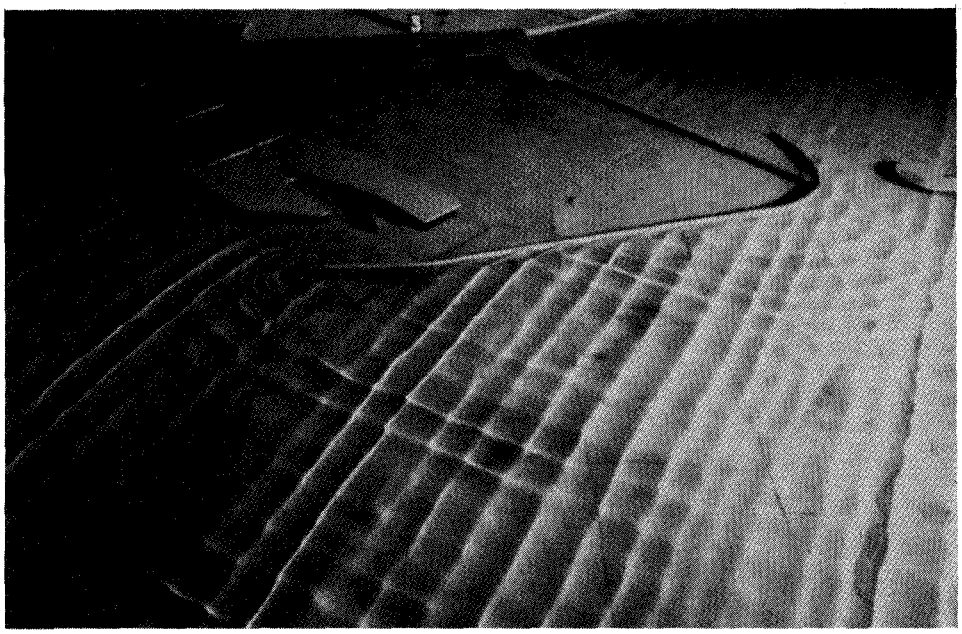

d. Typical irregular wave patterns for 3.6-sec, 3.4-ft waves from WNW

Figure 28. (Concluded)

conditions (with the exception of the Incident location). Also, the period bands of maximum significant wave height agree well between model and prototype. It is not possible to compare the spatial variation of maximum significant wave heights around the protected harbor between the model and prototype, because the spatial variation trends in the model are very dependent on incident wave direction. Note that the design wave height criteria were not exceeded under monochromatic waves at any of the second model's gaging locations.

Judging from the prototype Incident maximum H_s compared to the generated wave conditions, it appears that the prototype did not experience conditions as severe as those tested in the model. However, as noted above, a locational discrepancy for the Incident gage could have placed it in a node for short-period reflected waves so that it measured unusually low wave heights. If in fact the measured prototype wave climate was substantially less severe than design conditions, a complete test of the model's predictive capability has not yet occurred. Nevertheless, since wave height criteria were met in the available prototype data set and the model predicted the criteria would be met, the model appears to have correctly predicted interior harbor conditions.

In general, the second physical model study found that monochromatic conditions produced larger wave heights outside the breakwater than irregular conditions. Maximum wave heights in the entrance channel, along Hyde Street pier, and in the interior harbor were similar in magnitude, and occurred about equally often for monochromatic and irregular conditions.

Generally, the tests with waves from WNW with historic ship replicas in place resulted in slightly lower wave heights at the Basin and Alioto's Wharf locations compared to the equivalent tests without the ships. Thus, the inclusion of the ships appeared to improve the agreement between model and prototype, as might be expected.

In order to provide information for determining whether surge was increased by the breakwater, and for comparisons with CERC's numerical harbor oscillation model, SIO averaged large numbers of individual burst's energy spectra to produce a single long-term average energy spectrum at each surge sensor. A separate long-term average spectrum was formed for pre- and post-BW sub-data sets, respectively. Figures C67, C68, and C69 show these long-term averaged spectra from the various locations co-plotted to illustrate spatial trends and effects of the breakwater. The reader is reminded that the use of a logarithmic vertical scale makes differences in magnitude of peaks less obvious than they would be at linear scale. Subsets of the pre-BW data sets were chosen (to the extent possible) so that comparisons would not be biased by comparing different lengths of gaging record or different seasons. Long-term pre-BW average surge spectra appear for Alioto's, Alioto's Wharf, Hyde Street pier, Pier 47, and Pier 45. Post-BW average surge spectra appear for Alioto's, Alioto's Wharf, Basin, and Pier 45.

All five pre-BW average surge spectra indicate an energy peak in the vicinity of 228 sec, which CERC's model predicted to be the primary or "pumping"

mode of harbor oscillation. The model-predicted 80-sec peak was also present at all five locations, but other prototype peaks were not predicted by the model. Spatial trends of surge variation agree well between model and prototype. Both predicted that surge in the vicinity of the pumping mode would be strongest at the most interior locations (Alioto's and Alioto's Wharf).

In general, post-BW prototype surge data show that the breakwater did not change the frequencies of oscillation very much, but that some energy was redistributed. Surge energy at periods greater than 80 sec was reduced by the breakwater in the Hyde Street pier and Boat Basin area (Figure C68). Conversely, the surge energy at Pier 45 (Figure C69) appears to have generally increased after breakwater completion, as that location became enclosed within the protected harbor. Surge energy at long periods in the vicinity of the pumping mode appears to have increased at the Alioto's and Alioto's Wharf locations (Figure C67). Some of this apparent increase may be due to the relative short length of pre-BW record compared to the post-BW record.

Note that for all surge sensors, energy levels at the low frequencies (periods of several minutes) are 2 to 4 orders of magnitude higher than energy levels at the higher surge frequencies (periods of 20-50 sec), with or without the breakwater in place. The simplified numerical ship motion analysis conducted by CERC and also reported in Bottin, Sargent, and Mize (1985) indicated that motions of the historic fleet would be most influenced by surge periods less than about 50 sec. The average spectra show that surge energy levels in this critical range were very low before the breakwater was built, and remained essentially unchanged after breakwater completion. Note that monitoring of ship motion was not included in the MCCP study.

In summary, the prototype data show that overall, no large changes in surge energy levels or surge frequency distributions appear to have occurred as a result of the breakwater, considering the effects that differences in the lengths of record and wave climates might cause. CERC's numerical harbor oscillation model was reasonably accurate in predicting spatial trends and peaks, but not as accurate in predicting increases or decreases. The (perhaps overly general) performance criterion, "no increase in surge," has apparently been met for the boat basin/Hyde Street pier area, but apparently has been violated at Pier 45 and the innermost part of the traditional berthing area.

Paralleling the surge spectral analysis, SIO developed long-term average spectra for each of the energy sensors, plotted in Figures C70 through C73. Due to sensor depth and sampling rate considerations, the parts of these plotted spectra for short-period waves (from 4-sec to 2-sec periods) should be viewed with caution in making comparisons. All the pre-BW average spectra show broad incident energy peaks centered at 8 sec and 3.5 sec. These peaks presumably correspond to ocean-generated and locally generated waves, respectively. The pre-BW average spectra show the expected spatial trend of highest overall wind-wave and swell energy levels at Municipal pier, followed by Pier 47, then Pier 45, with Alioto's Wharf the lowest. The spectra at Pier 47 and Pier 45 are similar in shape, except for around the 8- to 12-sec period range, where Pier 47 had higher energy. The post-BW average spectra also

show the expected spatial trend where the Incident gage had the highest energy levels, followed by Pier 45, with Alioto's Wharf the lowest.

Figures C70 and C71 compare pre- and post-BW wind-wave and swell energy at Alioto's Wharf and Pier 45, respectively. Energy reductions were calculated by SIO, by computing the difference in total energy across the spectrum for each gage (proportional to the difference in area under the pre- and post-BW curves).

At Pier 45 (Figure C70), while the overall energy shows a significant reduction (77 percent), a greater proportion of the energy decrease took place at the longer, ocean-generated periods than at the locally generated periods. This is consistent with the position of the sensor at Pier 45 with respect to incident wave directions and blocking structures.

For Alioto's Wharf (Figure C71), the overall energy also shows a substantial reduction (47 percent) with much more of the reduction taking place at periods shorter than about 8 sec than at longer periods. This trend is not surprising, since the location of the Alioto's Wharf gage relative to the breakwater leaves a small window open to ocean-generated waves from westerly directions. The baffle system under Municipal pier has little effect in reducing waves at the longer periods typical of the ocean-generated energy.

How much of the energy reduction evident in Figures C70 and C71 is not due to the breakwater? In other words, are the energy reductions representative measures of breakwater wave attenuation? If pre- and post-BW wave climates were similar in severity and seasonal pattern of variation, and the pre/post gage records were about the same length and covered the same seasons, energy reduction could be attributed to the breakwater.

Can comparison of the pre-BW spectrum for Municipal pier (on Figure C72) with the Incident gage's post-BW spectrum (on Figure C73) indicate anything about the severity of the pre-BW versus post-BW wave climates? From 4.5- to 5.5-sec periods, the average energy at both gages was almost identical. The ratio of Municipal pier energy to Incident energy rises with increasing wave period beyond 5.5 sec. At 15 sec, Municipal pier energy is about 3.3 times the Incident energy. If the pre- and post-BW incident wave climates were similar, these two gages might be expected to have similar energy for the shorter periods, because the influence of reflection should be small for the shorter wave periods. However, if the breakwater is a stronger reflector than the wave baffle under Municipal pier, at longer periods the Incident gage's energy should be higher than that of the Municipal pier gage. Also, if the wave climates were similar, even if the detached breakwater is a perfect reflector and the wave baffle doesn't reflect at all, the ratio of energy should not be greater than 2, at any frequency. Therefore, this comparison of average energy spectra seems to suggest that the pre-BW wave climate for the Municipal pier gage was more severe than the post-BW climate for the Incident gage.

However, the differences between measured average energy at Municipal pier and the Incident gages could be caused by the combination of many factors besides the relative severity of the two gages' wave climates. These include, but are not limited to, the relative influence of reflection, the relative proximity of the two gages to the two reflectors, and the length and timing of the two gages' records. Perhaps this last factor is the most important in this case, since the Municipal pier record includes two winter seasons, whereas the Incident record only has one.

Since no single "incident" energy sensor operated for a long period of time both before and after breakwater construction, conclusions about the equivalence of the pre- and post-BW wave climates cannot be made from the available data sets. Therefore, the energy reductions at Alioto's Wharf and Pier 45 cannot be treated as quantitative measures of breakwater wave attenuation, even though the same location and depth are being compared.

A comparison of Figures C72 and C73 also qualitatively shows the effect of the breakwater. In the pre-BW record, wave energy reaching Pier 47 was about the same as that reaching Municipal pier, whereas in the post-BW period, the Basin gage experienced much less energy than the Incident gage. But for most of the same reasons noted above for Municipal pier versus Incident, not much can be made of a comparison between Pier 47 and Basin.

Figure C73, however, is the best available basis for quantifying the wave attenuation of the breakwater over a fairly wide variety of wind-wave and swell conditions. Note from Figure 24 that the gaging records for the Incident and Basin gages cover the same time period (14.5 months). A very large reduction in average energy (66 percent) for wave periods longer than 4.5 sec can be attributed primarily to the breakwater. The average spectrum for the Incident gage could not be reliably calculated for periods less than 4.5 sec, because of the relatively large depth of the sensor.

Currents

Monitoring objectives for currents. Extensive pre- and post-breakwater prototype current data would be required for a thorough quantitative examination of the effects of the breakwaters on currents and circulation within the harbor and surrounding areas. As noted in the Chapter 2 discussion, HEC's measurements were oriented towards establishing tidal boundary conditions for the numerical hydrodynamic model and verifying its results. The baseline prototype current data set is difficult to use for MCCP purposes. Although it provides detailed information for locations of interest for modeling, it is very limited in spatial and temporal extent, and does not provide a synoptic overview of general circulation patterns.

However, the hydrodynamic model results (e.g., Figure 19) do provide this information. Lacking baseline prototype data of the extent required to characterize the pre-breakwater conditions, the MCCP approach was to collect post-breakwater prototype current data for comparison to the numerical model.

Two field campaigns were conducted to measure general circulation. Stations were distributed throughout the area surrounding the breakwaters, and measurements were made at several depths at each station throughout a full tidal cycle. The data were used to develop a quasi-synoptic overview of general circulation that could be compared with the numerical model results. Thus the primary monitoring objective was addressed indirectly, and secondary MCCP objectives (review of design procedures and tools, provision of information useful for Operation and Maintenance) were addressed directly.

The performance criterion with respect to entrance channel currents (not to exceed 2 knots) was specifically addressed by measuring peak entrance currents at mid-channel on two occasions when strong tides were predicted.

General circulation measurements. Field measurement campaigns were conducted September 1-2, 1987, and July 28-29, 1988. Both campaigns were of approximately 25 hr duration, attempting to capture a full tide cycle of current measurements. The 1987 campaign covered a tide with a predicted range between lower low water (llw) and higher high water (hhw) of 5.7 ft at the Golden Gate. The predicted range for the 1988 campaign's tide was 8.4 ft--the second largest range for that year. Thus the 1987 campaign examined an average type of tide (recall that the diurnal range for the Golden Gate station is 5.8 ft), and the 1988 campaign's tide was an uncommonly strong spring tide. Since production runs of the hydrodynamic model simulated conditions on September 19, 1983 that had a tidal range of approximately 5.5 ft, the 1987 data should be relatively good for model:prototype comparisons, if non-astronomical influences (i.e., weather conditions) did not have a large influence. On the other hand, the more extreme 1988 data set provides a more pronounced illustration of spatial variability in the circulation pattern, and will be more useful for engineering design of future facilities in the study area.

Figure 29 shows the 11 current measurement stations used for both field campaigns. Station siting was based on the desire to obtain broad spatial coverage of the area where currents might be influenced by the breakwater structures. As always, the number and location of stations and frequency of sampling were constrained by the available resources (personnel, vessels, equipment) and configuration of the site. One-minute-average measurements of horizontal current speed and direction were collected at three vertical locations for each station: top, mid-depth, and bottom. Top measurements were approximately 10 percent of total depth below the surface. Bottom measurements were approximately 3 ft above the seabed (due to rigging constraints of the instruments). At some low tide stages, only a mid-depth reading could be obtained at station 3. Each station was occupied an average of 22 times during the collection period.

Figure 30 shows one of the side-cast, impeller-type current meters used for both general circulation and peak entrance channel measurements. This type of meter is designed to measure horizontal ocean currents which are relatively steady in direction and speed. Because of the size and mass of the meters, they have a slow response to directional fluctuations. Their neutral buoyancy and flexible-tether rigging arrangement cause them to "weathervane" to align

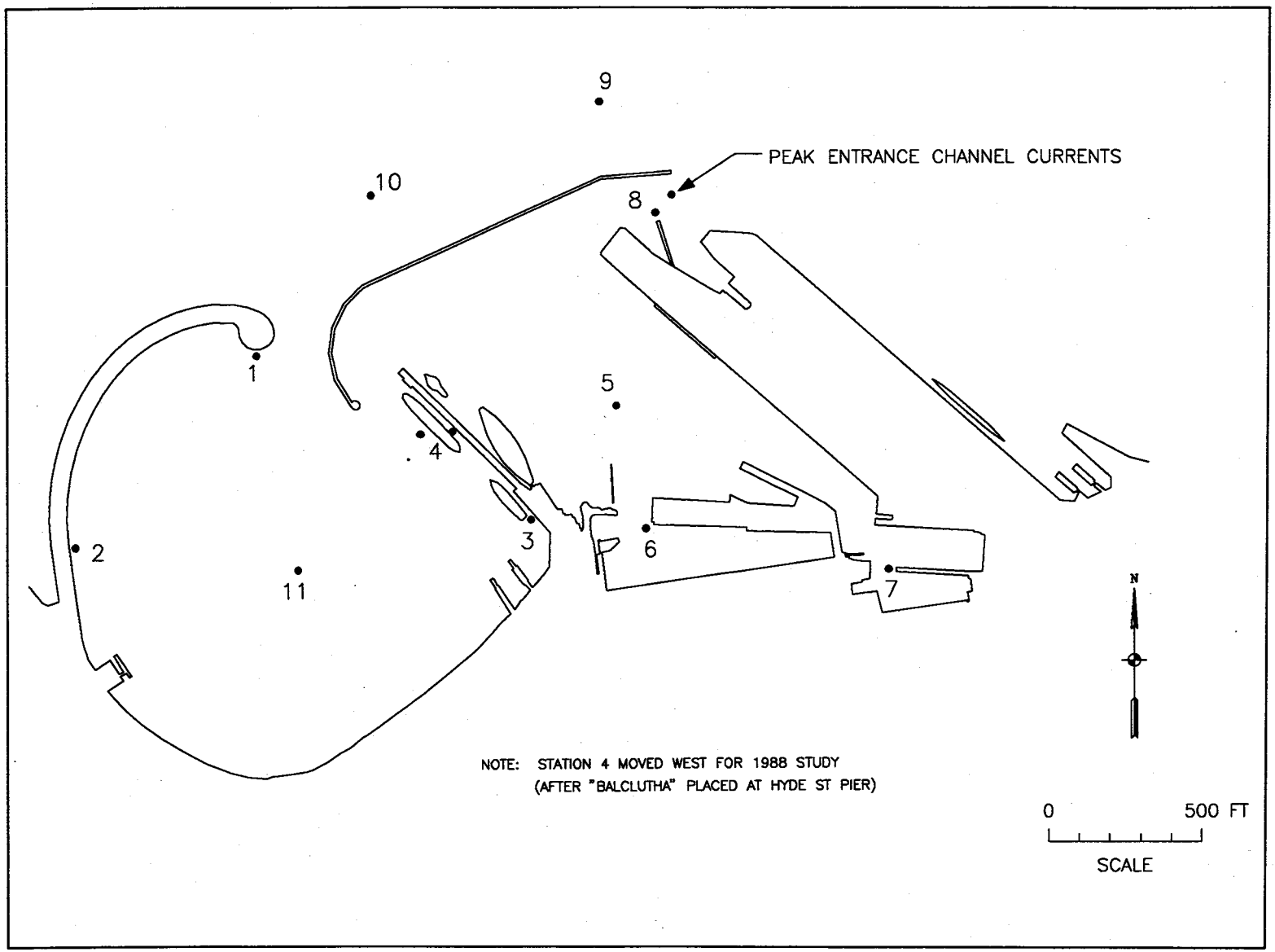

Figure 29. MCCP prototype current measurement stations

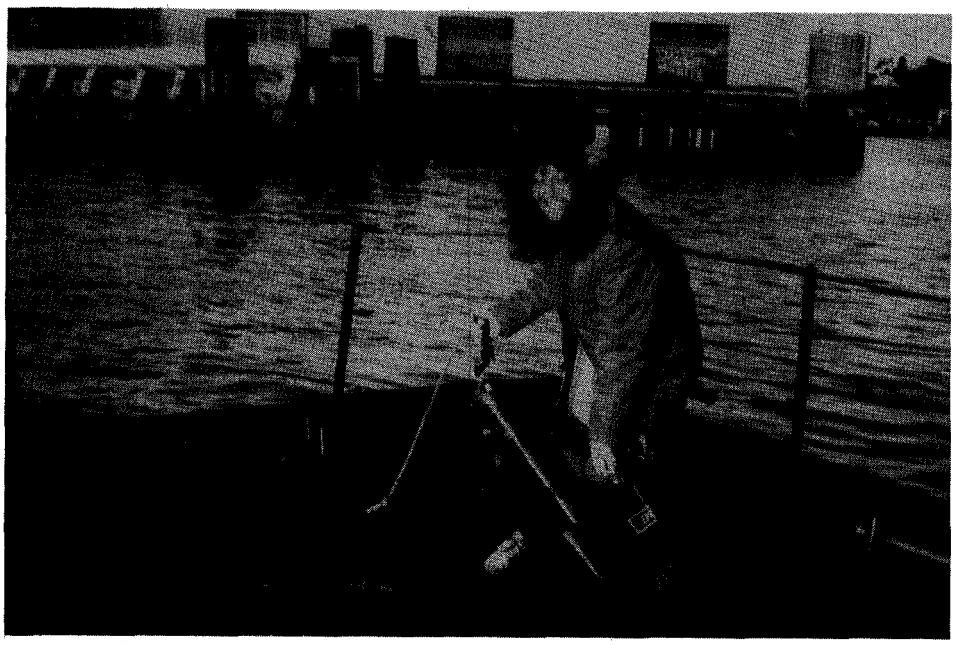

Figure 30. Endeco current meter used in prototype measurements

with the current, even if it has a vertical component. In cases where large-scale turbulence was generated by upstream structures (e.g., the under-pier wave baffle at stations 1 and 2), measurements from the impellor-type current meters were in some instances erratic and difficult to average, because of the meters' design. Also, these meters were not well-suited to measurement of very small currents (e.g., at stations 6 and 7).

The two field data sets were examined for errors, then processed by computer to produce tabular listings and vector (stick) plots showing variation of current magnitude (speed) and direction with time at each station and vertical location. Currents were assumed to be horizontal. Figure 31 shows resulting plots for top (T), middle (M), and bottom (B) data at station 4 (located west of the historic ship *Balclutha* during the 1988 campaign). The horizontal axis is incremented in hours for the two days of the campaign, but the vectors are plotted to scale (knots) with their tails at the actual time of measurement along an invisible line parallel to the time axis. The straight-up direction indicates currents flowing towards magnetic north (data in Figure 31 are not corrected to true north). Data for station 4 generally show no pronounced differences in speed or direction throughout the water column when flood or ebb is in full swing, but do show some depth-related differences near the change of tide, as might be expected. These data are typical of those obtained at the stations located well away from structures. Some of the other stations' data are less well-behaved due to the proximity of structures (1, 2, 3, and 8), or the low speeds in some zones (5, 6, and 7). Station 3 was sometimes influenced by swell waves breaking on the adjacent Aquatic Park beach.

The voluminous, complete sets of tabular listings and vector plots are archived at CERC's Prototype Measurement and Analysis Branch (PMAB). In

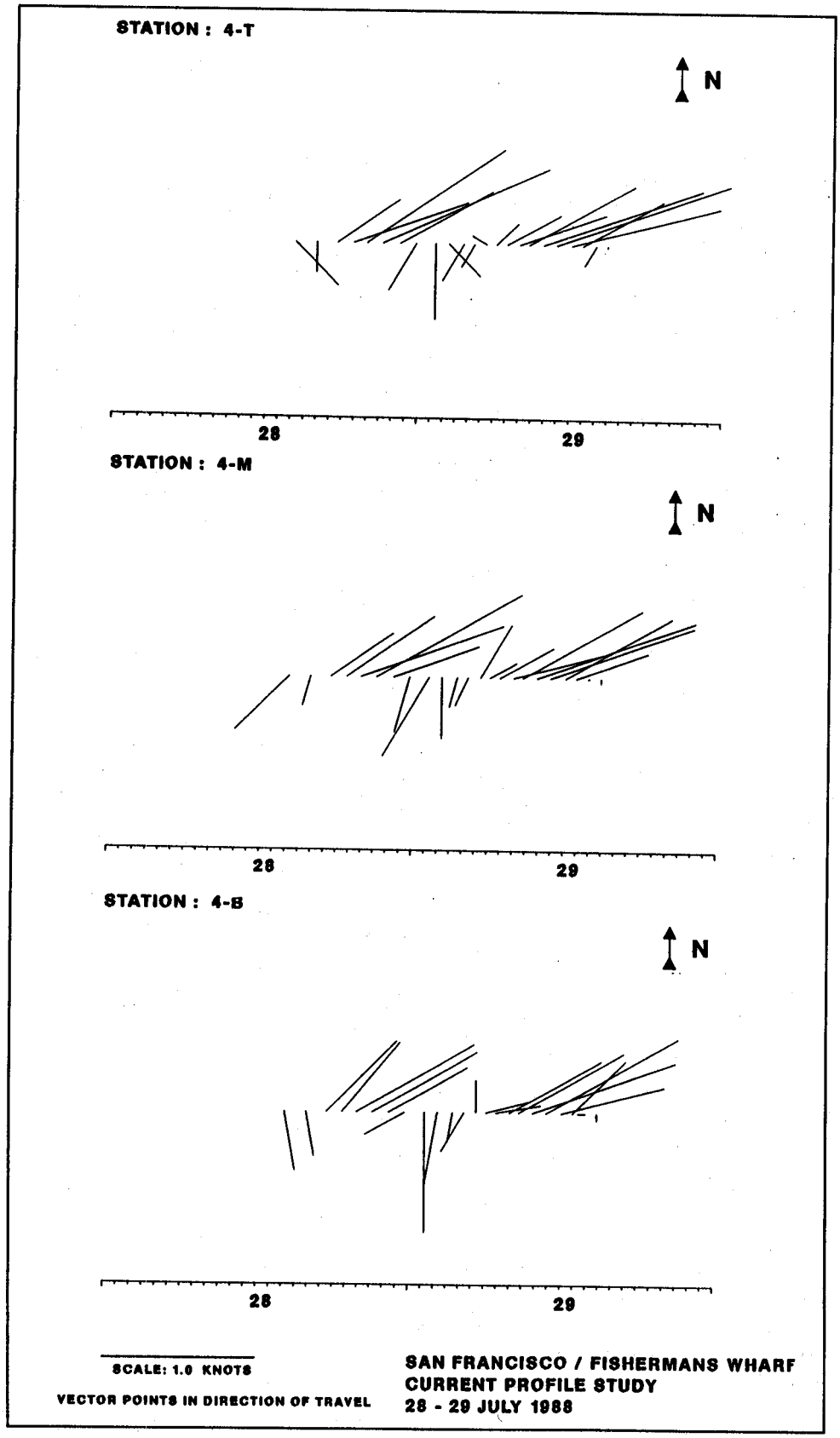

Figure 31. Typical prototype current variation with depth and time (station 4)

the fall of 1989 preliminary copies were released to SPN, the design consultant for the Port, and representatives of the rowing and swimming clubs. Those copies were used in studies for the Port of San Francisco's expansion of small-craft berthing facilities on the east side of Hyde Street pier.

Figures 32 through 35 are presented to allow comparison of numerical model versus prototype current patterns and speeds. The current pattern figures have common scales for geographic features and current speed so they can be overlaid for direct comparison. The speed scale is feet per second (fps). Figures 32 and 34, representing peak ebb and flood, respectively, are taken from HEC's numerical model report (USACE HEC 1984a) and are the same conditions shown previously in Chapter 2. MCCP current station locations are co-plotted on Figures 32 and 34 to provide reference for comparisons. Piers and wharves are not shown; only the shoreline, detached breakwater, and impermeable filled areas under Piers 45 and 47 are visible. However, the numerical model did incorporate estimated additional resistance to flow due to the segmented breakwaters and pier pilings, but not that due to moored vessels. Figures 33 and 35 show corresponding prototype currents using the mid-depth values only. Vectors shown for the numerical model represent depth-averaged values. It was felt that mid-depth prototype values are sufficiently representative of depth-averaged currents for most stations, since at peak flood and ebb, depth variations were generally minor. Also, the mid-depth values are least likely to include influences of wind-driven surface currents or local seabed irregularities.

Since stations were occupied on a rotating basis by three measurement crews covering the entire study area, the prototype vectors shown in each figure were not all measured at exactly the same time. To create the figures, the stick plots (e.g., Figure 31) and tabular data were examined in detail to select the appropriate peak flood and ebb measurements from each station. Selection of "the" peak value was somewhat judgmental for stations where currents were weak, or direction and speed changed rapidly or erratically. Values used in each figure are, however, all from the strongest one of the two floods or ebbs in each day. The figures are a reasonable approximation to a "snapshot." The time difference between the first and last measurements included in one of these "snapshots" was typically about 100 min. These differences reflect real variations in the timing of peak currents around the study area as well as the effects of monitoring logistics. Directions have been correctly referenced to true north for Figures 33 and 35.

Comparison of Figure 32 with Figure 33a shows generally good qualitative agreement for peak ebb speed and direction, especially for stations 4, 8, and 11. The prototype values generally show a larger difference in speed between interior and bayside locations than do model values. One of many possible sources of discrepancy might have been model underestimation of flow resistance due to pilings (including the batter piles of the breakwater) and moored vessels. The stronger tide of the 1988 campaign is evident in the larger interior speeds seen in Figure 33b. The model also correctly predicted the relatively weak currents of the innermost locations. Comparison of Figure 34 with Figure 35 also shows generally good agreement between model

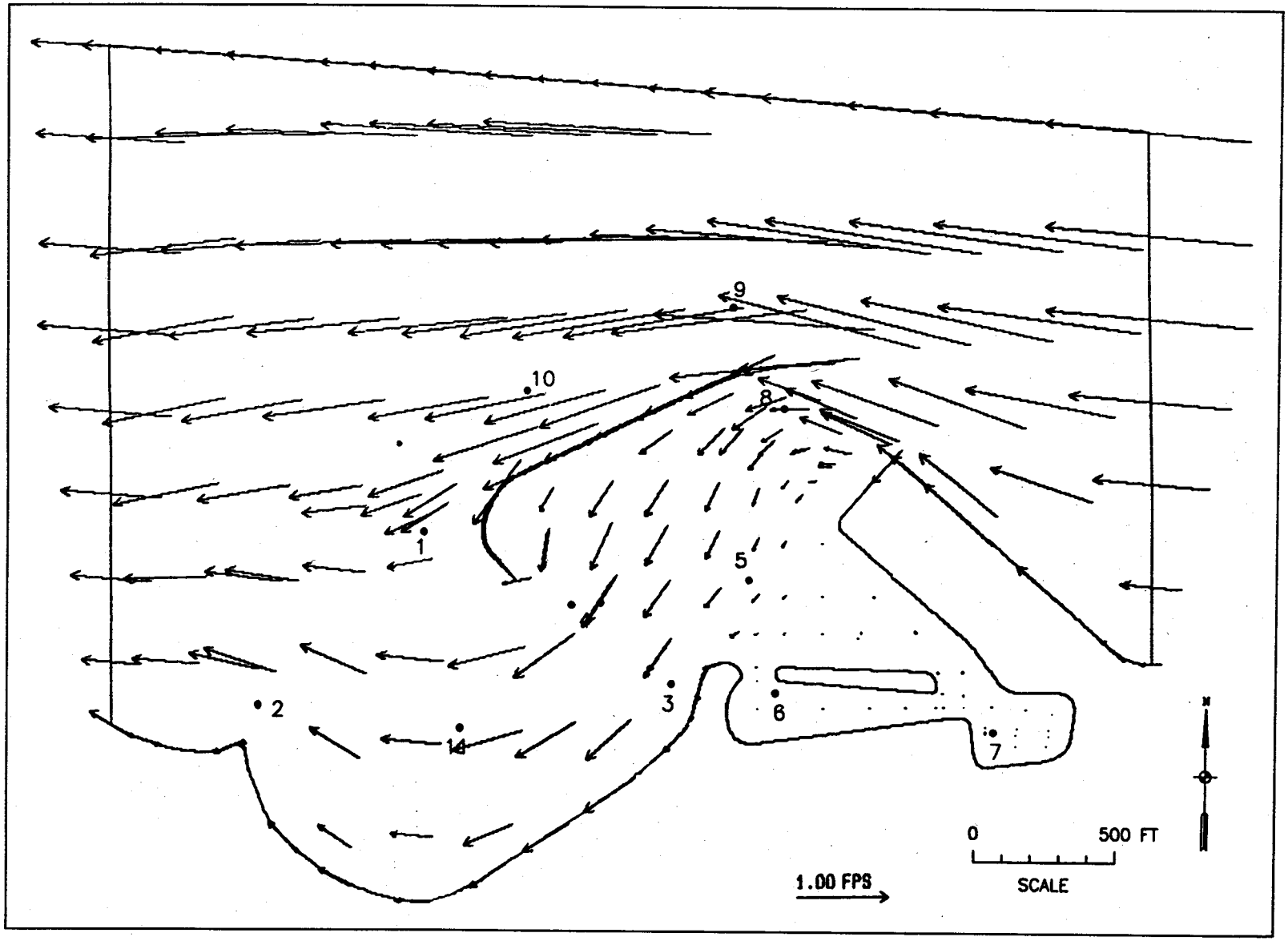

Figure 32. Hydrodynamic model currents at peak ebb with MCCP current stations

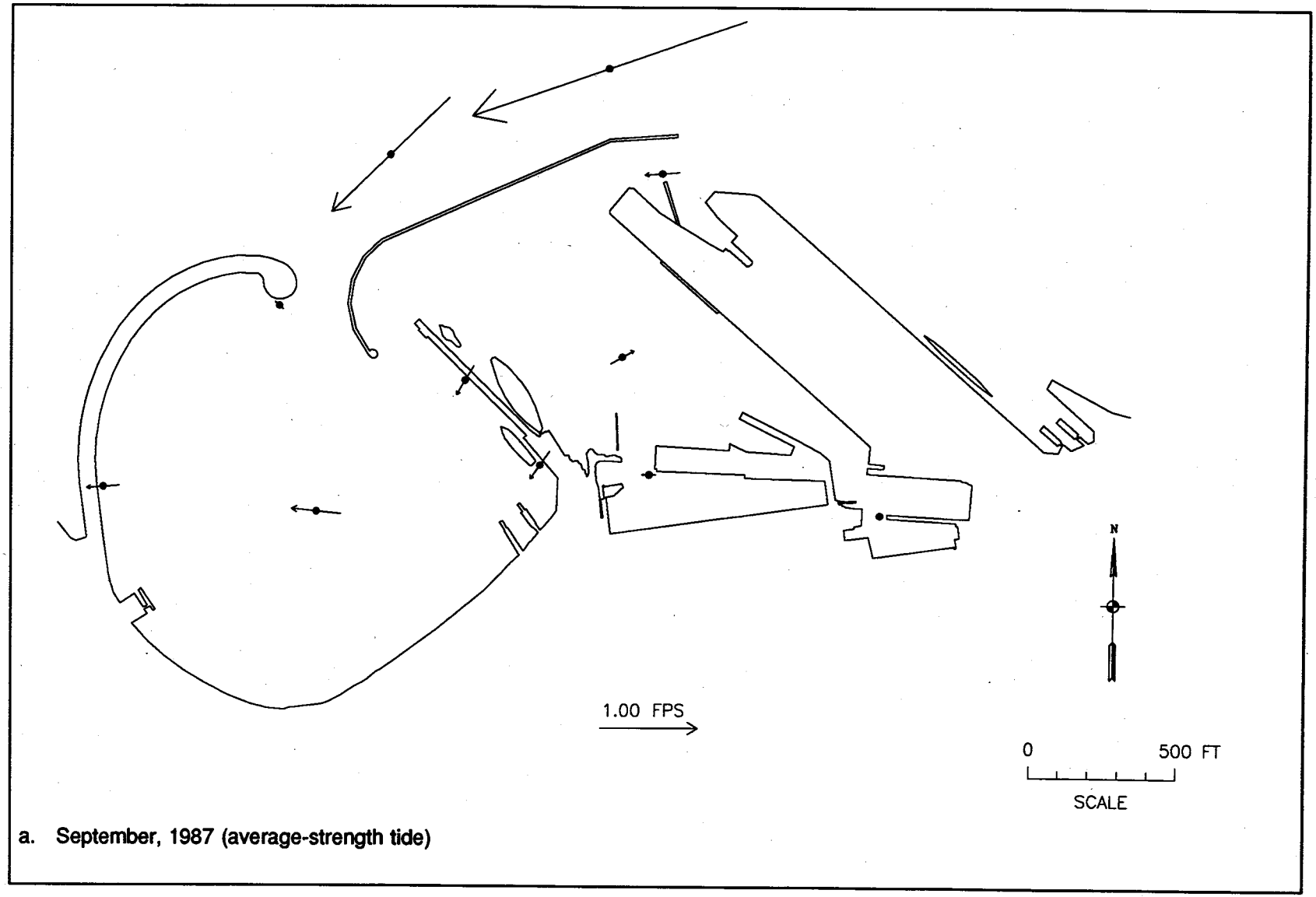

a. September, 1987 (average-strength tide)

Figure 33. MCCP prototype mid-depth currents at peak ebb (Continued)

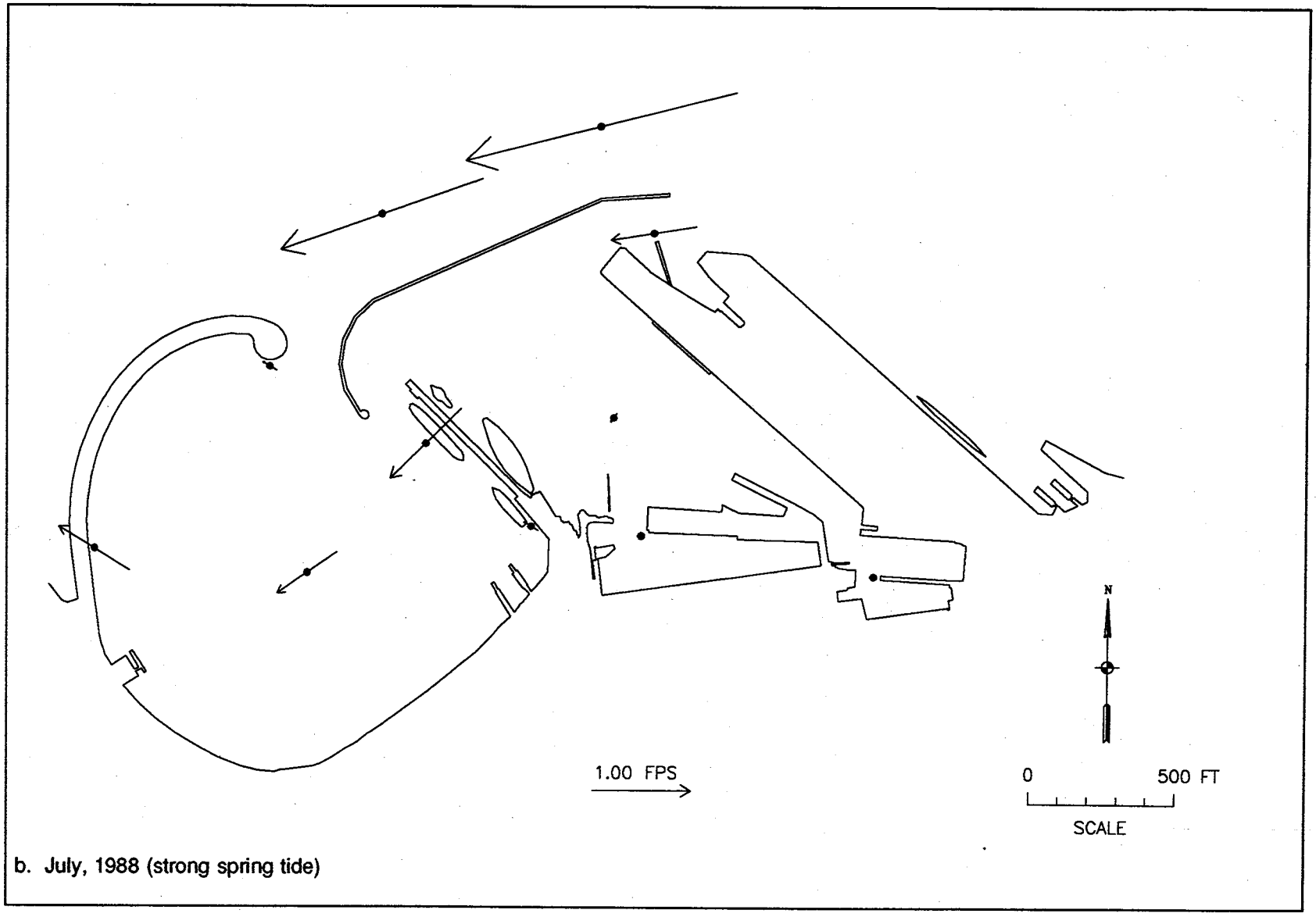

b. July, 1988 (strong spring tide)

Figure 33. (Concluded)

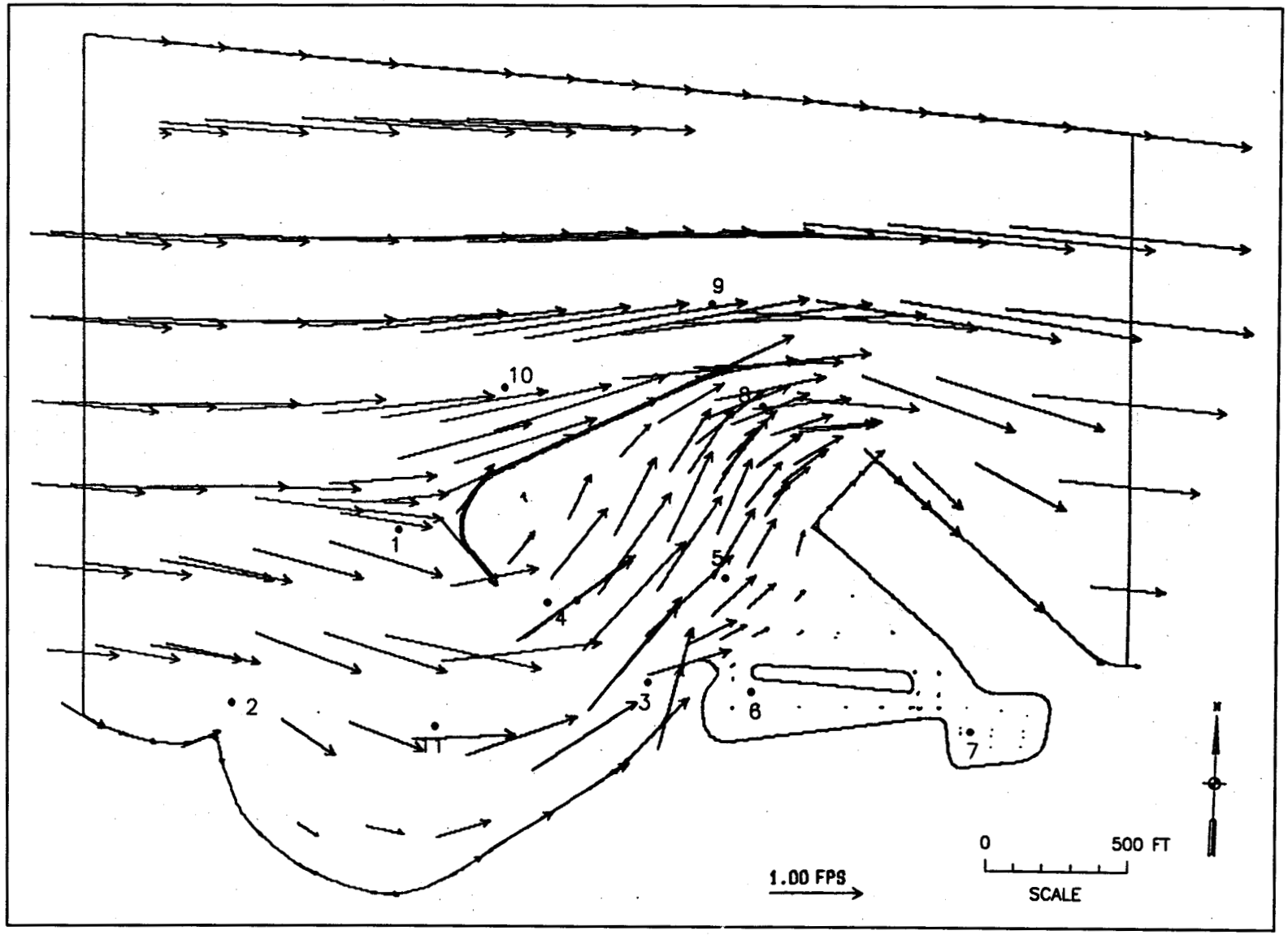

Figure 34. Hydrodynamic model currents at peak flood with MCCP current stations

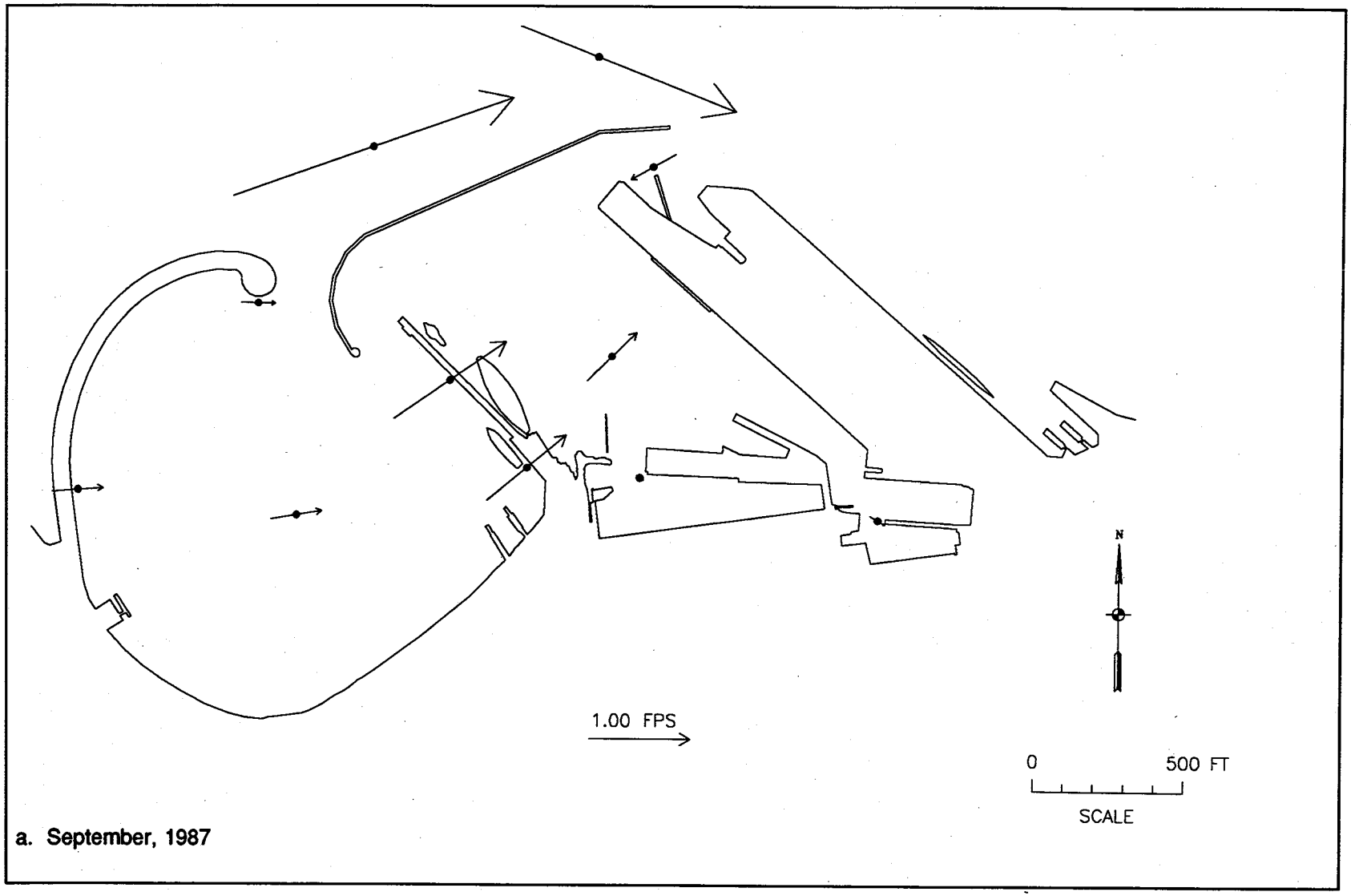

Figure 35. MCCP prototype mid-depth currents at peak flood (Continued)

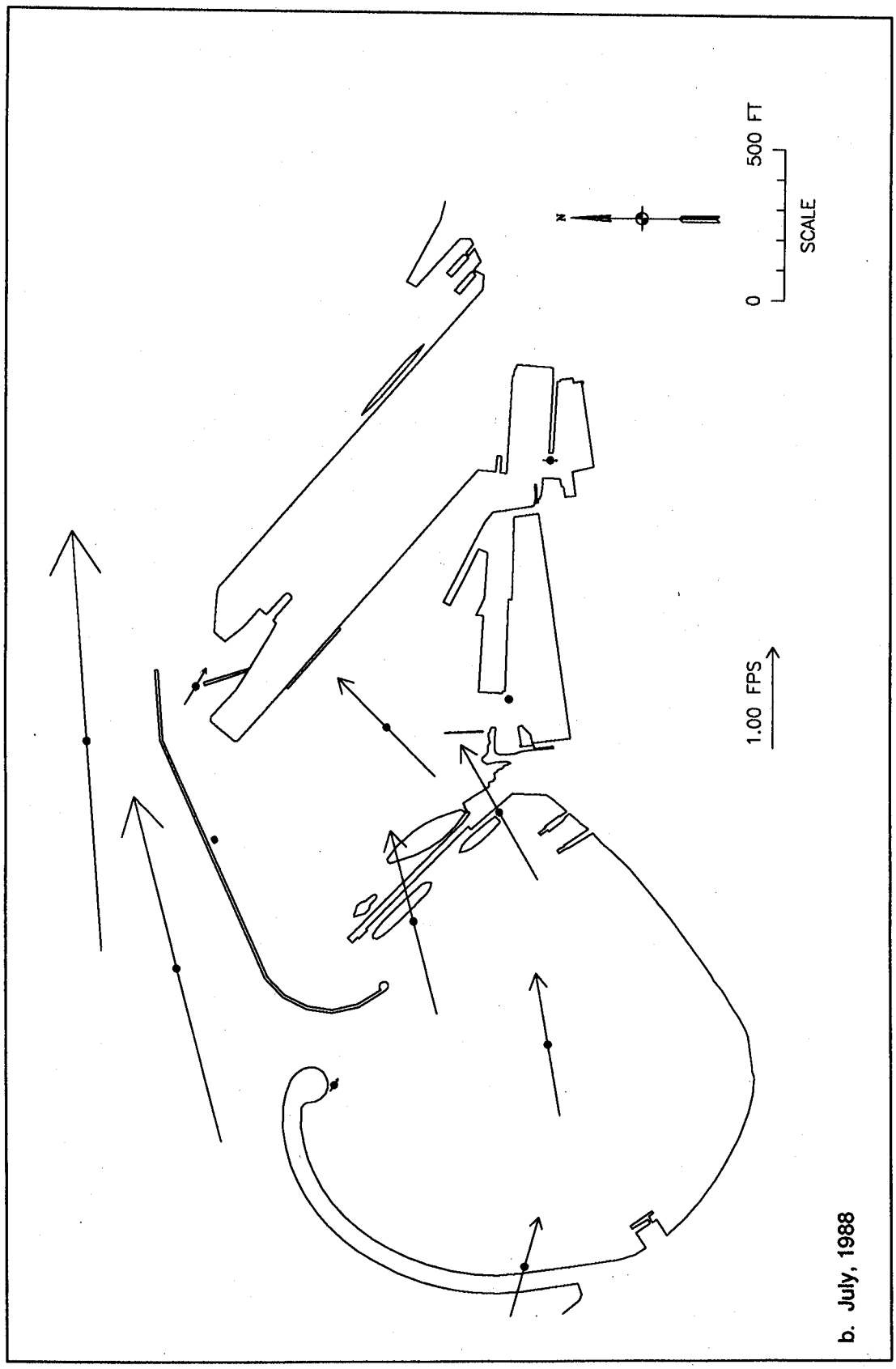

Figure 35. (Concluded)

and prototype. Comparison of the two sets of prototype figures indicates that peak flood speeds generally exceeded peak ebb speeds, especially at stations away from structures and along Hyde Street pier. The same trend was predicted by the model. Presence of a gyre at the end of the east segmented breakwater could have caused the inconsistent direction of the prototype vector at station 8 in Figure 35a. The numerical network appears to have been too coarse to accurately model smaller-scale flow behavior such as gyres at the abrupt ends of structures. However, the generally good overall agreement between model and prototype indicates that the numerical model was a good design tool, given the many possible sources of discrepancy, including differences in the characteristics of the tides, effects of weather, changes in bathymetry, etc.

Entrance channel measurements. Evidence from the general circulation measurements suggested that peak entrance channel currents should easily meet the performance criterion, "not to exceed 2 knots" (3.4 fps). However, in light of the apparent presence of a gyre at station 8, further prototype measurements were obtained on two other occasions for confirmation (May 5th and July 19th, 1989). Predicted tide ranges were relatively extreme on these dates, at 8.1 ft and 7.7 ft, respectively. The same type of current meter described previously was deployed from the stern of SPN's vessel while it was tied alongside the fender piles at the east end of the detached breakwater. The horizontal and vertical position of the meter was adjusted until the location of maximum entrance current speed was found. On May 5th, measurements were made during most of the predicted stronger ebb tide only, due to scheduling constraints. A peak speed of 1.2 knots was observed. On July 19th, measurements encompassed both the peak flood and the subsequent peak ebb. Peak speeds for both flood and ebb again only attained 1.2 knots. Therefore, it can be concluded that the entrance channel performance criterion is very unlikely to be violated. Field notes for both sets of measurements are archived at SPN.

Bathymetry (scour and deposition)

Monitoring objectives for scour and deposition. The monitoring plan specified that the actual scour should be measured and compared with that predicted, and that the cause of scour should be evaluated. The effect of the breakwaters on deposition within the harbor was also to be investigated. Relevant performance criteria were that scour "must be within the design scour depth of 10 ft along the wall" and that circulation "does not impact shoaling rates to the point of requiring maintenance dredging." These objectives and criteria were addressed by analysis and comparison of data sets collected by two bathymetric methods: lead-line surveys at points along the breakwater structures, and acoustic fathometer surveys of the wider surrounding area.

Lead-line surveys. Following breakwater completion, the MCCP Program funded collection of seven lead-line data sets. These data sets were obtained by contracted surveyors or Corps personnel over the period from June 1987 to August 1991. Figure 36 shows SPN personnel deploying the District's own lead line, consisting of a 7-lb lead weight attached to a cord labeled with depth

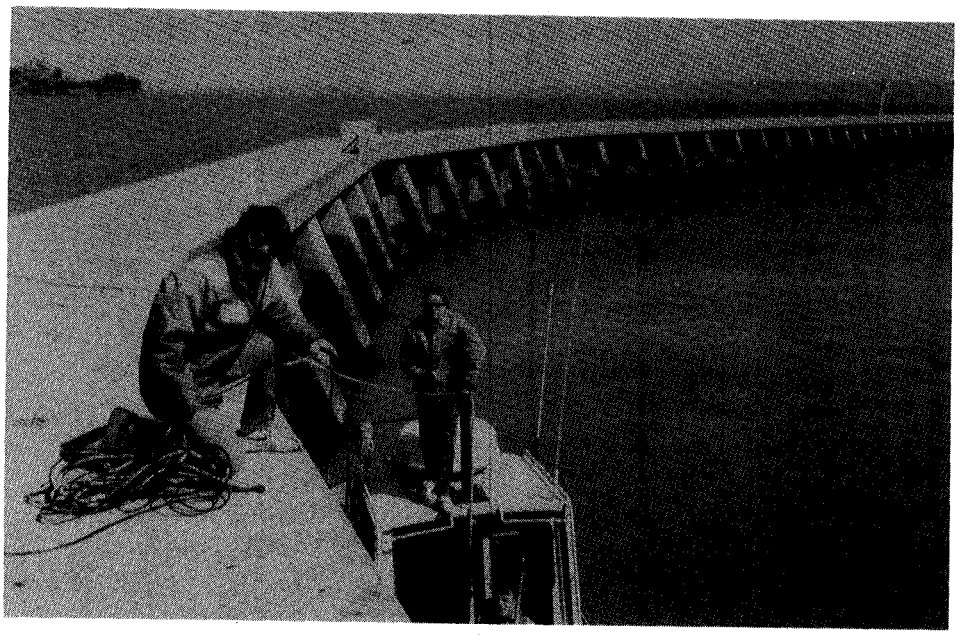

Figure 36. Taking lead-line soundings inside curvilinear section of detached breakwater

values. The lead (a standardized piece of survey equipment) is shaped like an elongated cone, with a concave bottom. For hard bottom materials, lead-line measurements can be reliable and repeatable. Soft materials are penetrated to a distance depending on their strength and density. The depression in the bottom of the lead is designed to trap a small sample of soft seabed materials. Cohesive (muddy) material was encountered at most points along the interior of the detached breakwater, and some points along the exterior. Hard bottom was found at the two ends. Contracted surveys were performed from small vessels; Corps surveys were performed from the breakwater cap, which is not accessible to the public. Differences in survey equipment and procedure are assumed to have had insignificant effects on resulting measurements.

Survey coverage was expanded and increased in resolution after the initial survey to avoid missing any "hot spots" of scour, and to provide some data along Hyde Street pier for the Park Service (GGNRA) as a return favor for their assistance with the general circulation studies. Some of the additional sites were dropped from later surveys as key locations became better defined. Also, some sites were occasionally inaccessible or not visited due to resource constraints. Generally, at each site along the breakwater several subsites were defined with bed elevation measurements recorded for each: immediately adjacent to the sheet pile at its point of penetration into the seabed; directly below the edge of the breakwater pile cap; and 5 ft out from the cap. Closer spatial resolution was obtained at the ends of the breakwater structures. A page-sized, plan-view figure cannot show all field measurements from a single date of survey, because the close spacing of subsites would prevent a readable display. To allow convenient comparison, each survey's data set was reduced to representative values for each site. Figures B8 through B14 show these

representative lead-line depths in one-page plan format for each of the seven surveys. Representative depths were selected by a judgmental process which estimated the spatially weighted average depth. Where large variation in subsite depths occurred, the representative depth for that site was estimated with a bias toward the deepest value, in order to be conservative considering the consequences of underestimating scour. The complete set of original field data are archived at CERC's PMAB and at SPN.

Near-structure scour and deposition. Figures 37 through 40 present results of comparisons of representative lead-line depths surveyed on different dates. Although no pre-construction lead-line data set was obtained, a set of depths at points along the future breakwater alignments (Figure B15) was extracted from the August 1984 Fathometer survey contours (shown in Figure B3). The spot-sounding data obtained by Woodward-Clyde, which were the basis for Figure B3 (but are not included in this report), were also consulted, to provide increased confidence about the precision and accuracy of Figure B15. Assuming no significant changes in bathymetry occurred between August 1984 and the completion of the breakwater, the depths of Figures B15 and B3 were considered representative of baseline conditions for the scour and deposition analyses. Another application of judgment was sometimes necessary in determining changes in depth between surveys at sites which were in close proximity, but not exactly aligned. Note that all depths in the figures have been rounded to the nearest integer value.

Figure 37 shows changes in depth between August 1984 and the most recent MCCP lead-line survey, August 1991. The figure is intended to show the net near-structure scour and deposition effects of the breakwaters. The deepest scour has taken place at the west end of the detached breakwater. Substantial scour has also appeared adjacent to the historic ship *Balclutha* (13-ft draft), moved to the location shown in April 1988. A substantial amount of net deposition has taken place at most locations along the landward side of the detached breakwater and near the tip of Hyde Street pier.

Since it is not possible from Figure 37 alone to know whether scour and deposition rates have changed over time, Figures 38 and 39 were prepared to show changes in depth between the baseline bathymetry and the initial lead-line survey, and between the initial and most recent lead-line surveys, respectively. Figure 38 can be considered a depiction of scour and deposition for the initial period between the start of pile-driving operations (November 6, 1985) and the first lead-line survey (April 21, 1987), assuming breakwater construction activities did not cause significant changes in bathymetry (no dredging was performed for construction). Figure 39 shows the net scour and deposition after the initial period. Values in Figure 37 are therefore the sum of those in Figures 38 and 39. It can be seen that most of the net scour of Figure 37 took place in the initial period, whereas deposition has been more steady over the years. Furthermore, Figures 38 and 39 show that trends at some sites (notably, those along the eastern-half landward side of the detached breakwater) reversed from erosional to accretional some time after the initial period. Conversely, some points along the segmented breakwaters reversed trend from accretional to erosional.

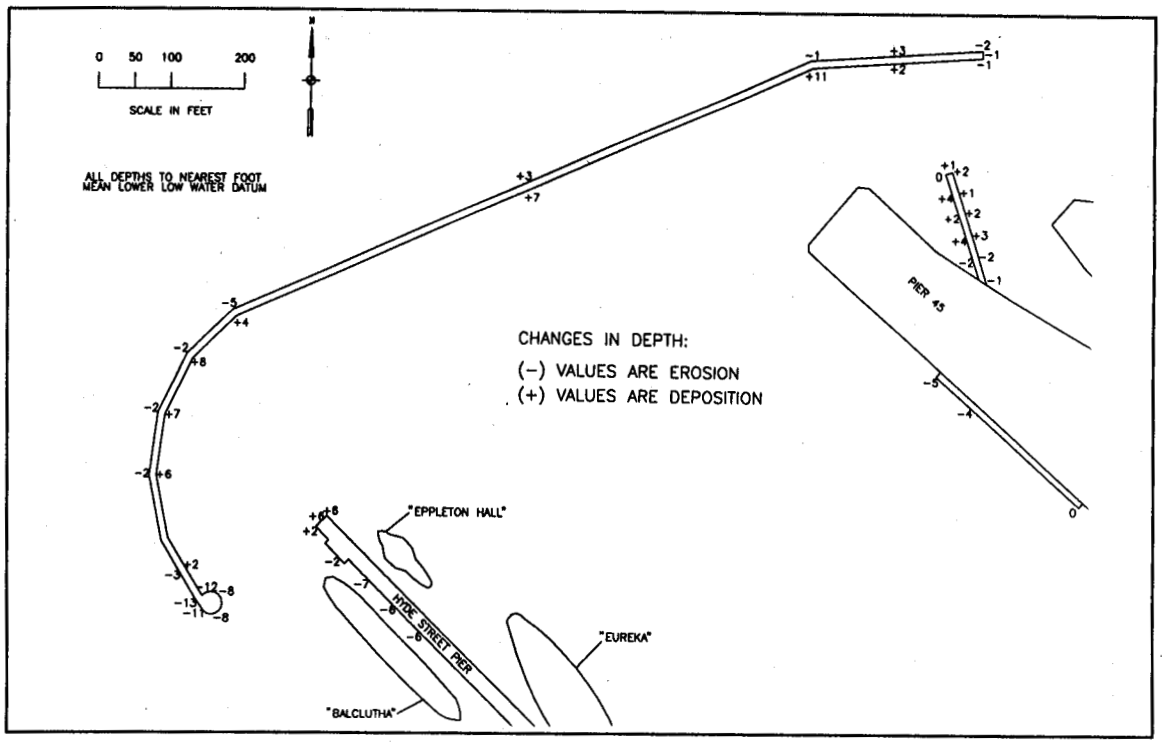

Figure 37. Comparison of August 1984 Fathometer and August 1991 lead-line depths

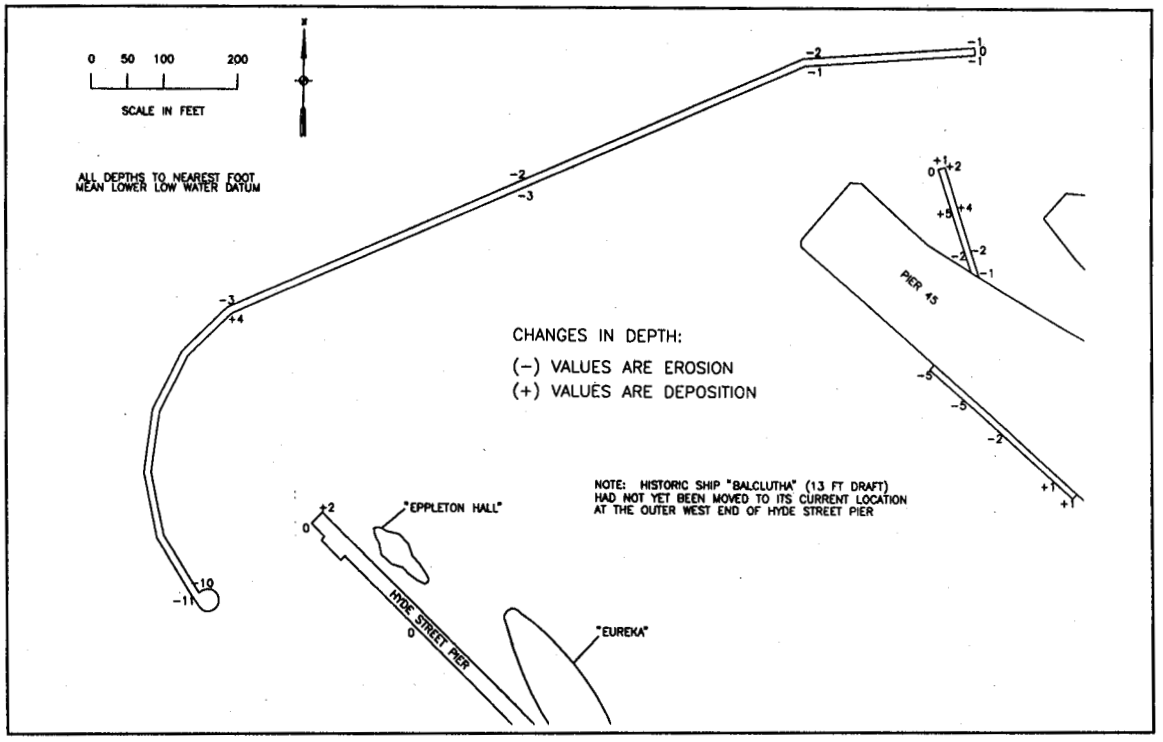

Figure 38. Comparison of August 1984 Fathometer and August 1987 lead-line depths

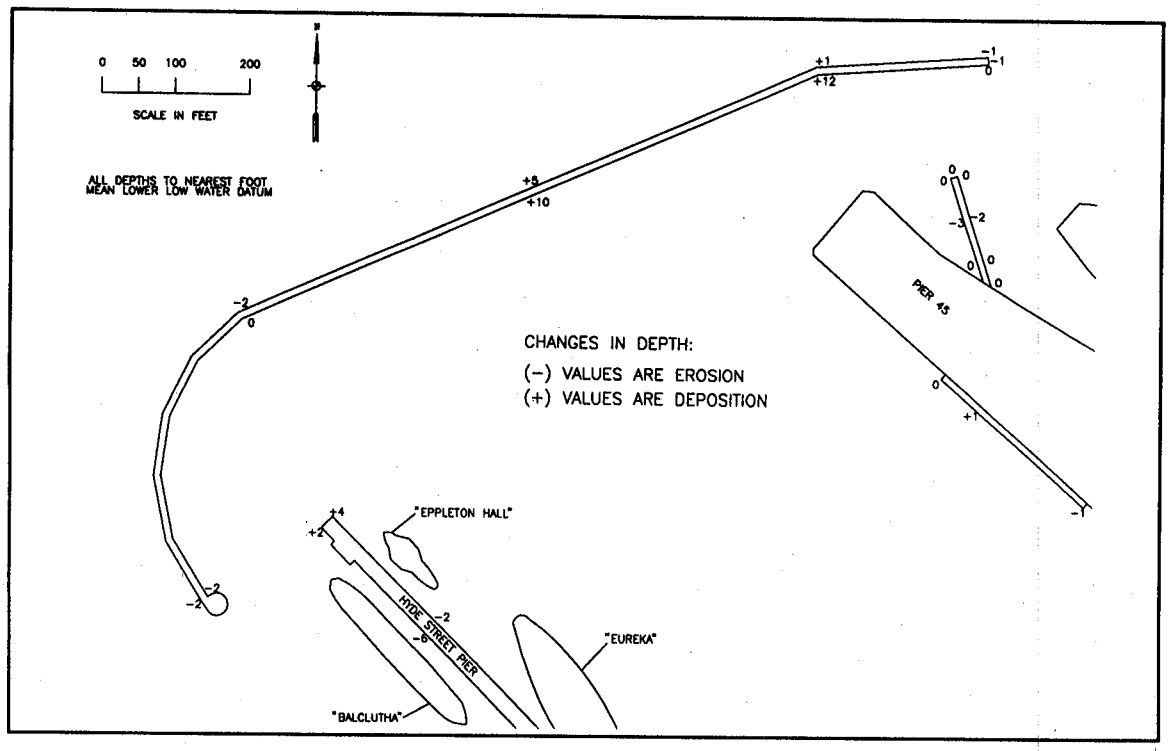

Figure 39. Comparison of April 1987 Fathometer and August 1991 lead-line depths

Figure 40 was prepared by scanning the representative lead-line depth figures (B8 through B14) for the deepest and shallowest depths observed at each site in all MCCP lead-line surveys (compiled into Figures B16 and B17), then plotting the differences between those depths and the August 1984 depths. For sites where both extremes of depth were deeper than the 1984 reference depth, only the deeper extreme was used to compute the plotted (negative) difference value. Positive plotted values resulted from the converse situation. For sites that had extremes both above and below the reference depth, both values were plotted. Therefore Figure 40 shows the envelope of depth values observed at each site over the 6-year period. The figure can be considered a "hypothetical worst case" scenario that did not occur at any one moment in time, but may be useful for a conservative evaluation of structural support of piles, including maximum across-wall mudline differentials. The figure conveys only a partial indication of erosional or accretional trends, however.

A detailed review of Figures B8 through B15 reveals that areas that appeared to have a continuous erosional trend include the two ends of the detached breakwater, the junction of the curved and straight sections of the detached breakwater, the area adjacent to the *Balclutha*, and a few spots adjacent to openings in the segmented breakwaters. Nearly all sites along the landward side of the detached breakwater (except close to the east end) appeared to have a relatively strong accretional trend since the initial period. Other bayward-side sites along the straight section of the detached breakwater showed occasional trend reversals, although they were primarily accretional since the initial period. Some of the trend reversals and rate changes may be

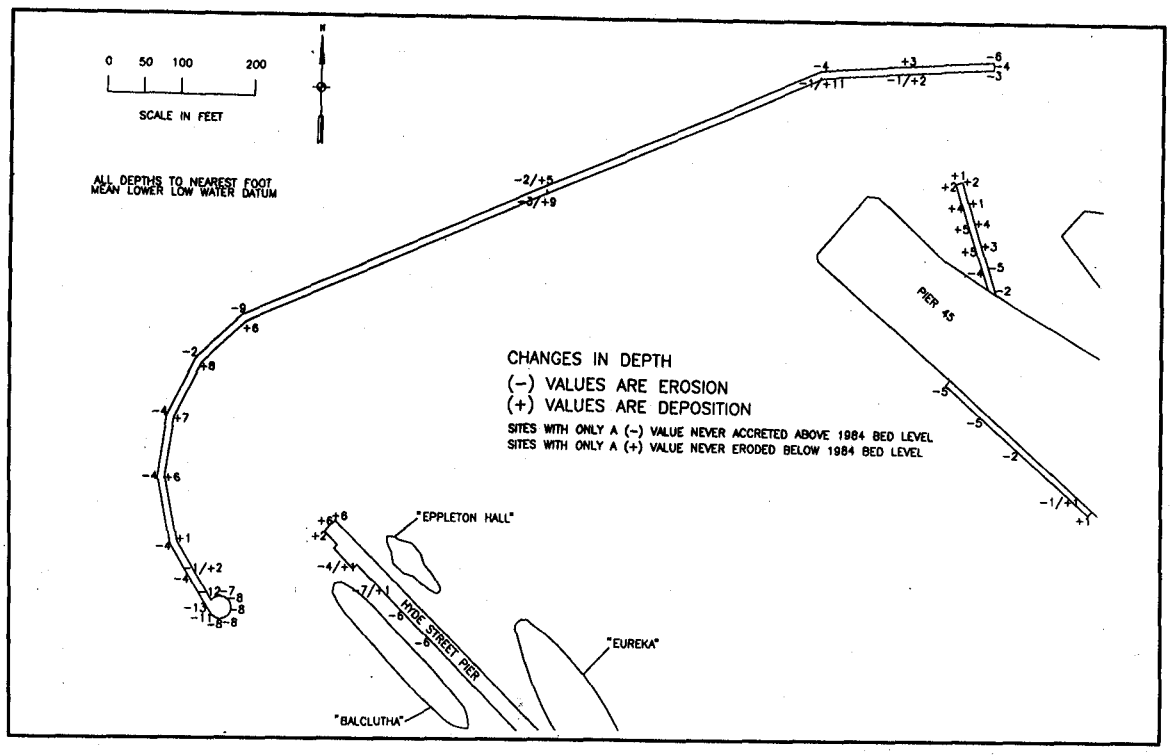

Figure 40. Extremes of scour and deposition observed in all MCCP lead-line surveys

due to seasonal effects related to cyclic changes in tidal current strength and variations in the sediment supply. It should be emphasized that the lead-line sites were not sampled frequently enough to allow a more complete definition of erosional/accretional trends over time.

Comparison of measured versus predicted scour. Figure 41 compares the predicted maximum likely scour depths of Figure 21 with measured maximum scours (negative values) and minimum depositions (positive values). Measured scour and deposition values in the figure were determined by taking the change in depth between the 1984 baseline reference depths (Figure B15) and the deepest observed depths in the lead-line surveys at each site (Figure B16). Accordingly, the measured scours and depositions in the figure are not implied to have existed simultaneously at any moment during the 6-year period, yet they represent a worst-case combination of measured values.

Another possible version of Figure 41 could be prepared based on the August 1991 depths (for example using the net scour values shown in Figure 37). Since the predicted scours were described in the GDM as "equilibrium" values, if the erosional trends due to the breakwaters had indeed leveled off by August 1991, such a figure would constitute a more appropriate comparison. Recall that Table 2 presents the more conservative predicted "maximum equilibrium scour depths." However, the lead-line sites were not sampled frequently enough to allow a determination of whether or not the absolute extremes of scour have already occurred. It is possible that a more frequent program of lead-line sampling (particularly in the initial

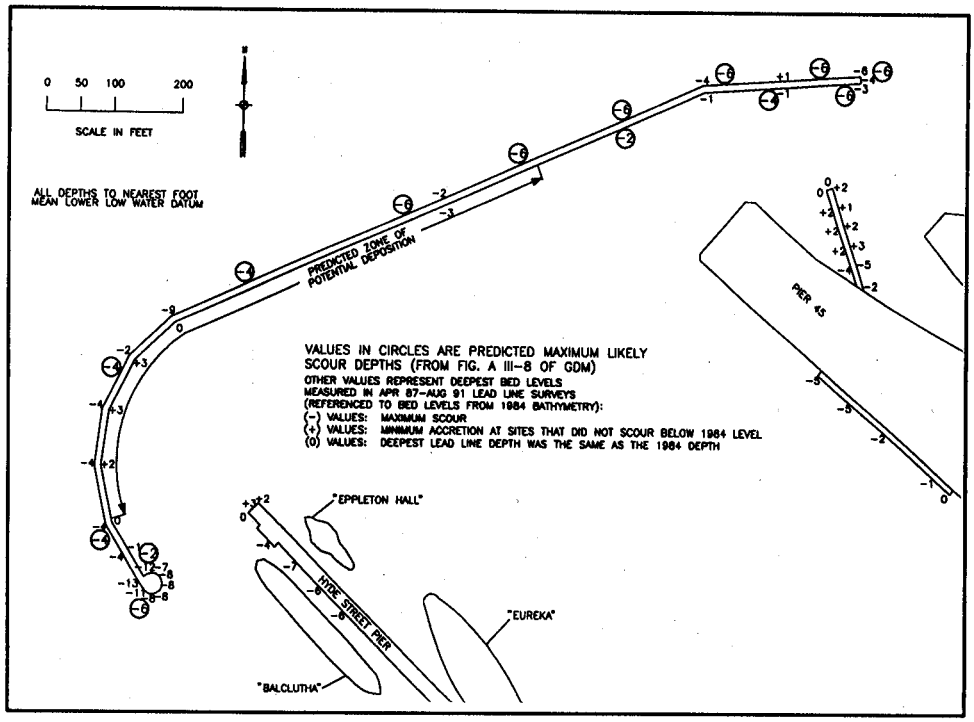

Figure 41. Comparison of predicted versus measured maximum scour

post-construction period) would have detected even more extreme depths than those used to prepare Figure 41.

From Figure 41, generally the zones of scour and deposition along the detached breakwater were predicted correctly. The magnitudes appear to have been overestimated for most of the eastern two thirds of the structure (except at the east end), and underestimated for the west end. The maximum scour depth range in Table 2, 10-12 ft for a water depth of 20 ft, appears to have been a better estimate of the measured scour at the west end of the detached breakwater.

Comparison of measured versus design scour. Figures 42 and 43 compare depths used for sheet pile structural design (a single depth for each of the six design sections discussed in Chapter 2) with measured lead-line depths. Measured depths for Figure 42 are the representative depths from the August 1991 lead-line survey. In Figure 43, the deepest observed depths (from Figure B16) are shown instead. Comments in the preceding section about equilibrium and worst-case conditions apply here as well. Accordingly, Figure 43 provides a more conservative basis for evaluating whether the nominal "design scour depth of 10 ft along the wall," has been exceeded, or whether piles have experienced critical minimum embedment conditions. A careful review of the GDM's wording indicates that the scour performance criterion should be applied to the bayward sides of all three breakwater components. Apparently the design scour depth of 10 ft was applied stepwise to each of the six design depths for the six classes of piles. Therefore, even if a location along the breakwater shows a measured scour (relative to 1984

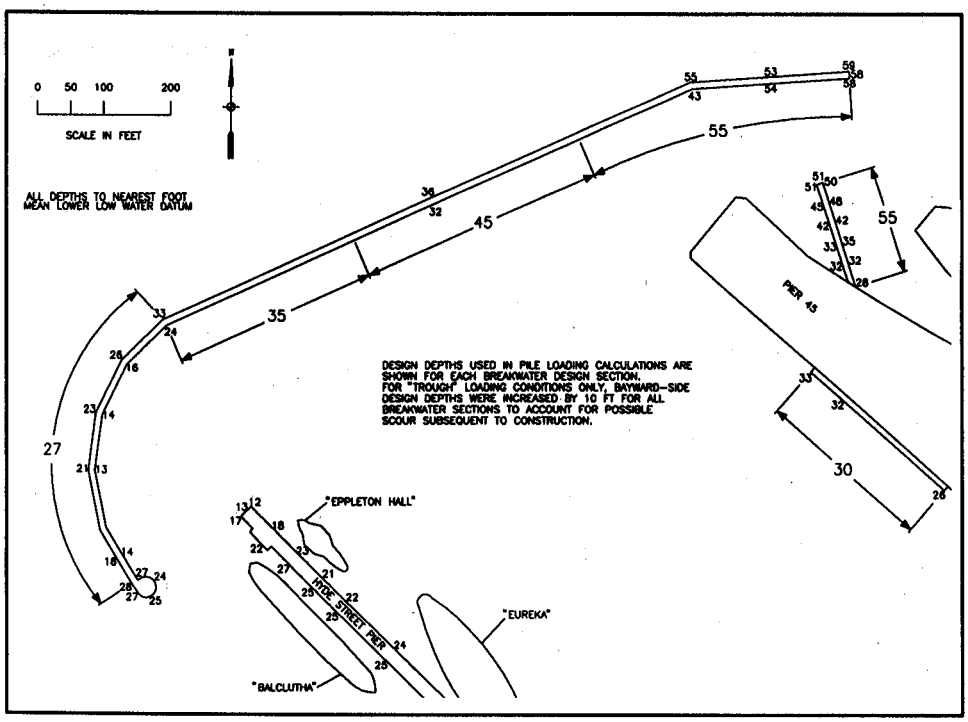

Figure 42. Comparison of pile design depths versus August 1991 lead-line depths

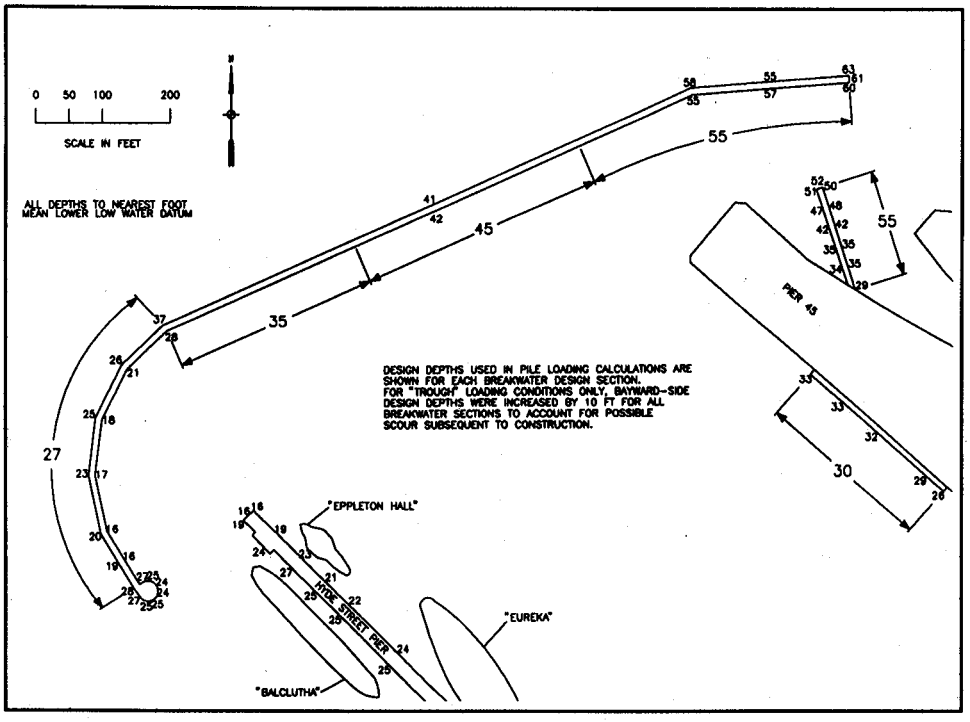

Figure 43. Comparison of design depths versus deepest observed lead-line depths

depths) greater than 10 ft--a violation of the scour performance criterion--it may not be approaching the actual structural design depth. For this reason the scour values from Figure 41 (to be conservative) or Figure 37 (to reflect more recent conditions) should be used to determine whether the performance criterion has been met. Figures 42 and 43 are more appropriate, however, for evaluating design versus measured depths of pile embedment.

For example, from Figure 41, it is seen that the scour performance criterion has been violated at the west end of the detached breakwater. The junction point between the curvilinear section and the straight sections has also been very close to violation. Yet from Figure 43, it is seen that piles at the western end could have had approximately 9 ft of additional scour before they reached the bayside structural design depth of 37 ft (section IV design depth of 27 ft plus 10 ft bayside scour). However, a few piles at the other end of section IV, at the end of the curvilinear section, have already seen a bayside depth of 37 ft. Although the scour performance criterion has been met at all other sites, the easternmost piles of the detached breakwater have been within 2 ft of their structural design depth of 65 ft.

Since the structures are tied together by cap beams and behave structurally as units, the severity of scour at the detailed, individual pile level is only one factor involved in determining the criticality of structural support. For example, a given loss of embedment at the ends of structural units (including on either side of expansion joints) could pose a more significant structural threat than the same embedment loss at locations within units supported by the adjoining structure on both sides. Furthermore, the increased earth pressures from the deposition along the landward side of the detached breakwater should also be considered in any analyses of the present situation's structural risks.

Cause of scour. Available resources and measured data were insufficient to permit investigating the cause of scour--that is, the processes involved and their relative contribution to the observed scour--in a detailed, scientific manner. On the other hand, it is clear that the breakwaters have resulted in local scour. It is reasonable to assume that where the breakwaters restrict or abruptly redirect the tidal flow, causing local accelerations, higher velocities, and instabilities (turbulence, vortices, vertical components, etc.), greater sediment-transport driving forces exist than at locations where there is little interference with the pre-breakwater flow pattern. Wave-induced bottom currents probably have played some role in the scour/deposition processes along the breakwaters, but the relative contributions of wave-related versus tidal current-related processes cannot be delineated from the observed data. Other regional-scale factors (such as seasonal variations in the sediment supply) may also be involved.

Prevention of further scour. Preliminary reviews of MCCP lead-line data through March 1989 suggested that the scour could eventually become a maintenance problem. Due to the long lead times required for fiscal planning of construction activities, SPN initiated the process in FY 1989, in anticipation of a possible scour-protection project. In February 1992, interim (partial) MCCP lead-line analyses were delivered to SPN for use in evaluating the need for the

scour protection and for design purposes. As a preventive measure, scour protection was constructed at the ends of the detached breakwater and the east segmented breakwater in October 1992. The protection consists of three layers: a base fill material (of varying thickness, depending on the depth of the scour zones); an intermediate rock filter material; and a top armor material (stone riprap). From the complete lead-line analysis described in this report, it appears that it may be prudent to evaluate the present adequacy of structural support on an individual pile and structural unit basis. The junction between design sections III and IV (end of curvilinear section) should be given a particularly careful examination. It is recommended that depths at that junction, adjacent to the openings in the segmented breakwaters, and in the recently protected areas continue to be monitored.

Fathometer surveys. Five fathometer surveys covering parts of the Fisherman's Wharf area were contracted by SPN over the period from August 1984 to September 1990. The resulting data are shown in Figures B3 through B7. The first of these (which has been discussed previously) formed the basis for the bathymetry sheet included in the as-built plan set. The subsequent surveys were conducted as part of the MCCP program. Areal coverage of the second survey (June 1987) was, like the pre-breakwater survey, limited to the immediate vicinity of the breakwater structures. The third survey (April 1988) was expanded to cover a greater area, including the zone west of the outer part of Hyde Street pier, and most of the protected basin, including the proposed berthing expansion area. The fourth and fifth surveys (August 1989 and September 1990) expanded coverage further to include the entire Aquatic Park small boat mooring basin. Data were collected using standard hydrographic surveying equipment (echo sounders) and procedures. A comparison of lead-line versus fathometer measurements showed that depths obtained are approximately the same by either method. All fathometer survey results were provided as blueprint-sized drawings (original Mylars are archived at SPN). In addition, the two most recent surveys were also delivered in digital form as computer drawings using a base map drawn based on aerial photography obtained at the time of the 1989 survey. The digital base map proved very useful as a background for many of the figures shown in this report. Due to resource constraints, it has not been possible to digitize the spot soundings, contour all five of the survey data sets, and perform inter-comparisons by computer-assisted methods. Also, the varying extent of survey coverage would complicate such an analysis. Nonetheless, a generalized comparison could be performed by examining depths at approximately corresponding locations.

Effect of the breakwaters on scour and deposition within the harbor. A point-by-point comparison of depths covered in all fathometer surveys might reveal details of scour and deposition not readily apparent in this less rigorous review of the five data sets. However, it is evident that most scour effects clearly attributable to the breakwaters have been better defined by the previously discussed lead-line data and analysis. Other than the relatively large scour zone at the west end of the detached breakwater, no other obvious widespread scour zones can be seen in the fathometer data. Given the relatively coarse resolution of the fathometer data (compared to the lead-line data), it would be difficult to detect scour features of the size occurring adjacent to the

structures, yet it is unlikely that any other large scour areas have been missed. On the other hand, depositional zones were found to cover relatively large areas.

Figure 44 summarizes net scour and deposition trends (over the time period covered by surveys) in the areas of common coverage by fathometer surveys. The local scour zones shown on the figure were primarily determined by the preceding lead-line data analysis. Scour rates (feet/year) for these zones have been roughly estimated and generalized from the measured data. They represent approximate average scour rates required to produce the measured net depth change. It is not implied that scour was constant at the rates shown. Indeed, at many locations the detailed data show that scour rates varied widely, and in some cases these locations experienced deposition for portions of the record.

The approximate boundaries of the depositional areas in Figure 44 were estimated by comparison of depths at several key points within the common fathometer coverage areas. The boundary outlining the "average deposition greater than 1 foot/year" zone should be considered very approximate, especially the portion of the boundary lying within the berthing expansion area, which was not surveyed prior to 1988. The deposition rates shown roughly approximate rates required to produce the measured net deposition. Clearly, the zone along the protected side of the breakwater from the curvilinear section up to about the end of Pier 45 has shown the highest net deposition rate. Review of Figures B3 through B7 reveals an eastward migration of the 20-, 30-, and 40-ft contours, and steady decreases in the minimum depths found in the area beyond the end of Hyde Street pier. The rate shown in the entrance channel is included to reflect that the measured data indicate a weak net depositional trend there. A careful examination of the fathometer data sets shows highly variable bathymetric evolution in the entrance channel zone. For example, at the east end of the detached breakwater, the 1989 data indicate a relatively deep scour "hole," which had essentially disappeared by the 1990 survey. The data clearly show that the historic ship *Balclutha* has had a significant erosional effect on adjacent bathymetry. For areas other than those indicated in Figure 44, either no clear scour and deposition trends were detected, or there is insufficient coverage to make a determination.

Since there are no successive pre-breakwater fathometer surveys covering the entire area, it is not possible to estimate "background" scour or deposition (shoaling) rates. Therefore it is difficult to evaluate whether, and to what extent, the breakwaters have altered shoaling rates, as required by the objectives and performance criteria of the monitoring plan. To date, the area has not been dredged, so it could be argued that the shoaling-related performance criterion has been met. Furthermore, the outer boundary of the zone where breakwaters have influenced scour and deposition is impossible to determine from the available data, although it is probably safe to say that scour effects have been limited to the immediate vicinity of the structures, and deposition effects have been relatively more widespread.

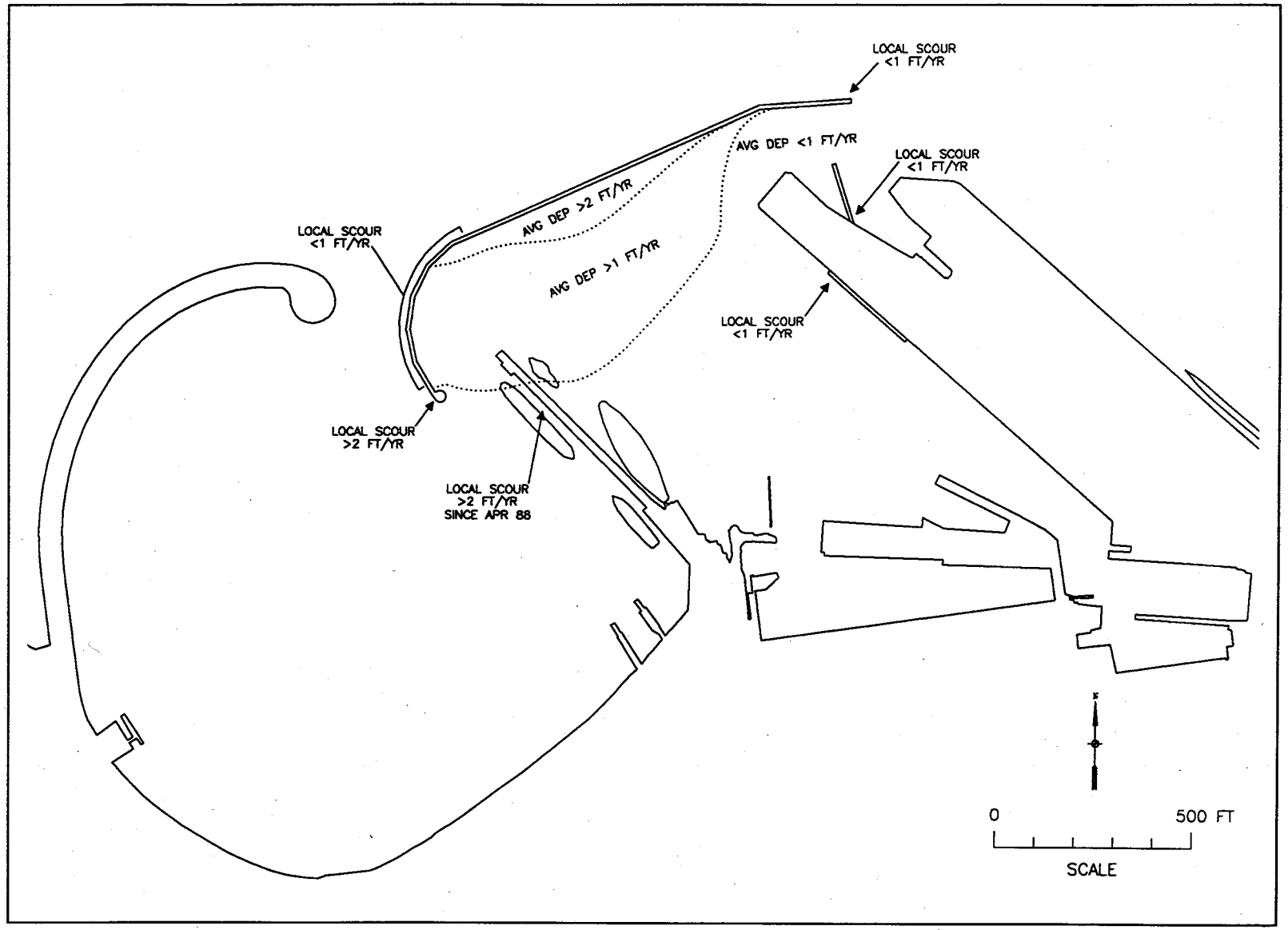

Figure 44. Summary of net scour and deposition trends

Littoral environment

Monitoring objectives for littoral environment. The monitoring plan calls for an evaluation of the effect of the breakwaters on "the littoral process, including shoreline response and deposition within the harbor." The "beach erosion" performance criterion specified that the breakwaters "not increase net sediment loss to the Aquatic Park system." Harbor deposition has been addressed in preceding sections. The MCCP data collection approach was to assemble any available beach-related information, and establish a "Littoral Environment Observation" (LEO) station at Aquatic Park. It was felt to be beyond the scope and resources of this MCCP study to rigorously examine the aforementioned performance criterion by determining the boundaries of the Aquatic Park littoral system and its sediment budget.

Littoral environment observations. In the late 1970s, CERC began a program to formalize and standardize procedures for low-cost, continuing measurements of beach and surf zone characteristics. The program, known as LEO (Schneider 1981), was carried out by human observers. Near the beginning of the Fisherman's Wharf MCCP effort, several employees of GGNRA (including lifeguards at Aquatic Park beach) were trained to collect LEO data at a location near the Maritime Museum building. A second purpose of the LEO at Fisherman's Wharf was to provide a check on wave measurements obtained by wave gages installed in the study area. Although LEO data are somewhat subjective and qualitative, long-term data sets with frequent observations (especially by the same observer) can have statistical validity and quantitative uses. Due to changes in personnel and funding cuts (including elimination of the lifeguard positions), the LEO data collection was sporadic, and was eventually discontinued. The observations were too infrequent and duration of coverage was too short to form a valid basis for analysis. This MCCP study found no other quantitative data on post-breakwater beach characteristics (such as repeated surveys of beach profiles or sequential aerial photographs).

However, qualitative observations during site visits throughout the MCCP study and discussions with GGNRA personnel indicated no noticeable changes in Aquatic Park beach attributable to breakwater effects. The description of the beach in the Noorgard Consultants report (1985) is a valid description of the present-day beach. Furthermore, the beach management practices described in Chapter 2 (see Figure 45) may be masking or mitigating breakwater-related beach changes. In summary, there is no evidence that beach erosion has increased due to breakwater effects.

Structural integrity and alignment

Monitoring objectives for structural integrity and alignment. The monitoring plan specified that "spalling, cracking and settlement of the wall" be investigated to address structural integrity. Acceptable performance was defined as "vertical and horizontal alignment changes, visual cracking and spalling not sufficient to impact the function of the structure." The MCCP

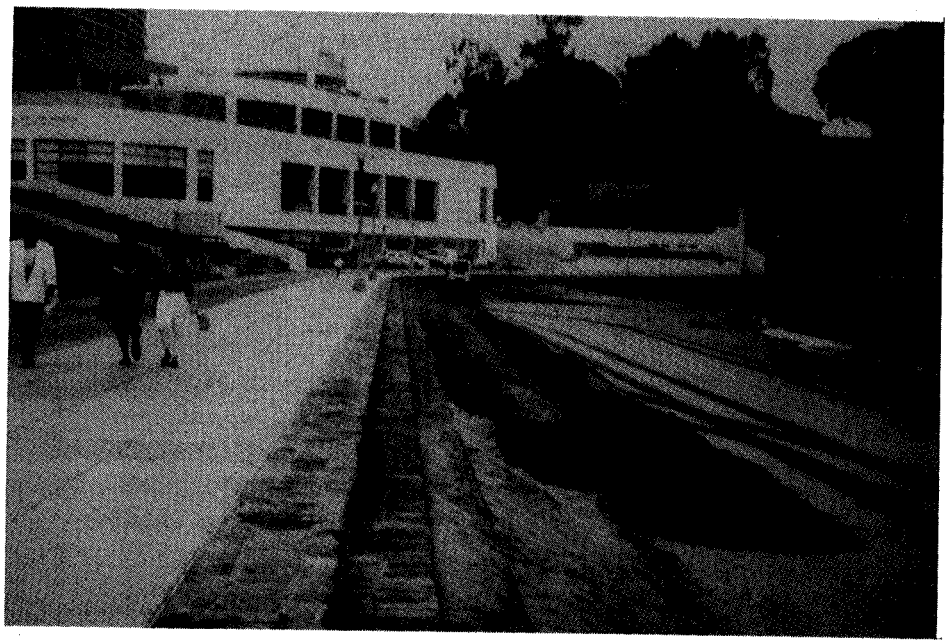

a. Looking west along promenade--Maritime Museum in background

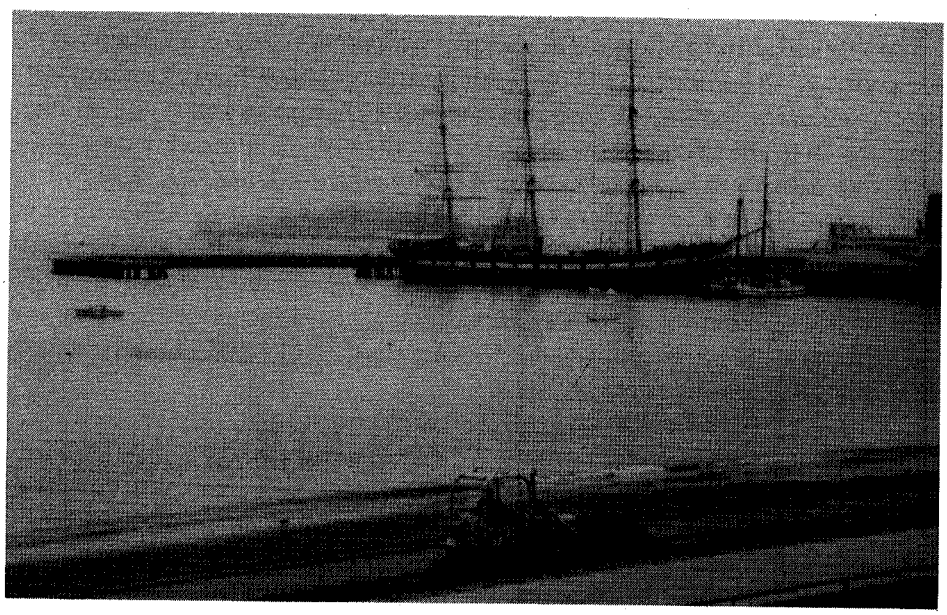

b. Looking north--Alcatraz Island in the distance

Figure 45. Beach management by front-end loader at Aquatic Park

approach was to perform qualitative visual inspections and quantitative surveys establishing and re-examining the horizontal and vertical absolute positions of selected points on the structures.

Visual inspections. The breakwaters are routinely subjected to visual inspections by SPN personnel as part of their annual Operation and Maintenance condition surveys program. During these inspections, a boat is driven alongside the breakwaters while observers take notes, photographs, and videotape to document any visible damages or deterioration. All visual inspection results are archived at SPN.

No significant evidence of deterioration (cracking, spalling) in the original concrete was found during visual inspections. At a few isolated locations, grout patches were applied at the end of construction to protect places where small portions of sharp sheet-pile edges broke off in construction handling. Some of these patches have fallen off, allowing some minor corrosion in the exposed areas. Figure 46a (at station 11+66, in the curvilinear section of the detached breakwater) shows the worst example of this type of deterioration. Also, some of the rubber expansion joint gaskets have loosened from the underside of the detached breakwater cap, but are still attached along the top side of the cap (see Figure 46b). The function of the structure has not been affected by these minor problems.

Supplemental inspection data. Several additional types of information were collected in addition to the routine inspection data, either in conjunction with the annual inspection or on an ad-hoc basis. Partial sets of lead-line data (measured from the detached breakwater cap) were obtained on two occasions. These data sets were included in the previously discussed analysis. SPN's side-scan sonar was also used on two occasions to search for evidence of scour holes along the structures. On one occasion, divers attempted to retrieve seabed core samples to provide additional qualitative information about the nature of the seabed at scour and deposition zones along the detached breakwater. A special inspection was conducted following the October 1989 Loma Prieta earthquake to check for related damage.

The side-scan sonar surveys (April 1989 and April 1990) provided qualitative images of seabed features along the detached and east segmented breakwaters. The high acoustic reflectivity of the concrete structures and lack of precise position and elevation information for the sonar towfish made the resulting images difficult to interpret. Nonetheless, the images provided evidence of local scour at the two ends of the detached breakwater, including at the base of batter piles, as well as adjacent to the openings in the east segmented breakwater. Evidence of scour was more clearly visible in the second side-scan survey's data. The original side-scan sonar records are archived at SPN.

Divers were deployed during July 1989 to attempt collection of short seabed cores (tube length about 2 ft) at four locations along the detached breakwater. Although surface currents were minimal at the location just landward of the east end, the dive there was aborted for safety reasons after encountering

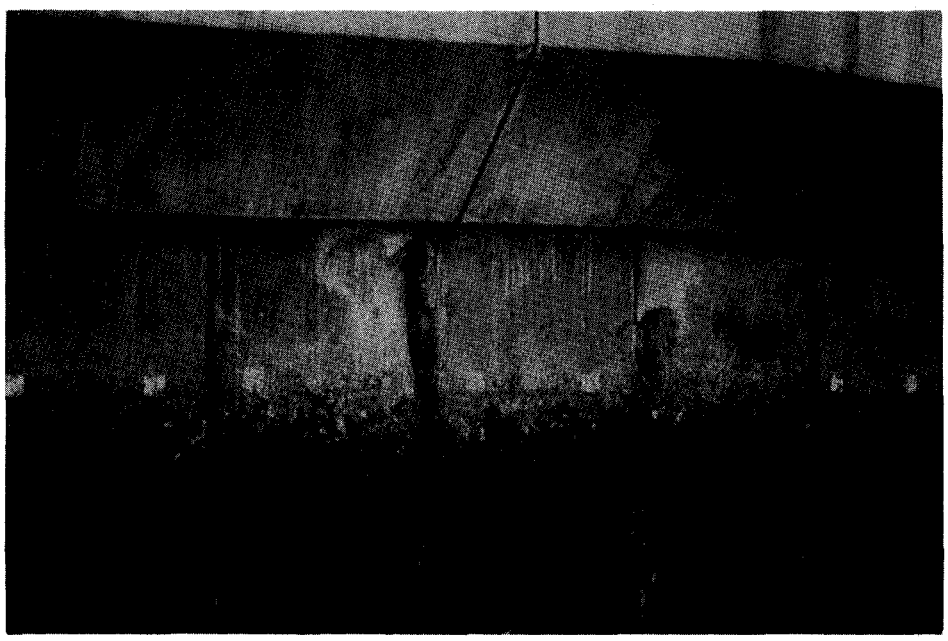

a. Missing concrete on west-facing side of sheet pile

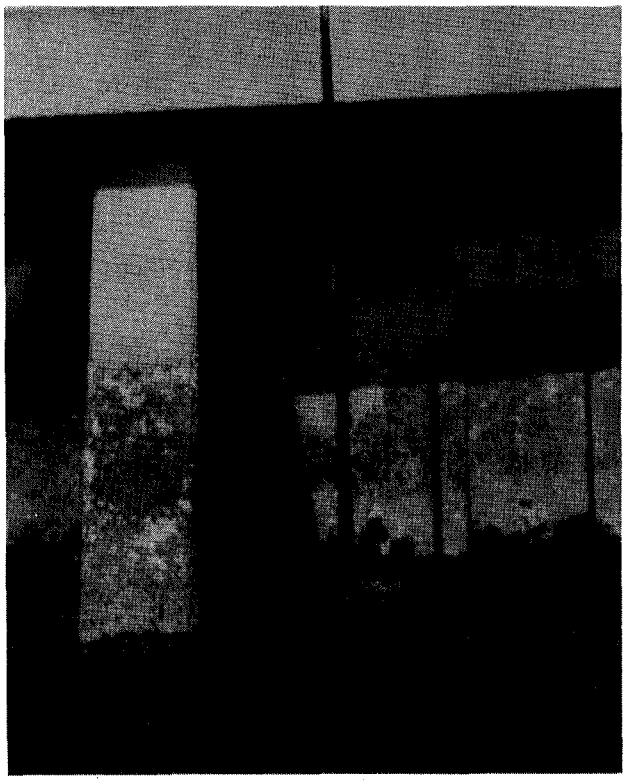

b. Dislodged expansion gasket

Figure 46. Minor damage and corrosion of detached breakwater sheet piles

relatively strong bottom currents and in consideration of the potential for entanglement with the batter and fender piles in the zero-visibility conditions. Core tubes were easily pushed by hand into the soft, mostly muddy material at the two locations within the depositional zone landward of the structure (near the midpoint, and about 75 ft north of the west end circular platform). It was not possible to insert the core vertically at the fourth location (immediately adjacent to the end of the sheet pile wall under the circular platform). The bottom material there was scooped into the core tube with a scraping motion. It consisted of hard materials, including shells, construction debris (small chunks of concrete, short pieces of rebar), sand, gravel, and some mud. A strong turbulent flow was encountered there, and a steeply sloped seabed depression was noted. The extent of the scour hole was not explored for safety reasons. The bottom samples were not subjected to laboratory analyses, and were discarded after being examined and photographed.

Structural alignment surveys. Four precise surveys of fixed monuments along the structures have been performed since breakwater completion. Locations of the monuments (including two on Municipal pier) are shown in Figure 47. The monuments on the breakwaters are brass disks embedded flush with the breakwater cap. The first survey, just after construction (November 1986), included monuments 1 through 6 and the two on Municipal pier. Additional monuments 7, 8, and 9 were installed for the April 1988 survey. Subsequent surveys including all 11 monuments were performed in September 1989 and October 1990. Standard land-surveying equipment and procedures were followed. Additional control benchmarks in the area, besides those shown in Figure 47, were used to establish absolute reference to the California State Plane Coordinate system for horizontal positions, and to mllw datum for elevations. All structural alignment data are archived at SPN.

The contractor for the 1988 survey was not asked to compute changes in monument positions from the original (1986) positions surveyed by SPN. However, the contractor for the 1989 and 1990 surveys was required to compare positions to prior surveys. The contractor found that positions supplied for the 1986 and 1988 surveys were in error, leading to apparent movements up to several feet. Errors in the 1988 survey were correctable, however. Although differences between the 1986 and 1990 positions were computed to the extent possible, the contractor was unable to make conclusions about the accuracy of those results (which showed generally larger movements than between other surveys) due to differences in the two surveys' methods, and lack of sufficient original field data. In the report following the 1989 survey, the contractor's opinion was that no detectable breakwater movement had taken place between the 1988 and 1989 surveys. Small apparent movements of the breakwaters between 1989 and 1990 were reported following the 1990 effort, however. The detached breakwater moved south by an average of 0.07 ft. The west segmented breakwater moved southwesterly by an average of 0.10 ft. The east segmented breakwater moved west-southwesterly by an average of 0.09 ft. Monument HL 57 moved easterly by 0.09 ft (HL 56 was used as a reference, and therefore was assumed to be stationary). The contractor's report emphasizes that the aforementioned movements are *apparent* movements, that

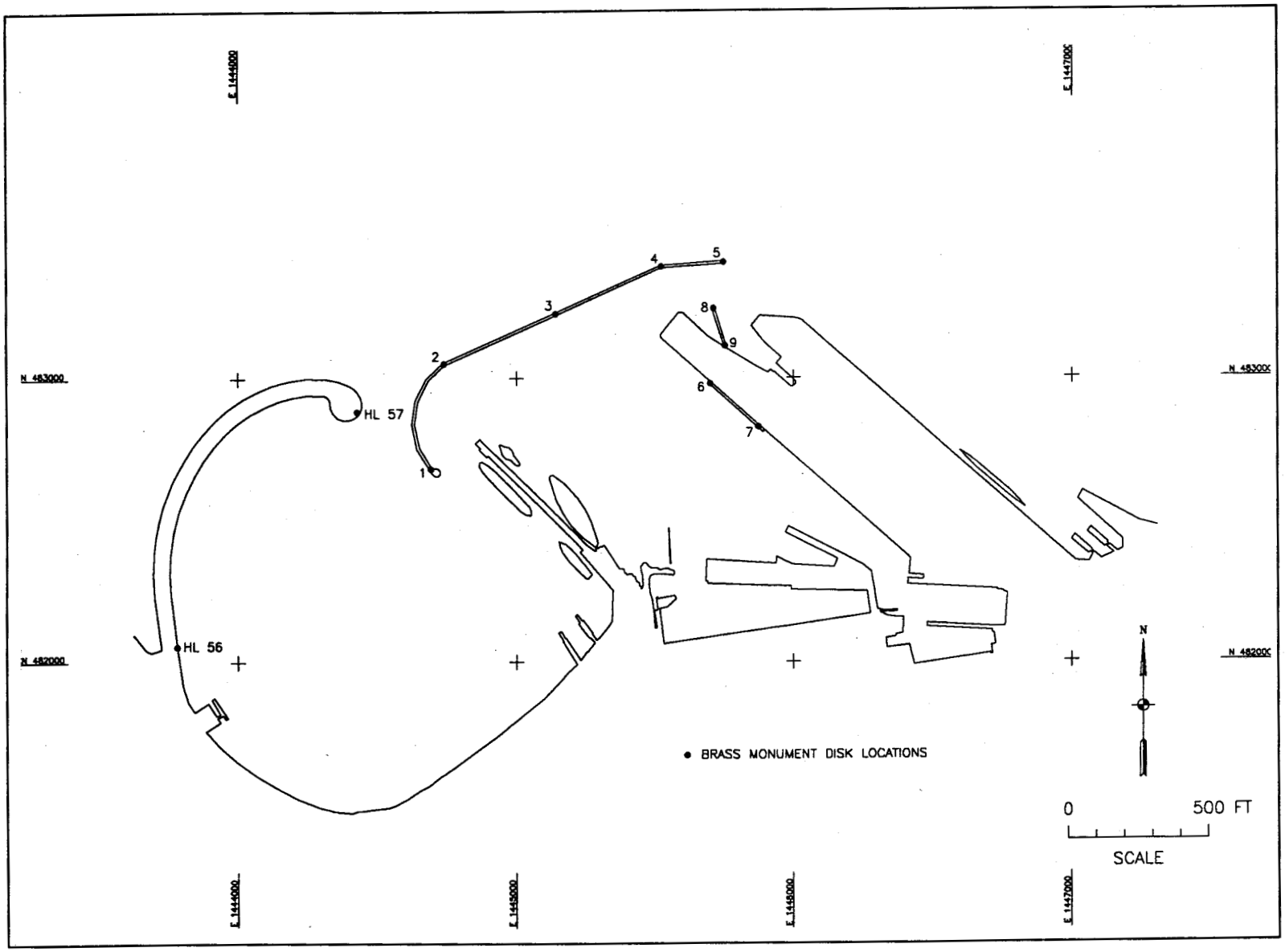

Figure 47. Locations of structural alignment monuments

is, movement of HL 56 and HL 57 in a north-northeasterly direction would have produced the same apparent movement of the breakwaters.

The contractor reported that movements at Fisherman's Wharf between the 1989 and 1990 surveys may have been caused by the October 1989 Loma Prieta earthquake, since a post-earthquake survey for a different client indicated a movement of 0.13 ft in an east-northeasterly direction at a location in eastern San Francisco. SPN personnel visually inspected the breakwaters immediately following the earthquake, and once again a few months later. No noticeable changes or damage were detected. Figure 48 shows earthquake damages to nearby structures (photographs were taken in March 1991). Figure 48a shows an example of differential settlement inside one of the buildings on Pier 45. The February 1991 issue of *The Fisherman's News* reported that over $9 million in damages to Pier 45 resulted from the earthquake. The same article states that when the earthquake hit, "the fill beneath the central portion of the pier liquified, causing extensive buckling and cracking to floors and foundations of the sheds, making continued operations unsafe." Figure 48b shows a partially collapsed section of decking near the landward end of Hyde Street pier. Some of the most dramatic damages in San Francisco occurred in the "Marina District," a residential area located about 1 mile west of the breakwaters.

Elevation differences between surveys were considered to be minor, although reported values for the latter three surveys have a consistent trend of very slight elevation decrease, with differences between 1988 and 1990 values ranging from 0.03 to 0.07 ft. These elevation decreases show no evidence of differential settling of the breakwaters, however. Elevations of the nine breakwater cap monuments for 1990 are within 0.07 ft of one another, confirming the visual impression that the caps remain level. State Plane coordinates and elevations of the 11 monuments from the October 1990 survey are given in Table A1.

From visual inspection, the breakwaters appear to be entirely stationary, i.e., there is no visible motion due to waves. The contractor's reports for 1989 and 1990 mention that vibrations (described as "chattering") due to waves striking the detached breakwater caused fluctuations in the readings obtained by the survey instruments. Also, the fender pile clusters protecting the ends of the breakwaters have been observed swaying back and forth with the passage of waves (range of motion up to several feet). Some of the piles within the clusters appear to have uplifted by several inches from their original position (see Figure 6b); also, the connections holding the piles together appear to be loose. The clusters are still performing their function, however. Maintenance of the pile clusters is not part of SPN's responsibility.

In summary, the breakwaters are meeting performance criteria for structural integrity and alignment. No significant deterioration, settlement, or changes in alignment have occurred. There is no evidence of damage due to the October 1989 earthquake.

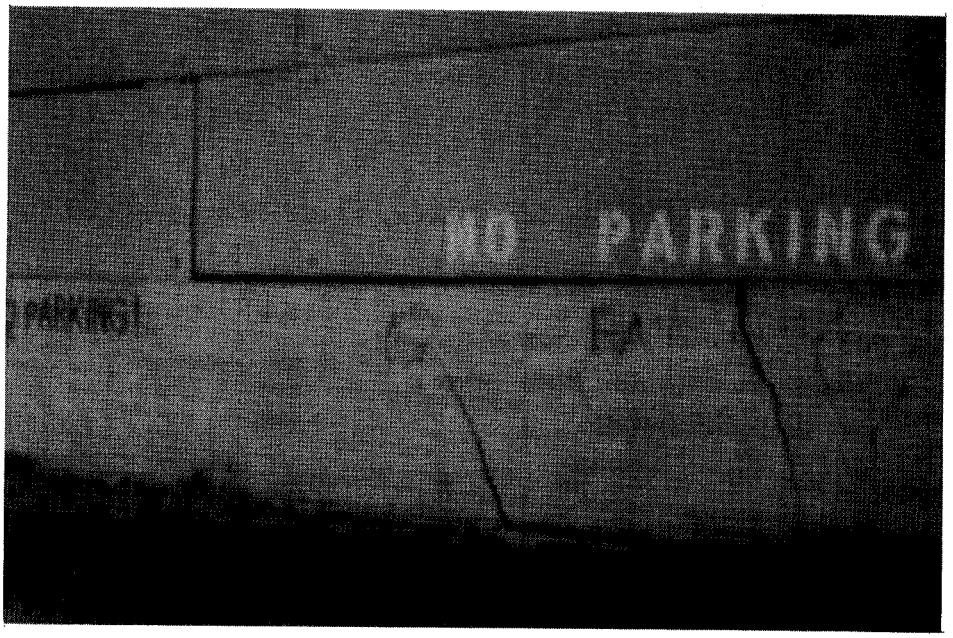

a. Settlement and cracking of structure on Pier 45

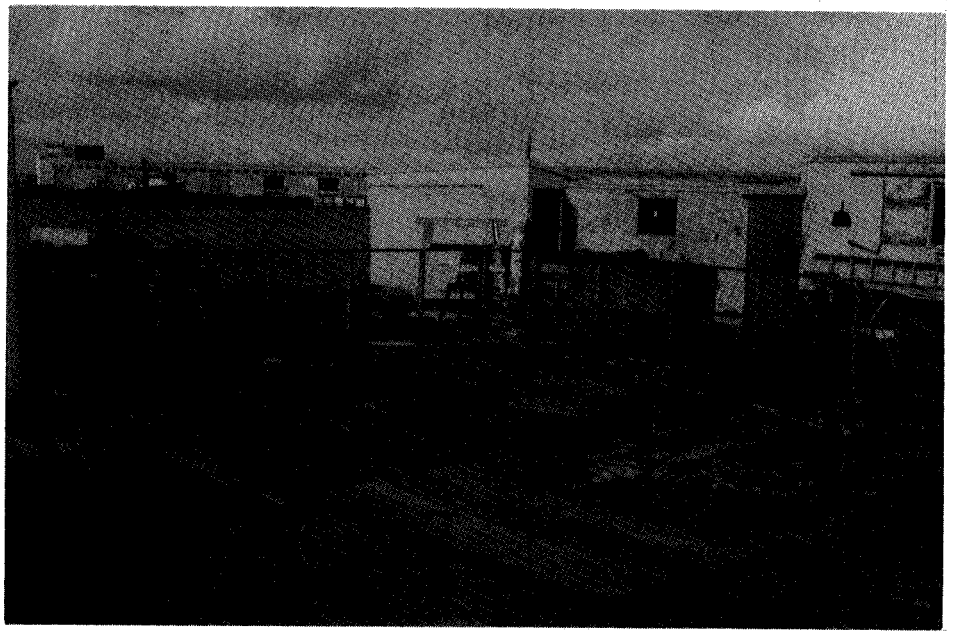

b. Partial collapse of Hyde Street pier deck near landward end

Figure 48. October 1989 earthquake damage in study area

4 Summary, Evaluation, and Recommendations

Breakwater Performance and Impact on the Surrounding Area

Waves and surge

Available measured wave data for the post-BW period show that significant wave heights (wind waves and swell) within the protected harbor did not exceed performance criteria. The breakwater is performing its primary purpose--to provide wave protection for the traditional Fisherman's Wharf small-craft berthing area, for the fleet of historic ships berthed at Hyde Street pier, and for the planned berthing expansion area between Hyde Street pier and Pier 45. Figure 49 shows wave conditions at Fisherman's Wharf during a "norther" on December 15, 1988. The largest significant wave height measured inside the protected harbor since breakwater construction occurred during this event.

The data also show that the qualitative performance criterion for surge ("no increase") was met for the central part of the harbor (Hyde Street pier and the berthing expansion area), but was violated at the end of Pier 45 and the innermost reaches of the traditional berthing area. Primarily, the breakwater appears to have caused some shifting of surge energy amongst pre-existing resonant peaks. Changes in surge were not large; some locations showed decreases. The breakwater has not caused surge to become a "new" problem in the harbor.

Currents and circulation

Measurements of entrance channel currents during relatively extreme tidal conditions found peak current speeds to be well below the performance criterion limit of 2 knots. Direct comparisons between pre- and post-BW prototype current data (as a means of evaluating the breakwater's effects) were

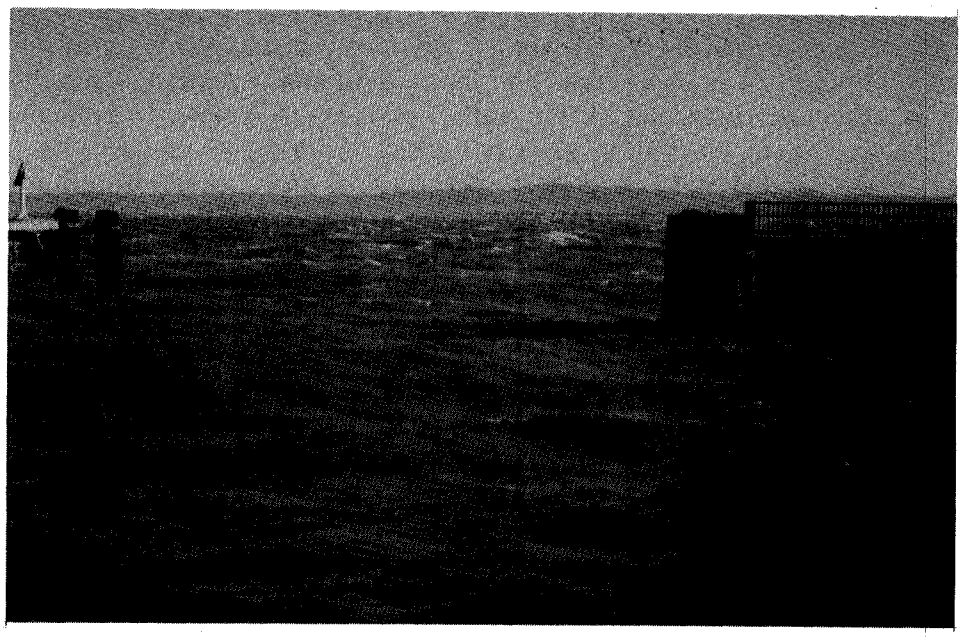

a. Looking northeast out of entrance channel

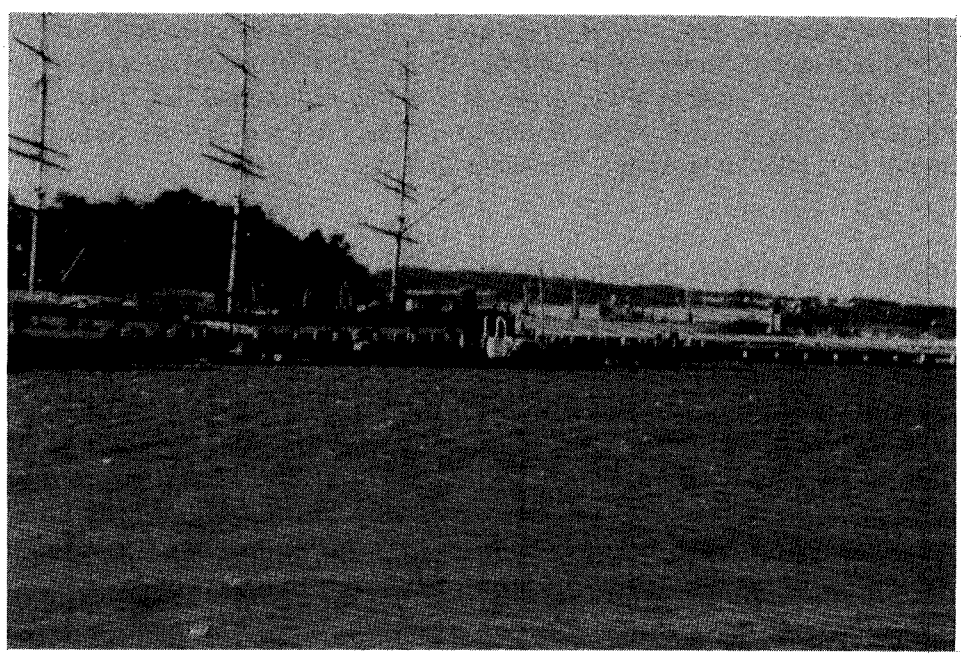

b. Looking southwest at basin and Hyde Street pier

Figure 49. December 15, 1988 Storm

not feasible. However, results from post-BW prototype measurements of general circulation (current patterns and speeds) compare reasonably well with numerical model predictions. The specified performance criterion for circulation is expressed in terms of impacts on shoaling (deposition) rates. Although the available bathymetric data do not permit evaluation of breakwater impacts on deposition rates, the analysis suggests that significant deposition has taken place along the landward side of the breakwater since construction. No maintenance dredging has been required, however, so the performance criterion is still being met at this time. It was not possible to establish outer boundaries of zones where circulation and deposition have been influenced by the breakwater from the available measured data.

Scour

Lead-line data show that the nominal "design scour depth of 10 ft along the wall" has definitely been violated at the westward end of the detached breakwater. This performance criterion has also been approached closely at the point of junction between the curvilinear and straight sections of the detached breakwater. Other locations may have been at or beyond the 10-ft scour limit for unknown periods of time. The lead-line data were not obtained often enough to unequivocally establish scour trends, or to permit concluding that maximum scour depths have already been reached. As a preventive measure, scour protection was constructed at the ends of the detached breakwater and the east segmented breakwater in October 1992. Scour effects of the breakwater appear to be limited to the immediate vicinity of the structure. It is emphasized that measured scour relative to the specified performance criterion may not be a reliable measure of structural stability or instability.

Littoral environment (beach erosion)

There is no evidence that the breakwater caused increased beach erosion at Aquatic Park. Insufficient quantitative data were available to rigorously determine beach changes, or the boundaries or sediment budget of the Aquatic Park littoral system. A quantitative analysis of beach changes due to the breakwater would be difficult, if not impossible, because of GGNRA's beach management practices (importation and movement of sand by mechanized equipment). From onsite visual observations, the present-day beach matches the pre-BW description.

Structural integrity and alignment

The breakwater structures have not moved or deteriorated significantly, despite the effects of the October 1989 Loma Prieta earthquake, which caused extensive damages in the immediate vicinity. No cracking or spalling of original concrete has occurred. The function of the breakwater has not been impacted at all by the very small changes in vertical and horizontal alignment.

Design Procedures and Tools

Selection of design waves

Measured wave heights met performance criteria and the breakwater has not been damaged by waves. Therefore, design waves (selected primarily using SPM methods) have not been shown to be incorrect or inappropriate. Because the directions of incident waves were not measured, it is unclear whether the site has experienced conditions similar to those used in design. Incident wave data measured during the MCCP study do not provide a better basis for statistical projection of extreme waves than the incident data measured prior to breakwater construction.

Numerical modeling of alternative breakwater alignments

Overall good agreement between prototype current data and numerical model-predicted currents indicates that the numerical model was a good design tool, given the assumptions and limitations involved.

Physical modeling to select and optimize breakwater configuration for short-period wave protection

Successful wave-attenuation performance during the post-BW measurement period confirms the physical model's prediction that the breakwater would meet design objectives for short-period wave height reduction. Spatial trends of wave height variation were similar in prototype and model. However, prototype wave conditions may not have been as severe as the design waves tested in the model. A complete test of the model's predictive capability for wave heights in the harbor under extreme conditions has not yet occurred.

The physical model was an effective and flexible design tool. The feedback and insight it provided allowed an interactive approach to optimization of breakwater configuration to meet diverse design requirements. More recent physical model tests, replicating the original wave conditions, showed that regular and irregular waves produced similar predicted maximum significant wave heights for interior locations. Results of the second model investigation emphasized the importance of precise correspondence between prototype and model wave gage locations, particularly when gages are located within zones affected by reflections off nearby structures.

Numerical modeling of breakwater impacts on harbor oscillation

Prototype surge data show that numerical surge modeling was useful as a qualitative design tool. The model was adequate for predicting peak resonant frequencies and the general spatial patterns of harbor oscillation throughout the site, but was only partially successful at predicting specific changes due to the

breakwater. The prototype surge information obtained at Fisherman's Wharf was not extensive enough to provide an improved basis for model application and/or a more complete evaluation of the model's performance.

Scour predictions

Scour prediction methods were reasonably accurate in identifying locations of scour and deposition but less successful in predicting magnitudes. Considering the limited information on site conditions and seabed materials and the complexity of the processes involved (particularly the behavior of cohesive materials), the combination of quantitative methods and engineering judgment used to make predictions was remarkably successful. A more thorough application of the same basic methodology may have produced even better predictions.

Structural loading calculations and design

Prototype data were not specifically collected to permit evaluation of structural loading and design calculations. However, the good structural performance to date shows that the methods used were at least not deficient. The fact that the breakwater sustained no detectable damages from the October 1989 earthquake shows that the seismic design was effective for that important event.

Monitoring Effort

Waves and surge

Prototype data for wind waves and swell were an adequate basis for documenting the actual post-construction wave-attenuation performance of the breakwater under a variety of conditions. They were also useful in evaluating the physical model. Lack of directional information and sufficient length of continuous gaging record for incident conditions prevented an independent determination of design waves for the site. The lack of directional information also hindered selection of prototype events for replication in the physical model, and prevented a more thorough test of the model's predictive capability.

In future monitoring at sites like Fisherman's Wharf, which are subject to simultaneous ocean-generated and locally generated waves, some modifications to standard open-coast wave data processing and analysis procedures should be considered. Specifically, analysis should avoid overlapping frequency coverage between surge, ocean-generated (swell), and locally generated waves. Sampling rates (both frequency of gage polling and frequency of pressure sampling within bursts) should be specifically tailored to the frequency regimes present. Sampling rate considerations and decisions about hard-wired versus

self-recording gage technology should also include examination of how fast wave conditions might change at the site. The directionality of incident wave conditions should definitely be obtained. Wave monitoring should be planned and initiated as early as possible *in the design process* to allow definition of baseline conditions. If rigorous evaluation of models used in design is anticipated, prototype gage siting should closely correspond to model gage siting. Water depth and zones of potential reflection from structures are important considerations in gage siting as well. It may be unrealistic to rely on visual observations, such as LEO, to provide useful information to supplement automated measurements.

Circulation and entrance currents

The prototype current data provided an acceptable description of post-BW general circulation for average and extreme tides, and were reasonably adequate as a basis for prototype:model comparisons. Discrepancies between the prototype and model should not be attributed entirely to model deficiencies, i.e., the measured data set is not extensive enough to be declared representative of "the" (only) true currents. Post-BW data may also prove useful for design of future facilities in the area, such as moorings, or when a generalized description of the present-day currents is needed as a baseline prior to anticipated major changes in circulation. It was not feasible to compare MCCP post-BW data sets with pre-BW prototype data, due to fundamental differences in data collection objectives and approach. Entrance channel current measurements were conducted with a very specific objective, and proved entirely satisfactory for that purpose.

Bathymetry

Lead-line depth measurement was a simple and direct method for examining near-structure scour and deposition. The resulting data were very useful for documenting actual scour behavior for comparison with predictions, and for providing advance knowledge of potential scour problems. For similar structures, the low-technology lead-line method of monitoring should be seriously considered.

Fathometer survey data were reasonably effective for determining far-field bathymetric changes likely to be due to the breakwater. A more confident assessment of breakwater-related changes would have been possible if more pre-BW data were available, and if all surveys had covered the same broad area at equivalent resolution.

For maximum usefulness, initial bathymetric data collection should cover a broad area at high resolution, and should commence as early as possible in the life of a project--preferably well before construction. High intensity data collection should continue during and immediately after construction. The Fisherman's Wharf lead-line and fathometer data sets suggest that the most dynamic seabed evolution may have occurred in the first two years after the end of

construction. Once the areal extent of the zone influenced by the structure and the critical locations are known, it may be permissible to reduce the extent and intensity of data collection.

Structural Integrity

Although visual inspections detected only minor changes in the breakwaters and the resulting data were essentially qualitative, they provided the very important information that the breakwater was holding up extremely well. An experienced and observant inspector can obtain detailed information and insight about a structure that no automated or remote-sensing method can provide. Notes, photographic, and videotape documentation can be extremely useful when supplemented with locational reference information (e.g., station markings).

Side-scan sonar proved useful as an efficient reconnaissance tool to detect and confirm the location of scour zones. Side-scan results are primarily qualitative; to fully exploit the records, an experienced operator/interpreter, towfish positioning information, and repeated measurements are required.

Precise surveys of fixed monuments along the structures were very successful in quantifying long-term structure movements, although ideally a more complete initial survey would have been desirable. If different survey organizations will be used to conduct the surveys, standard methods and thorough documentation requirements should be established from the beginning to ensure that all survey results are inter-comparable. The placement of indestructible monuments in the structures as reference points for surveys was a very wise decision by SPN, and is highly recommended for other structures. Acquisition of high-resolution vertical aerial photographs at the completion of construction is also very highly recommended.

Littoral environment

The scope of the MCCP study prevented a rigorous and complete examination of the littoral environment of Aquatic Park. However, more quantitative information might have been obtained if more resources had been committed to littoral environment data collection. Data collection planning placed perhaps too much reliance on human observers. CERC experience with the LEO program suggests that strongly motivated volunteers are more reliable observers than employees who are required to perform LEO in addition to their other duties. Use of high-quality sequential aerial photography is recommended as a reliable means of collecting objective shoreline data that can also serve other (sometimes unanticipated) purposes.

Other lessons learned from monitoring

Perhaps most importantly, it should be recognized that a successful MCCP monitoring project requires a relatively large front-end investment at the time data collection plans are being formulated. Preferably, this planning would commence during the feasibility study phase of a proposed coastal project. A large and thorough effort is required to locate and review all existing information concerning the site. A significant investment in organization is necessary to provide for convenient storage and retrieval of reports, drawings, photographs, and digital data as they accumulate throughout the several years of monitoring. Computer-aided drawing (CAD) systems, geographic information systems (GIS), and other digital databases can be a very useful framework for storage of data, and can greatly enhance the ability to conduct analyses and generate products such as report figures. However, the decision to apply these computer-based systems requires an understanding that costs to establish and maintain them and to train users are significant and continuing. For small projects, a non-computer-based organization may be suitable, but still requires planning. Also, the early planning needs to consider and provide funding for contingencies such as changes in monitoring objectives due to appearance of Operation and Maintenance problems, and changes in personnel. Elements of monitoring which are not routine may require much more funding per unit of product obtained. To focus the study for maximum effectiveness, the scope should be limited to those elements for which the required approach is reasonably well understood beforehand. Similarly, if pre- versus post-project or model versus prototype comparisons are desired, data collection should be planned to obtain information at corresponding locations, times, etc.

Since it is not possible to anticipate all of the potential uses of data sets and changes in responsible personnel are likely, detailed, self-explanatory documentation of methods, equipment, and conditions at the time of data collection is required, especially for field measurements. To the extent possible, data collection sites should be permanently marked in the field, and precise position information recorded along with notes and photographs.

Operation and Maintenance

Usefulness of MCCP data for prevention of problems and future planning

MCCP investigators and their District partners both benefit from the ongoing two-way exchange of data collected under the MCCP Program and the Districts' own Operation and Maintenance inspection programs. For example, at Fisherman's Wharf, MCCP bathymetric data provided to SPN have been used in maintenance planning. Those data and general circulation data have also been available to the Port of San Francisco for use in design of the berthing expansion, and to GGNRA for operation and maintenance of Hyde Street pier and the historic fleet. It is likely that future uses of MCCP data will arise.

Recommendations

SPN and CERC should cooperate in a follow-through effort to ensure that all pertinent data and analysis results are properly archived for future retrieval. For example, SPN may benefit from having copies of CERC's photographs.

A careful review of structural design assumptions and evaluation of the present structural support and loading conditions on an individual pile and structural unit basis is recommended. The junction between design sections III and IV (end of curvilinear section) should be given a particularly careful examination. Depths at that junction, adjacent to the openings in the segmented breakwaters, and in the recently protected areas should be the subject of continued monitoring. It may be beneficial to enter the original lead-line data sets (individual subsite depths) into a CAD or GIS database to permit further, more detailed analyses of scour and deposition trends.

It is suggested that all structural alignment monument positions and Fathometer data (spot soundings and contours) be entered into the same CAD database. Some of these data are already stored in CAD form, along with current measurement and wave measurement locations. Any further analyses of the fathometer data will be facilitated by having past and future data available in digital graphic format.

Structural alignment and visual inspection surveys should be continued. Any new occurrences of concrete deterioration should be promptly repaired. Expansion joint gaskets should be maintained. SPN should ensure that the fender pile clusters receive maintenance, so that they will protect the breakwater from vessel impacts.

References

Bechtel Civil & Minerals, Incorporated. (1983). "Hyde Street pier, Fisherman's Wharf: Preliminary engineering report," prepared for Port of San Francisco, San Francisco, CA.

Bottin, R. R., Jr., Sargent, F. E., and Mize, M. G. (1985). "Fisherman's Wharf area, San Francisco Bay, California design for wave protection: Physical and numerical model investigation," Technical Report CERC-85-7, U.S. Army Engineer Waterways Experiment Station, Coastal Engineering Research Center, Vicksburg, MS.

Chen, H. S. (1986). "Effects of bottom friction and boundary absorption on water wave scattering," *Applied Ocean Research* 8(2), 99-104.

Chen, H. S., and Mei, C. C. (1974). "Oscillations and wave forces in an off-shore harbor," Report No. 190, Department of Civil Engineering, Massachusetts Institute of Technology, Cambridge, MA.

Geotechnical Consultants, Inc. (1984). "Geotechnical investigation Fisherman's Wharf breakwater, Port of San Francisco, California," prepared for Port of San Francisco and U.S. Army Engineer District, San Francisco, San Francisco, CA.

Houston, J. R. (1976). "Long Beach Harbor numerical analysis of harbor oscillations; Report 1, Existing conditions and proposed improvements," Miscellaneous Paper H-76-20, U.S. Army Engineer Waterways Experiment Station, Vicksburg, MS.

LeMehaute, B. (1965). "Wave absorbers in harbors," Contract Report 2-122, U.S. Army Engineer Waterways Experiment Station, Vicksburg, MS; prepared by National Engineering Science Company, Pasadena, CA, under Contract No. DA-22-079-CIVENG-64-81.

Noda, E. K. (1972). "Equilibrium beach profile scale-model relationship," *Journal, Waterways, Harbors, and Coastal Engineering Division, American Society of Civil Engineers*, 98 (WW4), 511-28.

Norgaard Consultants International. (1985). "Sand transport, erosion, and accretion at Aquatic Park, San Francisco Bay," prepared for U.S. Army Engineer District, San Francisco, Anchorage, AK.

Raichlen, R. (1968). "Motions of small boats moored in standing waves," Contract Report H-68-2, U.S. Army Engineer Waterways Experiment Station, Vicksburg, MS.

Schneider, C. (1981). "The littoral environment observation program," Coastal Engineering Technical Aid No. 81-5, U.S. Army Engineer Waterways Experiment Station, Coastal Engineering Research Center, Vicksburg, MS.

Seymour, R. J., Sessions, M. H., and Castel, D. (1985). "Automated remote recording and analysis of coastal data," *Journal of Waterway, Port, Coastal and Ocean Engineering, American Society of Civil Engineers* 111, 388-400.

Shore Protection Manual. (1984). 4th ed., 2 Vol, U.S. Army Engineer Waterways Experiment Station, U.S. Government Printing Office, Washington, DC.

U.S. Army Corps of Engineers Hydrologic Engineering Center. (1983). "Second interim report for the Fisherman's Wharf harbor study: Data summary," Special Projects Memo No. 83-9, prepared for the U.S. Army Engineer District, San Francisco, and the U.S. Army Engineer Division, South Pacific, Davis, CA.

_____. (1984a). "Evaluation of scour potential around the proposed Fisherman's Wharf harbor breakwater, San Francisco, California," Special Projects Report No. 84-8, prepared for U.S. Army Engineer District, Los Angeles, Davis, CA.

_____. (1984b). "Numerical simulation of the circulation and water quality within Fisherman's Wharf Harbor," Special Projects Report No. 84-10, prepared for U.S. Army Engineer District, Los Angeles, Davis, CA.

U.S. Army Engineer District, San Francisco. (1976). "Fisherman's Wharf Area, San Francisco, California, breakwater study for light draft navigation," San Francisco, CA.

_____. (1985). *General Design Memorandum*, DM No. 1, San Francisco Harbor, California, Fisherman's Wharf Area, San Francisco, CA.

U.S. Department of Commerce. (1988). "Tide tables 1988, high and low water predictions, west coast of North and South America including the Hawaiian Islands," National Oceanic and Atmospheric Administration, National Ocean Survey, Washington, DC.

U.S. Army Corps of Engineers. (1983). "Determining sheltered water wave characteristics," Engineer Technical Letter 1110-2-305, Washington, DC.

U.S. Army Engineer Waterways Experiment Station. (1981a). "Method of determining adjusted windspeed, Ua, for wave forecasting," Coastal Engineering Tech Note CETN-1-5, Vicksburg, MS.

_____. (1981b). "Revised method for wave forecasting in deep water," Coastal Engineering Tech Note CETN-1-7, Vicksburg, MS.

_____. (1981c). "Revised method for wave forecasting in shallow water," Coastal Engineering Tech Note CETN-1-6, Vicksburg, MS.

Woodward-Clyde Consultants. (1984). "Geophysical and geotechnical exploration, proposed detached breakwater, Pier 45, San Francisco, California," prepared for the U.S. Army Engineer District, Los Angeles, CA, Santa Ana, CA.

Appendix A
Breakwater Plans From the General Design Memorandum (GDM)

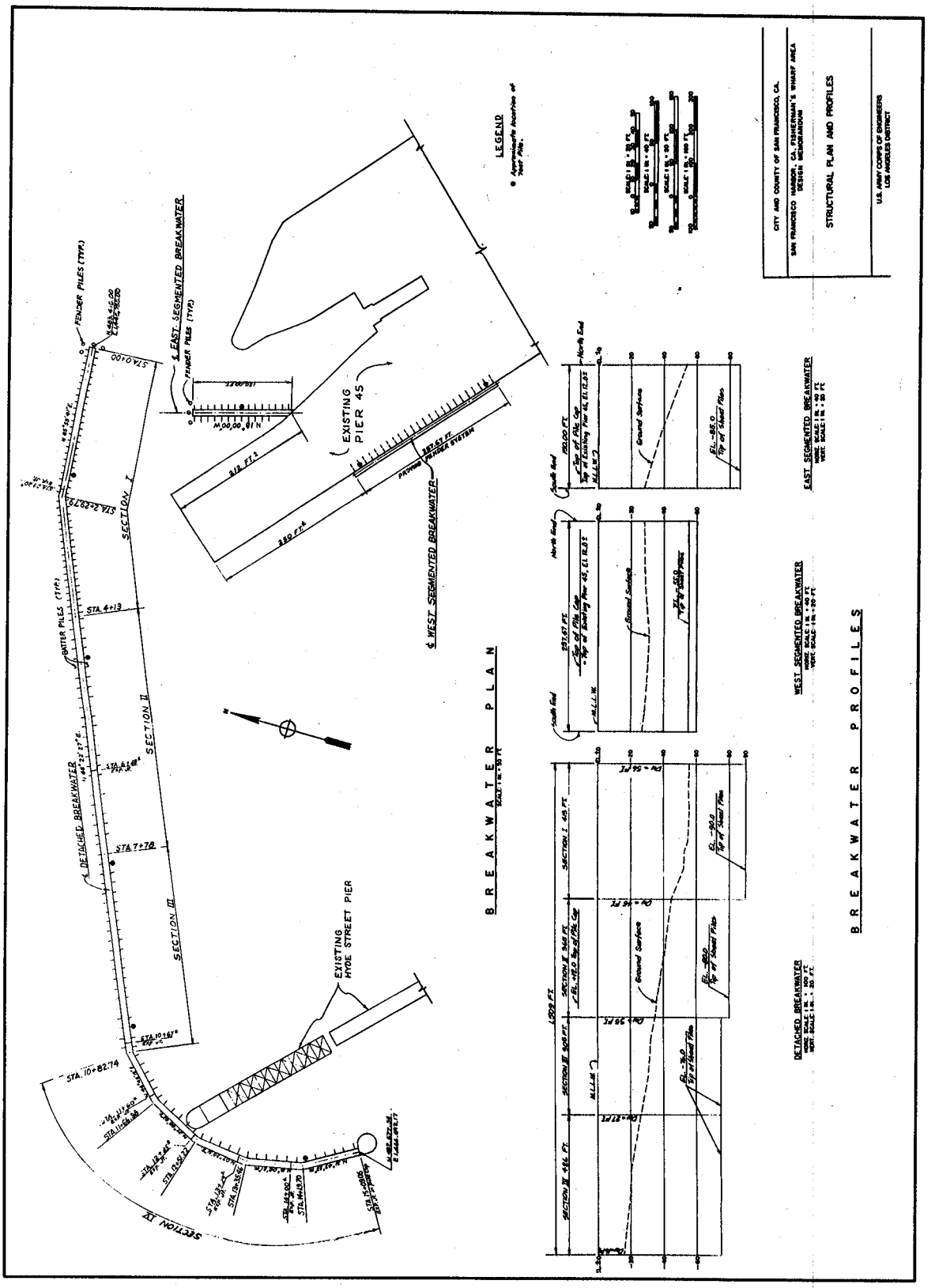

Figure A1. Breakwater plan and profiles

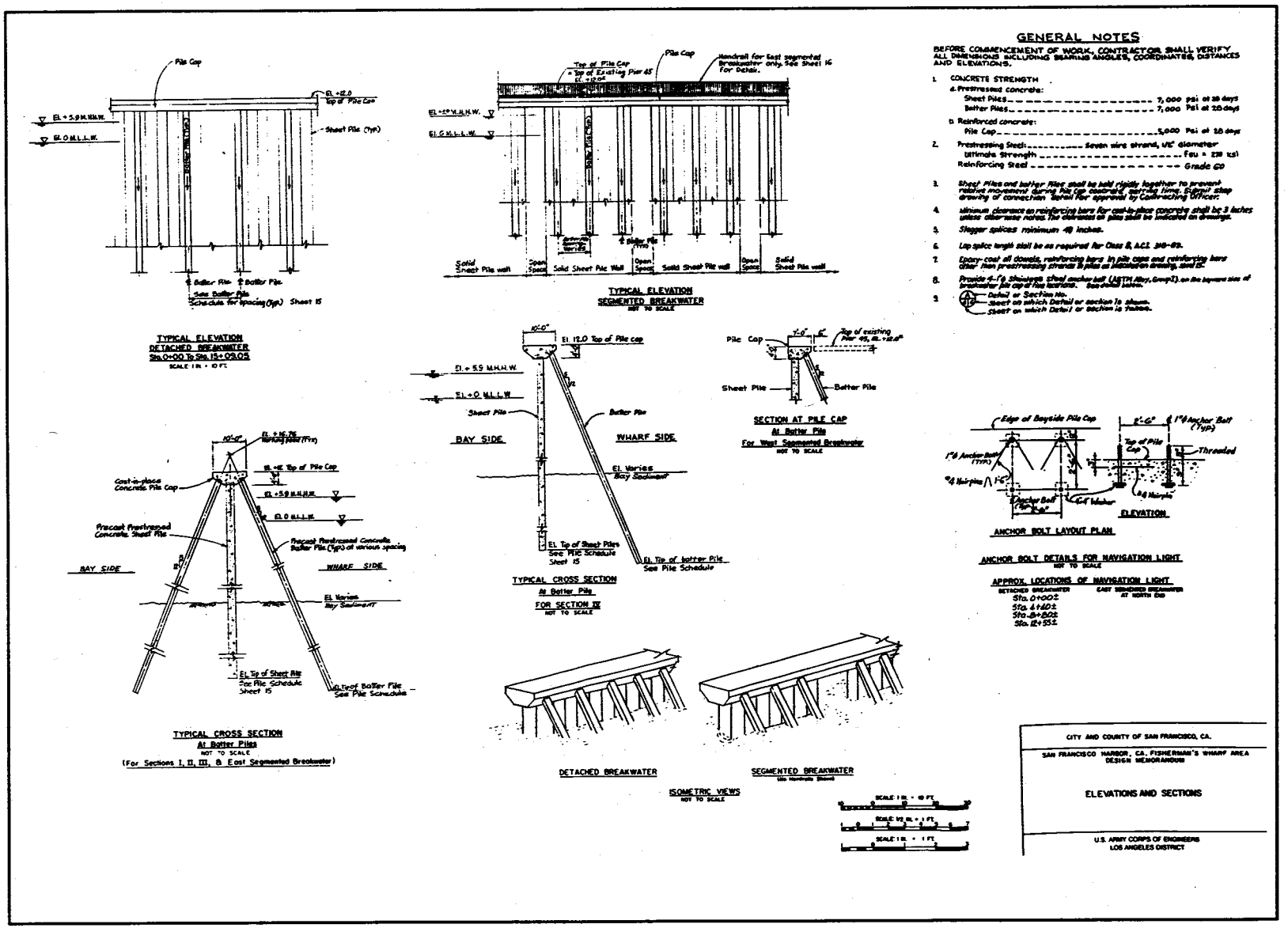

Figure A2. Breakwater elevations and sections

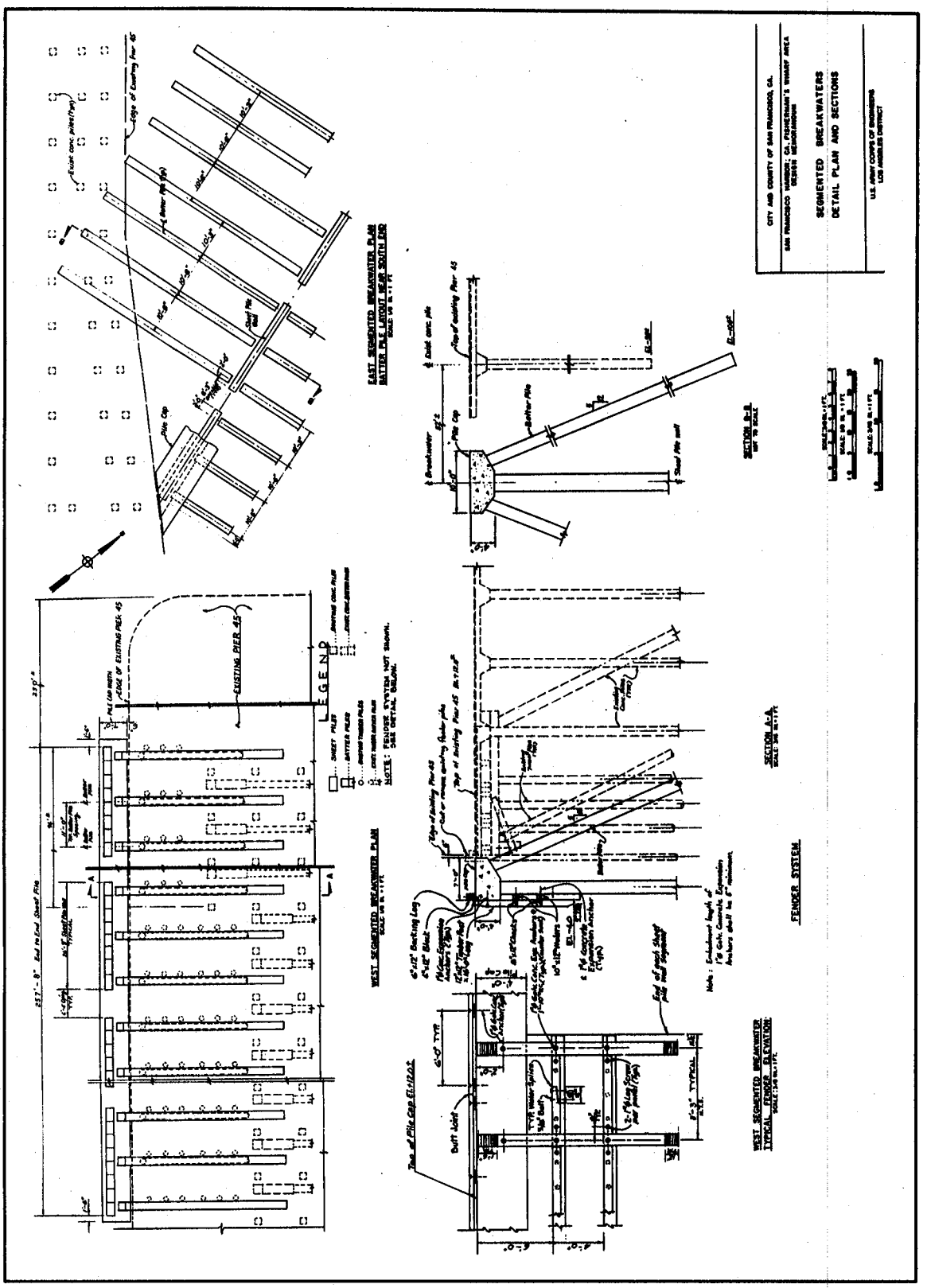

Figure A3. Detail plan and sections of segmented breakwaters

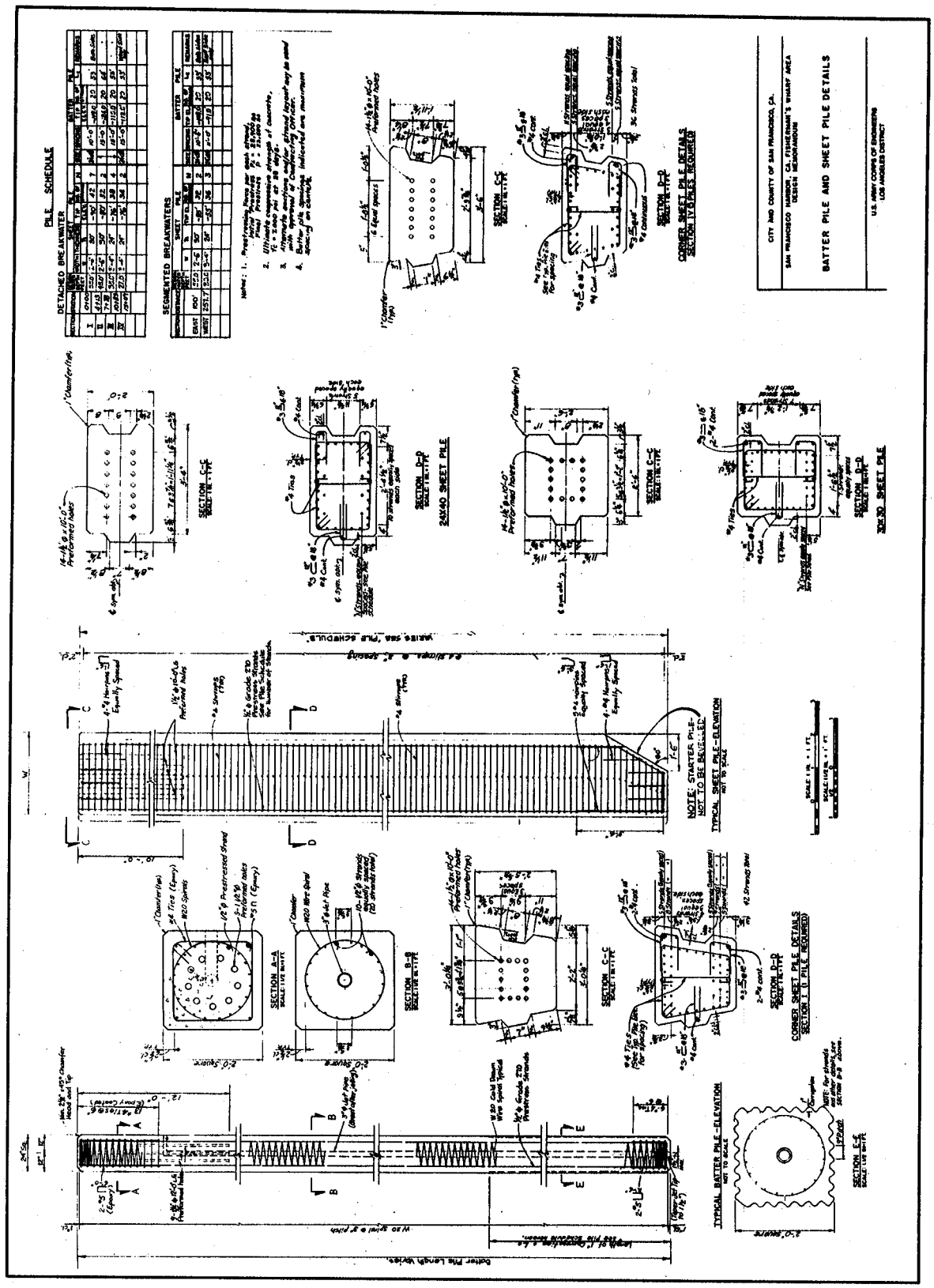

Figure A4. Details of batter and sheet piles

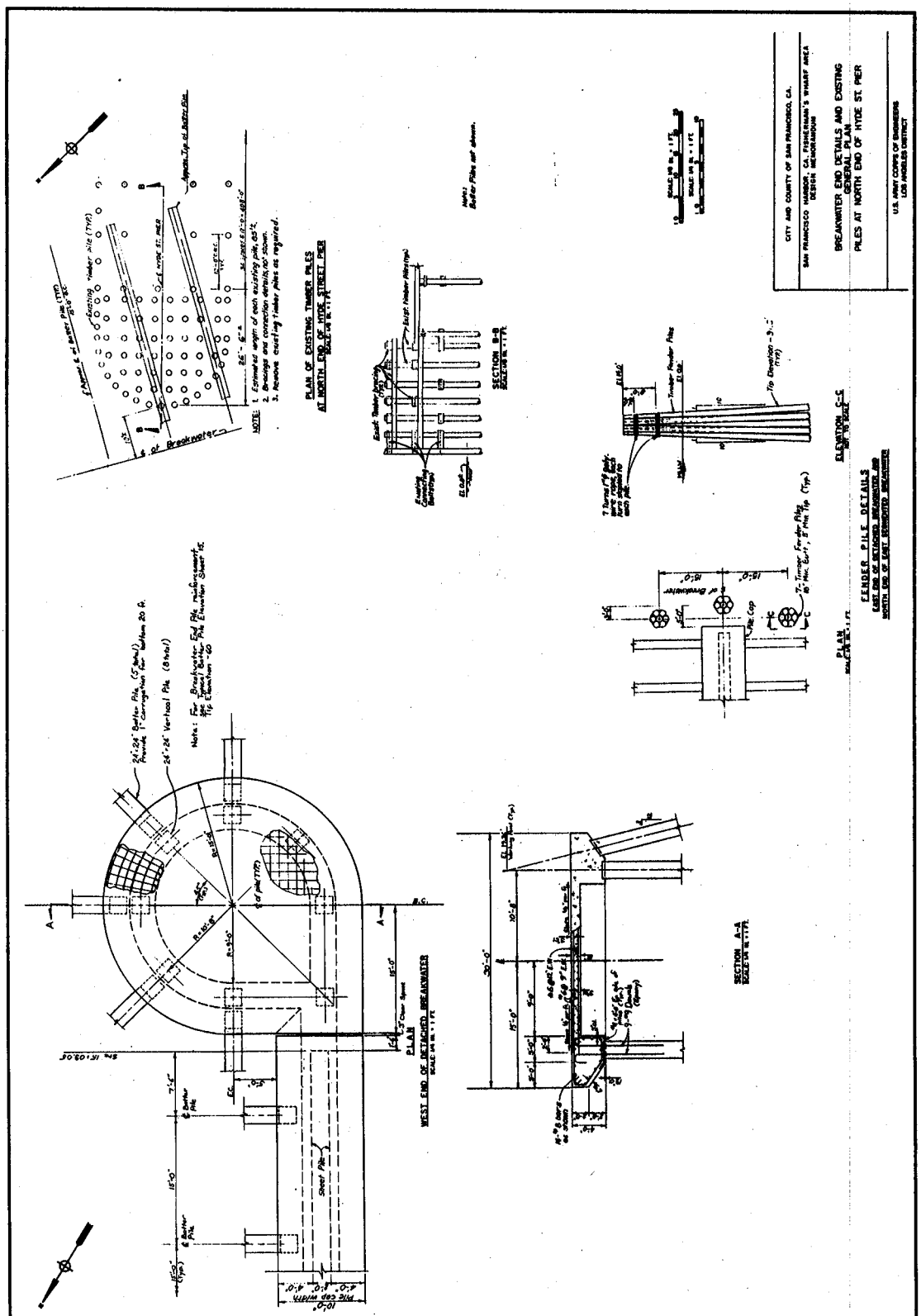

Figure A5. Details of breakwater ends and fender piles

Table A1
Coordinates and Elevations of Structural Alignment Monuments (October 1990 Survey)

Monument No.	California Zone 3 Plane Coordinates		Elevation (ft) MLLW Datum
	North (ft)	East (ft)	
1-Det. BW Sta 15+09	482680.12	1444691.57	12.10
2-Det. BW Sta 10+83	483051.37	1444737.84	12.08
3-Det. BW Sta 6+45	483226.82	1445138.88	12.06
4-Det. BW Sta 2+29	483393.50	1445520.15	12.03
5-Det. BW Sta 0+00	483409.63	1445746.83	12.05
6-W. Segm. BW North	482979.97	1445698.42	12.07
7-W. Segm. BW South	482827.98	1445873.37	12.04
8-E. Segm. BW North	483245.70	1445710.31	12.09
9-E. Segm. BW South	483114.52	1445752.43	12.10
HL56-Muni. Pier South	482056.11	1443781.79	12.78
HL57-Muni. Pier North	482881.85	1444426.06	13.56

Appendix B
Boring Locations, Geotechnical Profiles, and Bathymetry (Fathometer and Lead-Line Data)

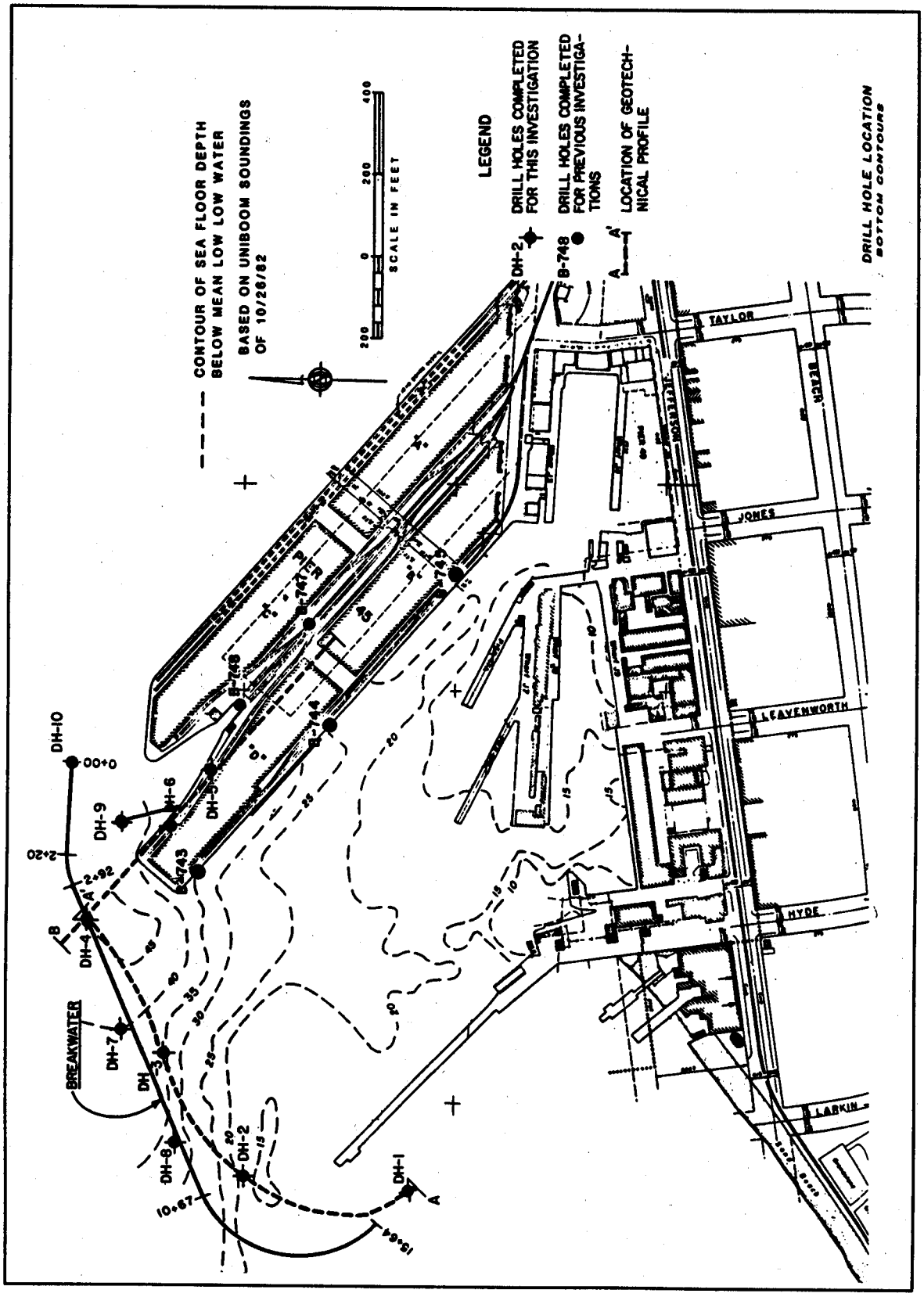

Figure B1. Plan view of boring and geotechnical profile locations (from GDM)

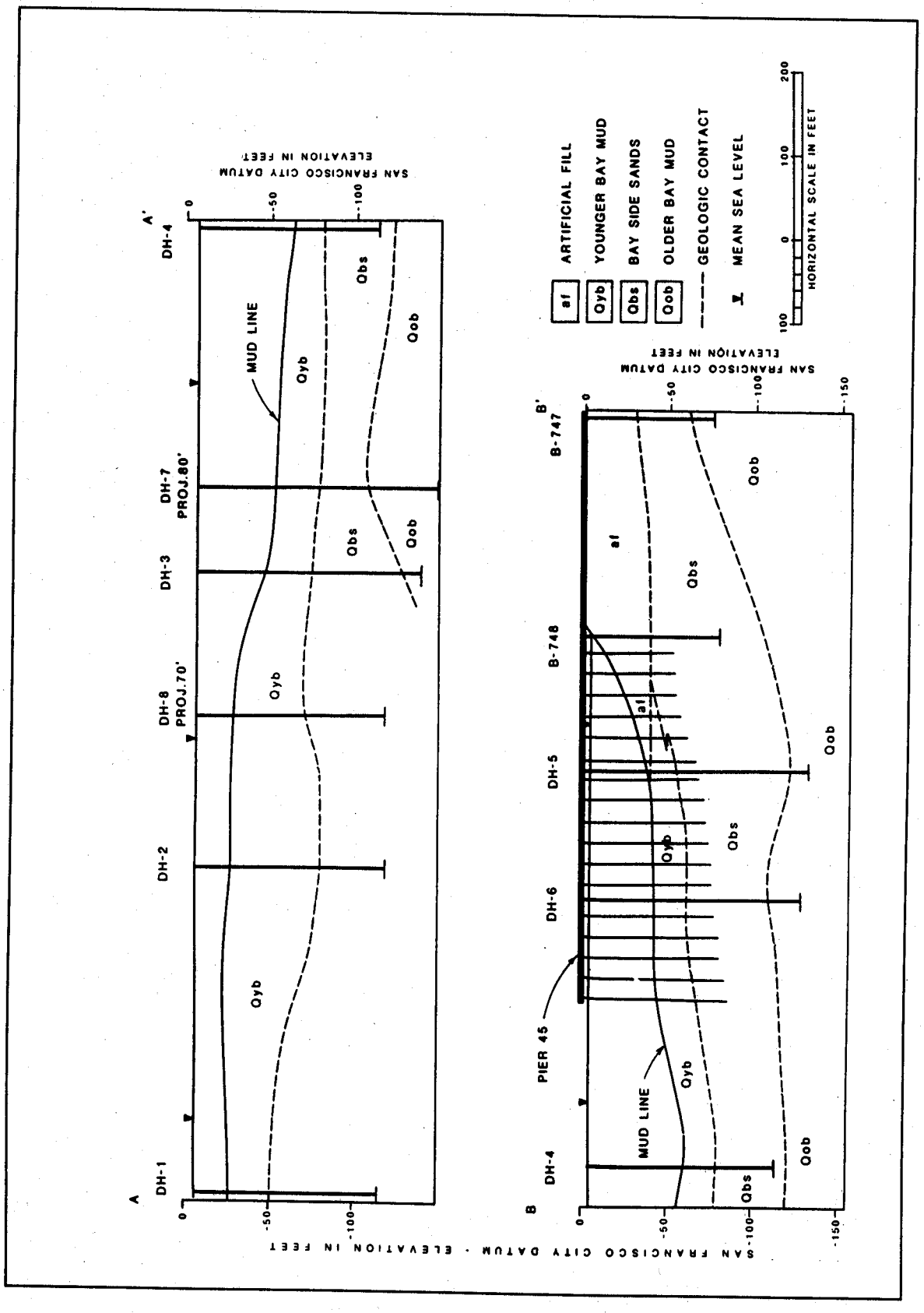

Figure B2. Geotechnical profiles (from GDM)

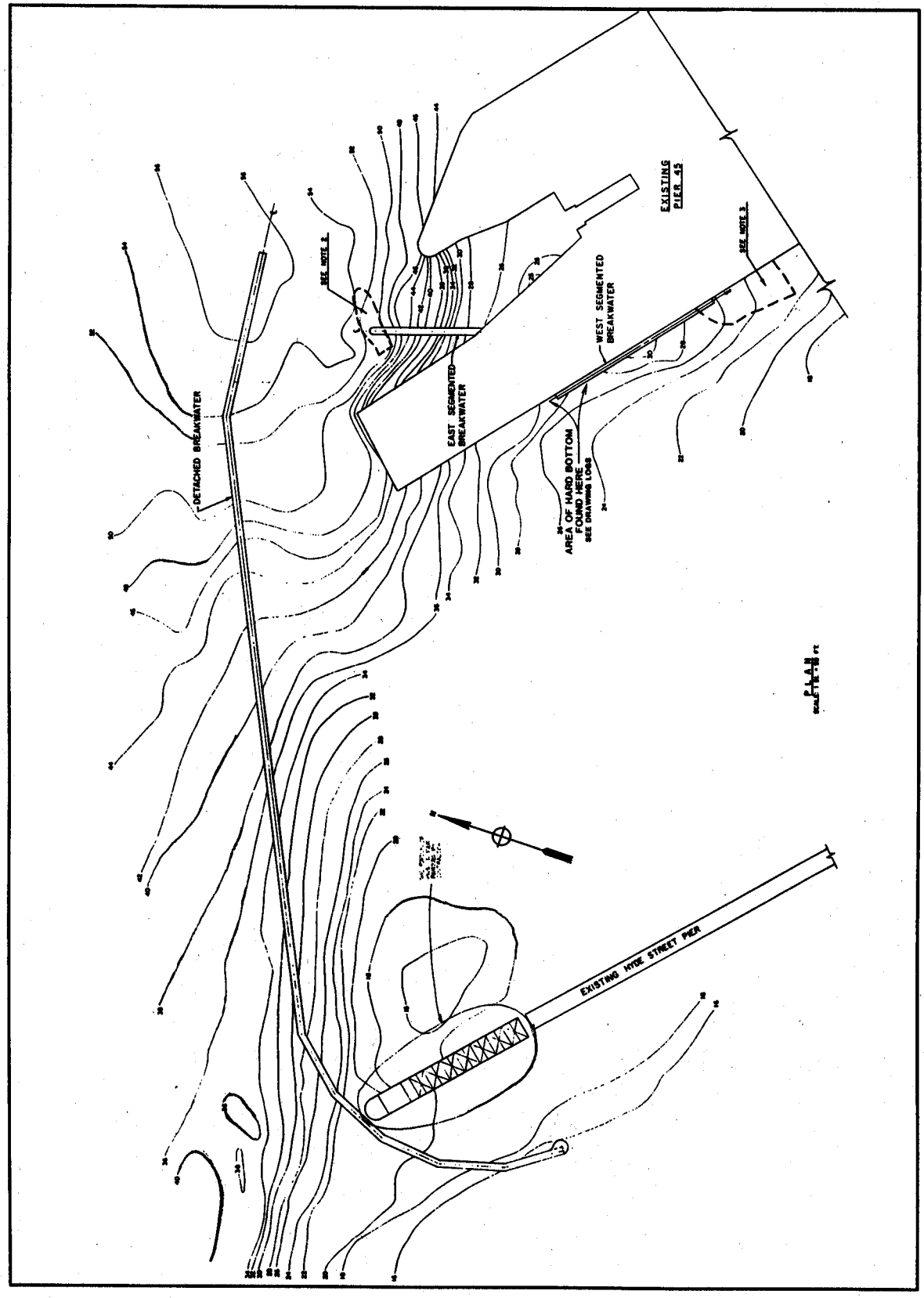

Figure B3. August 1984 bathymetry

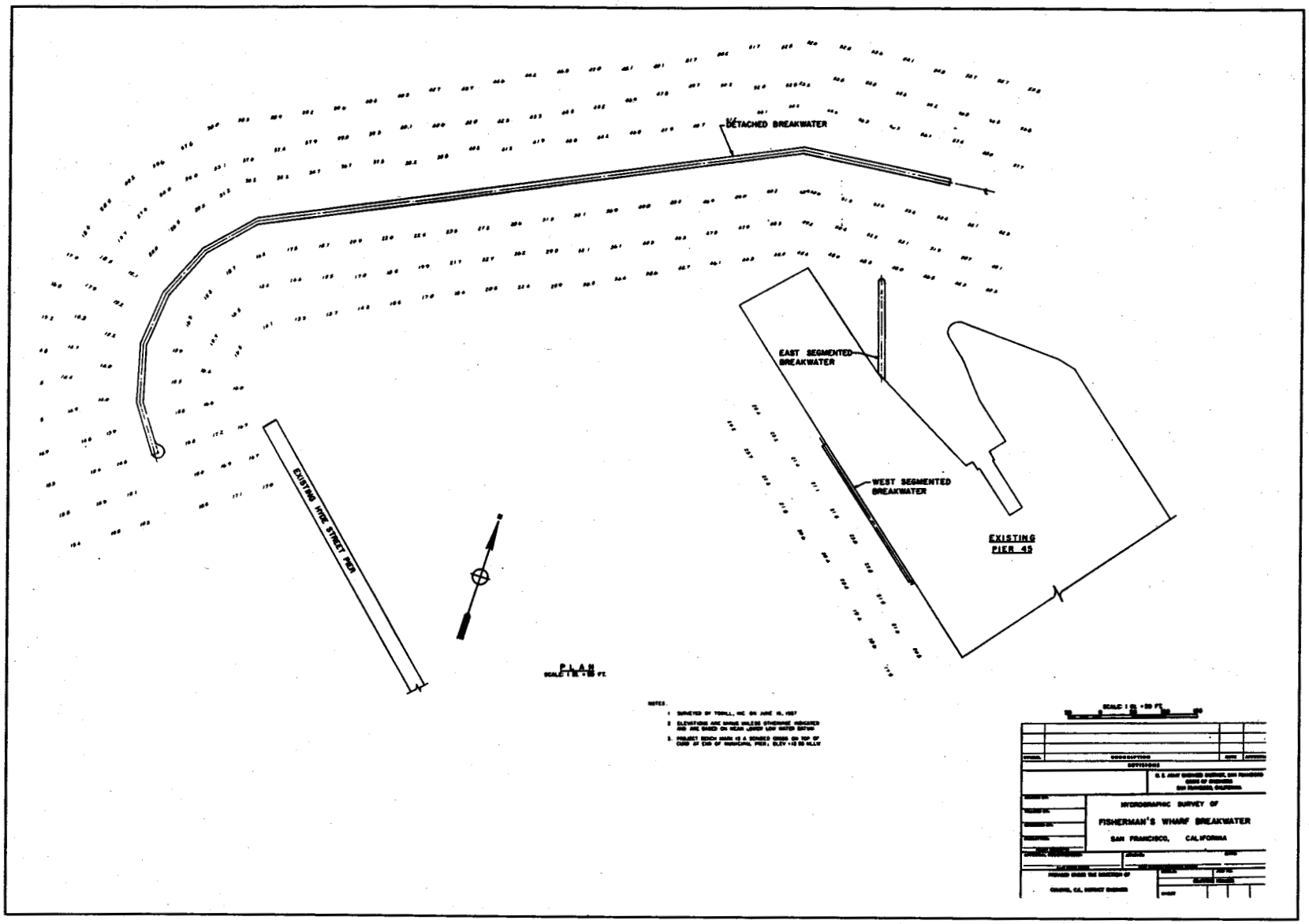

Figure B4. June 1987 bathymetry

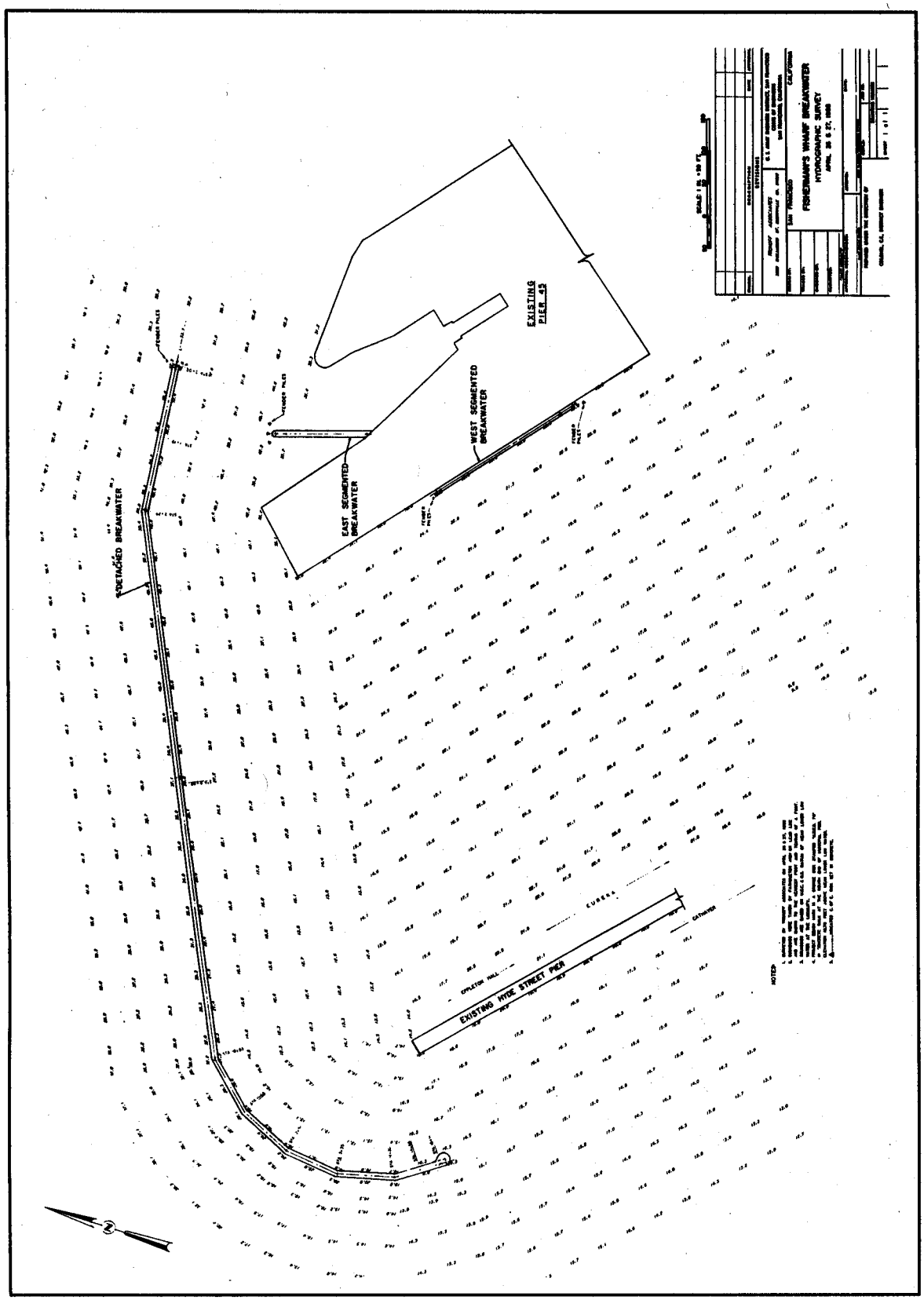

Figure B5. April 1988 bathymetry

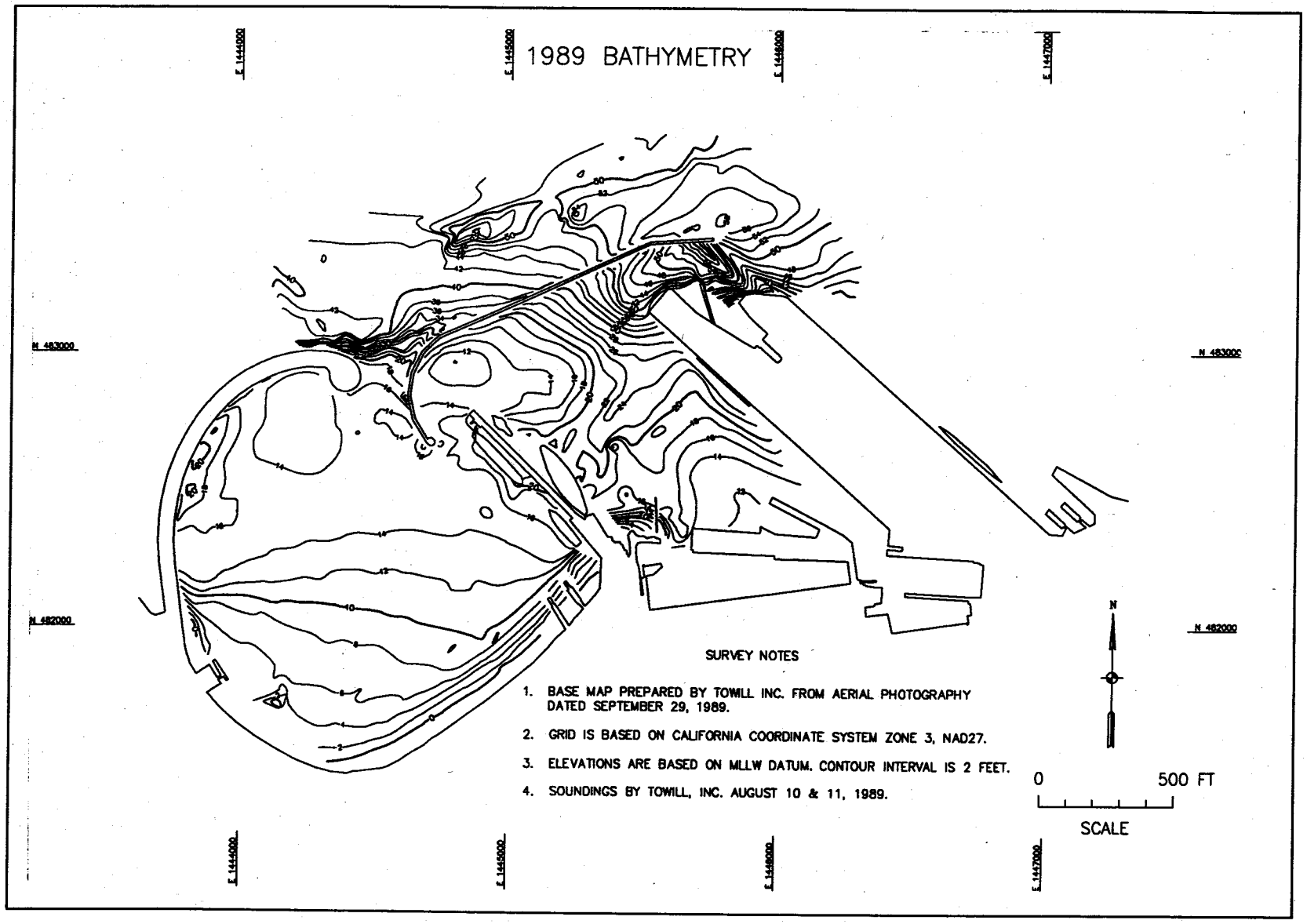

Figure B6. August 1989 bathymetry

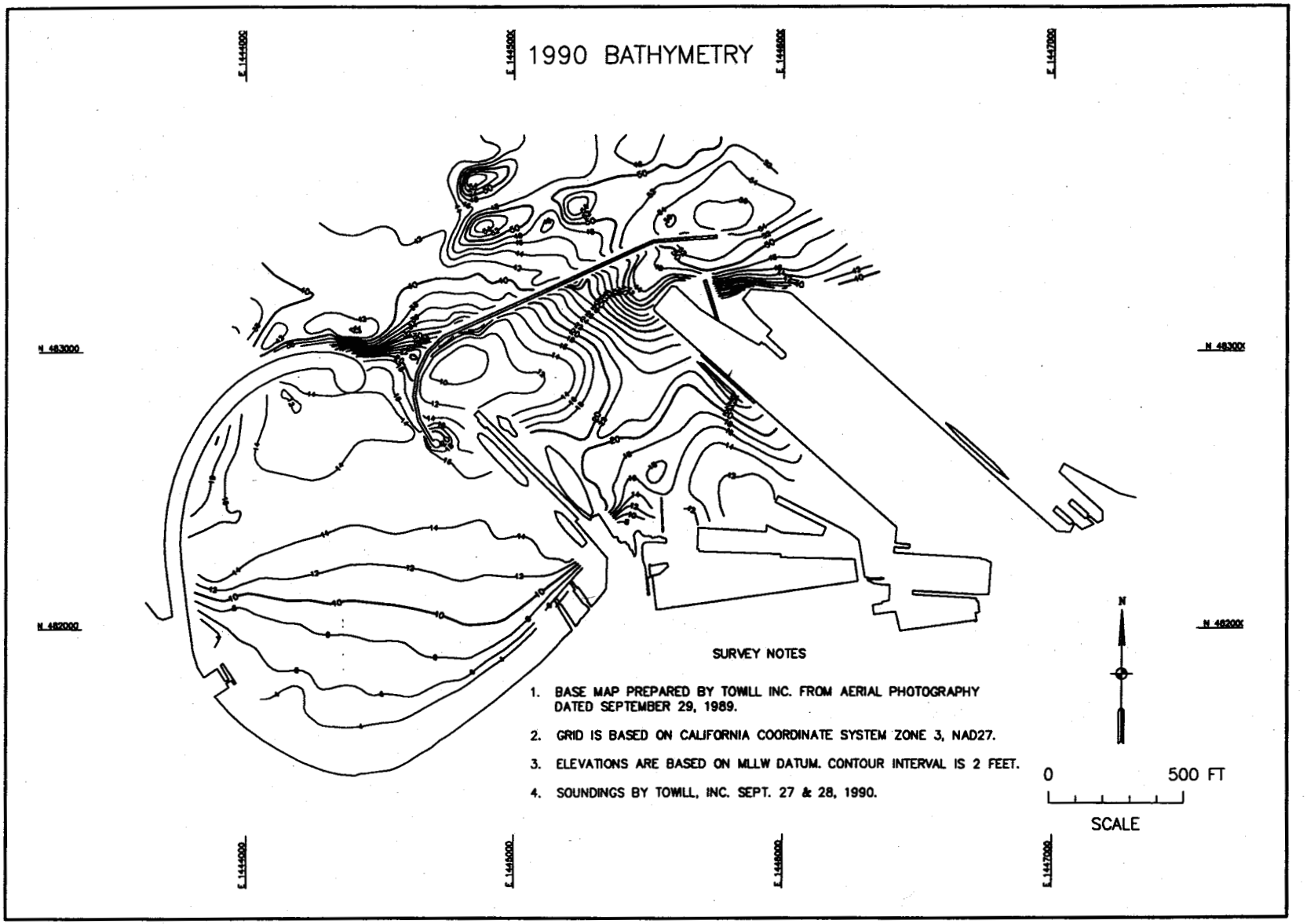

Figure B7. September 1990 bathymetry

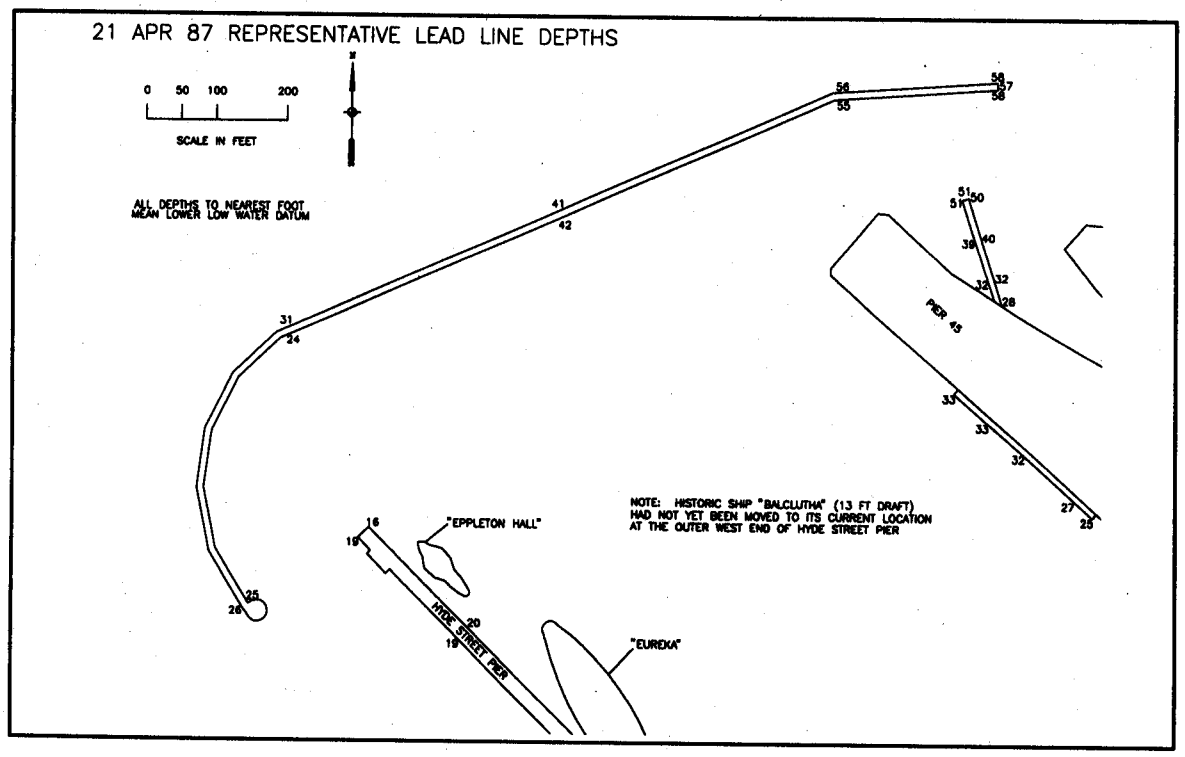

Figure B8. April 1987 representative lead-line depths

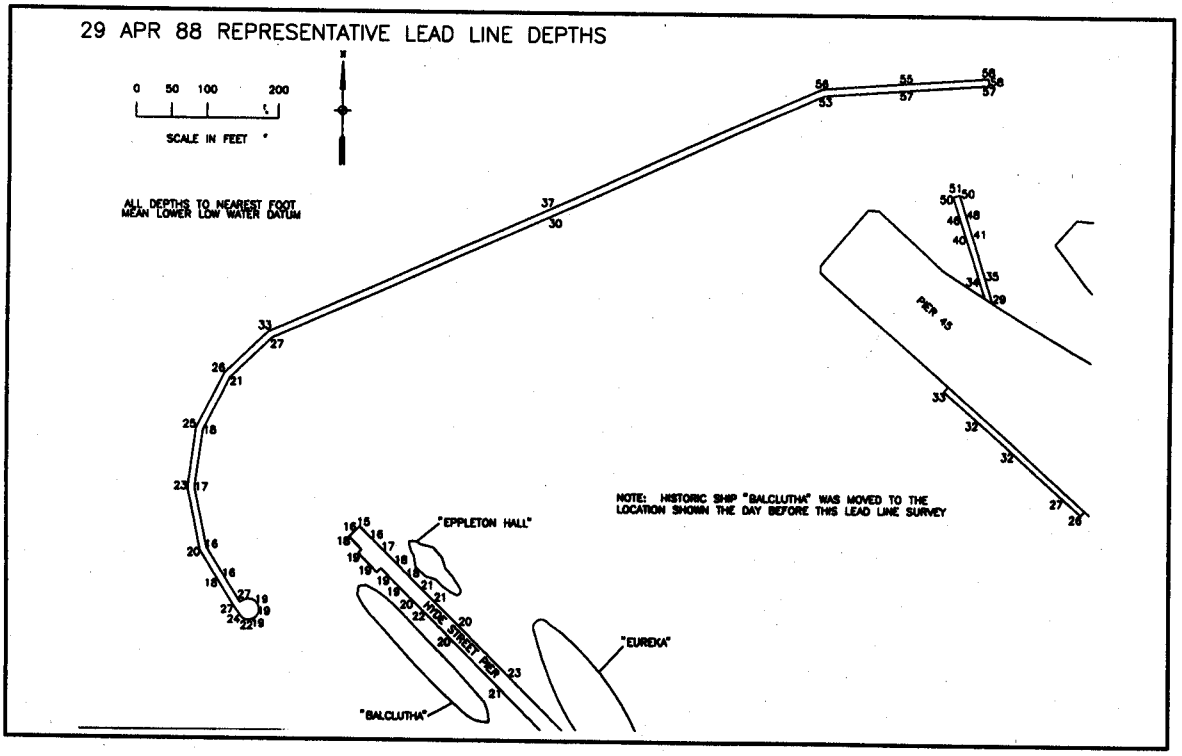

Figure B9. April 1988 representative lead-line depths

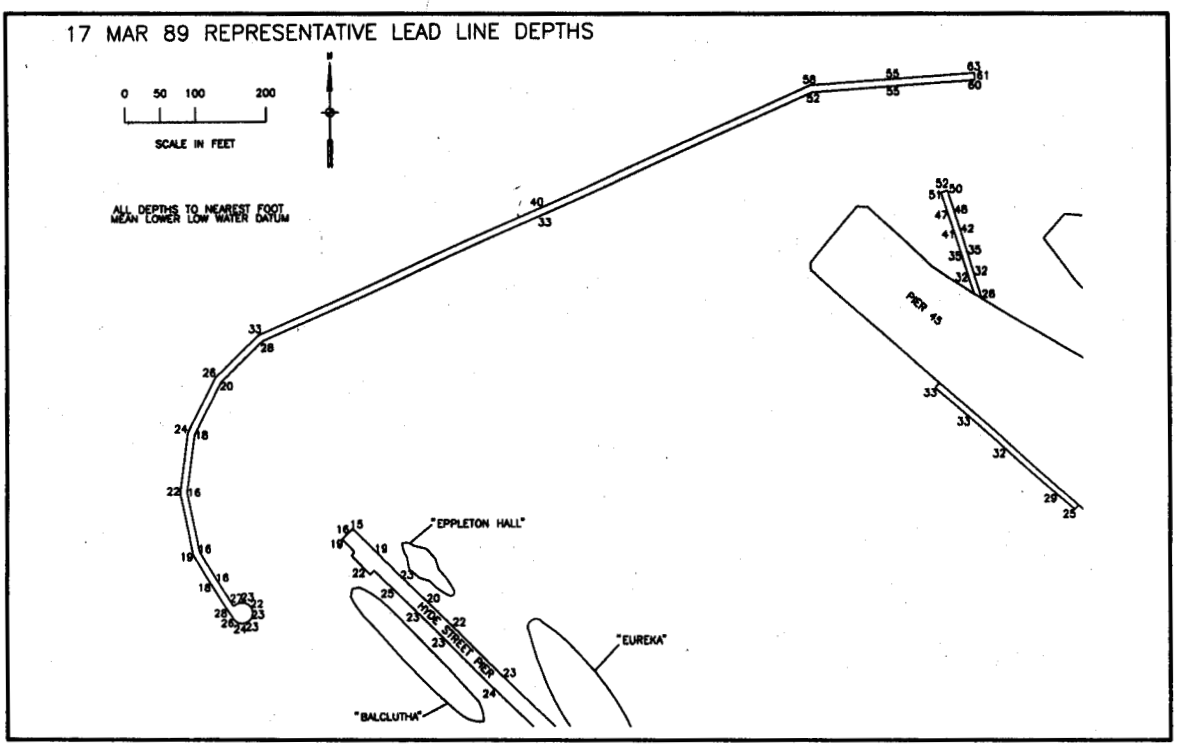

Figure B10. March 1989 representative lead-line depths

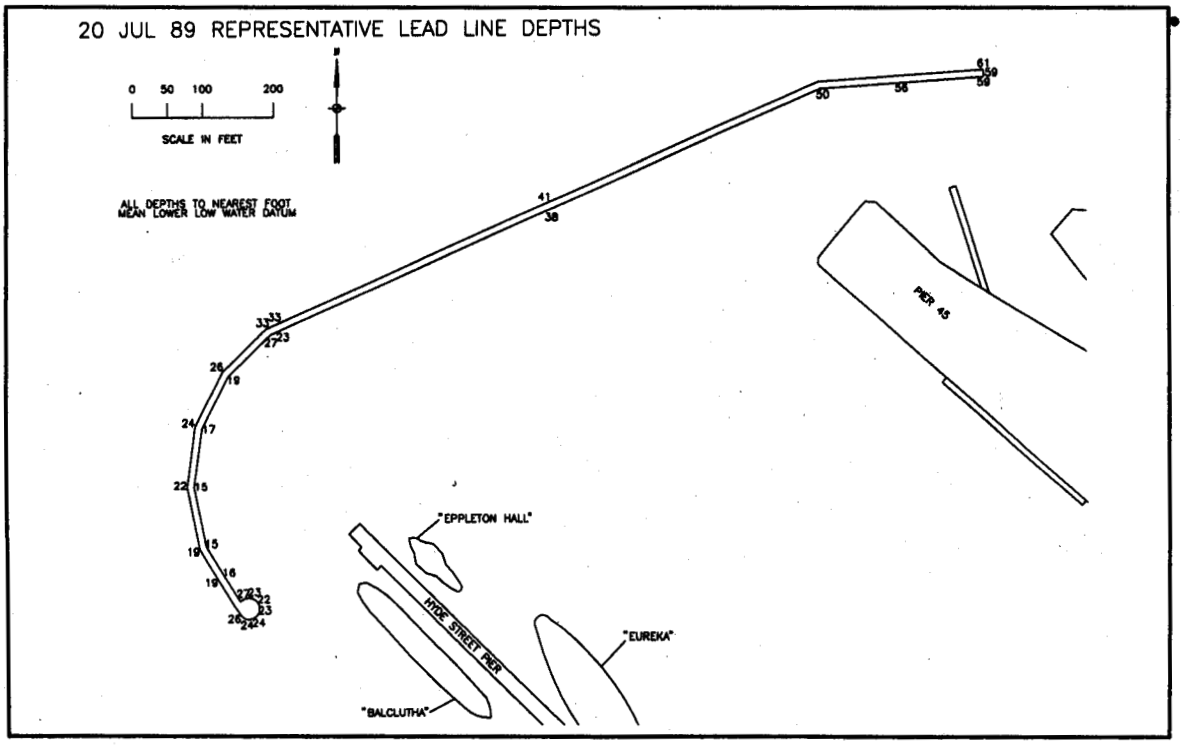

Figure B11. July 1989 representative lead-line depths

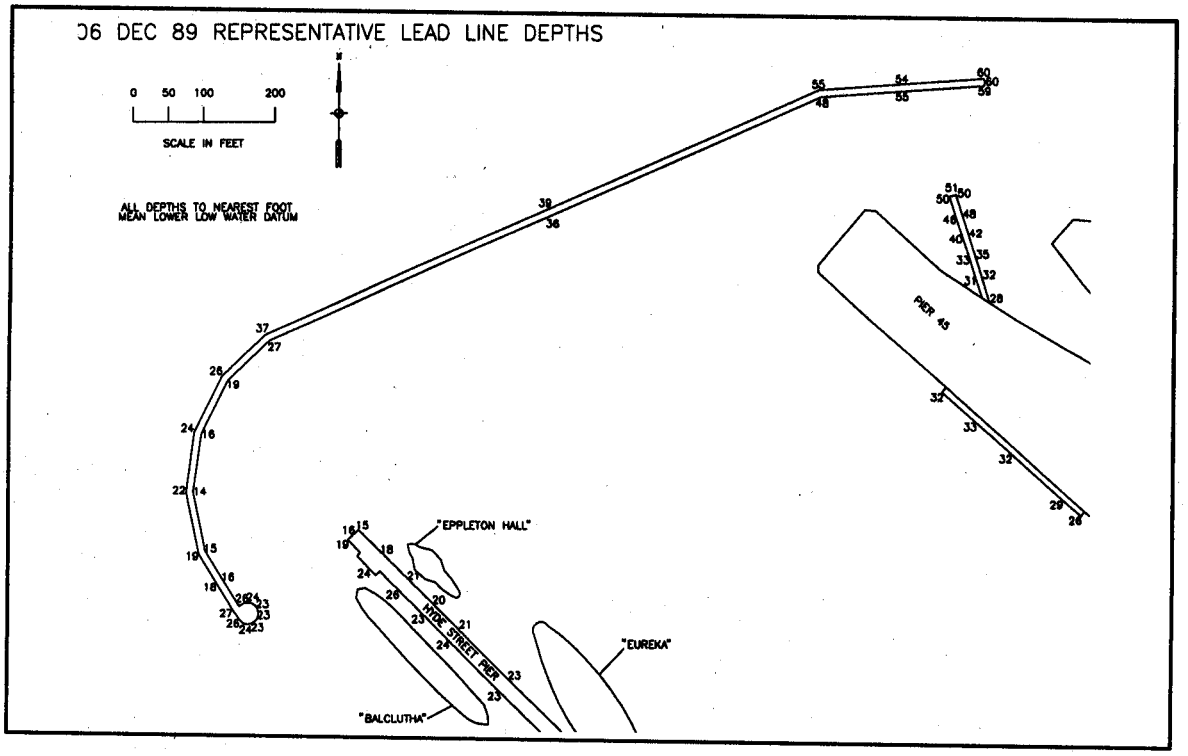

Figure B12. December 1989 representative lead-line depths

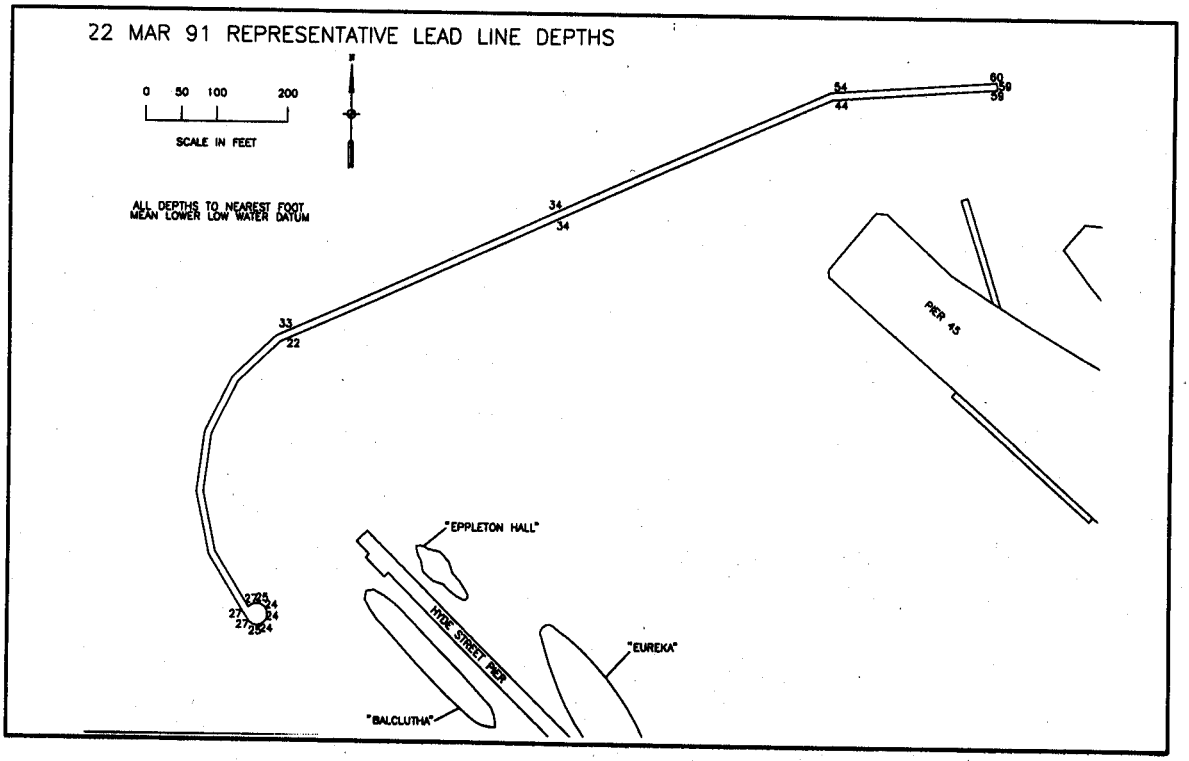

Figure B13. March 1991 representative lead-line depths

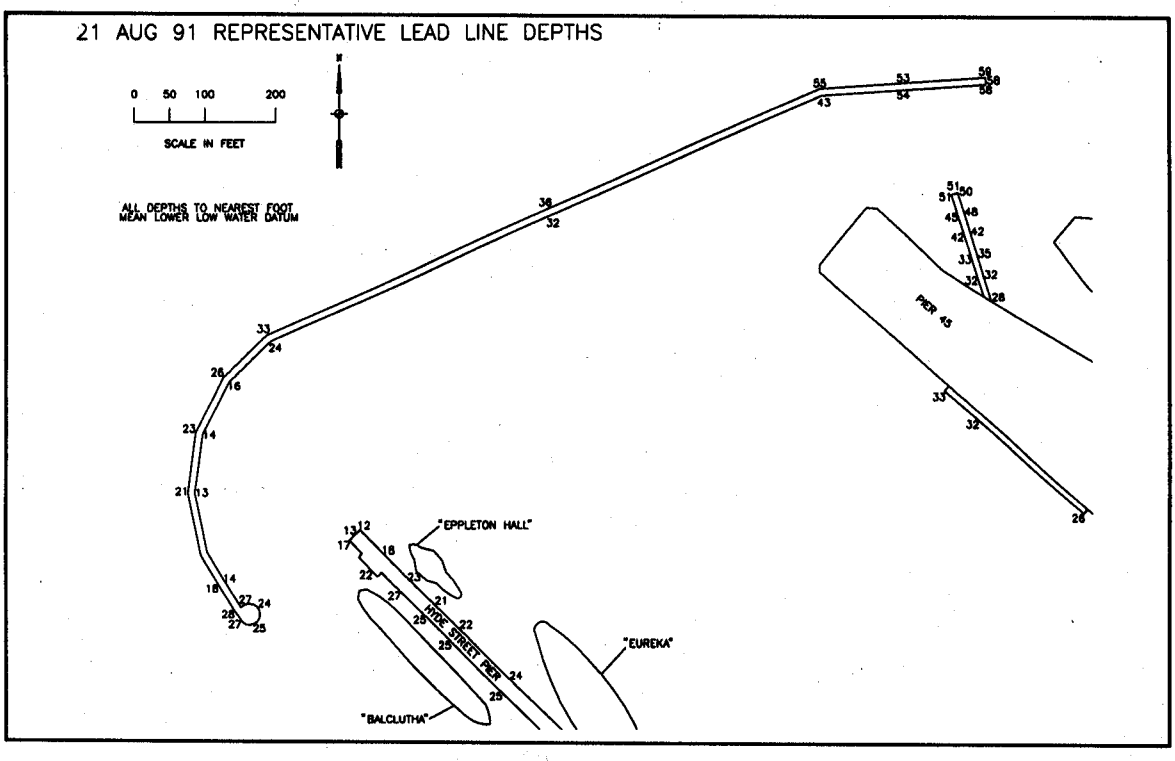

Figure B14. August 1991 representative lead-line depths

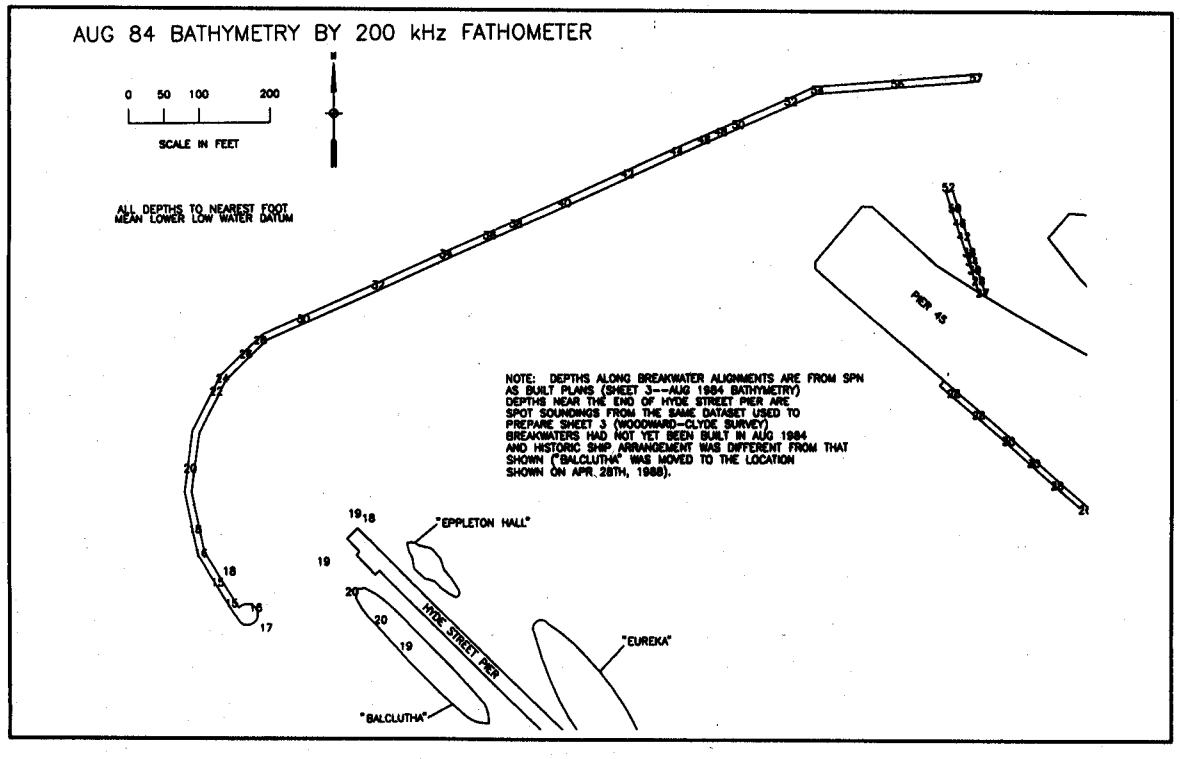

Figure B15. August 1984 fathometer depths along breakwater alignments

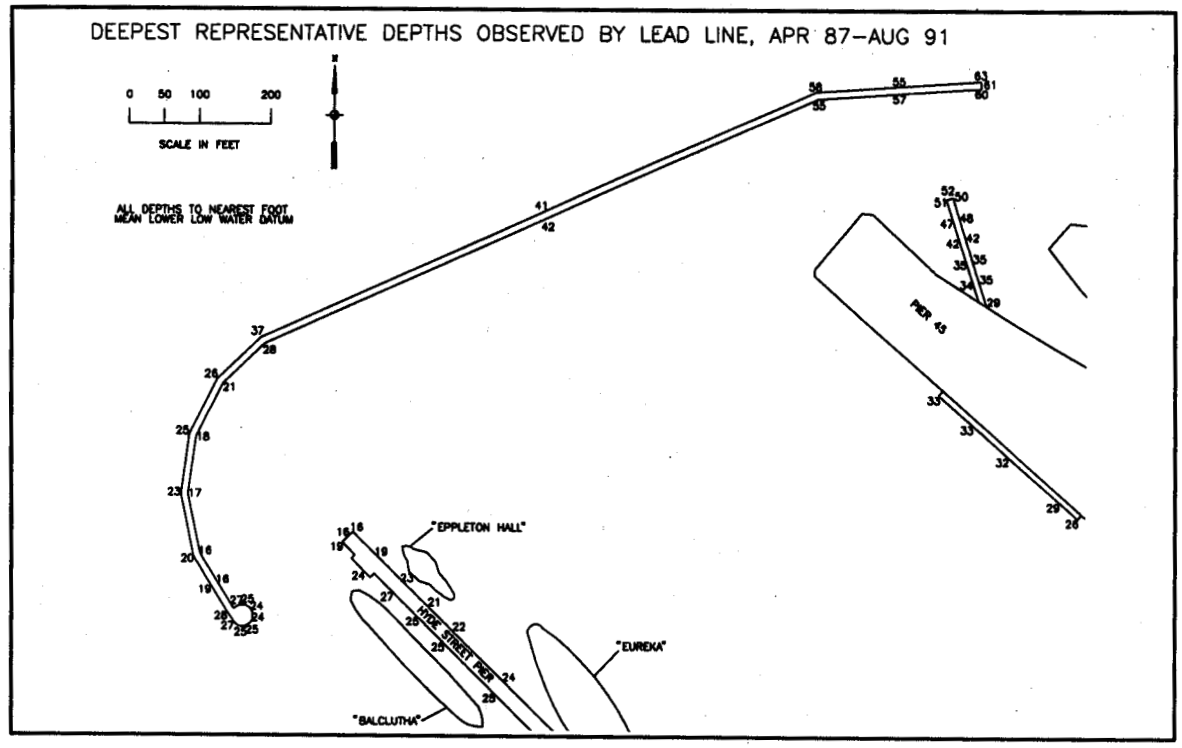

Figure B16. Deepest representative depths observed by lead-line, April 1987-August 1991

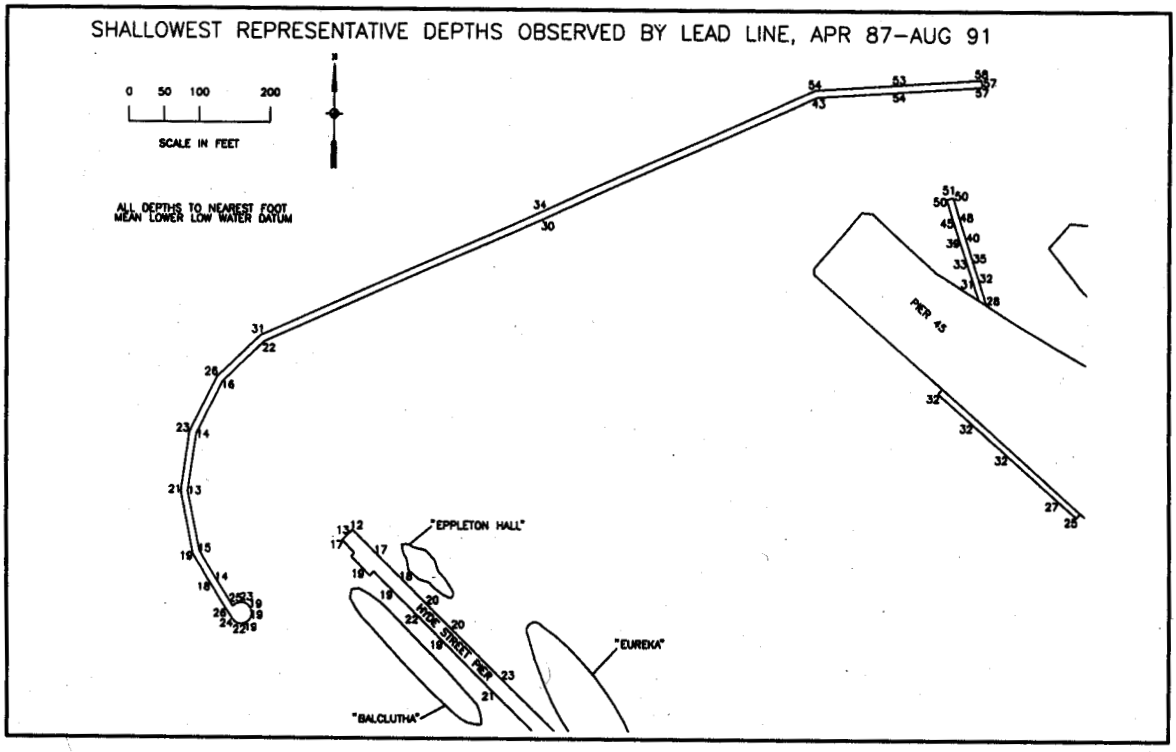

Figure B17. Shallowest representative depths observed by lead-line, April 1987-August 1991

Appendix C
Figures From Scripps' Wave Data Analysis Report

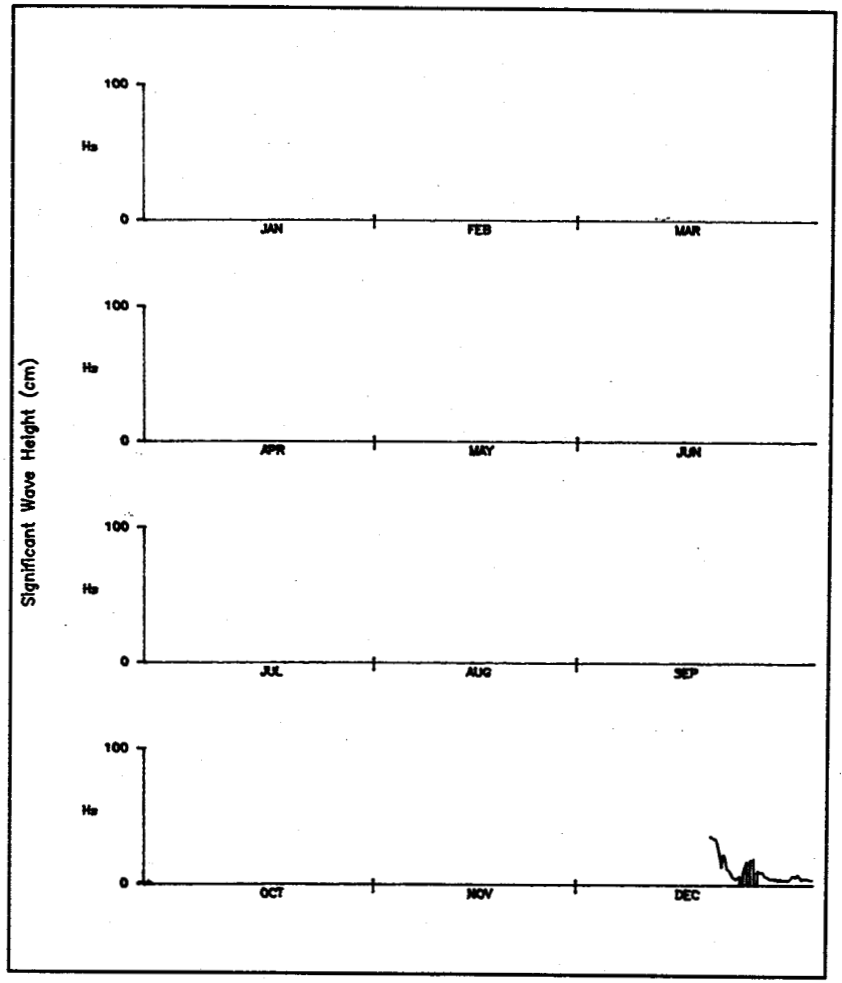

Figure C1. Surge significant wave height time-series plot for 1982 - Alioto's

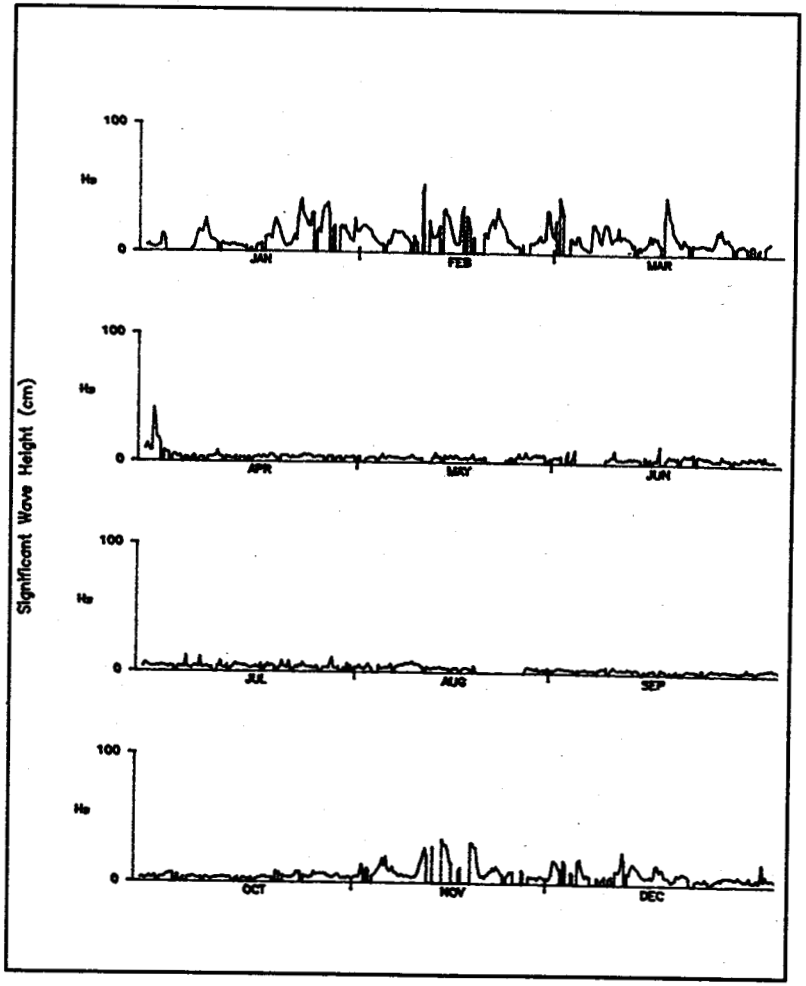

Figure C2. Surge significant wave height time-series plot for 1983 - Alioto's

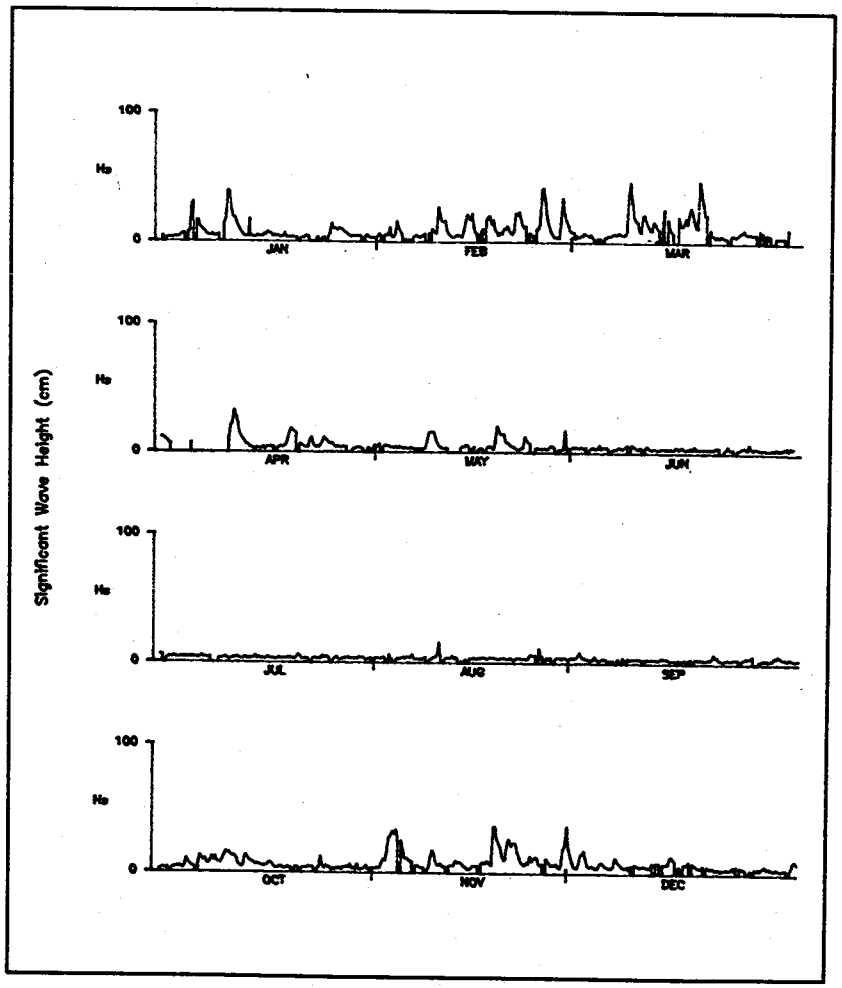

Figure C3. Surge significant wave height time-series plot for 1984 - Alioto's

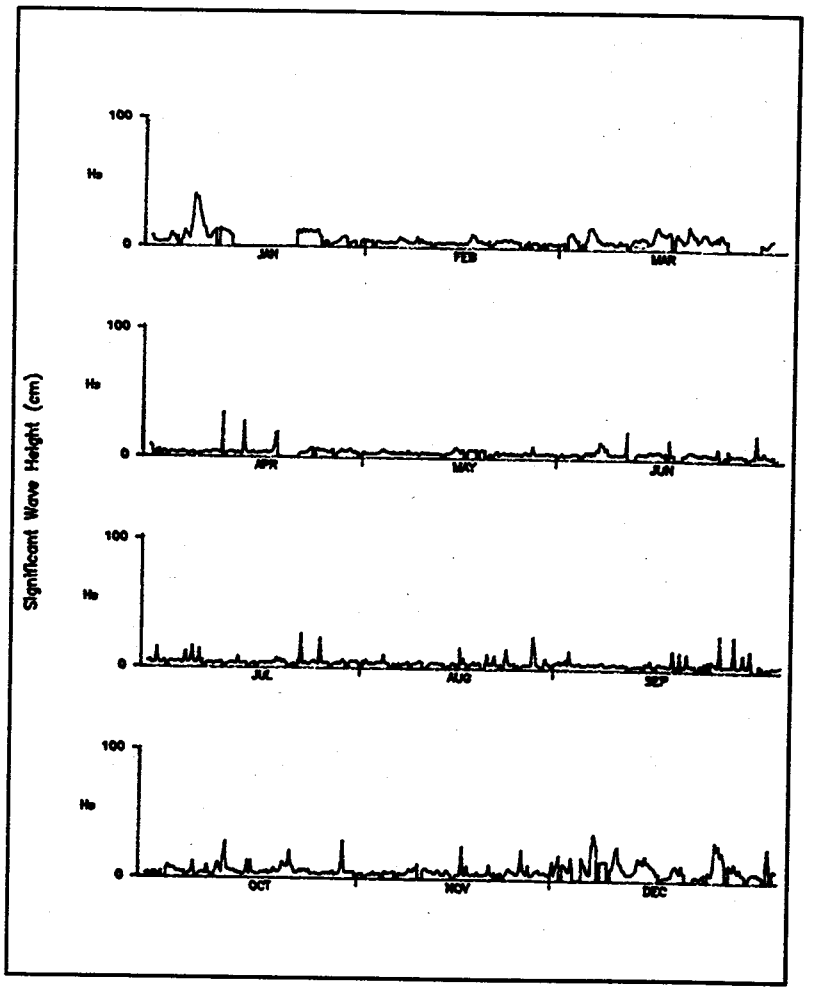

Figure C4. Surge significant wave height time-series plot for 1985 - Alioto's

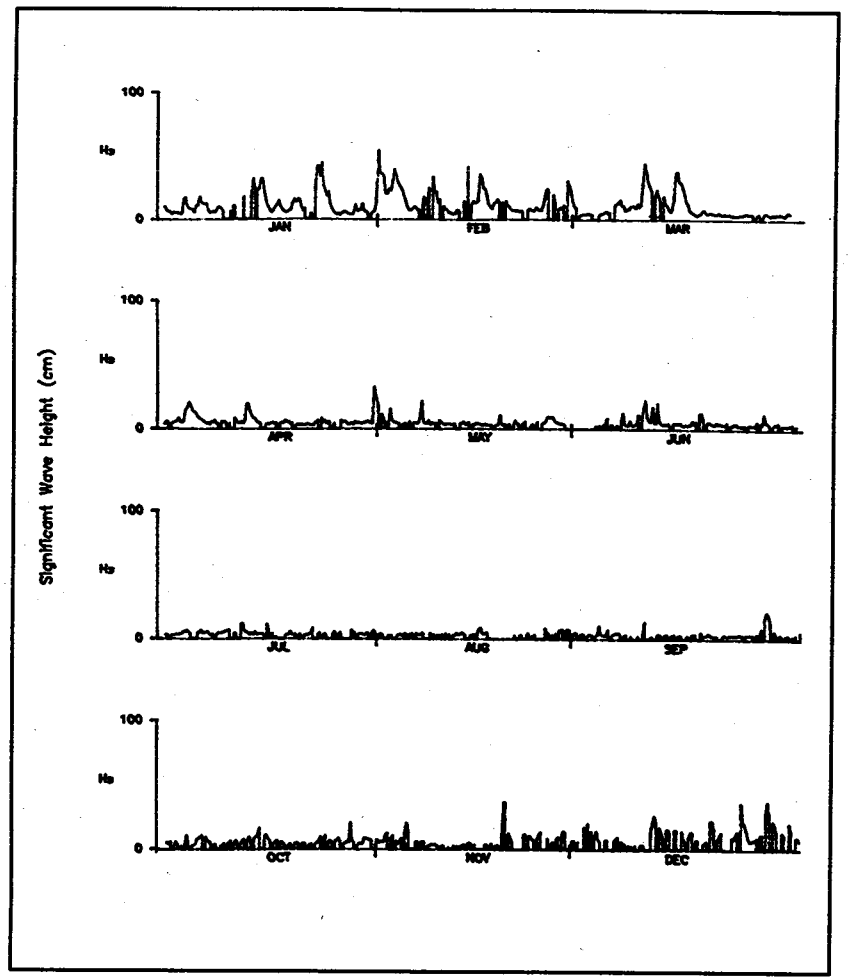

Figure C5. Surge significant wave height time-series plot for 1986 - Alioto's

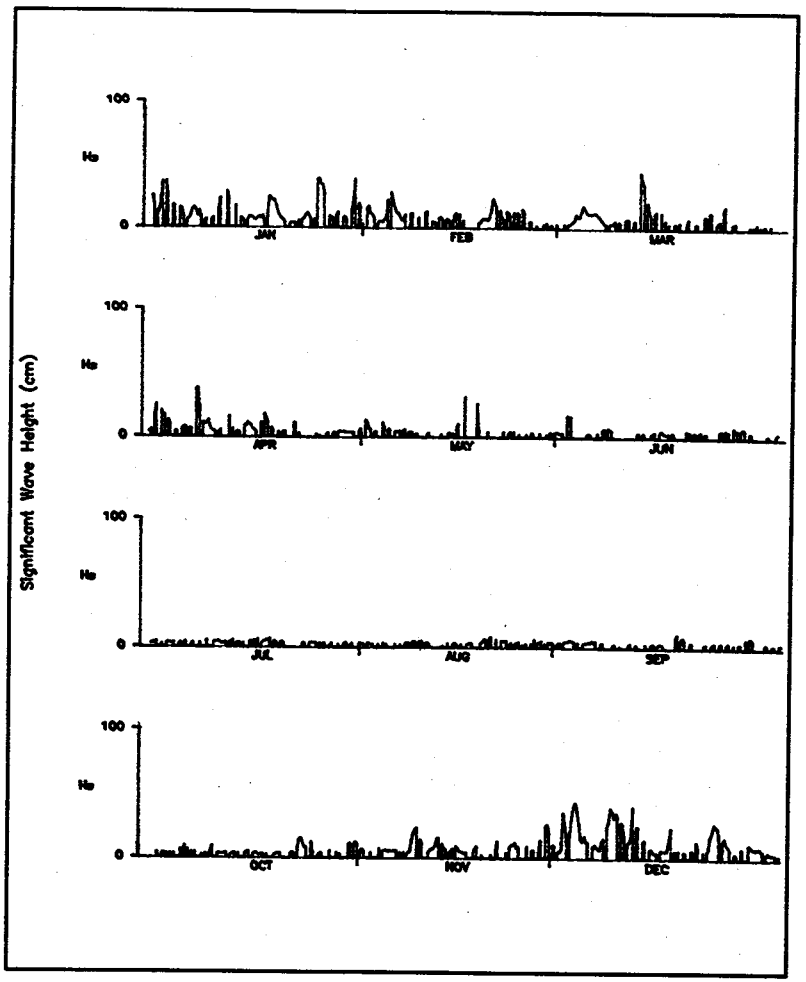

Figure C6. Surge significant wave height time-series plot for 1987 - Alioto's

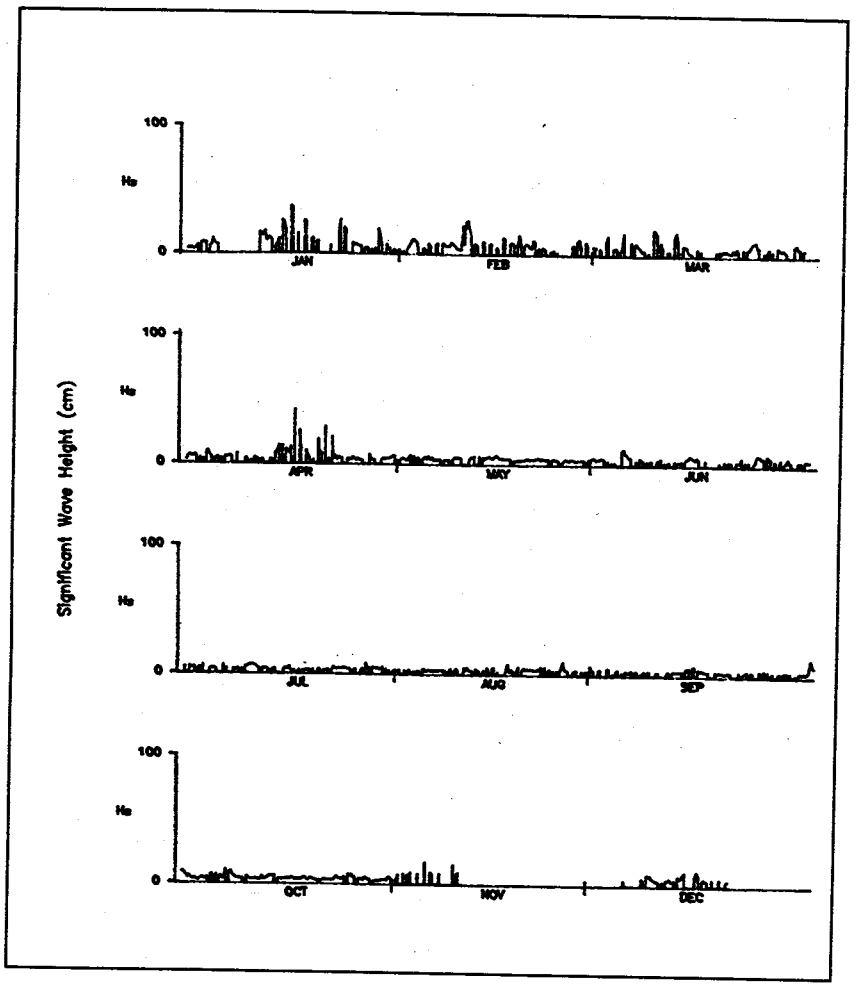

Figure C7. Surge significant wave height time-series plot for 1988 - Alioto's

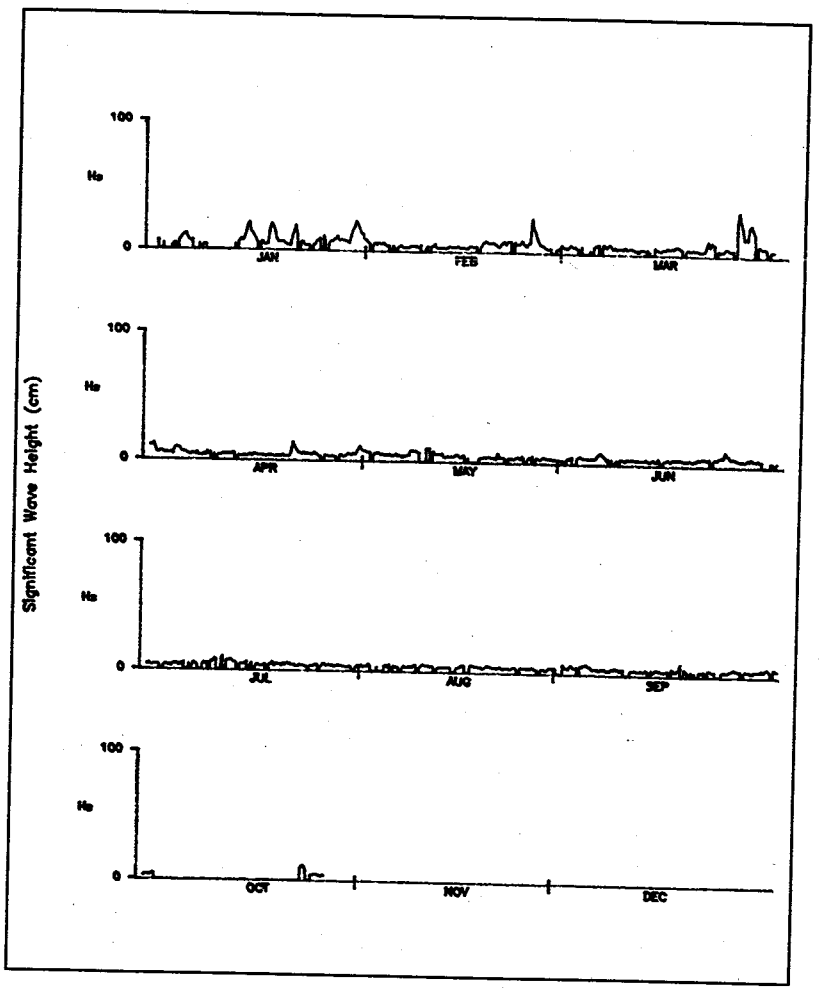

Figure C8. Surge significant wave height time-series plot for 1989 - Alioto's

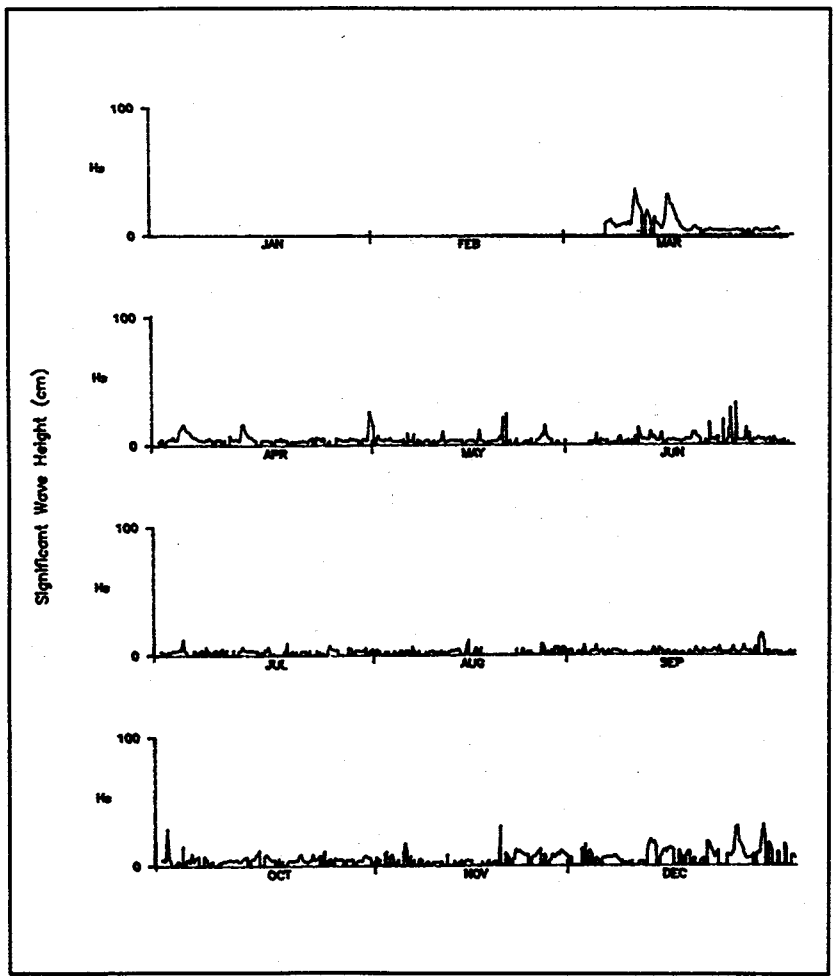

Figure C9. Surge significant wave height time-series plot for 1986 - Alioto's Wharf

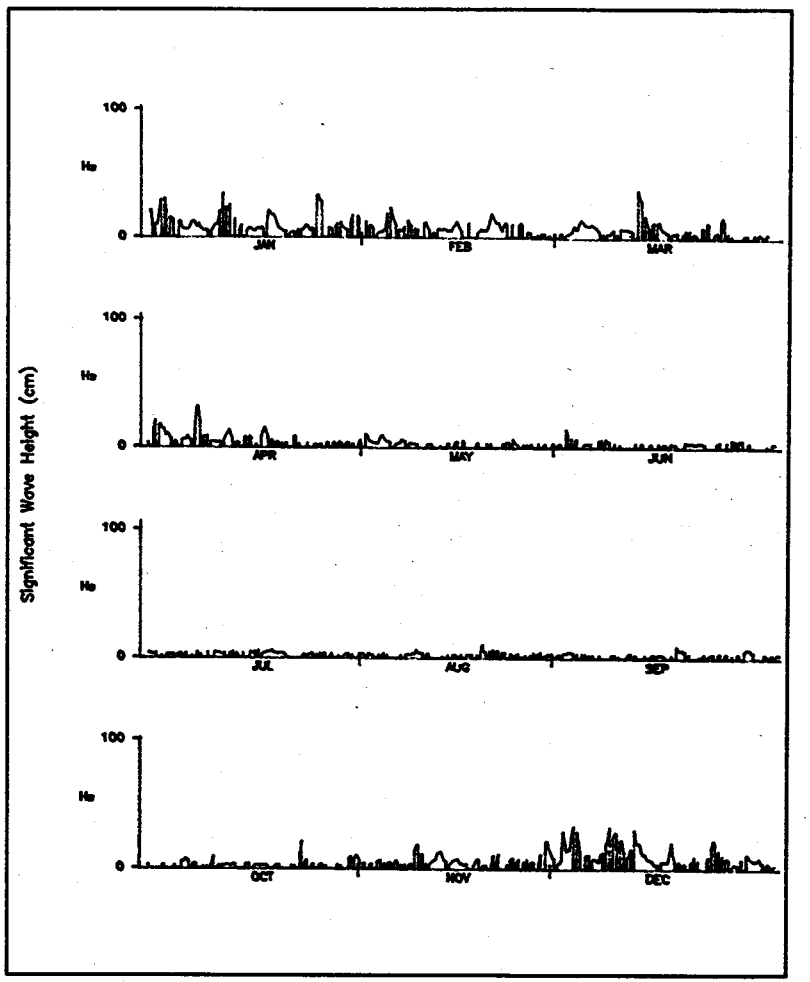

Figure C10. Surge significant wave height time-series plot for 1987 - Alioto's Wharf

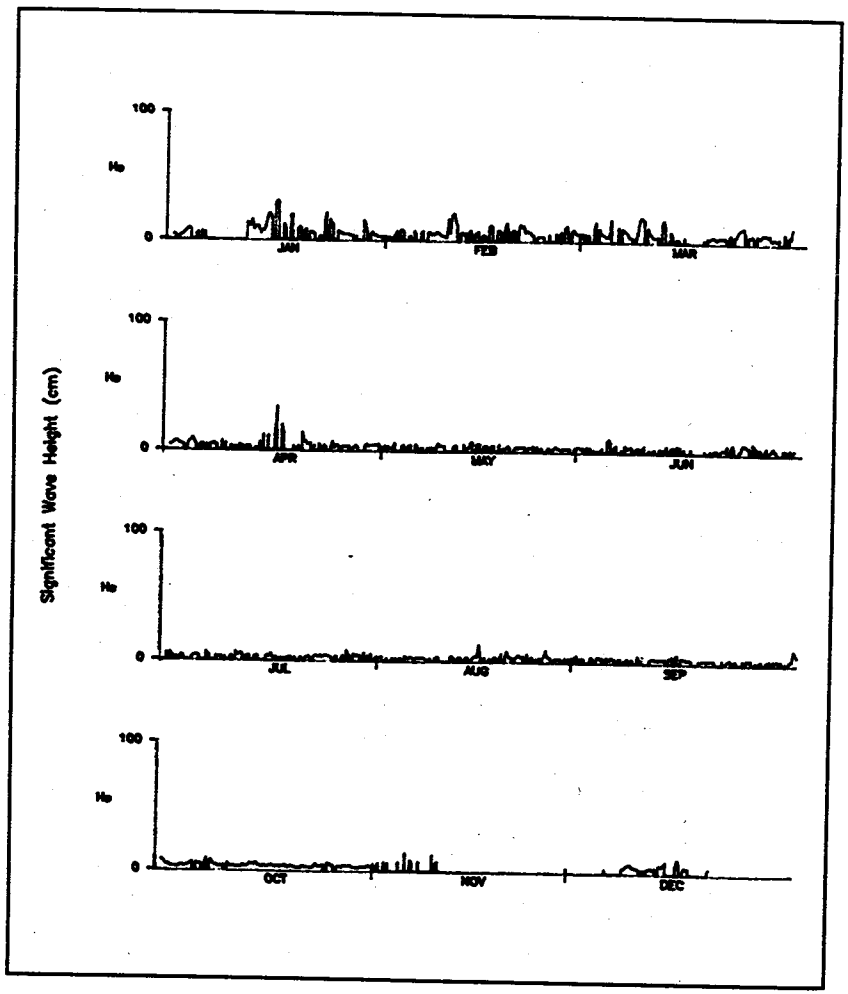

Figure C11. Surge significant wave height time-series plot for 1988 - Alioto's Wharf

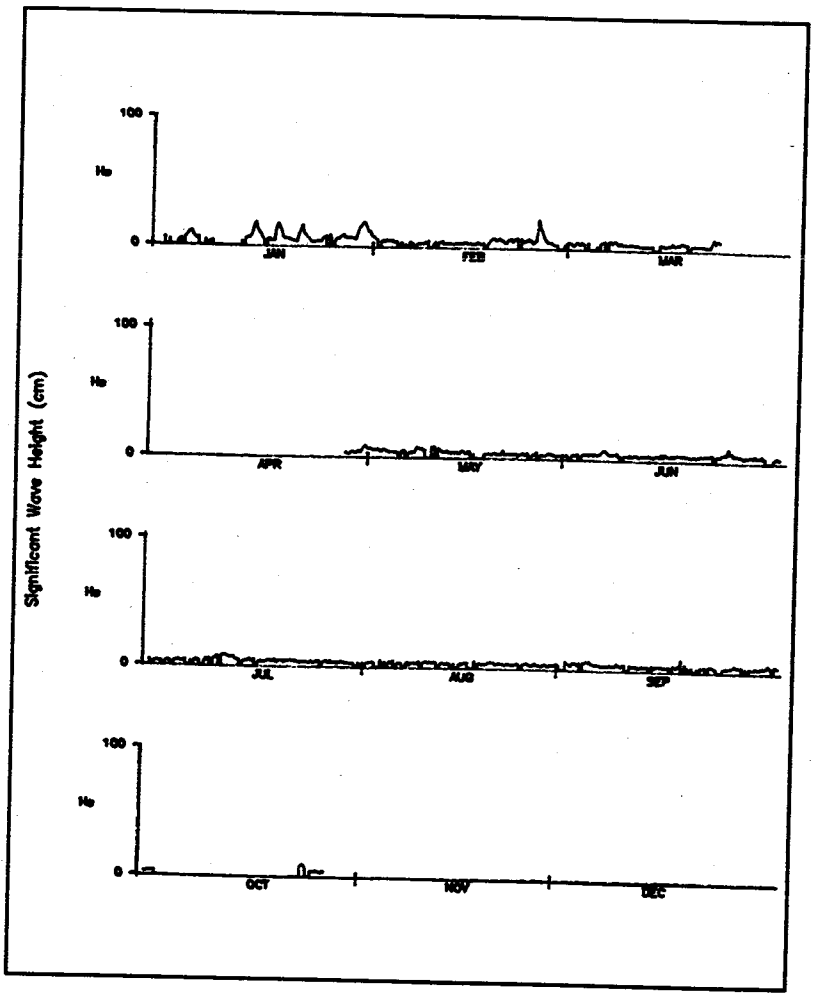

Figure C12. Surge significant wave height time-series plot for 1989 - Alioto's Wharf

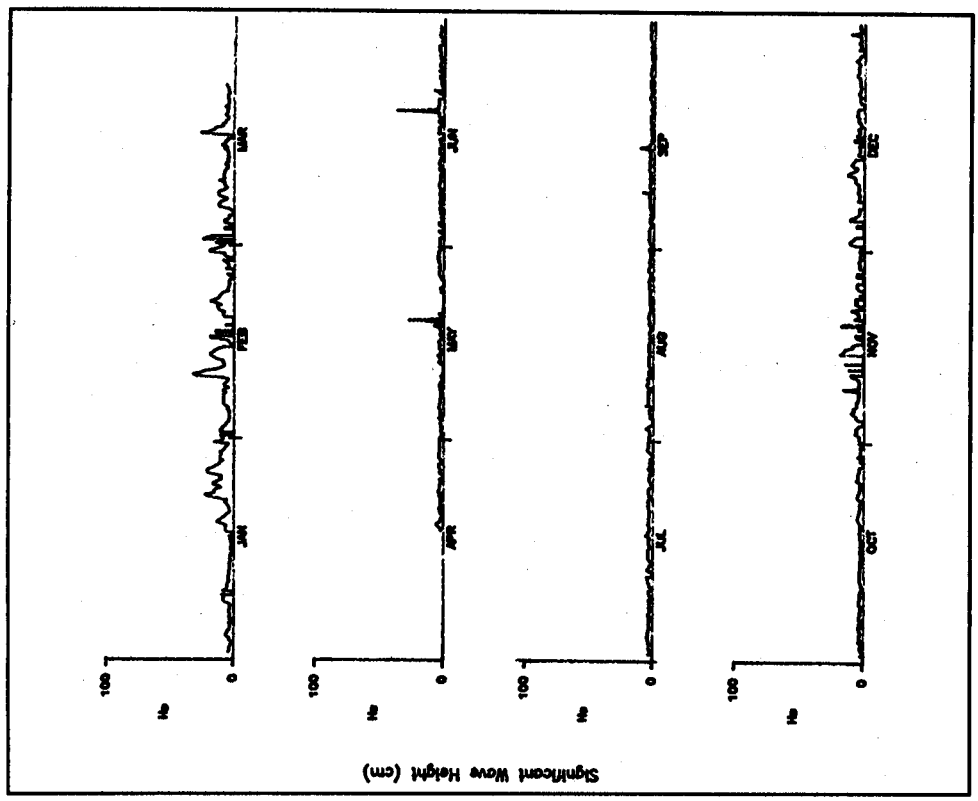

Figure C14. Surge significant wave height time-series plot for 1983- Pier 47

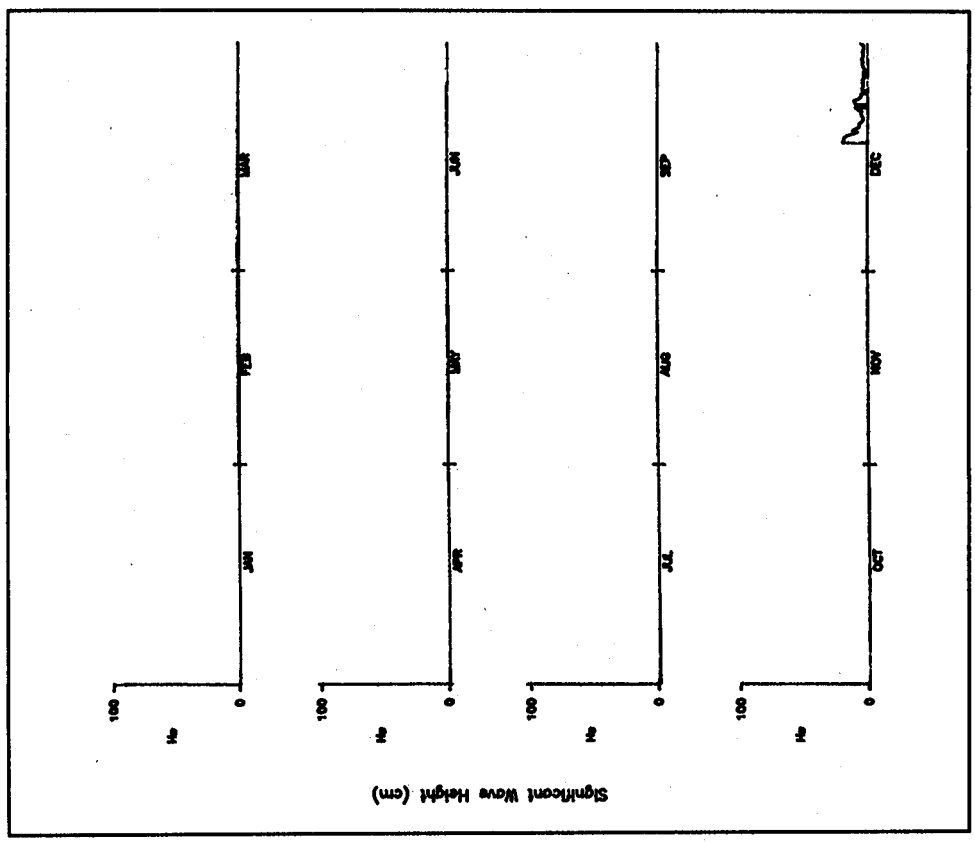

Figure C-13. Surge significant wave height time-series plot for 1982 - Pier 47

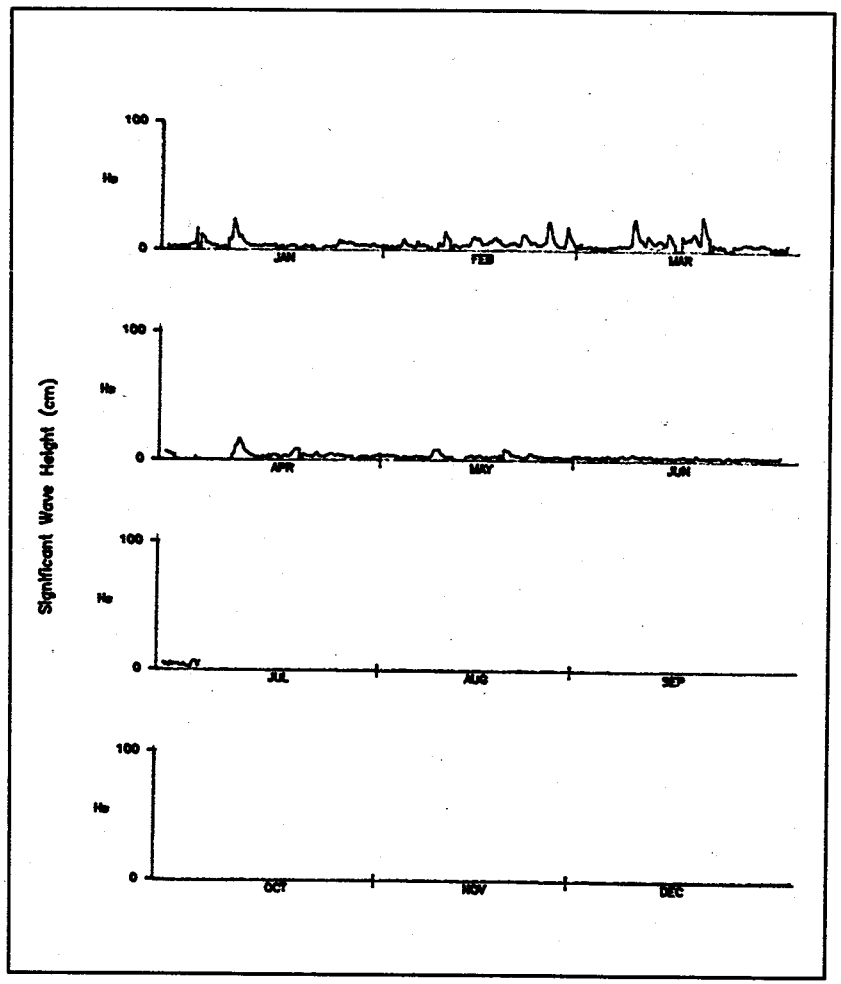

Figure C15. Surge significant wave height time-series plot for 1984 - Pier 47

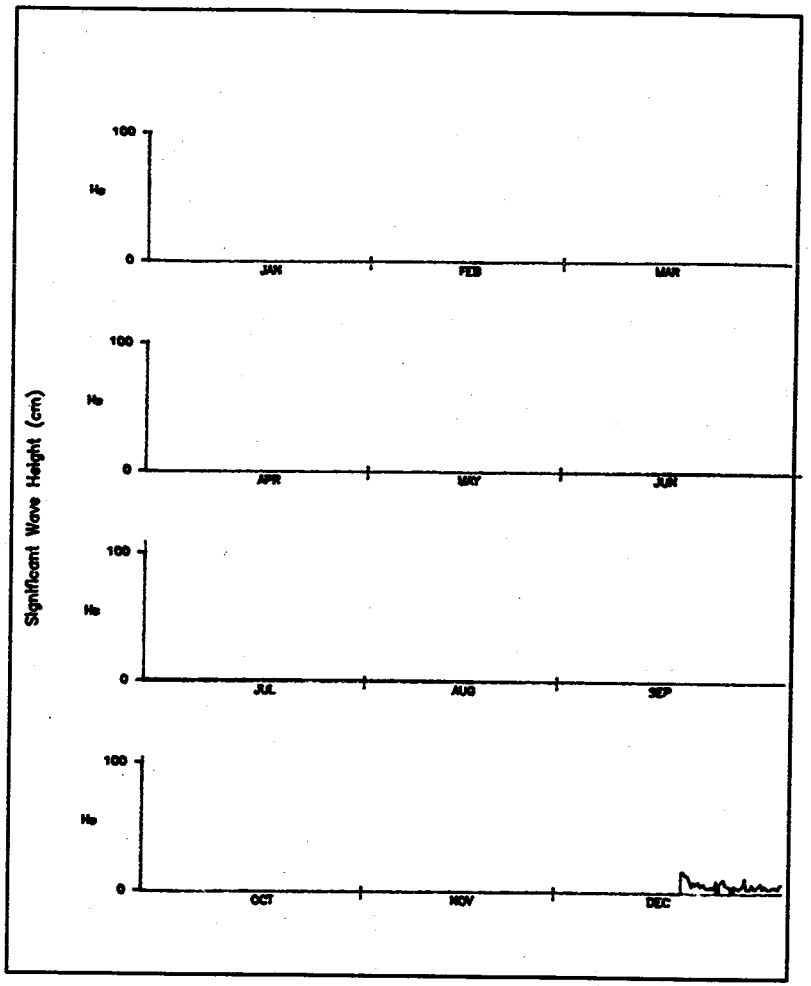

Figure C16. Surge significant wave height time-series plot for 1982 - Hyde St. pier

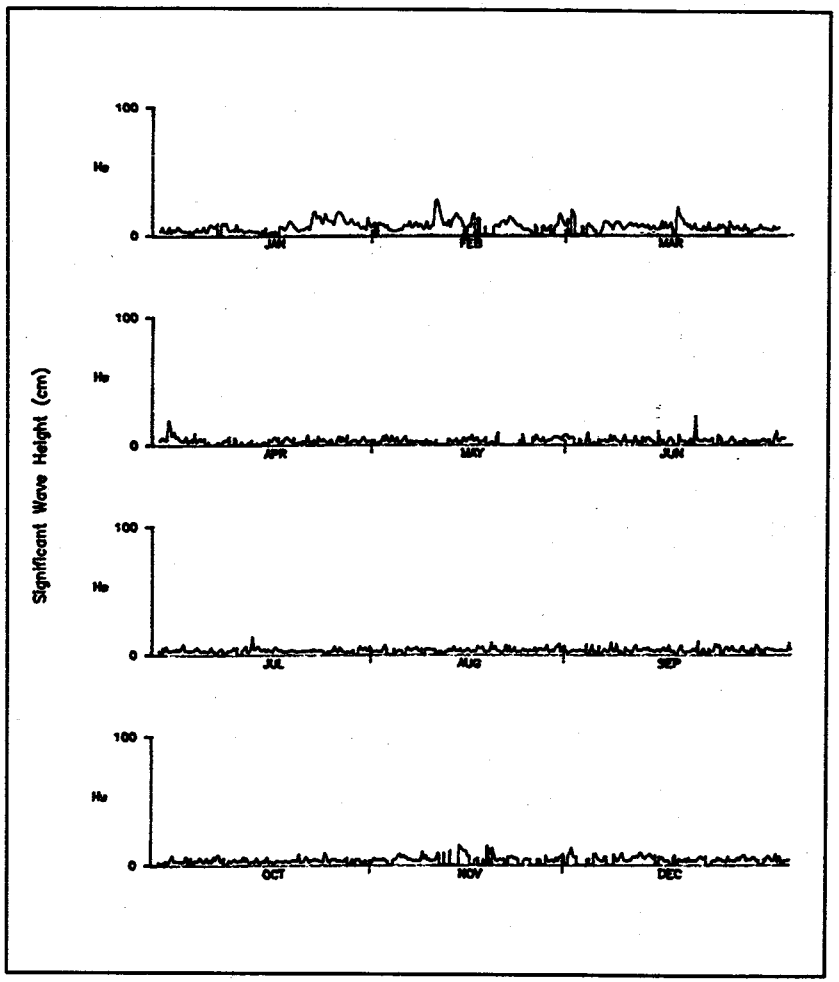

Figure C17. Surge significant wave height time-series plot for 1983 - Hyde St. pier

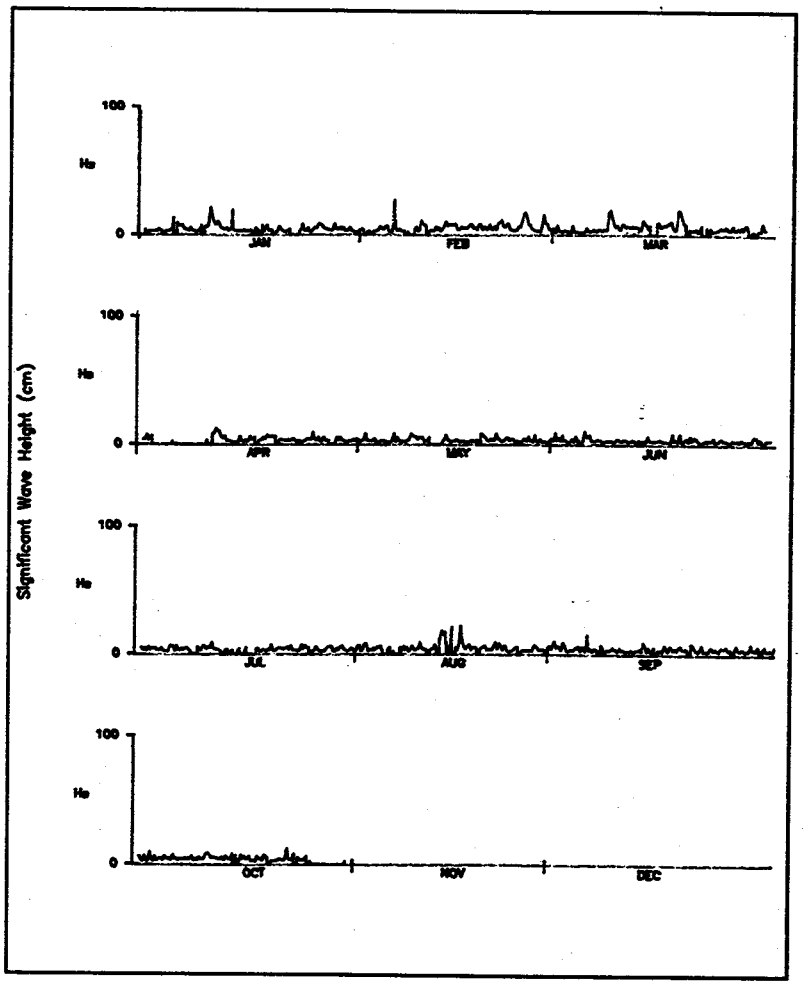

Figure C18. Surge significant wave height time-series plot for 1984 - Hyde St. pier

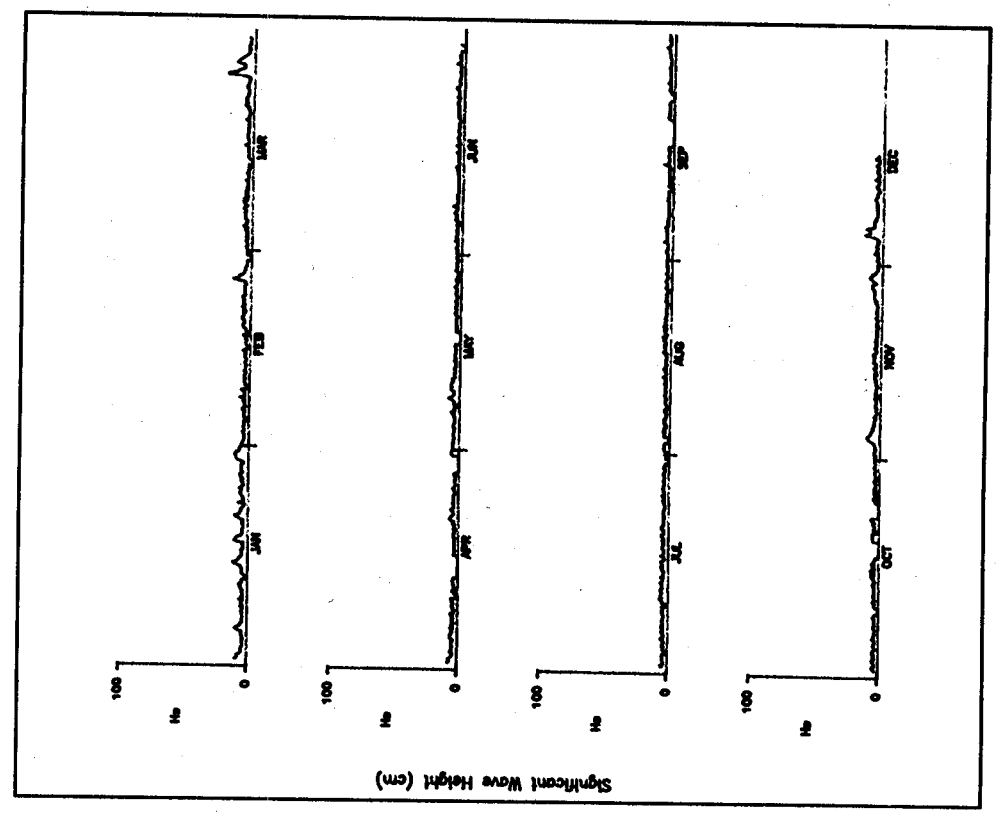

Figure C20. Surge significant wave height time-series plot for 1989 - Basin

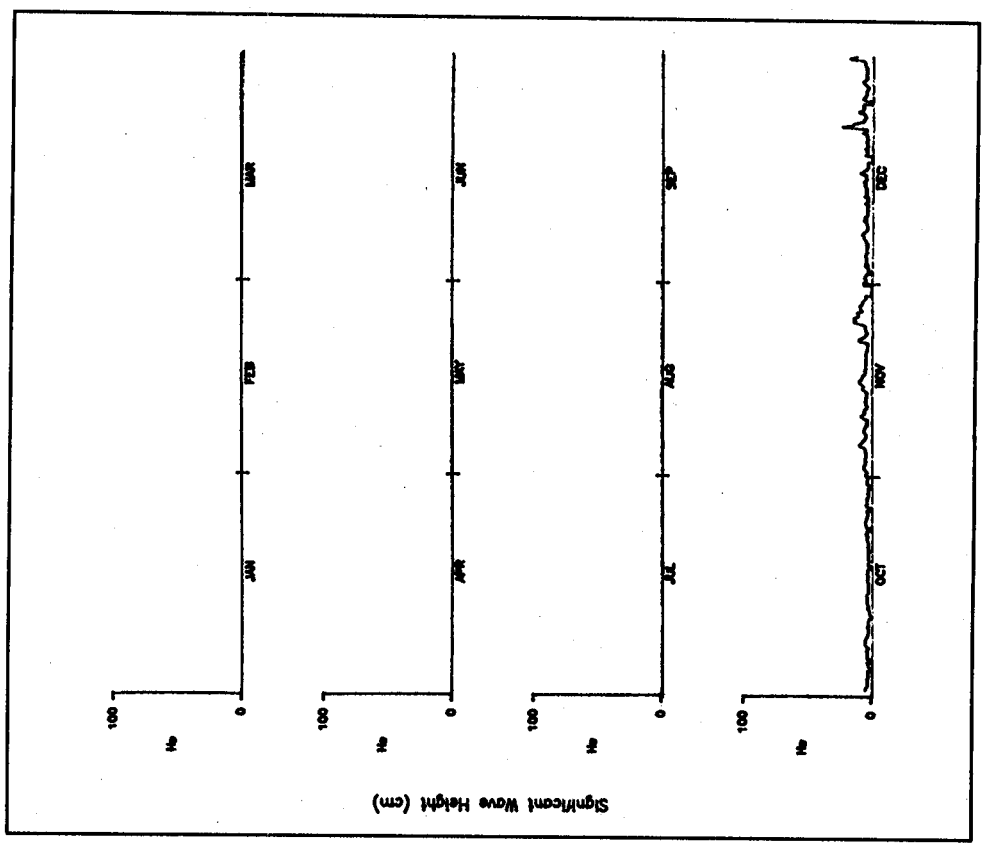

Figure C19. Surge significant wave height time-series plot for 1988 - Basin

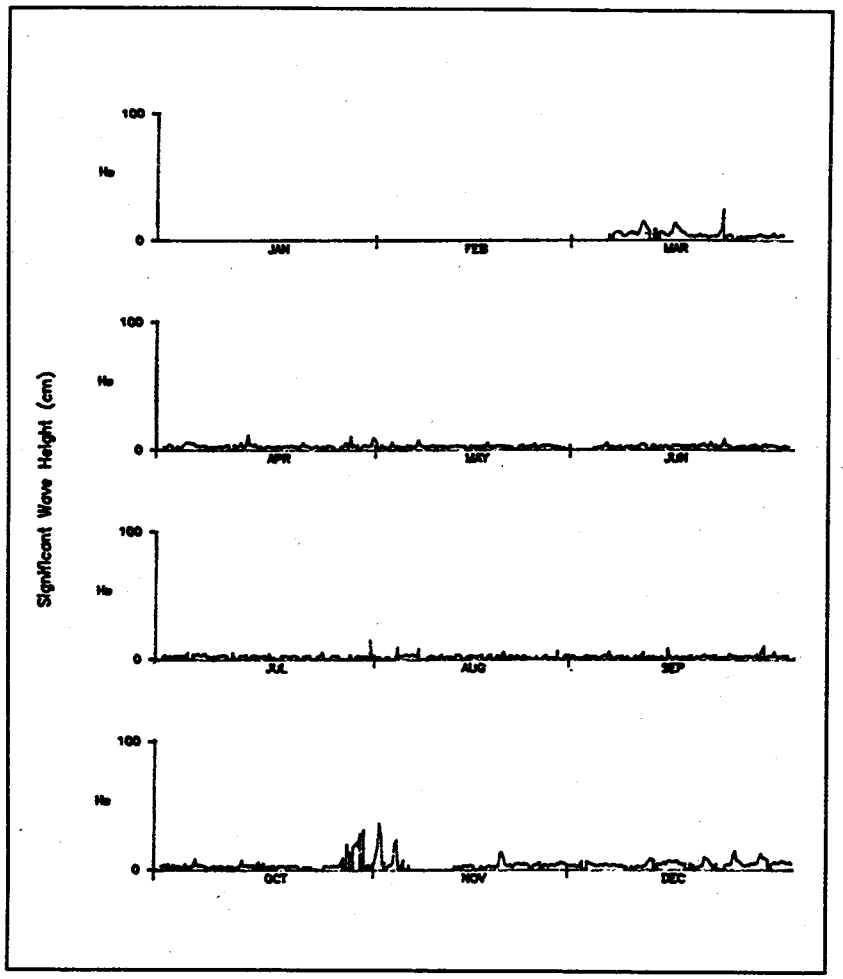

Figure C21. Surge significant wave height time-series plot for 1986 - Pier 45

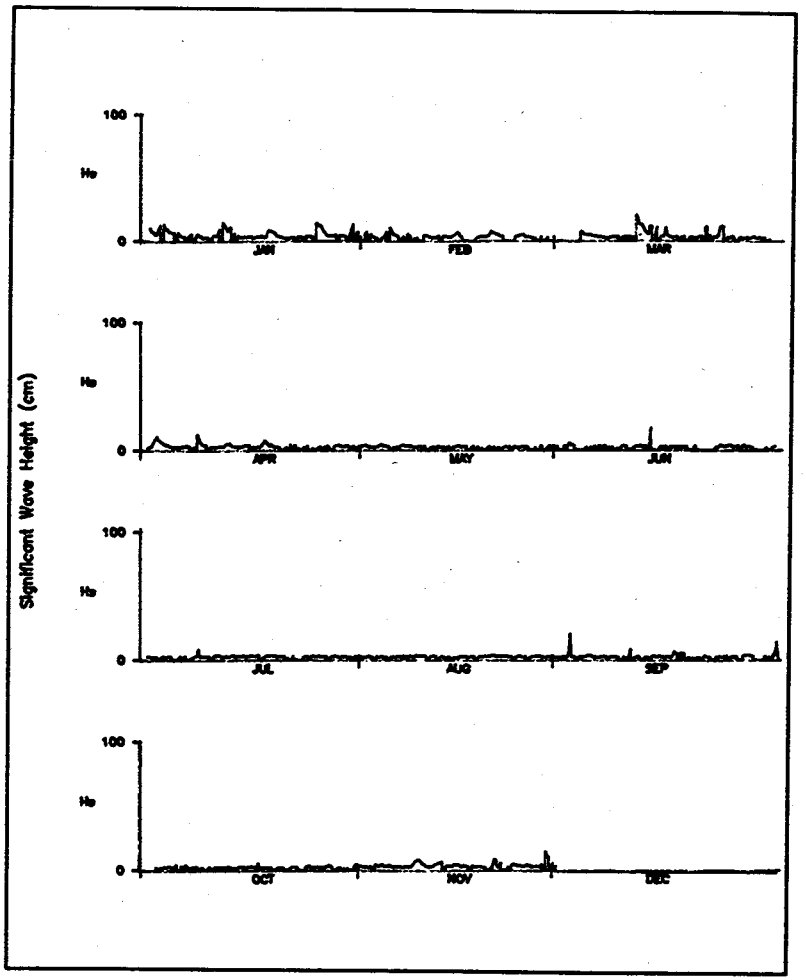

Figure C22. Surge significant wave height time-series plot for 1987 - Pier 45

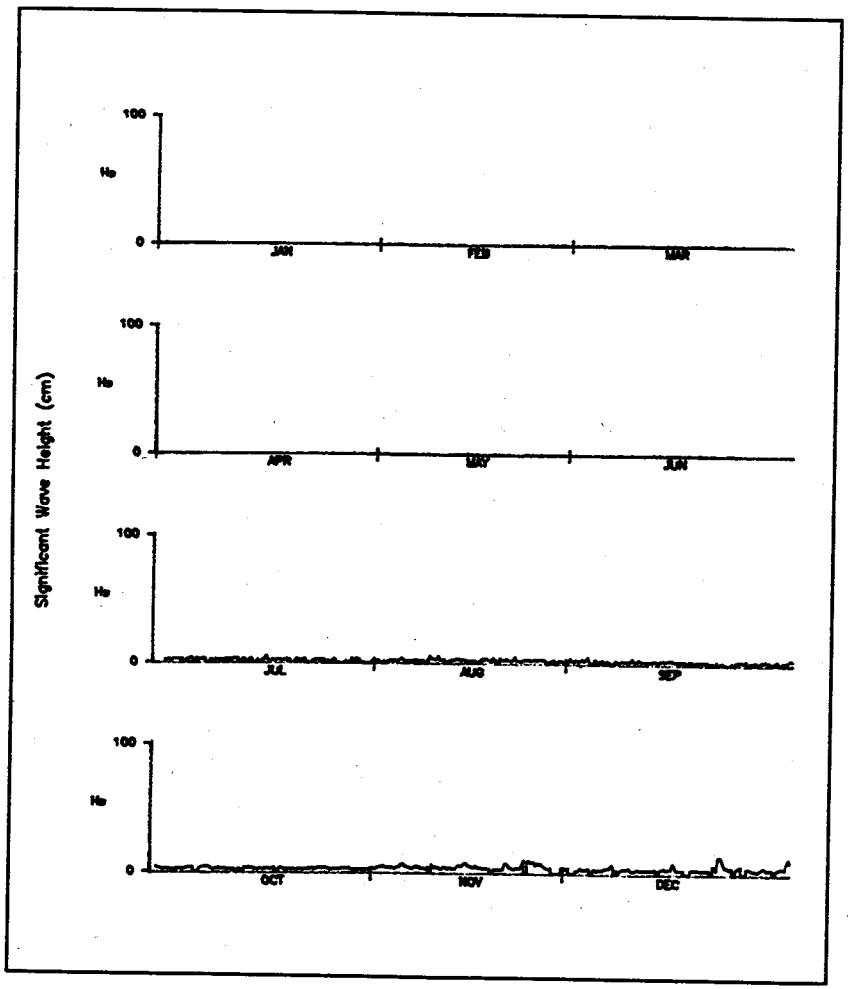

Figure C23. Surge significant wave height time-series plot for 1988 - Pier 45

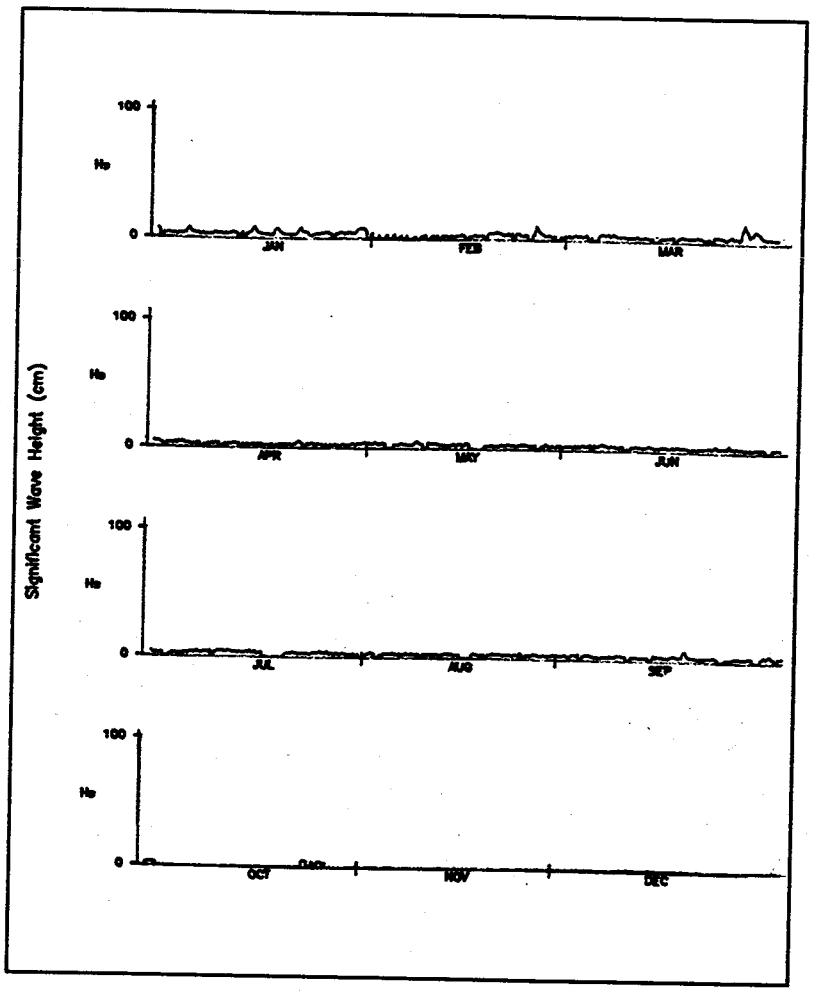

Figure C24. Surge significant wave height time-series plot for 1989 - Pier 45

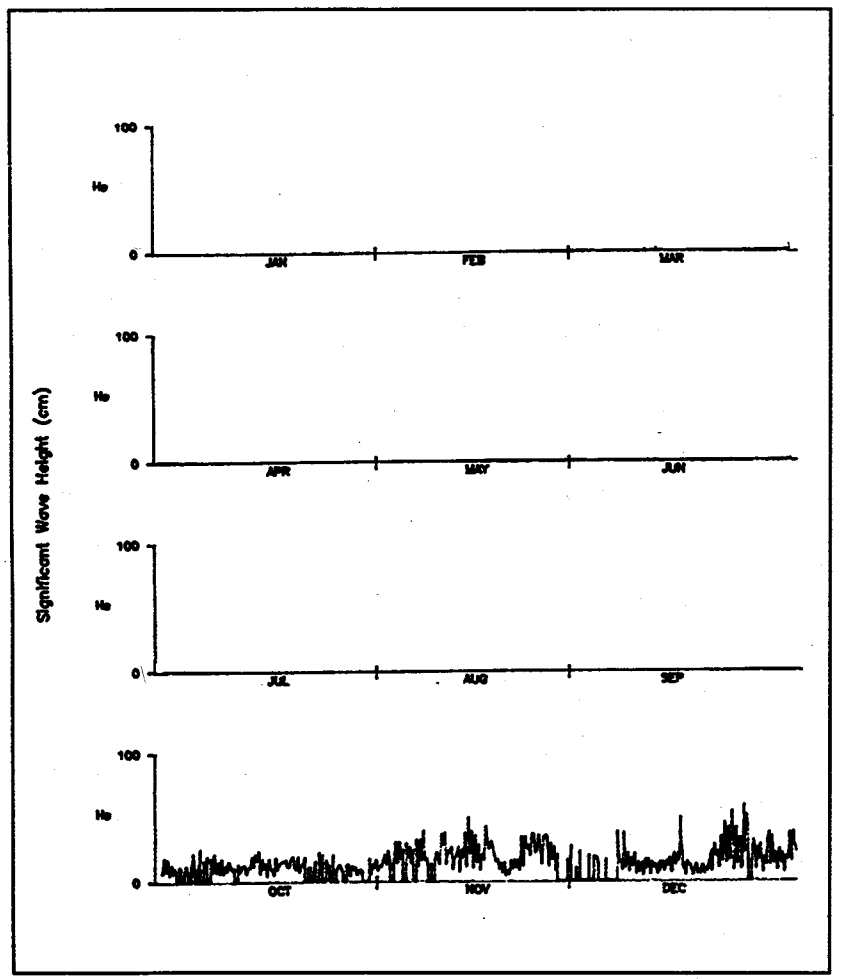

Figure C25. Energy significant wave height time-series plot for 1988 - Incident

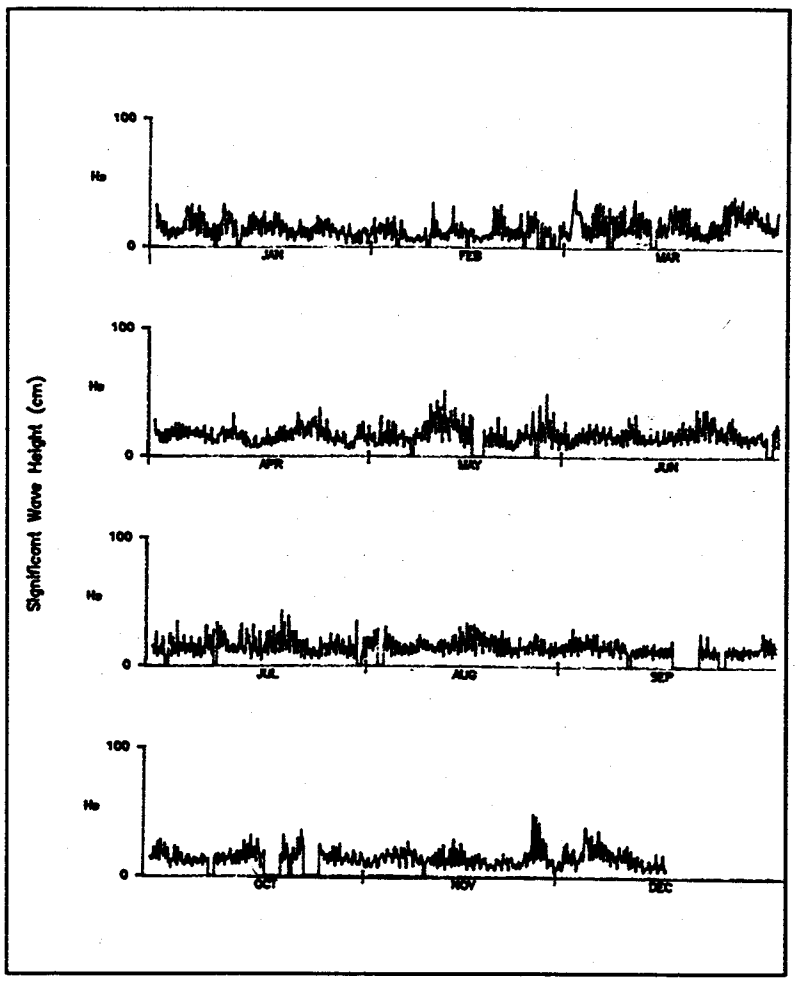

Figure C26. Energy significant wave height time-series plot for 1989 - Incident

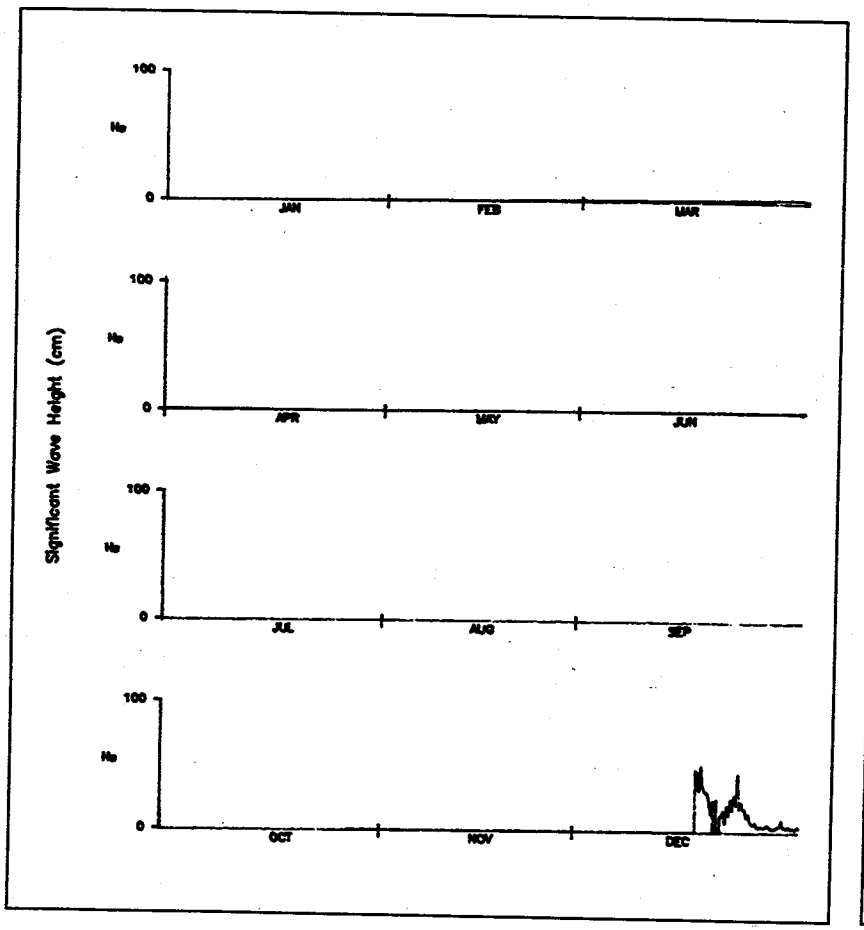

Figure C27. Energy significant wave height time-series plot for 1982 - Municipal pier

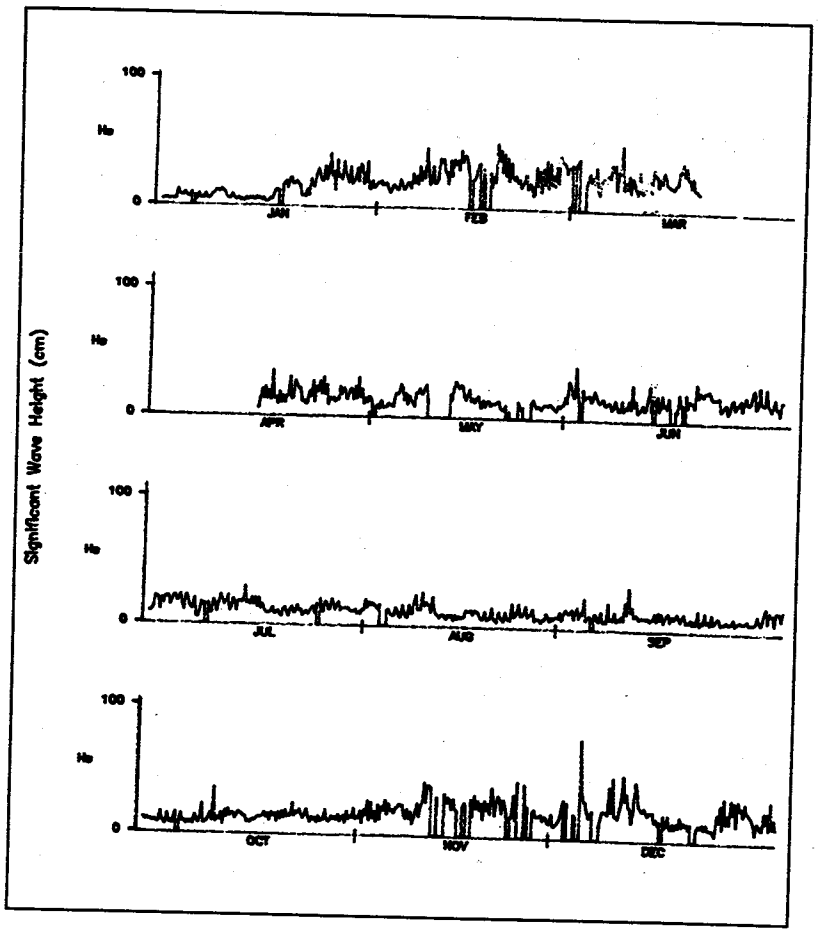

Figure C28. Energy significant wave height time-series plot for 1983 - Municipal pier

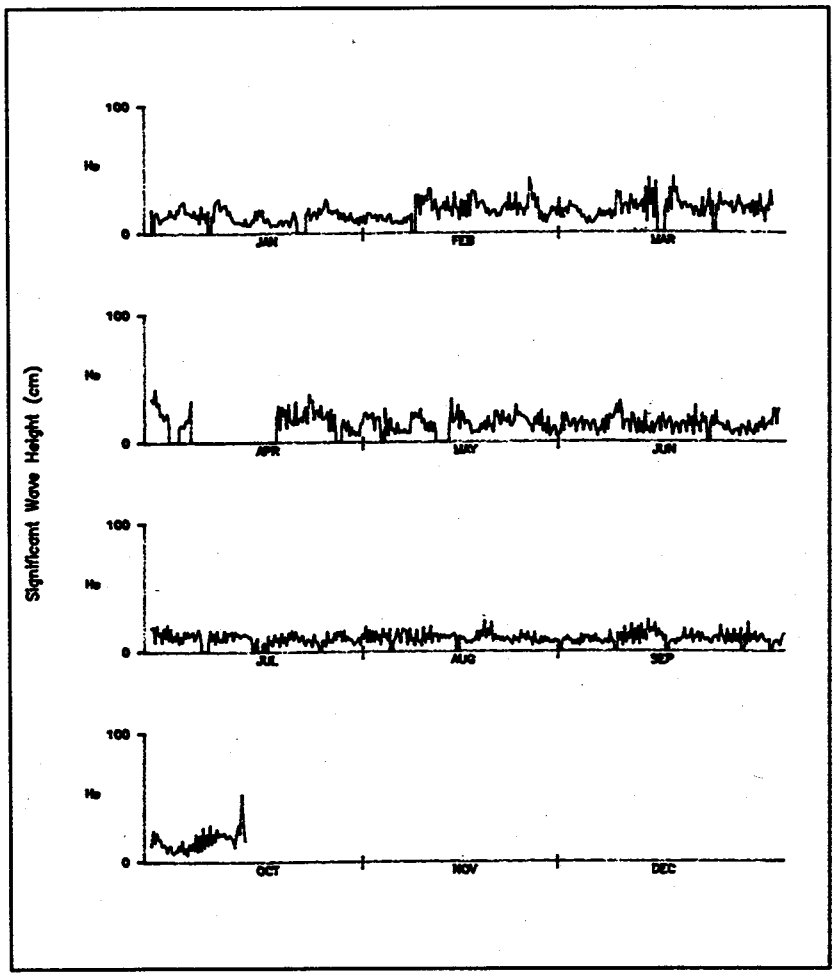

Figure C29. Energy significant wave height time-series plot for 1984 - Municipal pier

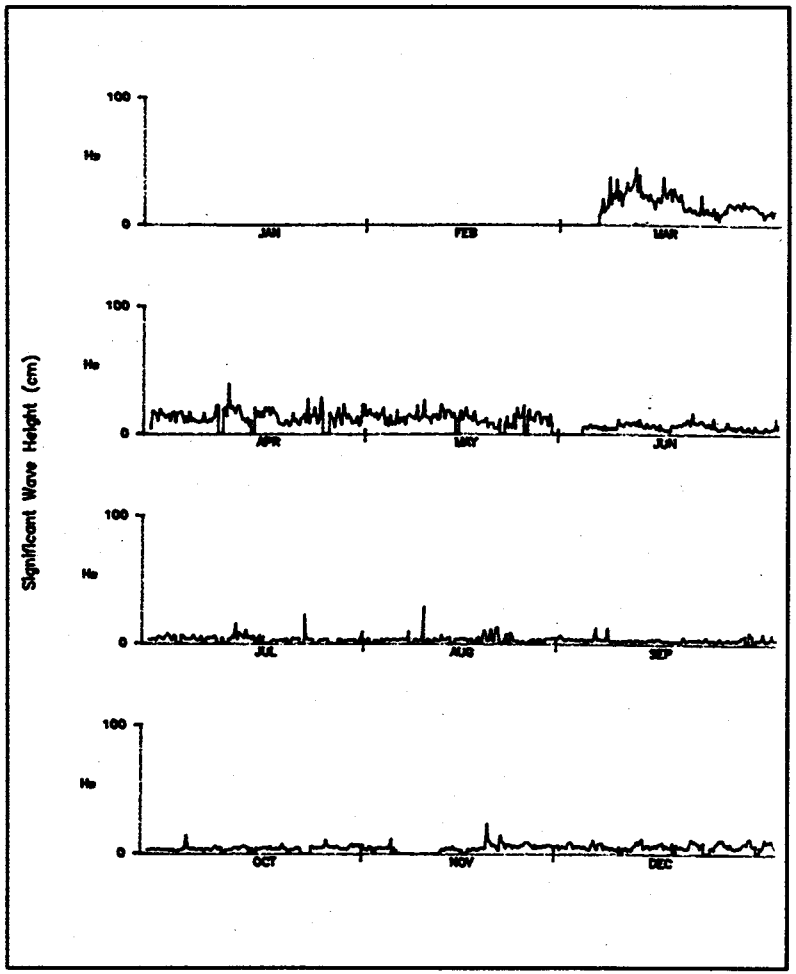

Figure C30. Energy significant wave height time-series plot for 1986 - Pier 45

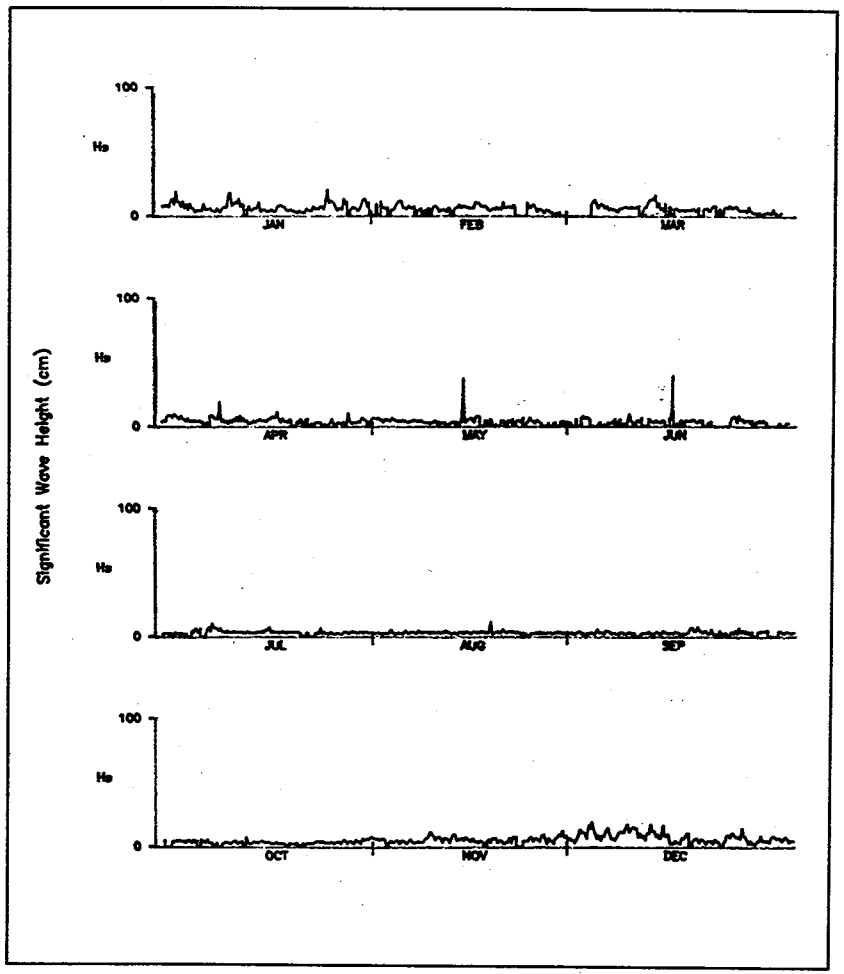

Figure C31. Energy significant wave height time-series plot for 1987 - Pier 45

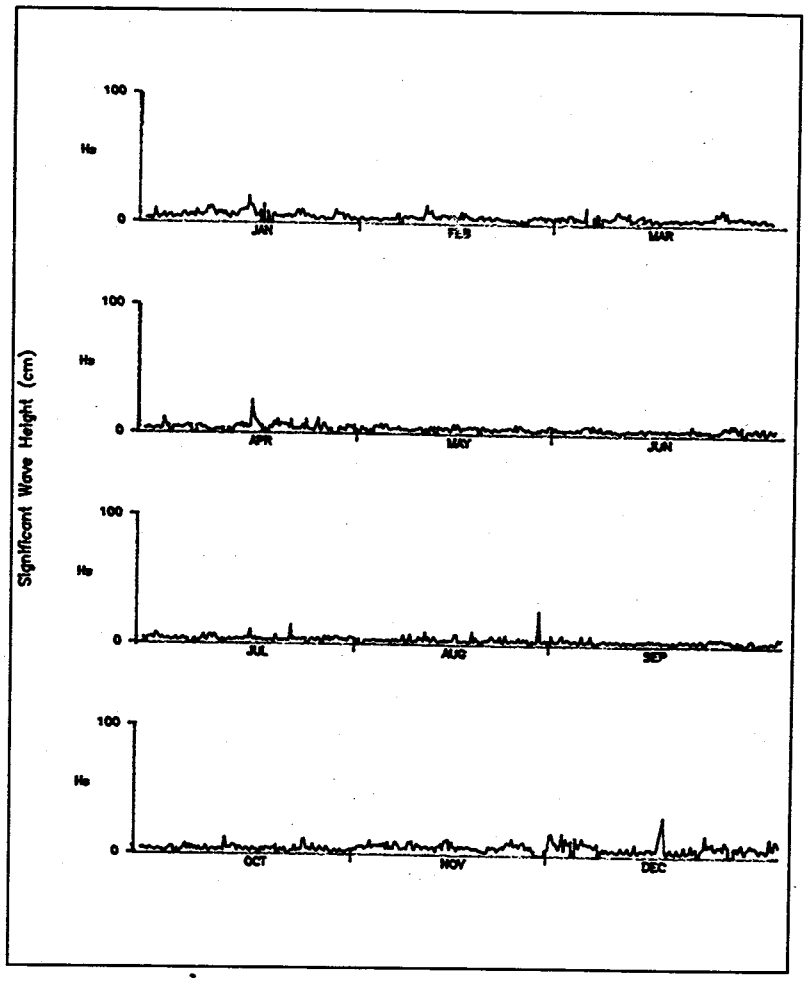

Figure C32. Energy significant wave height time-series plot for 1988 - Pier 45

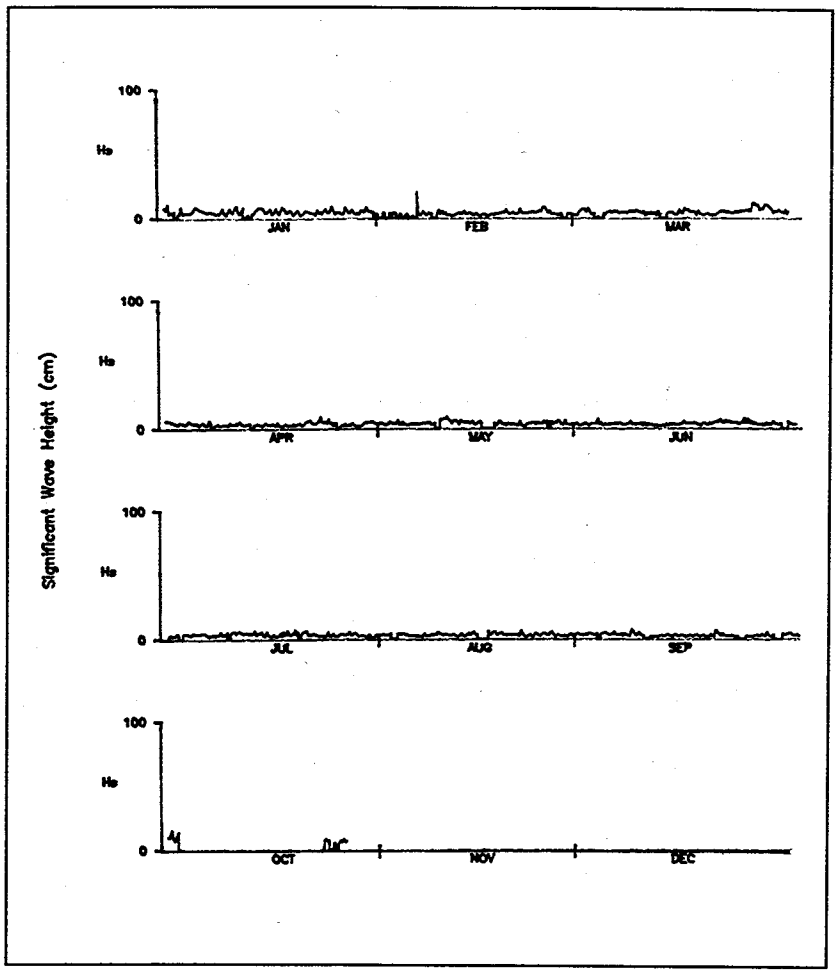

Figure C33. Energy significant wave height time-series plot for 1989 - Pier 45

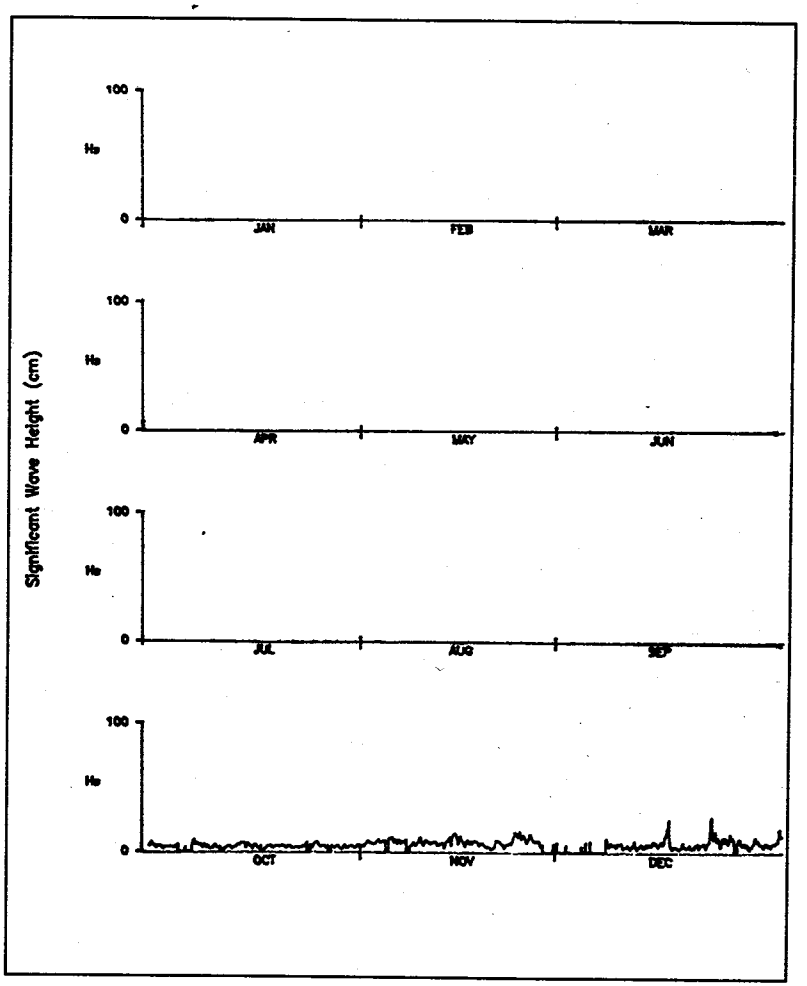

Figure C34. Energy significant wave height time-series plot for 1988 - Basin

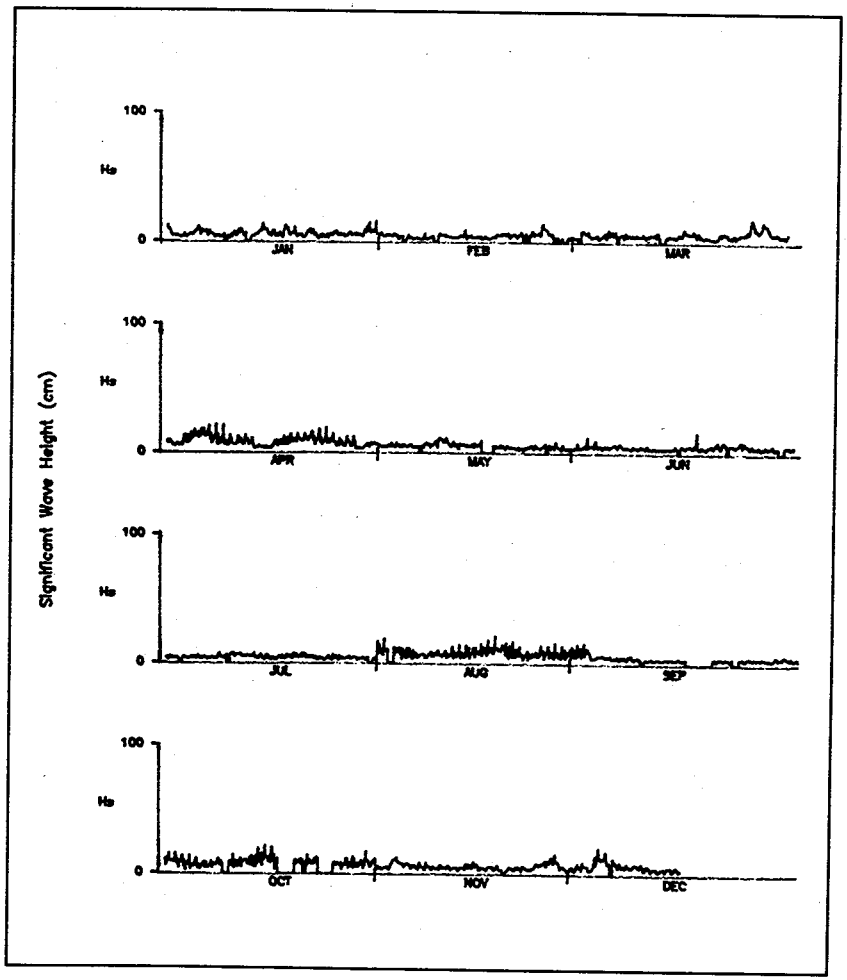

Figure C35. Energy significant wave height time-series plot for 1989 - Basin

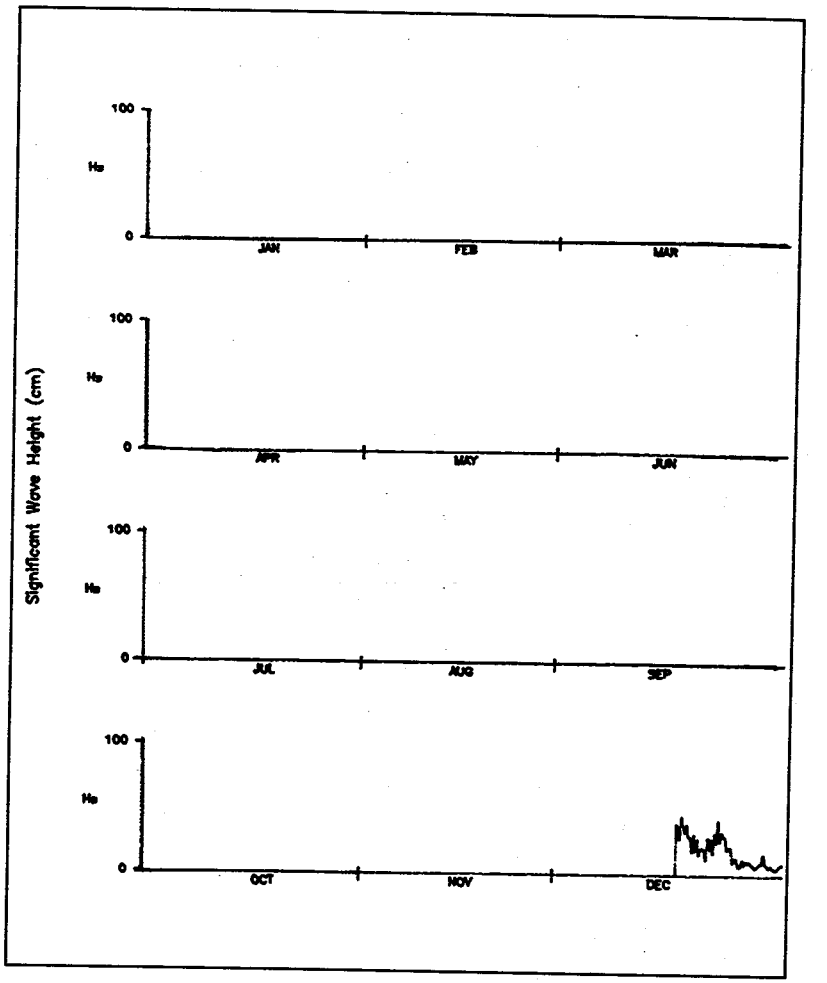

Figure C36. Energy significant wave height time-series plot for 1982 - Pier 47

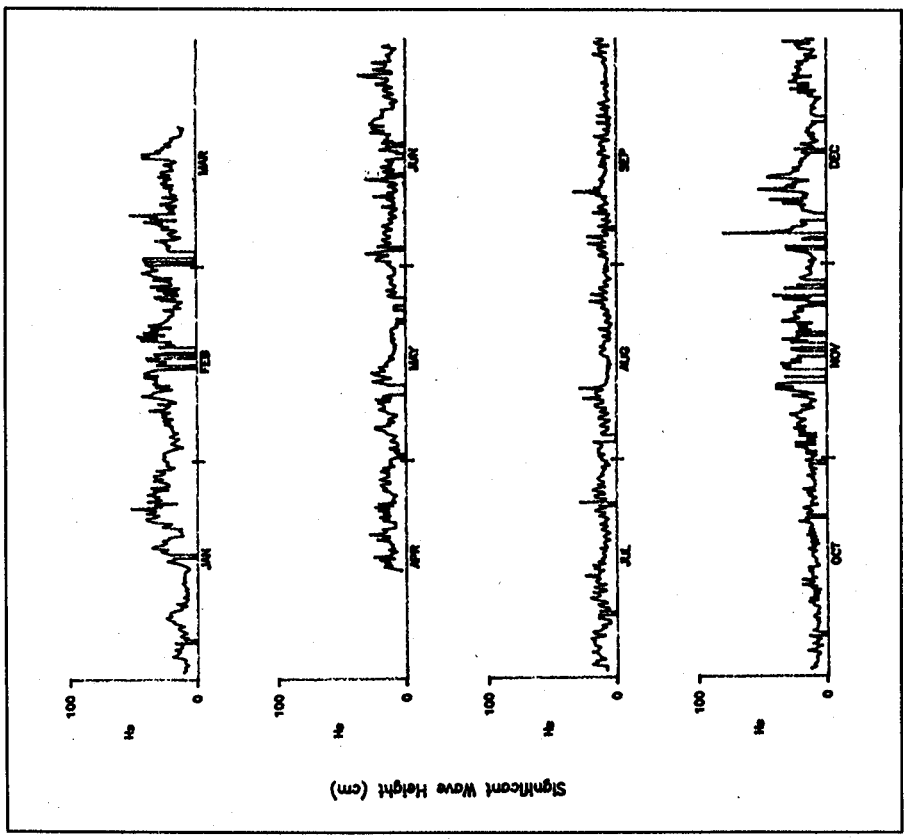

Figure C37. Energy significant wave height time-series plot for 1983 - Pier 47

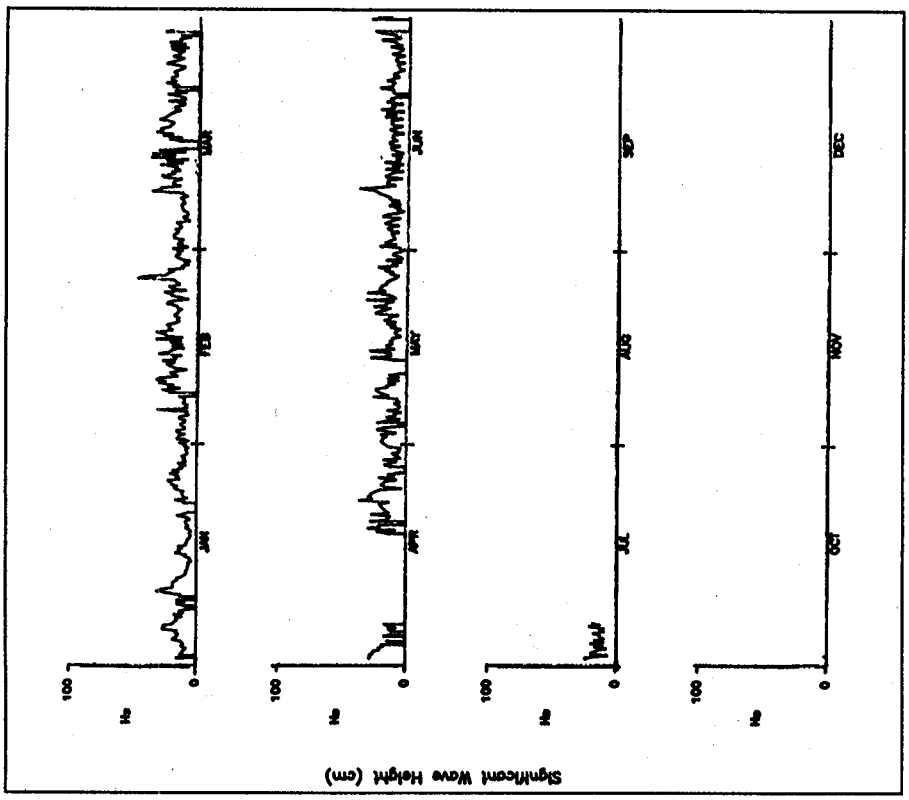

Figure C38. Energy significant wave height time-series plot for 1984 - Pier 47

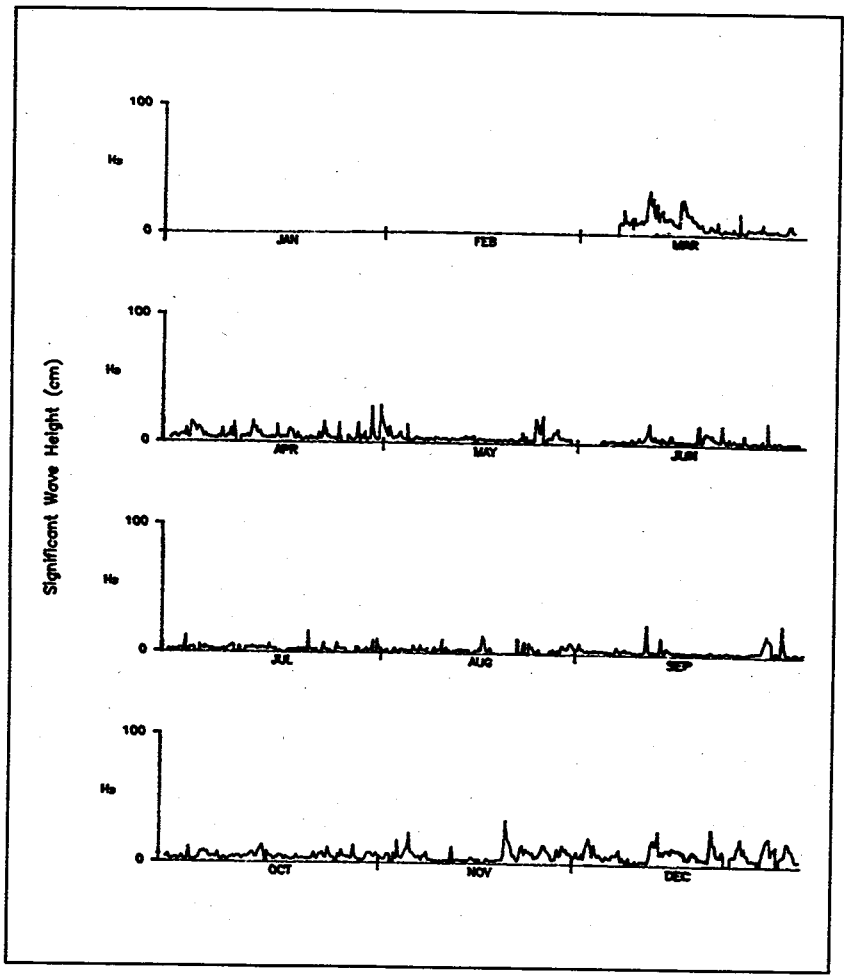

Figure C39. Energy significant wave height time-series plot for 1986 - Alioto's Wharf

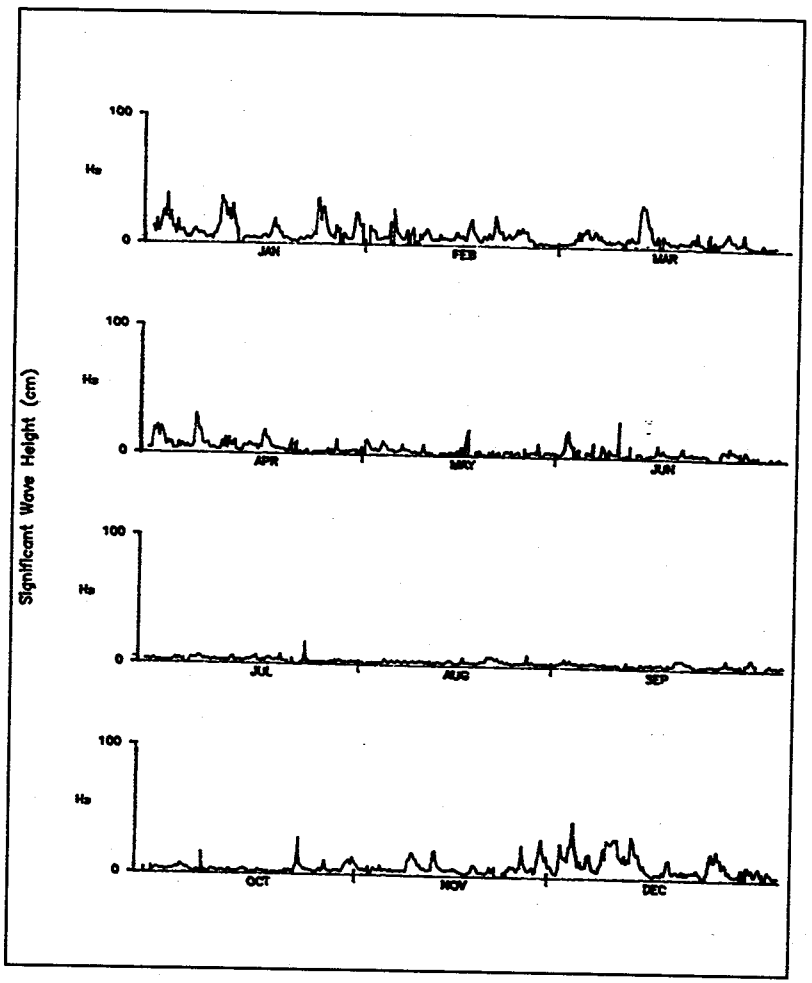

Figure C40. Energy significant wave height time-series plot for 1987 - Alioto's Wharf

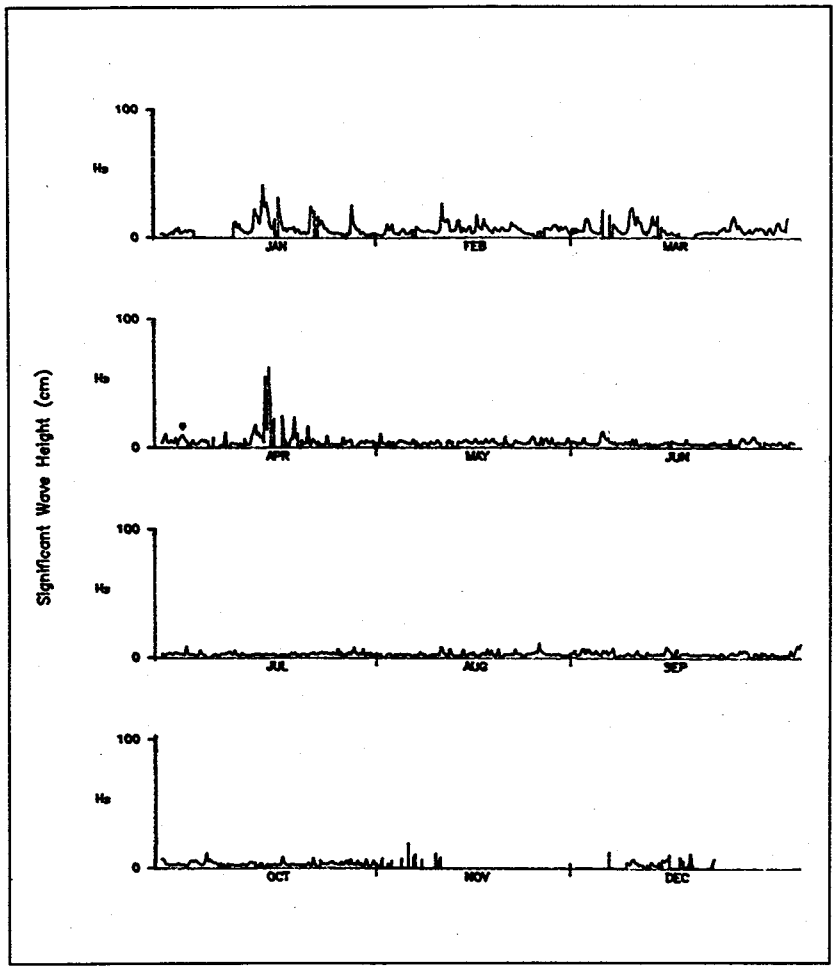

Figure C41. Energy significant wave height time-series plot for 1988 - Alioto's Wharf

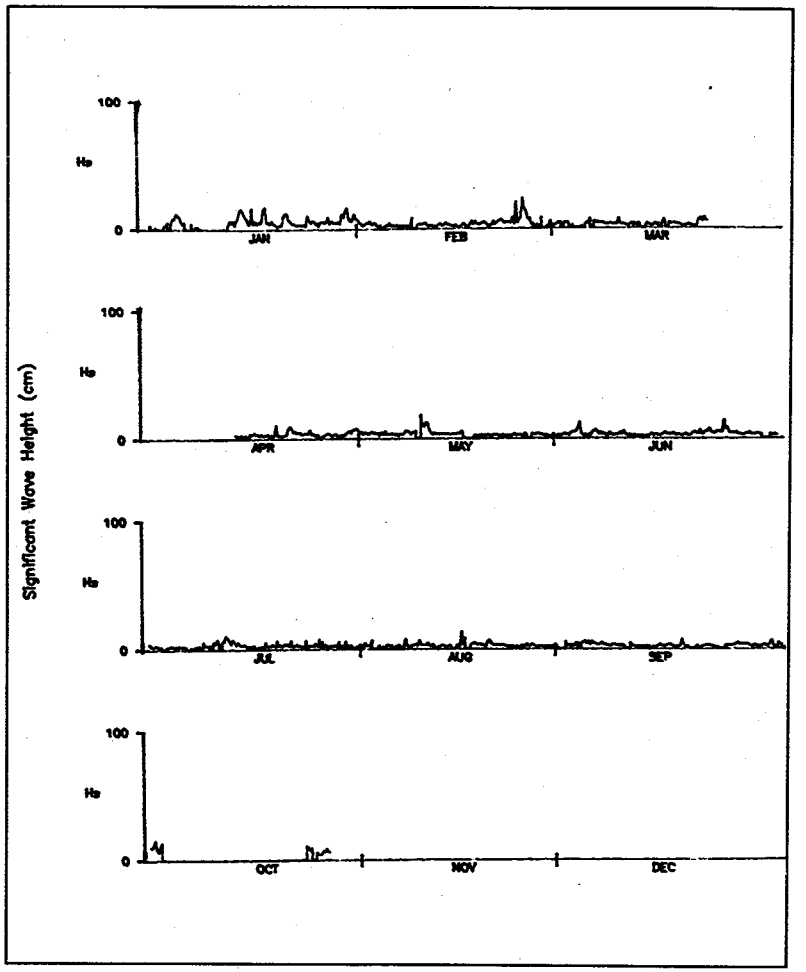

Figure C42. Energy significant wave height time-series plot for 1989 - Alioto's Wharf

TOTAL OBSERVATIONS =559

SIGNIFICANT WAVE HEIGHT (CM)	22+20	17	15	13	11	9	7	5
88-90+								
85-87								
82-84								
79-81								
76-78								
73-75								
70-72								
67-69								
64-66								
61-63								
58-60								
55-57								
52-54								
49-51								
46-48								
43-45								
40-42								
37-39								
34-36	1							
31-33								
28-30	5							
25-27	2							
22-24	3							
19-21	6							
16-18	10							
13-15	22					1		
10-12	34					1	1	
7 -9	45					1	1	
4 -6	132					5	3	8
1 -3	250			1	2	19	6	

PEAK PERIOD (SEC)

Figure C43. Joint distribution table, Alioto's Wharf, Energy, Pre-BW, Mar - Jun, 1986

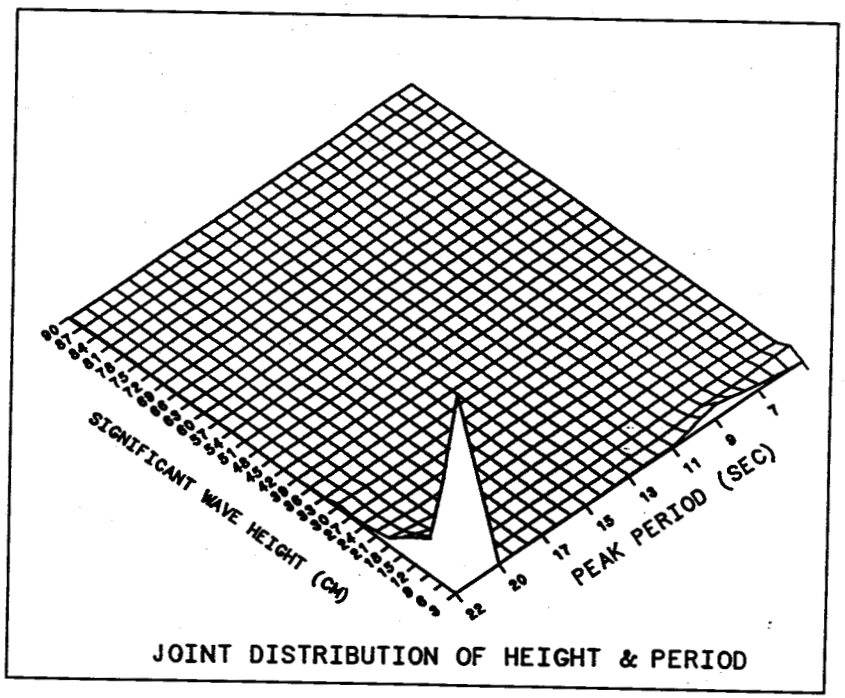

Figure C44. Joint distribution plot, Alioto's Wharf, Energy, Pre-BW, Mar - Jun, 1986

TOTAL OBSERVATIONS =4222

SIGNIFICANT WAVE HEIGHT (CM)

	22+20	17	15	13	11	9	7	5
88–90								
85–87								
82–84								
79–81								
76–78								
73–75								
70–72								
67–69								
64–66								
61–63	1							
58–60								
55–57	1							
52–54								
49–51								
46–48								
43–45	1							
40–42	2							
37–39	7							
34–36	4							
31–33	10							
28–30	12							
25–27	19							
22–24	19							
19–21	33							
16–18	55							
13–15	108							
10–12	170							
7 –9	412					2		
4 –6	1394					4	2	2
1 –3	1903	2	1	4	5	33	16	

PEAK PERIOD (SEC)

Figure C45. Joint Distribution table, Alioto's Wharf, Energy, Post-BW, Jul 1986 - Oct 1989

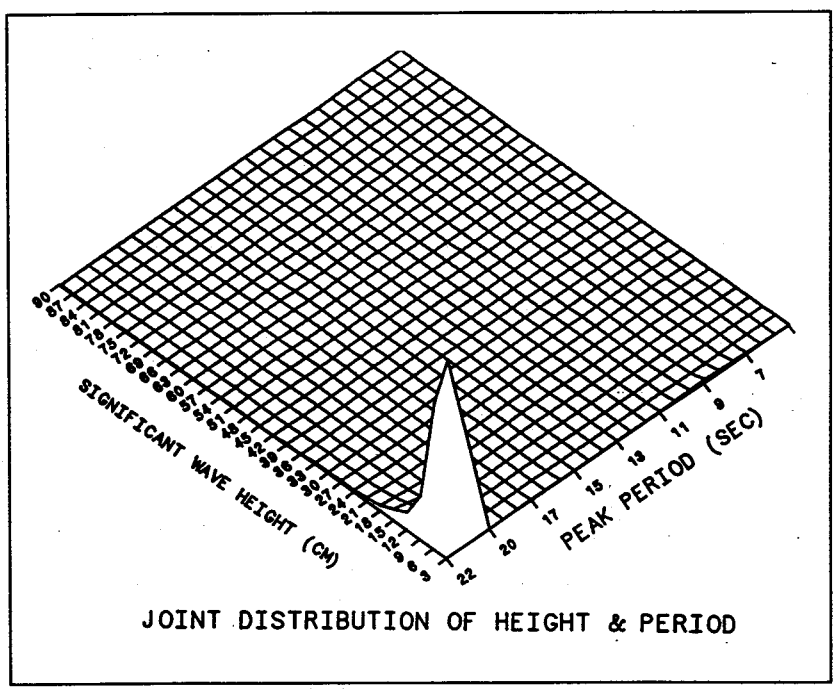

Figure C46. Joint distribution plot, Alioto's Wharf, Energy, Post-BW, Jul 1986 - Oct 1989

TOTAL OBSERVATIONS =2389

SIGNIFICANT WAVE HEIGHT (CM)

	22+20	17	15	13	11	9	7	5
88–90+								
85–87								
82–84								
79–81								
76–78								1
73–75								
70–72								
67–69								
64–66								
61–63								
58–60								
55–57								
52–54	1					1	1	
49–51					1	1	1	1
46–48						3	3	
43–45					1	2	1	2
40–42						6	7	
37–39					2	8	9	5
34–36	3					11	16	7
31–33	1			1	3	18	19	8
28–30	1				4	24	29	15
25–27	5			1	5	24	36	16
22–24	9			1	3	48	71	44
19–21	7				12	57	93	65
16–18	10		1	1	19	52	96	100
13–15	16		1	5	10	84	134	167
10–12	10	1	3	2	12	45	94	199
7 –9	3	2	8	11	16	44	78	185
4 –6	2	1	6	8	15	15	24	137
1 –3	8			8	14	9	11	

PEAK PERIOD (SEC)

Figure C47. Joint distribution table, Municipal pier, Energy, Pre-BW, Dec 1982 - Oct 1984

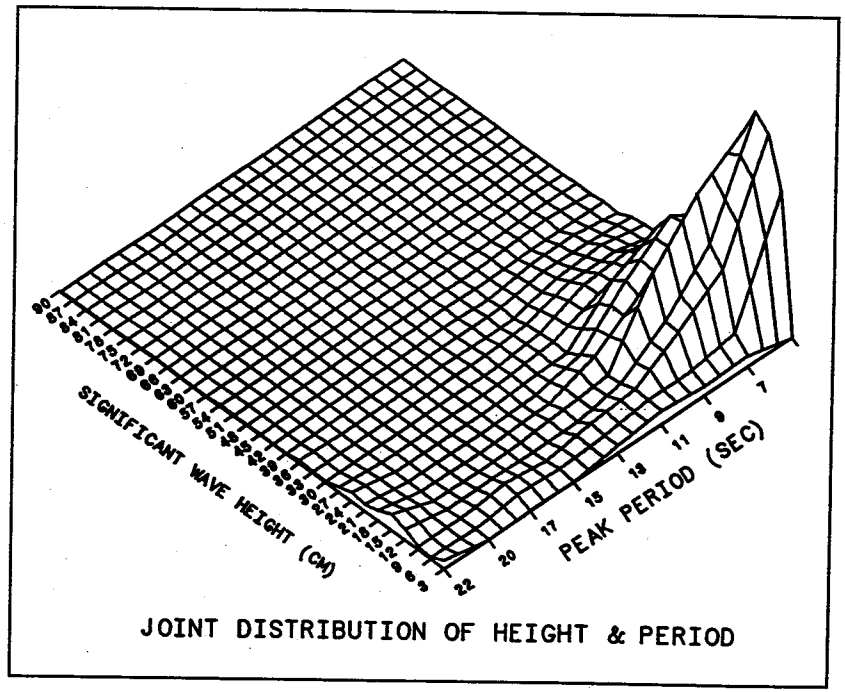

Figure C48. Joint distribution plot, Municipal pier, Energy, Pre-BW, Dec 1982 - Oct 1984

TOTAL OBSERVATIONS =2004

SIGNIFICANT WAVE HEIGHT (CM)	22+20	17	15	13	11	9	7	5
88–90+								
85–87								
82–84								
79–81								1
76–78								
73–75								
70–72								
67–69								
64–66								
61–63								
58–60								
55–57								
52–54	1				1	1		
49–51								
46–48					1		1	2
43–45	2					3		
40–42	7			1	2	8	2	3
37–39	2				1	2	3	4
34–36	6			2	8	10	4	3
31–33	7			3	4	12	5	13
28–30	7				3	21	12	12
25–27	9			3	15	42	13	21
22–24	10			3	11	43	15	33
19–21	9		1	4	27	55	17	51
16–18	14			8	16	68	27	70
13–15	27		3	8	30	86	35	156
10–12	16	1	2	15	39	73	44	159
7 –9	11	1	9	3	15	46	48	25	168
4 –6	4	3	12	1	14	16	23	10	115
1 –3	2	1	5	1	2	5	4	1	

PEAK PERIOD (SEC)

Figure C49. Joint distribution table, Pier 47, Energy, Pre-BW, Dec 1982 - Jul 1984

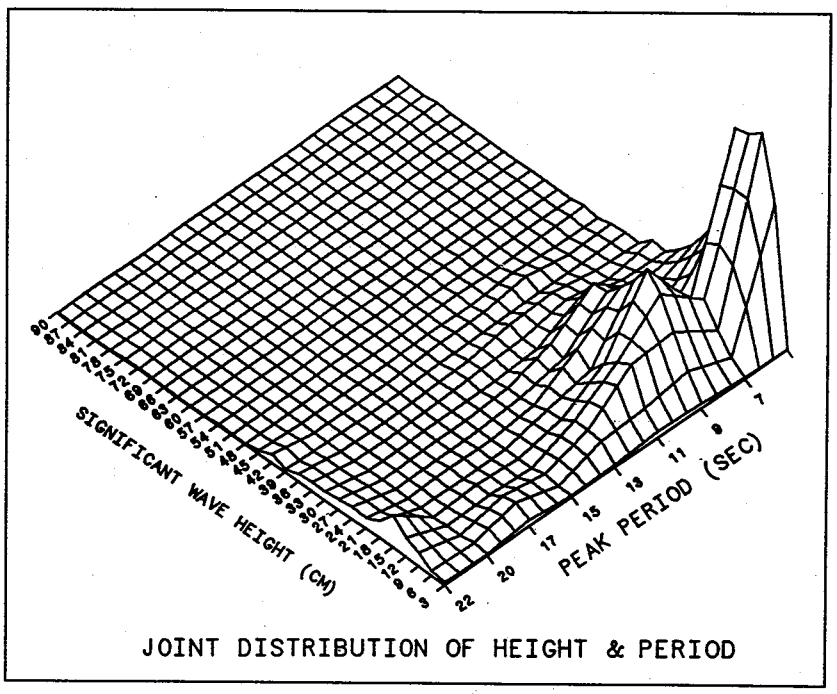

Figure C50. Joint distribution plot, Pier 47, Energy, Pre-BW, Dec 1982 - Jul 1984

TOTAL OBSERVATIONS =442

SIGNIFICANT WAVE HEIGHT (CM)	22+20	17	15	13	11	9	7	5
88–90								
85–87								
82–84								
79–81								
76–78								
73–75								
70–72								
67–69								
64–66								
61–63								
58–60								
55–57								
52–54								
49–51								
46–48								1
43–45								
40–42							2	
37–39							2	
34–36						2	1	
31–33							1	
28–30						1	3	1
25–27						2	3	5
22–24	3					3	3	13
19–21	2				1		5	6	18
16–18	1					2	6	14	21
13–15	8				1	5	6	15	49
10–12	1					5	8	11	53
7 –9	1			1	1	5	11	11	42
4 –6						1	11	8	47
1 –3	2	2		2		1	8	4	

PEAK PERIOD (SEC)

Figure C51. Joint distribution table, Pier 45, Energy, Pre-BW, Mar - Jun 1986

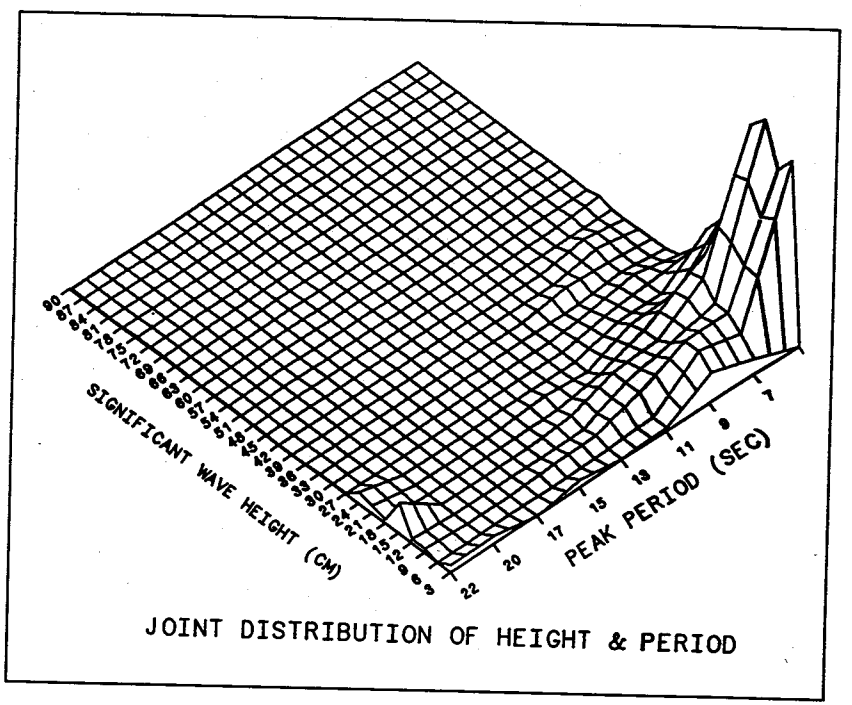

Figure C52. Joint distribution plot, Pier 45, Energy, Pre-BW, Mar - Jun 1986

TOTAL OBSERVATIONS =3148

SIGNIFICANT WAVE HEIGHT (CM)	22+20	17	15	13	11	9	7	5
88–90+								
85–87								
82–84								
79–81								
76–78								
73–75								
70–72								
67–69								
64–66								
61–63								
58–60								
55–57								
52–54								
49–51								
46–48								
43–45								
40–42	1							
37–39	1							
34–36								
31–33								1
28–30	1							
25–27	2							
22–24	4							1
19–21	4							
16–18	11							1
13–15	36							3
10–12	110				1	4	3	15
7 –9	224			2	23	46	25	96
4 –6	354		1	1	4	90	110	59	654
1 –3	471	4	21	32	44	184	334	170	

PEAK PERIOD (SEC)

Figure C53. Joint Distribution table, Pier 45, Energy, Post-BW, Jul 1986 - Oct 1989

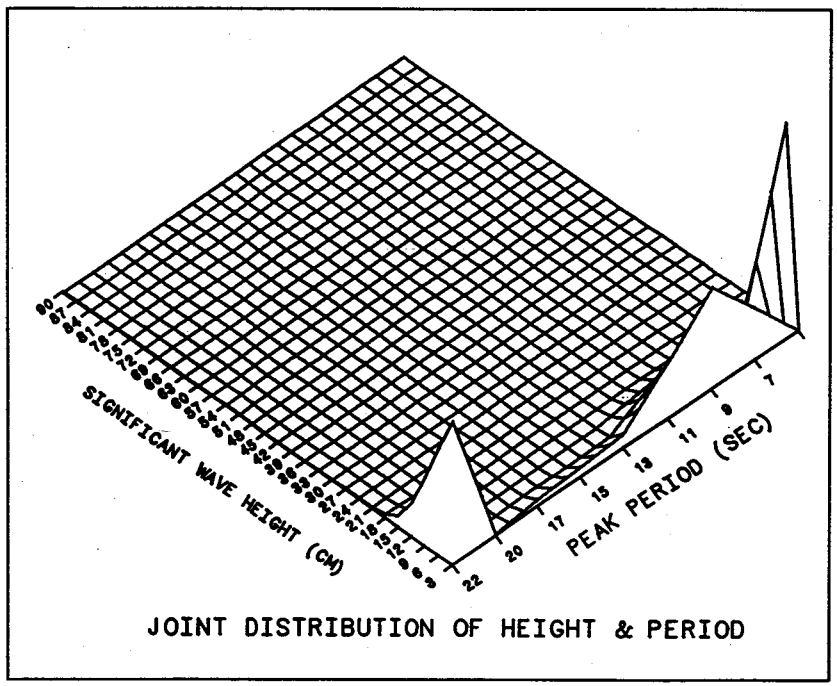

Figure C54. Joint distribution plot, Pier 45, Energy, Post-BW, Jul 1986 - Oct 1989

TOTAL OBSERVATIONS =2949

SIGNIFICANT WAVE HEIGHT (CM)	22+20	17	15	13	11	9	7	5
88–90+								
85–87								
82–84								
79–81								
76–78								
73–75								
70–72								
67–69								
64–66								
61–63								
58–60								1
55–57						1		
52–54						2		
49–51							2	1
46–48						1	3	1
43–45							4	2
40–42						1	5	1
37–39	1				1	3	9	9
34–36					1	12	15	19
31–33	3				1	12	15	27
28–30	3				1	16	19	43
25–27	17				1	23	37	64
22–24	27				5	19	47	118
19–21	43			3	1	29	42	165
16–18	69			7	6	38	49	229
13–15	107			2	10	38	51	410
10–12	76		1	2	7	26	30	330
7 –9	31	1		1	3	9	20	20	298
4 –6	10	1	4		7	2	2	5	161
1 –3	2		1		3	3		1	

PEAK PERIOD (SEC)

Figure C55. Joint Distribution table, Incident, Energy, Post-BW, Oct 1988 - Dec 1989

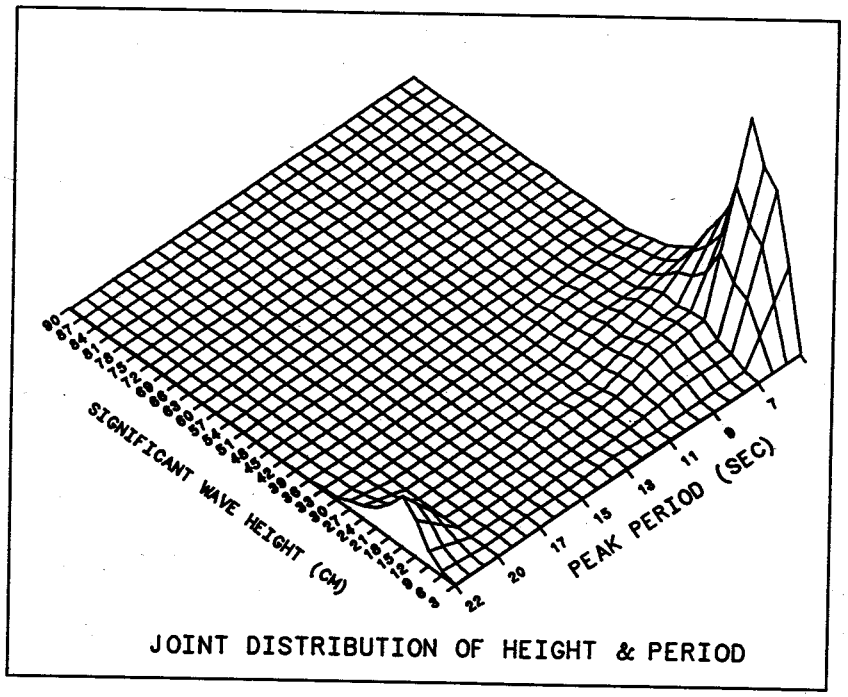

Figure C56. Joint distribution plot, Incident, Energy, Post-BW, Oct 1988 - Dec 1989

TOTAL OBSERVATIONS =2631

SIGNIFICANT WAVE HEIGHT (CM)	22+20	17	15	13	11	9	7	5
88–90+								
85–87								
82–84								
79–81								
76–78								
73–75								
70–72								
67–69								
64–66								
61–63								
58–60								
55–57								
52–54								
49–51								
46–48								
43–45								
40–42								
37–39								
34–36								
31–33								
28–30								
25–27	1							1
22–24	4							
19–21	13							
16–18	27							1
13–15	99					1		2
10–12	189			2	8	16	1	6
7 –9	300	3	1	12	34	41	13	38
4 –6	496	7	7	1	23	88	90	29	280
1 –3	428	10	19	15	81	89	93	62	

PEAK PERIOD (SEC)

Figure C57. Joint Distribution table, Basin, Energy, Post-BW, Oct 1988 - Dec 1989

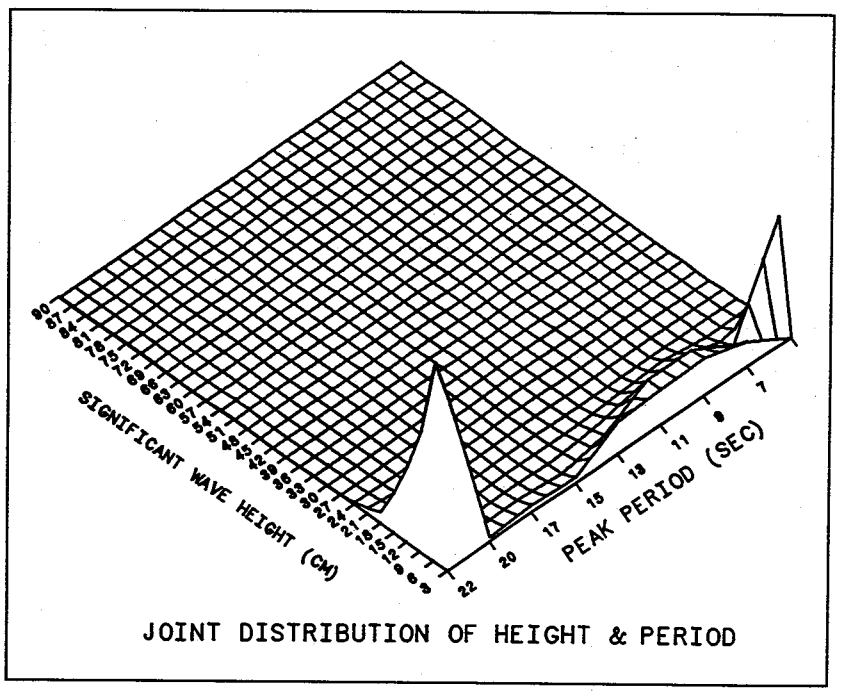

Figure C58. Joint distribution plot, Basin, Energy, Post-BW, Oct 1988 - Dec 1989

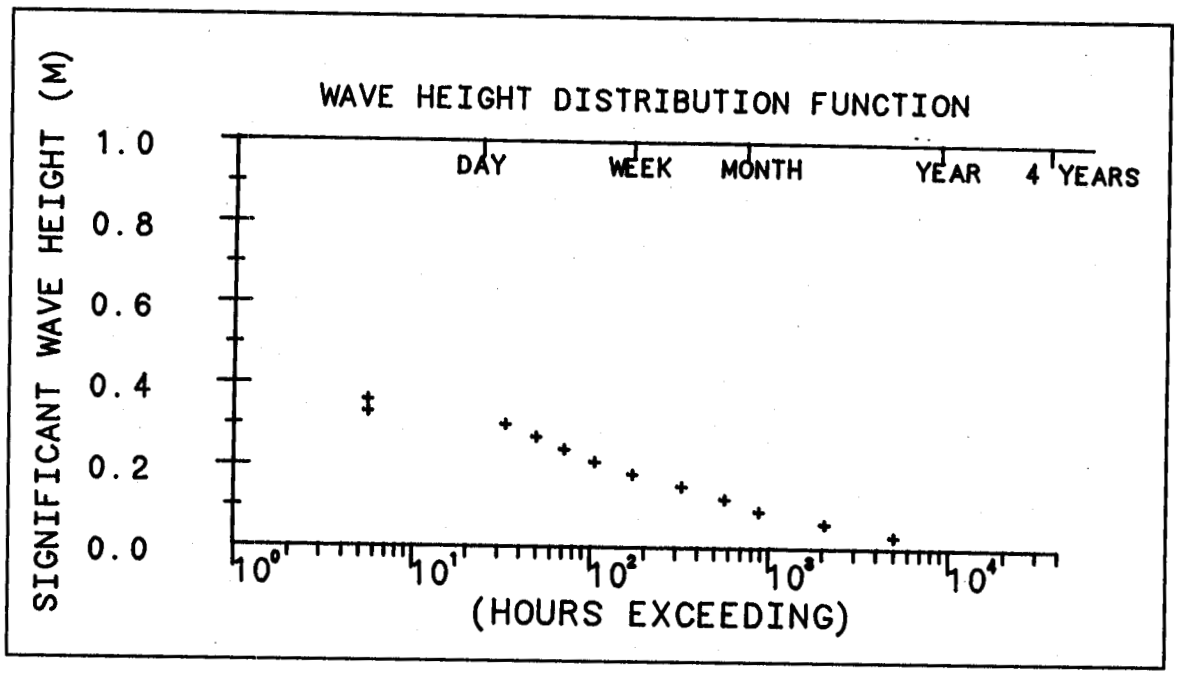

Figure C59. Cumulative wave height distribution plot, Alioto's Wharf, Energy, Pre-BW, Mar - Sep 1986

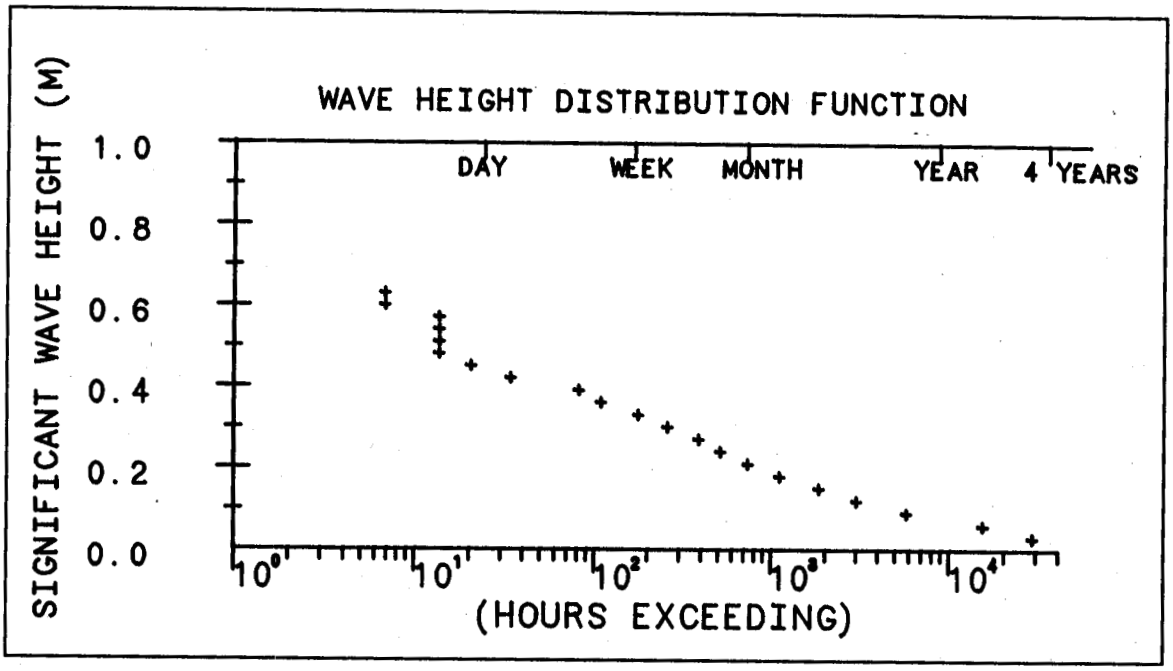

Figure C60. Cumulative wave height distribution plot, Alioto's Wharf, Energy, Post-BW, Jul 1986 - Oct 1989

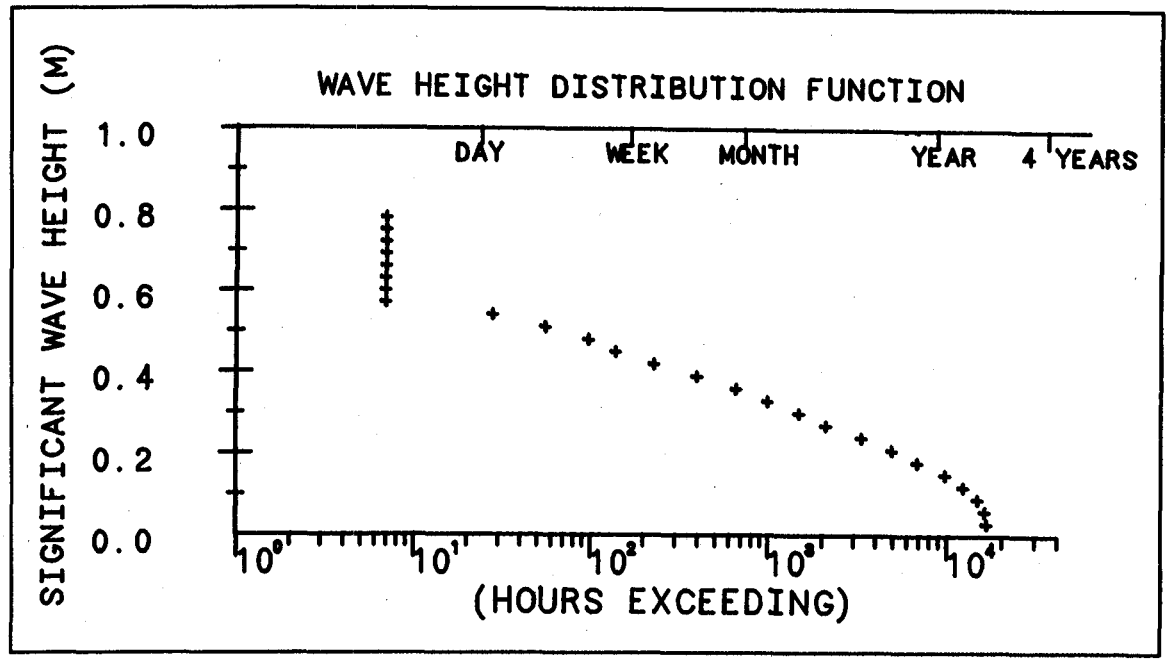

Figure C61. Cumulative wave height distribution plot, Municipal pier, Energy, Pre-BW, Dec 1982 - Oct 1984

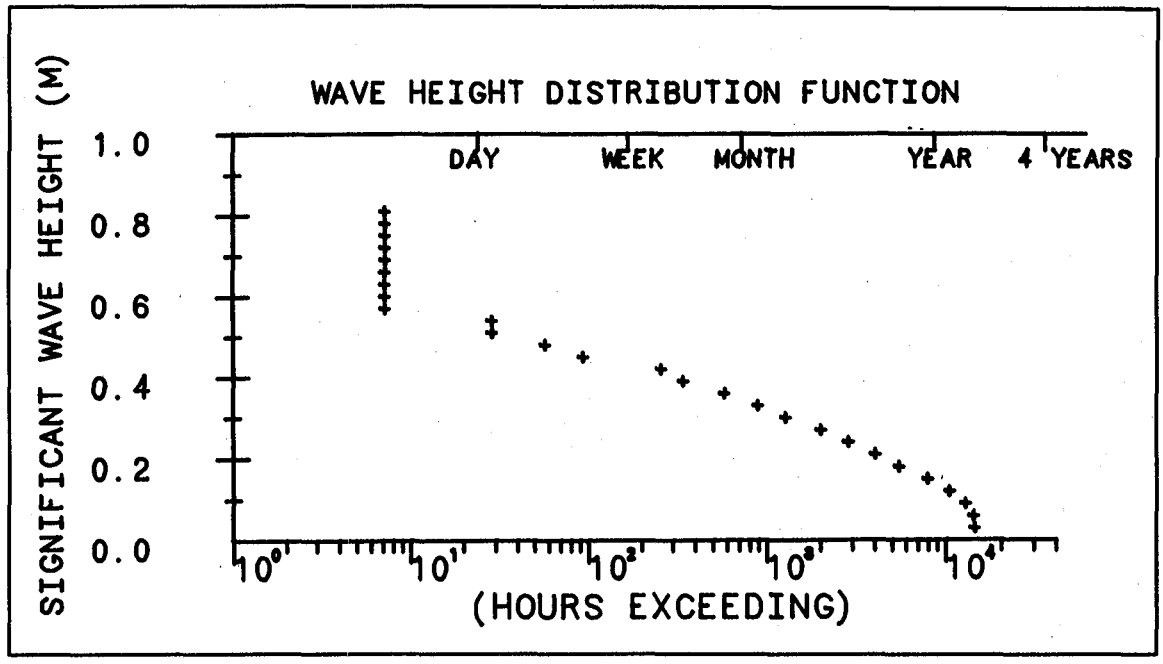

Figure C62. Cumulative wave height distribution plot, Pier 47, Energy, Pre-BW, Dec 1982 - Jul 1984

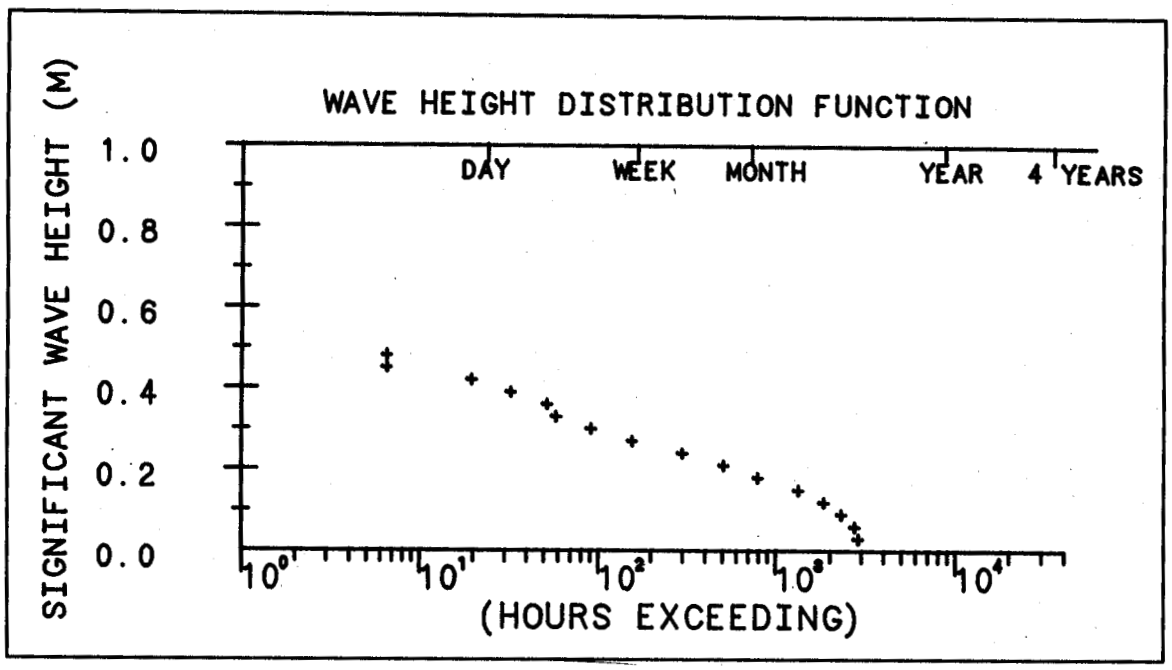

Figure C63. Cumulative wave height distribution plot, Pier 45, Energy, Pre-BW, Mar - Jun 1986

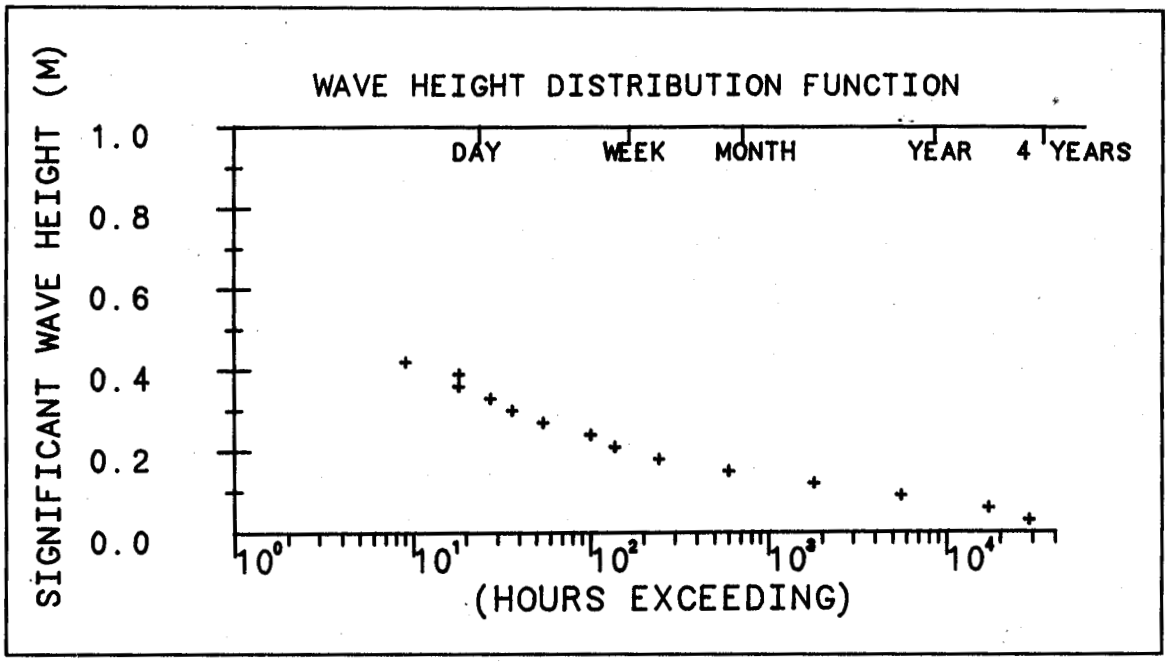

Figure C64. Cumulative wave height distribution plot, Pier 45, Energy, Post-BW, Jul 1986 - Oct 1989

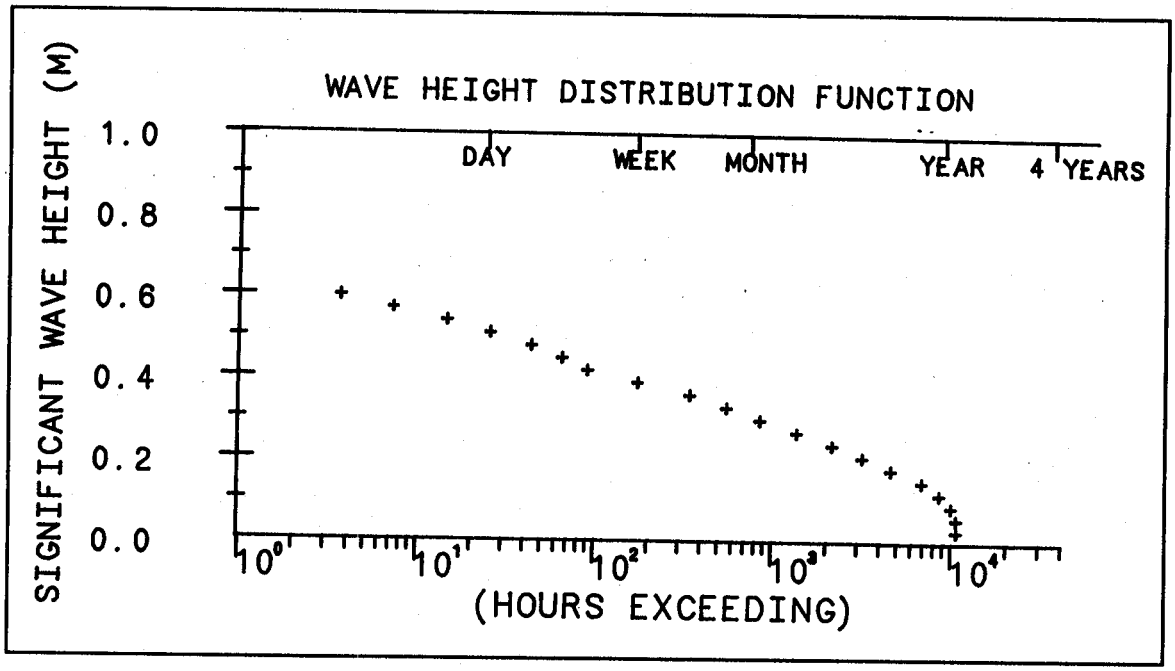

Figure C65. Cumulative wave height distribution plot, Incident, Energy, Post-BW, Oct 1988 - Dec 1989

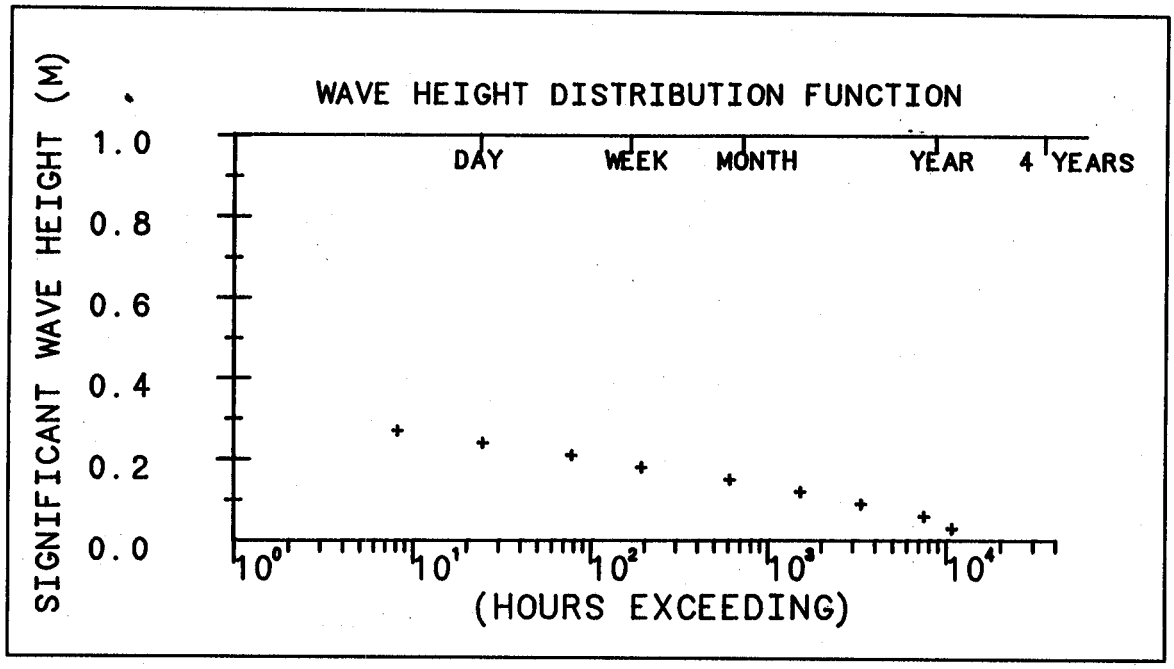

Figure C66. Cumulative wave height distribution plot, Basin, Energy, Post-BW, Oct 1988 - Dec 1989

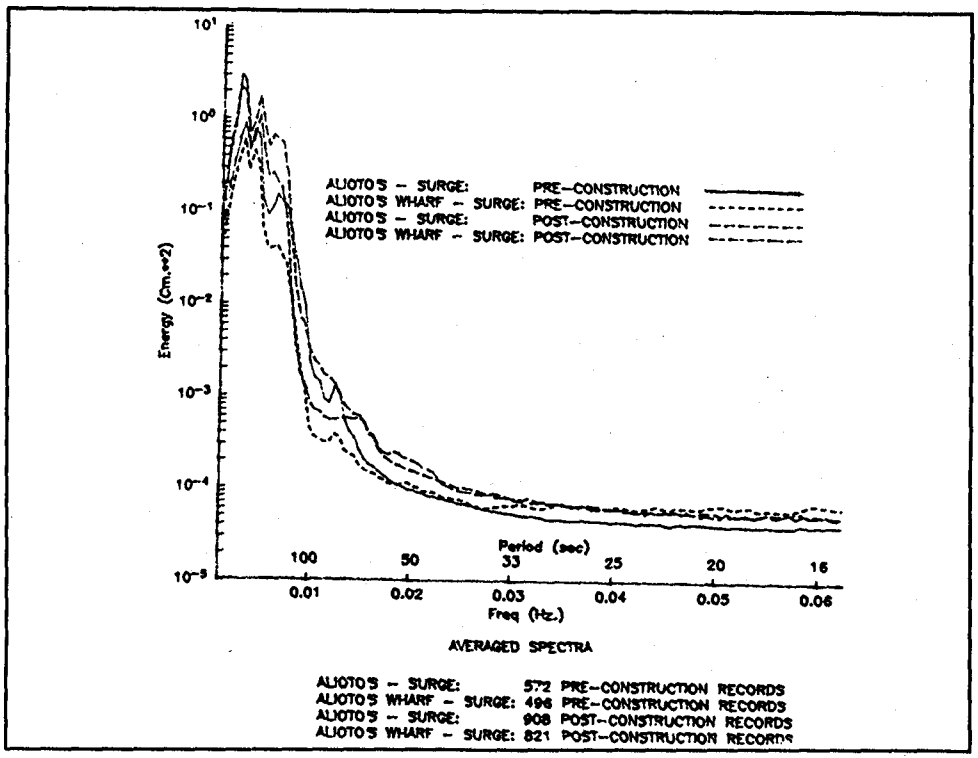

Figure C67. Long-term average surge spectra - Alioto's, Alioto's Wharf

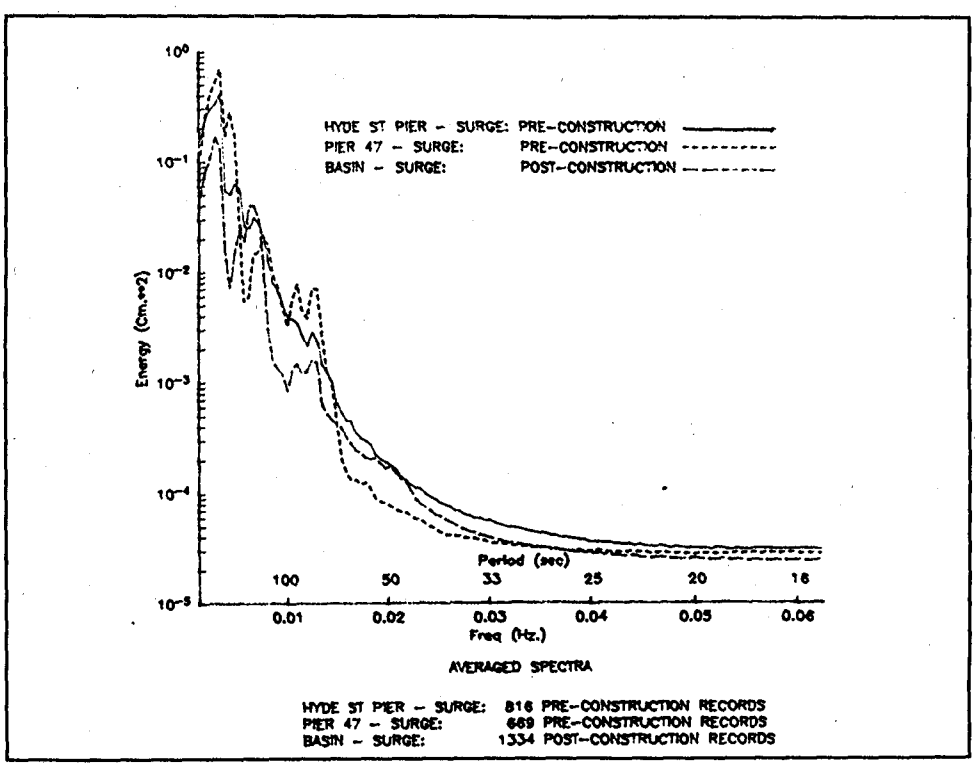

Figure C68. Long-term average surge spectra - Hyde St. pier, Pier 47, Basin

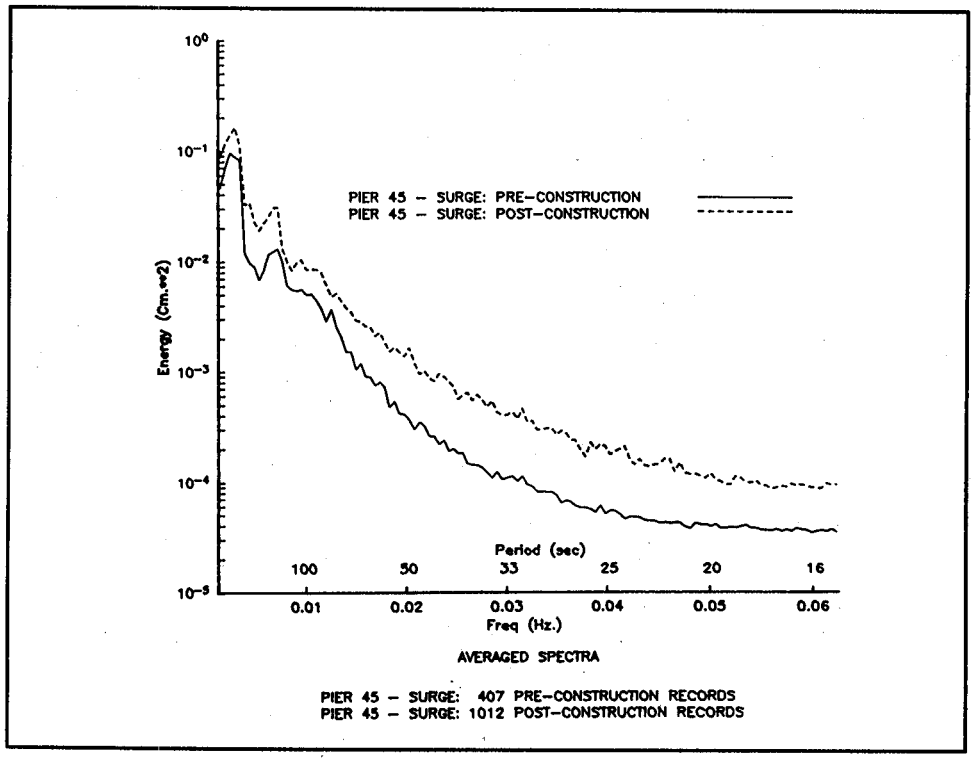

Figure C69. Long-term average surge spectra - Pier 45

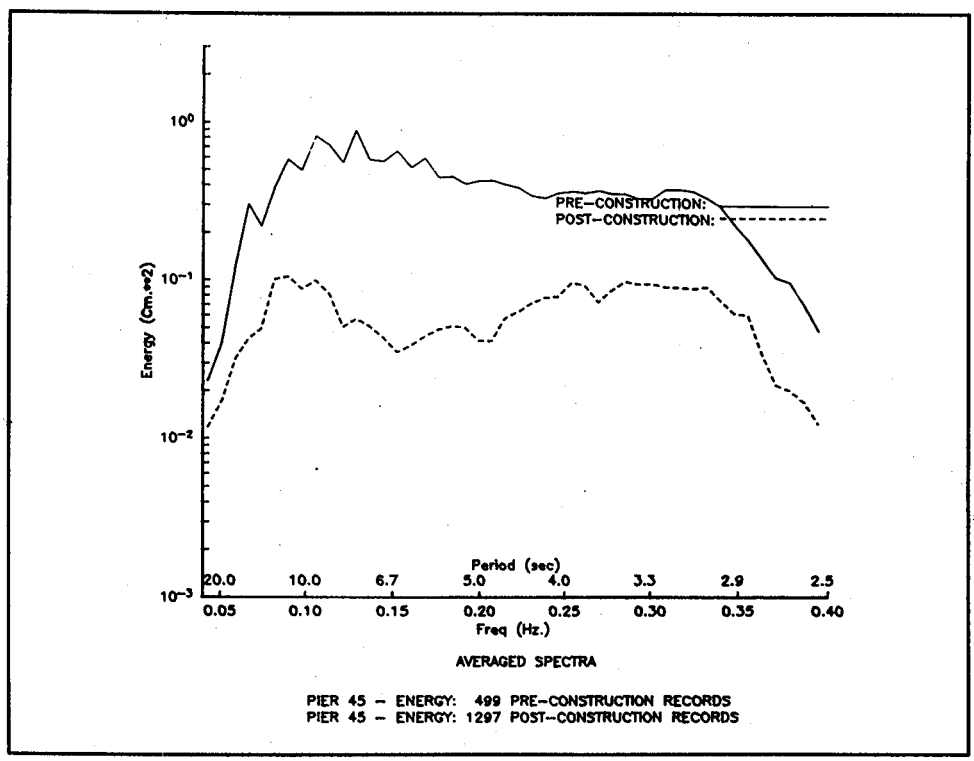

Figure C70. Long-term average energy spectra - Pier 45

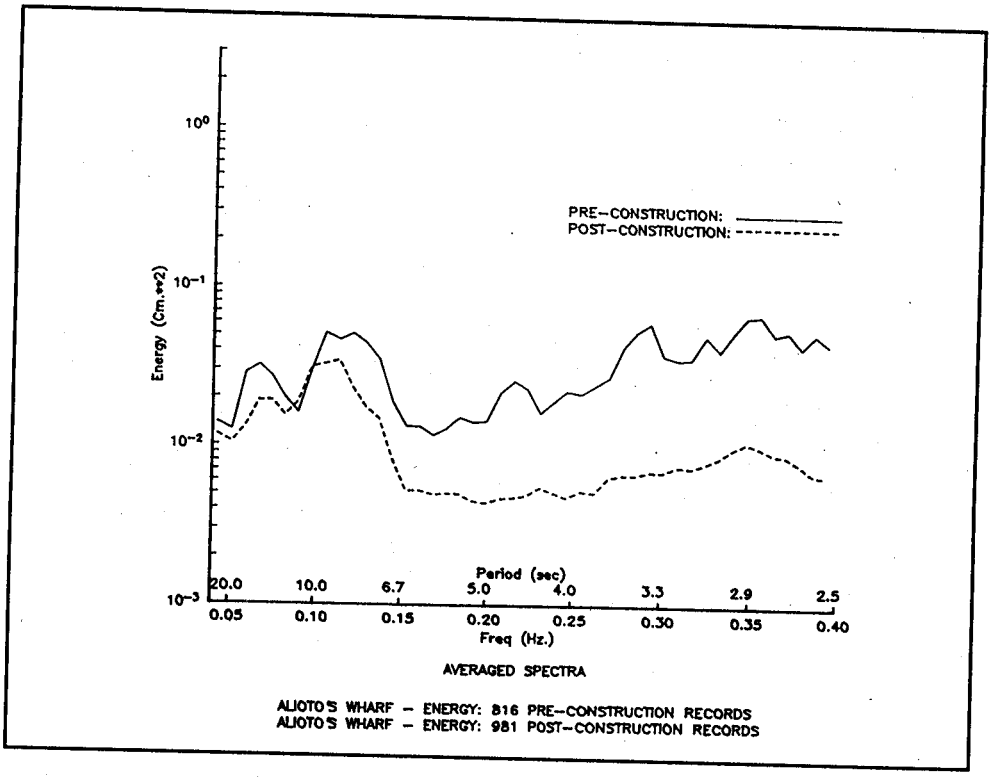

Figure C71. Long-term average energy spectra - Alioto's Wharf

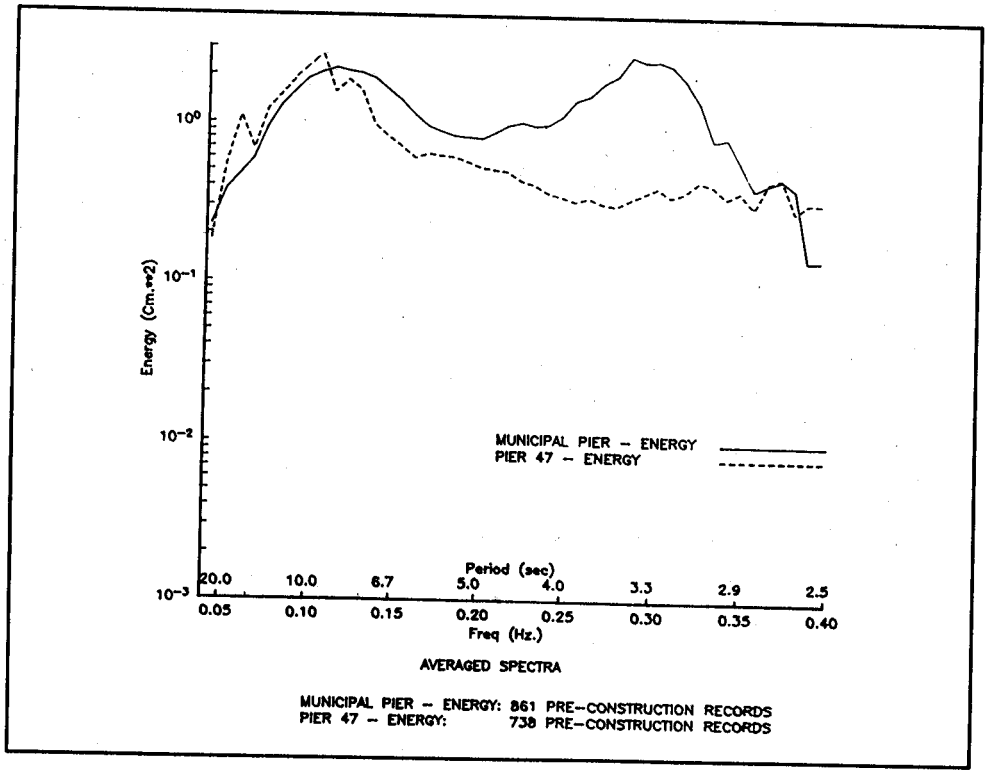

Figure C72. Long-term average energy spectra-Municipal pier, Pier 47

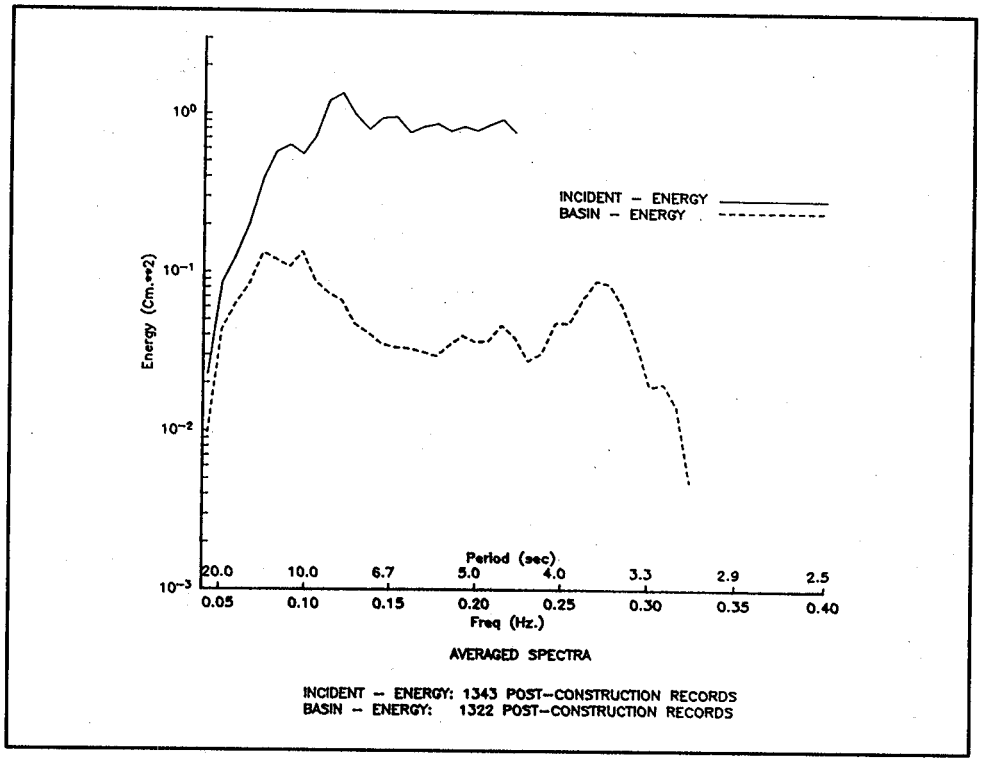

Figure C73. Long-term average energy spectra - Incident, Basin

REPORT DOCUMENTATION PAGE

Form Approved
OMB No. 0704-0188

1. AGENCY USE ONLY *(Leave blank)*	2. REPORT DATE	3. REPORT TYPE AND DATES COVERED
	May 1994	Final report

4. TITLE AND SUBTITLE
Fisherman's Wharf Breakwater Monitoring Study, San Francisco, California

5. FUNDING NUMBERS
WU 22115

6. AUTHOR(S)
Jonathan W. Lott

7. PERFORMING ORGANIZATION NAME(S) AND ADDRESS(ES)
USAE Waterways Experiment Station
Coastal Engineering Research Center
3909 Halls Ferry Road, Vicksburg, MS 39180-6199

8. PERFORMING ORGANIZATION REPORT NUMBER
Miscellaneous Paper
CERC-94-8

9. SPONSORING/MONITORING AGENCY NAME(S) AND ADDRESS(ES)
U.S. Army Corps of Engineers
Washington, DC 20314-1000

10. SPONSORING/MONITORING AGENCY REPORT NUMBER

11. SUPPLEMENTARY NOTES
Available from National Technical Information Service, 5285 Port Royal Road, Springfield, VA 22161

12a. DISTRIBUTION/AVAILABILITY STATEMENT
Approved for public release; distribution is unlimited.

12b. DISTRIBUTION CODE

13. ABSTRACT *(Maximum 200 words)*

A field monitoring study of the Fisherman's Wharf breakwater was conducted as part of the Monitoring Completed Coastal Projects (MCCP) program. The Corps project referred to as the "Fisherman's Wharf breakwater" in this report consists of a combination of three discrete reinforced concrete sheet-pile structures. The main detached breakwater is an impermeable vertical wall structure with additional support provided by batter piles. The other two structural elements are similar, except that they have openings to allow the passage of tidal flows. The breakwater is located on the north-facing waterfront of the city of San Francisco, California, adjacent to the world-famous Fisherman's Wharf small-craft harbor, bordered by Aquatic Park, Municipal pier, Hyde Street pier, and Pier 45. The site is subject to both local waves from fetches within San Francisco Bay and ocean-generated waves which penetrate to the site via the Golden Gate.

The breakwater was designed primarily to attenuate the damaging short-period waves that are largest from the north to northeast directions. The breakwater also provides protection for the historic ships berthed at Hyde Street pier and allows for expansion and improvement of the commercial fishing berthing facilities. Concurrent requirements were to prevent increases in harbor oscillations (surge) and to permit sufficient tidal circulation to avoid degradation of water quality.

(Continued)

14. SUBJECT TERMS
Aquatic Park
Baffled breakwater
Coastal structure design
Coastal structures
Current measurements
(Continued)

15. NUMBER OF PAGES
189

16. PRICE CODE

17. SECURITY CLASSIFICATION OF REPORT	18. SECURITY CLASSIFICATION OF THIS PAGE	19. SECURITY CLASSIFICATION OF ABSTRACT	20. LIMITATION OF ABSTRACT
UNCLASSIFIED	UNCLASSIFIED	UNCLASSIFIED	

13. ABSTRACT (Concluded).

Primary monitoring objectives were to document and evaluate breakwater performance with respect to waves and surge, circulation, scour, littoral processes and deposition, and structural integrity. Prototype measurements of waves and surge, currents, near-structure and harbor bathymetry, and structural alignments were obtained through the MCCP monitoring study. Prototype data were used to evaluate the breakwater's performance and its effects on the site, and to evaluate the procedures and tools, such as physical and numerical models, used to develop the project design.

The breakwater (completed in November 1986) has performed well to date with respect to the design objectives. Design wave height criteria for the protected harbor have been met thus far, although prototype conditions as severe as the most extreme design wave conditions apparently have not been experienced since breakwater completion. Effects on surge, circulation, scour, deposition, and the beach processes at Aquatic Park are generally close to performance criteria. Preliminary MCCP lead-line sounding data suggested that local scour at the ends of the structures could eventually become a maintenance problem (the possible need for scour protection was anticipated during breakwater design). As a preventive measure, the seabed was armored with stone riprap at critical locations in October 1992. The breakwater shows no evidence of damage or significant displacements from the Loma Prieta earthquake of October 1989, which caused significant damage to Pier 45 and Hyde Street pier. No unexpected operation and maintenance problems have developed.

From project performance to date, procedures and tools used in breakwater design appear to have been appropriate given the state of the art available at the time of design. However, the monitoring experience has pointed out the desirability of initiating prototype data collection well in advance of structure completion and continuation of monitoring long enough to establish a proper basis for comparisons. Prototype incident wave direction should be measured. Standard prototype wave gaging methodology and analysis may not be fully satisfactory when used to characterize or monitor sites such as Fisherman's Wharf that are subject to simultaneous short- and long-period waves. Similar sites may require non-standard wave-gaging approaches. The experience of this MCCP monitoring study has emphasized the desirability of planning monitoring in conjunction with the modeling studies for the design process.

14. Subject Terms (Concluded)

Fisherman's Wharf
Harbor circulation
Harbor oscillations
Impermeable breakwater
Lead-line soundings
MCCP
Monitoring
Physical modeling
Pile-supported breakwater
Reinforced concrete breakwater
San Francisco Bay
Scour
Surge
Vertical-wall breakwater
Wave attenuation
Wave data analysis
Wave gages